

THESIS

4

MICHIGAN STATE UNIVERSITY LIBRARIES



3 1293 01400 0578

**LIBRARY
Michigan State
University**

This is to certify that the
dissertation entitled

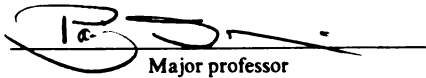
**ACCELERATED PROCESSING OF HIGH-
PERFORMANCE WOOD-CEMENT COMPOSITES**

presented by

Jong-Pil Won

has been accepted towards fulfillment
of the requirements for

Ph.D. degree in Civil Engineering


Major professor

Date August 4, 1995

PLACE IN RETURN BOX to remove this checkout from your record.
TO AVOID FINES return on or before date due.

DATE DUE	DATE DUE	DATE DUE
DEC 10 2000		
AUG 31 2003		
AUG 08 2011		

**ACCELERATED PROCESSING OF HIGH-
PERFORMANCE WOOD-CEMENT COMPOSITES**

By

Jong-Pil Won

A DISSERTATION

Submitted to
Michigan State University
in partial fulfillment of the requirements
for the degree of

DOCTOR OF PHILOSOPHY

Department of Civil and Environmental Engineering

1995

ABSTRACT

ACCELERATED PROCESSING OF HIGH- PERFORMANCE WOOD-CEMENT COMPOSITES

By

Jong-Pil Won

This research developed accelerated curing processes for wood-cement composites using the vigorous reactions between carbon dioxide and cement paste. Two wood-cement systems were considered: wet-processed cellulose fiber reinforced cement, and dry-processed cement-bonded wood particleboard. In cellulose fiber reinforced cement, carbonation curing was used to complement conventional accelerated curing, while in cement-bonded wood particleboard accelerated curing was accomplished solely through carbonation.

A comprehensive experimental parametric study followed by optimization investigations indicated that carbonation curing can enhance the productivity and energy-efficiency of manufacturing wood-cement composites. Carbonated boards showed reduced capillary porosity, increased CaCO_3 content and improved bonding to wood fibers. Under diverse accelerated weathering effects, carbonated boards also provided improved longevity and weathering resistance. This could be attributed to the chemical stability of carbonated products and reduced the capillary porosity of the composite system.

Lower CO₂ concentrations were as effective as pure CO₂ in carbonation curing of wood-cement composites. This indicates that CO₂-rich industrial emissions can find value-added applications in carbonation curing of building panels. This would add environmental benefits to the technical and economic advantages of the technology.

To

**my parents and parents-in-law for their love, support and
encouragement.**

ACKNOWLEDGMENTS

I wish to thank my advisor, Dr. Parviz Soroushian, for his guidance and patience during this research project. I especially appreciate his endless constructive critiques and intellectually challenging questions that initiated many meaningful research directions and significantly improved my abilities as a researcher. The indispensable help of Dr. Otto Suchsland is also gratefully acknowledge. Appreciation is extended to Dr. Ronald Harichandran and Dr. James Lucas for serving on the author's guidance committee.

Financial support for the performance of this research was provided by the U.S. Department of Agriculture and the Research excellence Fund of the State of Michigan. The technical support from the Composite Materials and Structures Center of Michigan State University is also gratefully acknowledged.

I would like to thank all the people who helped me during my stay at Michigan State University. Special appreciation, admiration, and love are given to the author's family for their continuous encouragement, love and support. Further thanks also go to the author's mother, Jung-Yun Lee, for her encouragement and patience in these years. Finally, I wish to extend my thanks to my wife Me-Yang Choi and two lovely daughters, Sung-Yeon (Teresa) and Ji-Yun (Rosa), for their constant love, patience and support.

TABLE OF CONTENTS

LIST OF TABLES	x
LIST OF FIGURES	xvii
CHAPTER 1 Introduction	1
1.1 Background	1
1.2 Fiber Reinforced Cement Composites	3
1.3 Applications of Natural Fiber Reinforced Cement Composite in Construction	4
1.3.1 Cement-Bonded Particleboard	4
1.3.2 Cellulose Fiber Reinforced Cement Composites	5
1.4 Research Objectives	5
CHAPTER 2 Natural Fibers and Particles	8
2.1 Introduction	8
2.2 Processing of Natural Fibers/Particles and Cementitious Composites	9
2.2.1 Wood Particles	9
2.2.2 Cellulose Fibers	13
2.3 Special Problems of Wood Particles and Fibers in Cementitious Materials	15
2.3.1 Setting and Curing of Wood-Cement Composites	16
2.3.2 Treatment of Fibers/ Particles	16
2.3.3 Mechanical Properties	17
2.3.4 Seasoning Effects on Fiber/ Particle Properties	17
2.3.5 Attack by Micro-Organisms	17
2.3.6 Humidity Condition	18
2.3.7 Temperature	18
CHAPTER 3 Literature Review	21
3.1 Introduction	21
3.2 History and Development of Wood-Cement Composites	21
3.2.1 Cement-Bonded Wood Particleboard	21

3.2.2 Cellulose Fiber Reinforced Cement Composites	22
3.3 Wood-Cement Compatibility	23
3.4 Overview of Earlier Carbonation Studies	26
3.4.1 Influence of Carbon Dioxide	26
3.4.2 Durability Characteristics	39
3.4.3 Economy	42
3.5 Design of Natural Fiber Reinforced Cement Composites	43
3.5.1 Volume Fraction of Fiber and Particle	43
3.5.2 Fiber and Particle Forms	45
3.5.3 Fiber/ Particle Length and Aspect Ratio	46
3.5.4 Fiber Orientation	47
3.5.5 Fiber Shape	47
3.5.6 Effect of Voids	47
3.5.7 Constituent Behavior	48
3.6 Theoretical Principles	49
CHAPTER 4 Manufacturing and Early Age Characteristics	
under Carbonation Effects	58
4.1 Introduction	58
4.2 Objectives	59
4.3 Cement Hydration Characteristics in the Presence of Wood Particles	59
4.4 Cement-Bonded Particleboard	62
4.4.1 Materials and Manufacturing Procedures	62
4.4.2 Experimental Design	65
4.4.3 Test Results and Statistical Analysis	70
4.5 Cellulose Fiber Reinforced Cement Composites	82
4.5.1 Materials, Manufacturing Procedures and Experimental Program	82
4.5.2 Experimental Set-Up	87
4.5.3 Test Results and Statistical Analysis	88
4.6 Summary and Discussion	101
4.6.1 Cement-Bonded Wood Particleboard	101
4.6.2 Cellulose Fiber Reinforced Cement Composites	103
CHAPTER 5 Optimization and Assessment of Mechanical	
and Physical Properties	104
5.1 Introduction	104
5.2 Objective	104
5.3 Cellulose Fiber Reinforced Cement Composites	104
5.3.1 Optimization of the Manufacturing Variables of Cellulose Fiber Reinforced Cement Composite by CO ₂ Curing: Unpressed Case	104
5.3.2 Test Results and Analysis	105
5.3.3 Mechanical and Physical Properties of Cellulose Fiber Reinforced Cement Composites	110
5.4 Cement-Bonded Particleboard	118

5.4.1 Mechanical Properties	118
5.4.2 Physical Properties	131
5.5 Summary and Conclusions	133
5.5.1 Cellulose Fiber Reinforced Cement Composite	134
5.5.2 Cement-Bonded Particleboard	134
CHAPTER 6 Durability Characteristics of Carbonated	
Wood-Cement Composites	135
6.1 Introduction	135
6.2 Test Procedures	136
6.2.1 Accelerated Wetting and Drying	136
6.2.2 Accelerated Freezing and Thawing	137
6.2.3 Warm Water Immersion	138
6.2.4 Repeated Wetting-Drying-Carbonation	139
6.2.5 Moisture Sensitivity	139
6.3 Test Results	141
6.3.1 Cement-Bonded Particleboard	141
6.3.2 Cellulose Fiber Reinforced Cement Composite	164
6.4 Dimensional Stability of Cellulose Fiber Reinforced Cement under Repeated Wetting-Drying-Carbonation	214
6.5 Summary and Discussion	216
6.5.1 Cement-Bonded Particleboard	216
6.5.2 Cellulose Fiber Reinforced Cement Composite	217
CHAPTER 7 Microstructure of Wood-Cement Composites	221
7.1 Introduction	221
7.2 Test Procedures	221
7.2.1 X-Ray Diffraction (XRD)	221
7.2.2 Environmental Scanning Electron Microscope (ESEM)	222
7.2.3 Thermogravimetric Analysis (TGA)	222
7.2.4 Mercury Intrusion Porosimetry	223
7.3 Test Results	224
7.3.1 Cement-Bonded Particleboard	224
7.3.2 Cellulose Fiber Reinforced Cement Composite	247
7.4 Summary and Conclusions	271
7.4.1 Cement-Bonded Particleboard	271
7.4.2 Cellulose Fiber Reinforced Cement Composites	272
CHAPTER 8 Summary and Conclusions	273
8.1 Manufacturing and Early Age Characteristics under Carbonation Effects	273
8.1.1 Cement-Bonded Particleboard	274
8.1.2 Cellulose Fiber Reinforced Cement Composites	274
8.2 Optimization and Assessment of Mechanical and Physical Properties	275

8.2.1 Cellulose Fiber Reinforced Cement Composites	275
8.2.2 Cement-Bonded Particleboard	276
8.3 Durability Characteristics of Carbonated Wood-Cement Composites	276
8.3.1 Cement-Bonded Particleboard	276
8.3.2 Cellulose Fiber Reinforced Cement Composites	278
8.4 Microstructure of Wood-Cement Composites	281
8.4.1 Cement-Bonded Particleboard	281
8.4.2 Cellulose Fiber Reinforced Cement Composites	282
APPENDIX A: A Framework to Model Restrained Shrinkage Cracking of Cellulose Fiber Reinforced Cement Composites	284
APPENDIX B: Standard Specifications	294
BIBLIOGRAPHY	295

LIST OF TABLES

Table 2.1	Areas of Forestland in the World	9
Table 2.2	Organic Constituents of Wood	10
Table 3.1	Industrial Production of Inorganic-Bonded Wood Composites	22
Table 3.2	Chemical Composition of Type I Portland Cement	24
Table 3.3	The New Carbonizing Technology	28
Table 3.4	Influence of Carbon Dioxide Injection on Cement-Bonded Particleboard	29
Table 3.5	Influence of Carbon Dioxide Pressure on Cement-Bonded Particleboard	31
Table 3.6	Summary of Comparison Between Carbonated, Fungal Cellar- Exposed and Uncarbonated, Unexposed Cellulose Fiber Cement Composites	40
Table 3.7	Comparative Durability of Conventionally and Rapidly Setting Cement-Bonded Wood Particleboard form Spruce	41
Table 3.8	Comparison of Raw Materials and Energy	43
Table 3.9	The Effect of Fiber Orientation on Strength of Composite	47
Table 3.10	Effect of Aspect Ratio and Fiber Content	55
Table 4.1	Wood Particle Dimension	62
Table 4.2	Chemical Composition of the Type I Portland Cement used In this Investigation	64
Table 4.3	Experimental Program to Evaluate Various CO ₂ Concentrations	67

Table 4.4	Experimental Program for the Evaluation of Various Mix Compositions	68
Table 4.5	Flexural Performance of Cement-Bonded Wood Particleboards Subjected to Methods I and II of CO ₂ -Curing	71
Table 4.6	Effects of Various CO ₂ Concentrations on the Flexural Performance of Cement-Bonded Wood Particleboard	74
Table 4.7	Flexural Test Results	78
Table 4.8	The Results of the Analysis of Variance	78
Table 4.9	The Composition of Cellulose Fiber Reinforced Cement Composite	82
Table 4.10a	Design of Experimental (Pressed Composite)	87
Table 4.10b	Design of Experimental (Unpressed Composite)	87
Table 4.11a	Flexural Performance of Cellulose Fiber Reinforced Cement Composites (Pressed)	89
Table 4.11b	Flexural Performance of Cellulose Fiber Reinforced Cement Composites (Unpressed).....	90
Table 4.12	Analysis of Variance of the Flexural Test Results for Cellulose Fiber Reinforced Cement Composites (Pressed)	91
Table 4.13	Analysis of Variance of the Flexural Test Results for Cellulose Fiber Reinforced Cement Composites (Unpressed)	92
Table 4.14	Results of Analysis of Variance after Transformation (Pressed)	93
Table 4.15	Results of Analysis of Variance after Transformation (Unpressed) ..	94
Table 4.16	Test Results of Evaluated Oven Temperature (Unpressed)	100
Table 5.1	Optimization Experimental Design and Test Results	107
Table 5.2	Flexural Performance of Optimized CO ₂ -Cured Unpressed Cellulose Fiber Reinforced Cement Composites Versus Those of Controls	110

Table 5.3	The Percentage Difference in Flexural Performance of CO ₂ -Cured Boards Versus Controls	112
Table 5.4	Flexural Performance of CO ₂ Cured Pressed Cellulose Fiber Reinforced Cement Composites Versus Those of Controls	113
Table 5.5	The Percentage Difference of Flexural Performance of CO ₂ Cured Boards Versus Controls	115
Table 5.6	Water Absorption and Specific Gravity Test Results	115
Table 5.7	The Experimental Program	119
Table 5.8	Flexural Test Results at 28 Days of Age	120
Table 5.9	Results of Analysis of Variance: CO ₂ Versus Conventionally Cured Boards	123
Table 5.10	Results of Analysis of Variance: CO ₂ Cured Boards	123
Table 5.11	Internal Bond Test Results	128
Table 5.12	Results of Analysis of Variance for IB: CO ₂ Versus Conventionally Cured Boards	129
Table 5.13	Results of Analysis of Variance for IB: CO ₂ Cured Boards	129
Table 6.1	The Properties of Cement Phases	135
Table 6.2	Repeated Wetting-Drying Effects on Flexural Strength of Cement-Bonded Particleboard	145
Table 6.3	Repeated Wetting-Drying Effects on Flexural Toughness of Cement-Bonded Particleboard	146
Table 6.4	Repeated Wetting-Drying Effects on Initial Stiffness of Cement-Bonded Particleboard	147
Table 6.5	Results of Analysis of Variance After Wetting-Drying: CO ₂ Cured Boards	148
Table 6.6	Results of Analysis of Variance After Wetting-Drying: CO ₂ Versus Conventionally Cured Boards	149

Table 6.7	Repeated Freezing-Thawing Effects on Flexural Strength of Cement-Bonded Particleboard	156
Table 6.8	Repeated Freezing-Thawing Effects on Flexural Toughness of Cement-Bonded Particleboard	157
Table 6.9	Repeated Freezing-Thawing Effects on Initial Stiffness of Cement-Bonded Particleboard	158
Table 6.10	Results of Analysis of Variance of After Repeated Freezing-Thawing: CO ₂ Cured Boards	159
Table 6.11	Results of Analysis of Variance of After Repeated Freezing-Thawing: CO ₂ Versus Conventionally Cured Boards	160
Table 6.12	Results of the statistical Analysis of Data: Unaged Cases	165
Table 6.13	Statistical Analysis of Test Results: Unaged Cases (Unpressed)	165
Table 6.14	Statistical Analysis of Test Results: Unaged Cases (Pressed)	166
Table 6.15	Effects of Repeated Wetting-Drying on the Flexural Performance of Cellulose Fiber Reinforced Cement Composites	170
Table 6.16	Results of the Analysis of Test Data (Unpressed)	171
Table 6.17	Results of the Analysis of Test Data (Pressed)	171
Table 6.18	Results of the Analysis of Test Data: Aged Cases	172
Table 6.19	Results of the Analysis of Test Data: Unaged/Aged Ratio	173
Table 6.20	Statistical Analysis of Test Results: Aged Cases (Unpressed)	174
Table 6.21	Statistical Analysis of Test Results: Aged Cases (Pressed)	174
Table 6.22	Statistical Analysis of Test Results: Unaged/Aged Ratio (Unpressed)	174
Table 6.23	Statistical Analysis of Test Results: Unaged/Aged Ratio (Pressed)	174
Table 6.24	Effects of Repeated Freeze-Thaw on the Flexural Performance of Cellulose Fiber Reinforced Cement Composites	179

Table 6.25	Results of the Analysis of Test Data (Unpressed)	180
Table 6.26	Results of the Analysis of Test Data (Pressed)	180
Table 6.27	Results of the Analysis of Test Data: Aged Cases	181
Table 6.28	Results of the Analysis of Test Data: Unaged/Aged Ratio	182
Table 6.29	Statistical Analysis of Test Results: Aged Cases (Unpressed)	183
Table 6.30	Statistical Analysis of Test Results: Aged Cases (Pressed)	183
Table 6.31	Statistical Analysis of Test Results: Unaged/Aged Ratio (Unpressed)	183
Table 6.32	Statistical Analysis of Test Results: Unaged/Aged Ratio (Pressed) ..	183
Table 6.33	Effects of Warm Water Immersion on the Flexural Performance of Cellulose Fiber Reinforced Cement Composites	188
Table 6.34	Results of the Analysis of Variance of Test Data (Unpressed)	189
Table 6.35	Results of the Analysis of Variance of Test Data (Pressed)	189
Table 6.36	Results of the Analysis of Variance of Test Data: Aged Cases	190
Table 6.37	Results of the Analysis of Variance of Test Data: Unaged/Aged Ratio	191
Table 6.38	Statistical Analysis of Test Results: Aged Cases (Unpressed)	192
Table 6.39	Statistical Analysis of Test Results: Aged Cases (Pressed)	192
Table 6.40	Statistical Analysis of Test Results: Unaged/Aged Ratio (Unpressed)	192
Table 6.41	Statistical Analysis of Test Results: Unaged/Aged Ratio (Pressed) ..	192
Table 6.42	Effects of Repeated Wetting-Drying-Carbonation Cycles on the Flexural Performance of Cellulose Fiber Reinforced Cement Composites	197
Table 6.43	Results of the Analysis of Variance of Test Data (Unpressed)	198
Table 6.44	Results of the Analysis of Variance of Test Data (Pressed)	198

Table 6.45	Results of the Analysis of Variance of Test Data: Aged Cases	199
Table 6.46	Results of the Analysis of Variance of Test Data: Unaged/Aged Ratio	200
Table 6.47	Statistical Analysis of Test Results: Aged Cases (Unpressed)	201
Table 6.48	Statistical Analysis of Test Results: Aged Cases (Pressed)	201
Table 6.49	Statistical Analysis of Test Results: Unaged/Aged Ratio (Unpressed)	201
Table 6.50	Statistical Analysis of Test Results: Unaged/Aged Ratio (Pressed) ..	201
Table 6.51	Effects of Moisture Condition on the Flexural Strength	207
Table 6.52	Effects of Moisture Condition on the Flexural Toughness	208
Table 6.53	Effects of Moisture Condition on the Initial Stiffness	209
Table 6.54	Results of Analysis of Variance Regarding Moisture Sensitivity	210
Table 6.55	Statistical Analysis of the Flexural Strength Test Results for Cellulose Fiber Reinforced Cement under Various Moisture Conditions (Unpressed)	211
Table 6.56	Statistical Analysis of the Flexural Toughness Test Results for Cellulose Fiber Reinforced Cement under Various Moisture Conditions (Unpressed)	211
Table 6.57	Statistical Analysis of the Initial Stiffness Test Results for Cellulose Fiber Reinforced Cement under Various Moisture Conditions (Unpressed)	212
Table 6.58	Statistical Analysis of the Flexural Strength Test Results for Cellulose Fiber Reinforced Cement under Various Moisture Conditions (Pressed)	212
Table 6.59	Statistical Analysis of the Flexural Toughness Test Results for Cellulose Fiber Reinforced Cement under Various Moisture Conditions (Pressed)	213
Table 6.60	Statistical Analysis of the Initial Stiffness Test Results for Cellulose Fiber Reinforced Cement under Various Moisture Conditions (Pressed)	213

Table 6.61	Dimensional Stability Test Results	214
Table 7.1	Thermogravimetric Compositional Analysis	229
Table 7.2	Comparison of Pore Volumes of Unaged and Aged Cement-Bonded Particleboards	234
Table 7.3	Thermogravimetric Test Results	253
Table 7.4	Comparison of Pore Size Distribution of Unaged and Aged Specimens of Cellulose Fiber Reinforced Cement Composite (Unpressed)	255
Table 7.5	Comparison of Pore Size Distribution of Unaged and Aged Specimens of Cellulose Fiber Reinforced Cement Composite (Pressed)	255

LIST OF FIGURES

Figure 1.1	Typical Application of Natural Fiber Reinforced Cement Composites	7
Figure 2.1	A Schematic Representation of the Substructure of a Tree	8
Figure 2.2	Organization of the Wood Cell Wall	11
Figure 2.3	Hardwood and Softwood Structure.....	12
Figure 2.4	Elements of a Knife-Ring Flake	13
Figure 2.5	Main Components and Plates of a Disk Refiner	13
Figure 2.6	Weight Loss of Wood and Wood components as a Function of Temperature	19
Figure 2.7	Hydrogen Bonds Between two Cellulose Chains	19
Figure 2.8	Attractive Forces Between Fibers due to Surface Tension of Evaporating Water	20
Figure 3.1	Hydration Rate of Cement and Wood-Cement Mixtures in the Early Stages and the Setting and Hardening Stages	25
Figure 3.2	Weight Gain Vs. Compacted Wood Specific Gravity and Water/Cement Ratio	30
Figure 3.3	Gas Consumption and Board Weight Gain by Board Type	30
Figure 3.4	Influence of Various Carbon Dioxide Pressure on Maximum Hydration Temperature and Setting Time of Cement in Wood/Cement Specimens	32
Figure 3.5	Influence of Water-Cement Ratio on Maximum Hydration Temperature and Setting Time of Cement in Wood/Cement Specimens	32

Figure 3.6	Influence of Binder Composition on Carbon Dioxide Content and Calcium Hydroxide Content of Specimens by the Carbon Dioxide Injection Process	32
Figure 3.7	Initial Modulus of Elasticity (MOE)	33
Figure 3.8	Modulus of Elasticity	34
Figure 3.9	Modulus of Rupture	34
Figure 3.10	X-Ray Patterns of Cement and Various Wood-Cement Specimens Fabricated by Conventional Method and Carbon Dioxide Process after 5 Hours or 28 Days	35
Figure 3.11	Effect of Heat Treatment at 40 and 60°C and Subsequent CO ₂ Curing, in CO ₂ on WF Values of Cast Specimens	36
Figure 3.12	Effect of Heat Treatment and Subsequent CO ₂ Curing for 1 and 2 Days on the WF Values of Compacted Specimens	36
Figure 3.13	Effect of Drying Time and Length of CO ₂ Treatment on the WF after Exposure to Different Conditions	37
Figure 3.14	Effect of Carbonation on Mechanical Properties of Asbestos-Cement Sheet	38
Figure 3.15	Effect of Carbonation on Mechanical Properties of Cellulose-Fiber Reinforced Cement Sheet	39
Figure 3.16	The Composite Stress-Strain Curves for Fiber-Reinforced Brittle Matrices	44
Figure 3.17	Flexural Strength and Toughness Versus Fiber Weight Fraction for Cement and Mortars reinforced with Wood Fiber (Kraft Pulp)	44
Figure 3.18	Compressive Strength of red Maple Wood-Cement Composites after 28 Days of Curing as A Function of Wood-Cement Ratio	45
Figure 3.19	Effect of the Fiber Aspect Ratio on the Tensile Strength of Fiber Reinforced Composites	46
Figure 3.20	Effect of Cellulose Pulp Fiber Content and Void Content of Air Cured Composites	48

Figure 3.21	Schematic Representation of Crack Traveling Through a Fiber Reinforced Matrix	49
Figure 3.22	Load-Deflection Curves for a Range of Cellulose Fiber Reinforced Cement Composites Tested in Flexure	51
Figure 3.23	Tensile Load-Deflection Curves for Different Failure Modes of Sisal Slives Embedded in Cement	53
Figure 4.1	Experimental Set-Up to Determine the Heat of Hydration of Wood-Cement -Water Systems	60
Figure 4.2	The Heat of Hydration Test Results	61
Figure 4.3	Wood Particles	63
Figure 4.4	Processing System Incorporating CO ₂ Curing	65
Figure 4.5	The Sequence of Experiments on Cement-Bonded Wood Particleboard	66
Figure 4.6	The Two Alternative Processing Sequences	67
Figure 4.7	The Three Point Flexural Test Set-Up	69
Figure 4.8	Typical Flexural Load-Deflection Curves Obtained with the Two Process Sequence.....	70
Figure 4.9	Effects of the Processing Sequence on Flexural Performance	71
Figure 4.10	Board Temperature under Method I and II of CO ₂ Curing	72
Figure 4.11	Effects of CO ₂ Concentration of Flexural Load-Deflection Curves ..	73
Figure 4.12	Effects of Various CO ₂ Concentrations on the Flexural Performance of Cement-Bonded Wood Particleboard	75
Figure 4.13	Methodology of Analysis	77
Figure 4.14	The Trends in Flexural Strength	79
Figure 4.15	The Trends in Flexural Toughness	79
Figure 4.16	The Trends in Initial Stiffness	80

Figure 4.17	Cube Plot of Flexural Test Results	81
Figure 4.18	Gradation of Silica Sand	83
Figure 4.19	Schematic of Formation of Two-Ply Cellulose Fiber Reinforced Cement Composite Sheet	84
Figure 4.20	Time-Pressure Cycles in Autoclave	85
Figure 4.21	Carbonation Curing Facilities for Cellulose Fiber Reinforced Cement Composites	86
Figure 4.22	Photograph of the Flexural Test Set-Up for Cellulose Fiber-Cement Composite	88
Figure 4.23a	Flexural Test Results (Pressed)	95
Figure 4.23b	Flexural Test Results (Unpressed)	96
Figure 4.24	The Trends in Flexural Strength	97
Figure 4.25	The Trends in Flexural Toughness	98
Figure 4.26	The Trends in Initial Stiffness	99
Figure 4.27	Flexural Performance at the Different Oven Temperature	102
Figure 5.1	Typical Load-Deflection Curves with CO ₂ Curing for Unpressed Cellulose Fiber Reinforced Cement Composites	105
Figure 5.2	Response Surface of Flexural Performance for Unpressed Cellulose Fiber Reinforced Cement Composites	108
Figure 5.3	Optimum Manufacturing Conditions of Unpressed Cellulose Fiber Reinforced Cement Composites	109
Figure 5.4	Flexural Performance of Optimized CO ₂ Cured Unpressed Cellulose Fiber Reinforced Cement Composite Versus Those of Controls	111
Figure 5.5	Flexural Performance of Pressed Cellulose Fiber Reinforced Cement Composites	114
Figure 5.6	Water Absorption of Cellulose Fiber Reinforced Cement Composites	116

Figure 5.7	Dimensional Stability Test Results	117
Figure 5.8	Schematic Diagram of Cement-Bonded Particleboard Manufacturing by Conventional Method	119
Figure 5.9	Typical 28 Days Flexural Load-Deflection Behavior of Cement-Bonded Particleboard	121
Figure 5.10	28 Days Flexural Performance of Cement-Bonded Particleboard	122
Figure 5.11	The Trends in Flexural Performance: CO ₂ Versus Conventionally Cured Boards	124
Figure 5.12	The Trends in Flexural Performance: CO ₂ Cured Boards	125
Figure 5.13	Time-Property Relationship of CO ₂ and Conventionally Cured Cement-Bonded Particleboard	126
Figure 5.14	Internal Bond Test Set-Up for Cement-Bonded Particleboard	127
Figure 5.15	Internal Bond Test Results	128
Figure 5.16	The Trends in Internal Bond Strength: CO ₂ Versus Conventionally Cured Boards	130
Figure 5.17	The Trends in Internal Bond Strength: CO ₂ Cured Boards	130
Figure 5.18	Dimensional Stability	132
Figure 5.19	Moisture Content	133
Figure 5.20	Swelling in Water of Cement-Bonded Particleboard	133
Figure 6.1	Test Set-Up for wetting-Drying	137
Figure 6.2	Effects of Repeated Wetting-Drying on the Flexural Load-Deflection Behavior of Cement-Bonded Particleboard	143
Figure 6.3	Effects of Repeated Wetting-Drying Cycles on Flexural Behavior ...	144
Figure 6.4	The Trends in Flexural Performance: CO ₂ Cured Boards	150
Figure 6.5	The Trends in Flexural Performance: CO ₂ Versus Conventionally Cured Boards	151

Figure 6.6	Effects of Repeated Freezing-Thawing Cycles on the Flexural Load-Deflection Behavior of Cement-Bonded Particleboard	154
Figure 6.7	Effects of Repeated Freezing-Thawing Cycles on Flexural Behavior	155
Figure 6.8	The Trends in Flexural Performance: CO₂ Cured Boards	161
Figure 6.9	The Trends in Flexural Performance: CO₂ Versus Conventionally Cured Boards	162
Figure 6.10	Typical Flexural Load-Deflection Behavior after Repeated Wetting-Drying Cycles of Cellulose Fiber Reinforced Cement Composites	167
Figure 6.11	Flexural Performance of after Wetting-Drying of Unpressed Cellulose Fiber Reinforced Cement Composites	168
Figure 6.12	Flexural Performance After Wetting-Drying of Pressed Cellulose Fiber Reinforced Cement Composites	169
Figure 6.13	Typical Flexural Load-Deflection Behavior after Repeated Freezing-Thawing Cycles of Cellulose Fiber Reinforced Cement Composites	176
Figure 6.14	Effects of Repeated Freezing-Thawing on the Flexural Performance of Unpressed Cellulose Fiber Reinforced Cement Composites	177
Figure 6.15	Effects of Repeated Freezing-Thawing on the Flexural Performance of Pressed Cellulose Fiber Reinforced Cement Composites	178
Figure 6.16	Typical Flexural Load-Deflection Behavior Before and After Warm Water Immersion of Cellulose Fiber Reinforced Cement Composites	185
Figure 6.17	Flexural Performance Before and After Warm Water Immersion of Unpressed Cellulose Fiber Reinforced Cement Composites	186
Figure 6.18	Flexural Performance Before and After Warm Water Immersion of Pressed Cellulose Fiber Reinforced Cement Composites	187
Figure 6.19	Typical Flexural Load-Deflection Behavior after Wetting-Drying-Carbonation Cycles of Cellulose Fiber Reinforced Cement Composites	194

Figure 6.20	Flexural Performance Before and After Wetting-Drying-Carbonation of Unpressed Cellulose Fiber Reinforced Cement Composites	195
Figure 6.21	Flexural Performance Before and After Wetting-Drying-Carbonation of Pressed Cellulose Fiber Reinforced Cement Composites	196
Figure 6.22	Typical Flexural Load-Deflection Behavior in Various Moisture Conditions (Unpressed)	203
Figure 6.23	Typical Flexural Load-Deflection Behavior in Various Moisture Conditions (Pressed)	204
Figure 6.24	Flexural Performance in Various Moisture Conditions (Unpressed) .	205
Figure 6.25	Flexural Performance in Various Moisture Conditions (Pressed)	206
Figure 6.26	Dimensional Stability	215
Figure 7.1	X-Ray Patterns for Unaged Specimens of Cement-Bonded Particleboard after 28 Days of Curing	225
Figure 7.2	X-Ray Patterns After Repeated Wetting-Drying Cycles for Cement-Bonded Particleboard	226
Figure 7.3	X-Ray Patterns After Repeated Freezing-Thawing Cycles for Cement-Bonded Particleboard	227
Figure 7.4	Thermogravimetric Analysis of Southern Pine and Aspen	229
Figure 7.5	Thermogravimetric Analysis of Cement-Bonded Particleboard after 28 Days of Curing	230
Figure 7.6	Thermogravimetric Analysis of Cement-Bonded Particleboard after Repeated Wetting-Drying Cycles	231
Figure 7.7	Thermogravimetric Analysis of Cement-Bonded Particleboard after Repeated Freezing-Thawing Cycles	232
Figure 7.8	Pore Size Distribution of Southern Pine and Aspen Species	234
Figure 7.9	Pore Size Distribution of Unaged Cement-Bonded Particleboard after 28 Days of Curing	235
Figure 7.10	Pore Size Distribution of Unaged Cement-Bonded Particleboard after Wetting-Drying Cycles	236

Figure 7.11	Pore Size Distribution of Cement-Bonded Particleboard after Freezing-Thawing Cycles.....	237
Figure 7.12	Cross-Section of Southern Pine and Aspen	239
Figure 7.13	Surface of Particles	241
Figure 7.14	Unaged Cement-Bonded Particleboard	242
Figure 7.15	After Repeated Wetting-Drying on Cement-Bonded Particleboard ..	243
Figure 7.16	After Repeated Freezing-Thawing on Cement-Bonded Particleboard	245
Figure 7.17	X-Ray Patterns for Unaged Specimens of Cellulose Fiber Reinforced Cement	248
Figure 7.18	X-Ray Pattern After Repeated Wetting-Drying Cycles for Cellulose Fiber Reinforced Cement	249
Figure 7.19	X-Ray Pattern After Repeated Freezing-Thawing Cycles for Cellulose Fiber Reinforced Cement	250
Figure 7.20	X-Ray Pattern After Warm Water Immersion for Cellulose Fiber Reinforced Cement	251
Figure 7.21	X-Ray Pattern After Repeated Wetting-Drying-Carbonation Cycles for Cellulose Fiber Reinforced Cement	252
Figure 7.22	Typical Weight Loss Curve for Cellulose (Kraft) Fiber	254
Figure 7.23	Typical Weight Loss Curves for Cellulose Fiber Reinforced Cement	254
Figure 7.24	Pore Size Distribution of Equilibrium Condition on Cellulose Fiber Reinforced Cement Composite	256
Figure 7.25	Pore Size Distribution after Repeated Wetting-Drying on Cellulose Fiber Reinforced Cement Composite	257
Figure 7.26	Pore Size Distribution after Repeated Freezing-Thawing on Cellulose Fiber Reinforced Cement Composite	258
Figure 7.27	Pore Size Distribution Immersed Warm Water on Cellulose Fiber Reinforced Cement Composite	259

Figure 7.28	Pore Size Distribution after Repeated Wetting-Drying-Carbonation on Cellulose Fiber Reinforced Cement Composite	260
Figure 7.29	Petrified Fibers in CO₂ Cured Cellulose Fiber Reinforced Cement Composites	262
Figure 7.30	Kraft Fiber in CO₂ Cured Cellulose Fiber Reinforced Cement Composites	262
Figure 7.31	Unaged Cellulose Fiber Reinforced Cement Composites	263
Figure 7.32	After Wetting-Drying Cycles of CO₂ Cured Cellulose Fiber Reinforced Cement	265
Figure 7.33	After Freezing-Thawing Cycles of CO₂ Cured Cellulose Fiber Reinforced Cement	266
Figure 7.34	After Warm Water Immersion of CO₂ Cured Cellulose Fiber Reinforced Cement	267
Figure 7.35	After Wetting-Drying-Carbonation Cycles of CO₂ Cured Cellulose Fiber Reinforced Cement	268
Figure 7.36	Saturated Conditions of CO₂ Cured Cellulose Fiber Reinforced Cement	269
Figure 7.37	Oven-Dried Condition of CO₂ Cured Cellulose Fiber Reinforced Cement	270
Figure A.1	Typical Construction Pattern of Cellulose Fiber Reinforced Cement Composites	284
Figure A.2	Response of Concrete Subjected to Uniaxial Cyclic Loading	290
Figure A.3	Flow Chart for Restrained Shrinkage Modeling	292

CHAPTER 1

INTRODUCTION

1.1 BACKGROUND

Cement and concrete products are notable for their weakness in tension unless they are reinforced by some means, and for their lack of toughness which gives rise to early cracking under impact loads or thermal shock. The use of reinforcing fibers to overcome such deficiencies is well known, and polypropylene, steel and glass fiber reinforced cement are now established construction materials.

Natural fiber reinforced cement composites are reconstituted wood products with desirable longevity, fire resistance and life-cycle cost position. The low productivity of cement-based wood composite plants resulting from the slow setting and hardening of cement has led to relatively high initial cost. Early exposure of cement binders to carbon dioxide (CO₂) can substantially reduce the setting and hardening times.

The commercially successful combination of wood and cement to produce a board dates back to early nineteen thirties with the development of light-weight wood wool slab (excelsior board) using initially magnesite as a binder, but later adopting Portland cement. Nearly two decades ago the smooth-surfaced high-density cement-bonded particleboard was first commercially produced in Switzerland [1]. Changes in the late 1970s and early 1980s in building board manufacturing technology was caused by asbestos health problems, together with changes in construction techniques and environmental problems, which resulted in rapid growth of the cement-bonded wood particleboard industry in Europe, Japan and Asia [2]. This rapid market penetration has been facilitated by the desirable balance of the following key qualities provided by cement-bonded particleboard [2, 3, 4]: resistance to fire, weather, insects and vermin, acoustic performance, workability, dimensional stability, and environmental safety. The high endurance of cement-bonded particleboard under various severe exposures places the product favorably in terms of life-cycle cost position.

The cellulose fibers derived from softwood or hardwoods present highly cost effective means of reinforcement for thin cement products. While in cement-bonded particleboard wood constitutes most of the end product volume, here cellulose fibers typically comprise less than 20% of the volume. Industrial developments in this area have focused on the use of the chemical (kraft) softwood fibers, while other fiber types (e.g. kraft hardwood or thermomechanical pulp) have also performed satisfactorily in cement composites. Wood fibers possess adequate stiffness, strength and bonding capacity to cement-based matrices for substantial enhancement of their flexural strength, toughness and impact resistance. These improvements are achieved through the stopping and deflection of cracks propagating in brittle cement matrices by wood fibers. Desirable technical qualities and low cost of wood fibers have made them the reinforcing materials of choice to substitute asbestos fibers in the broadly utilized thin cement products. The slurry-dewatering (Hatschek) method of asbestos cement productions (which is typically followed by compaction under pressure and high-pressure steam curing) also suits the production of cellulose fiber reinforced cement composites; this has been a key factor facilitating the replacement of asbestos with wood fibers in the industrial arena. Cellulose fiber reinforced cement composites are sensitive to moisture effects; saturated composites possess substantially increased toughness characteristics while flexural strength tends to be reduced upon wetting. Cellulose fiber reinforced cement composites present desirable dimensional stability, fire resistance and durability characteristics. Upon aging these composites actually gain strength and stiffness, but they tend to lose ductility with time. Partial substitution of cement with pozzolans can help maintain ductility of cellulose fiber reinforced cement products over time and also reduce moisture sensitivity. Cellulose fiber reinforced thin cement products are used in both exterior and interior applications in residential and commercial buildings.

The processing and properties of natural fiber reinforced cement composites, in the form of cement-bonded particleboard or cellulose fiber reinforced cement board, are sensitive, among other factors, to the specific wood species and wood fiber type. The setting and hardening of natural fiber reinforced cement composite is a slow process. The conventional cement-bonded wood boards require pressing and clamping for several hours

until they have hardened; the result is reduced productivity and increased initial cost. Wet processed cellulose fiber reinforced cement also needed to be autoclaved for several hours before it gains sufficient strength. Efforts towards substantially increasing the setting and hardening rate of cement should still provide sufficient “open time” during which the wood-cement-water furnish stays plastic to be mixed, formed and pressed.

Tremendous reductions in the setting time of cement-based binders, from few hours to few minutes, can be achieved through the addition of carbon dioxide (CO_2) [6,7]. The predominant chemical reaction occurring with carbonation involves $\text{Ca}(\text{OH})_2$ resulting from the hydration of cement, which reacts with CO_2 to produce CaCO_3 (limestone). CaCO_3 provides the initial strength necessary for early release of the board from press in dry processed cement-bonded particleboard. In wet processing of cellulose fiber cement also, the rapid carbonation reaction may help reduce the accelerated curing time.

1.2 FIBER REINFORCED CEMENT-BASED COMPOSITES

Although the first patent for fiber reinforced cement [8] dates from before the general use of reinforced concrete, and indeed the use of fibers to toughen bricks and pottery can be traced to the very beginning of civilization, it is only in the last decade that the principles governing the fiber reinforcement of brittle matrices have begun to be understood. As a matrix, Portland cement has some extremely attractive properties, e.g. it is about six times stiffer and one hundred times cheaper than typical resins; it has however, one over-riding disadvantage - a very low failure strain.

Fiber reinforced cements differ, both in their production processes and in their behavior, from other composites where the matrix is ductile. The ductile matrix is normally an organic, polymeric material which has an elongation at rupture of the same order of magnitude as that of the most common fibers.

The properties of fiber composites are controlled by a number of factors, of which the most important are;

1. The magnitudes of both the fiber and the matrix modulus (E_f and E_m)
2. The ratio of modulus of elasticity of the fiber to that of the matrix (E_f/E_m)
3. Type and properties of the matrix (ductile or brittle)

4. Fiber content, fiber length and orientation
5. Interfacial bond strength between the fibers and matrix

Fibers with a high modulus of elasticity yield a considerable increase in tensile strength over that of the hardened cement paste, whereas fibers with a low modulus of elasticity inhibit crack propagation in cement-based materials, thus improving the impact resistance of the composites.

1.3 APPLICATIONS OF NATURAL FIBER REINFORCED CEMENT COMPOSITES IN CONSTRUCTION

The possibilities offered by natural fiber concrete products are endless. These products are suitable for almost any light, non-load bearing or load bearing structures. They are also suitable for condition where properties of other materials are exceeded, such as resistance to fire, acoustics, humidity, durability, and lightness.

1.3.1 Cement-Bonded Particleboard

There are numerous applications for cement-bonded particleboard where other board types such as wood chipboard and gypsum cardboard do not resist humidity and climate, when the resistance could only be obtained by expensive overlaying, or when insufficient static values limit their use. Typical applications for internal use are sound insulating and fire resisting partitions, lining for timber frame housing, fire resistant floors, walls, and ceiling linings, fire doors, fire and moisture resistant furniture and built-in furniture, steel support beam and column castings, shaft and duct linings, paneling for electrical and gas applications, wet room linings, livestock building linings, glue laminated structural members, air ventilation ducts, refuse shafts, "Heat sink" roofing for low energy buildings, lining for industrial buildings and warehouses, fire resistant partitioning, sound resistant partitioning, and substrates. Outdoor applications are flat roofing, walling for prefabricated housing, permanent formwork, balcony parapets and floors, cladding for industrial buildings and warehouses, tunnel linings, sound barrier walls, fire barriers, pavilions and stadia, separating walls, sidings and soffits, and sound insulation walls along roads and highways.

1.3.2 Cellulose Fiber Reinforced Cement Composites

Due to the dimensional stability, structural capability, impact strength, thermal, and acoustic insulation, and fire resistant characteristics, these products are used for heat shields and spray booths, sound barriers and modular flooring, duct lining and air shafts, gaskets and seals, laboratory tops and splashbacks, and fire walls in dry kilns. These are some of the typical industrial components made of cellulose fiber reinforced cement composites. Commercial and residential use of cellulose fiber reinforced cement composite is mainly for the production of flat and corrugated sheet roofing elements, exterior and interior wall paneling, equipment screens, fascias, facades and soffits, substrate for tiles, window sills and stools, stair treads and risers, substrate for applied coatings, and utility building cladding panels. Agricultural uses of cellulose fiber reinforced cement composites are mainly for farm building, sidings, stalls, walls, poultry houses, incubators, green house panels, work surfaces, fencing, and sunscreens [8, 9, 10, 11].

Typical applications of natural fiber reinforced cement composites are shown in Figure 1.1.

1.4 RESEARCH OBJECTIVES

The ultimate goal of this research is to develop rapid, cost-effective and energy-efficiency processing techniques which yield wood-cement composite panels with improved engineering properties. The project relies of CO₂ curing of cement-based materials to accomplish these objectives.

The introduction of carbon dioxide into fresh cement paste accelerates the hydration process and, through changing the stoichiometry of reaction products, improves the longevity and dimensional stability of cementitious binders.

The objectives of this research are as follows.

1. Optimize the CO₂ curing conditions to increase the rate of strength gain in wet and dry processing of wood-cement composite panels and broaden the wood species basis for the panels.
2. Optimize the use of low-concentration CO₂ in the processing of wood-cement composites.

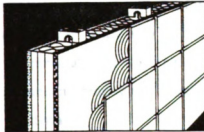
3. Enhance the engineering properties of wood-cement composites with CO₂ curing.
4. Investigate the effect of CO₂ curing on the microstructure of wood-cement composites, and develop structure-property relationship.

A secondary objective of the research is to model the restrained shrinkage cracking characteristics of wood-cement composites.

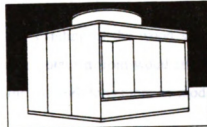
The research is presented in Chapters 2 through 8. Chapter 2 deals with wood fibers and particles. A literature review in the area of wood-cement composites is presented in Chapter 3. The basics of the manufacturing process and preliminary evaluation of CO₂ curing are introduced in Chapter 4. Chapter 5 and 6 describe comprehensive investigation of the CO₂ curing process, and describe the impacts of CO₂ curing on the processing and engineering properties of wood-cement composites. Microstructural investigations relevant to the CO₂ curing process are describe in Chapter 7. Finally, The project findings and conclusions are presented in Chapter 8.



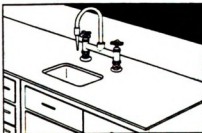
(a) Residential and Commercial Construction



SUBSTRATE FOR TILE



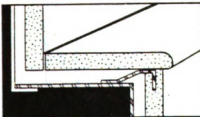
SPRAY BOOTH COMPONENTS



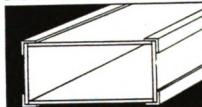
LABORATORY TOPS AND SPLASHES



EXTERIOR FENCING



STAIR TREADS & RISERS



DUCT WORK

(b) Industrial and Commercial Components

Figure 1.1 Typical Application of Natural Fiber Reinforced Cement Composites [10, 11]

CHAPTER 2

WOOD FIBERS AND PARTICLES

2.1 INTRODUCTION

The use of natural fibers as discrete reinforcement has been known since mankind started making straw reinforced sunbaked clay or mud bricks. Wood fibers exist in reasonably large quantities all over the world. They might be only minimally processed (natural fibers and wood particles) or could be subjected to various combinations of thermal, chemical and mechanical processing (cellulose fibers).

Wood possesses the strength, toughness and stiffness characteristics needed to withstand the forces of nature in forest and more importantly, the strains and stresses imposed on timber when used in construction. Understanding of the wood structure can help us appreciate that wood particles (fibers) can be obtained from wood and employed as an abundant, renewable, cheap and effective discrete reinforcement in modern composite materials.

Figure 2.1 briefly illustrates the structure of wood. A piece of clear timber may attain a tensile strength of approximately 69 MPa (10 ksi). But lumber pieces often contain defects. Individual fibers which constitute the reinforcing unit of timber may have tensile strengths as high as 690 MPa (100 ksi) or more. Cellulose, the primary chemical constituents of natural fibers, exhibits a tensile strength of approximately 6400 MPa (930 ksi). Even within the same tree species, fiber strengths can vary considerably.

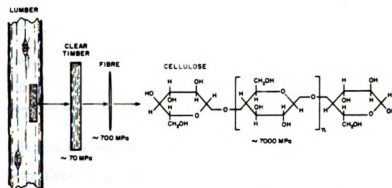


Figure 2.1 A Schematic Representation of the Substructure of a Tree [8]

2.2. PROCESSING OF WOOD FIBERS/PARTICLES AND CEMENTITIOUS COMPOSITES

2.2.1 Wood Particles

Wood is divided into two broad classes, usually referred to as “hardwood” and “softwood”. The terms are not very definitive, since some softwoods are harder than certain hardwoods. The term ‘softwood’ refers to conifers, which have needle-like or scale-like leaves; they are nearly all evergreens. The term ‘hardwood’ refers to the broad-leaved trees, which are nearly all deciduous. The particles of softwoods and hardwoods are fundamentally different in their anatomy and morphology. Table 2.1 shows the distribution of hardwoods and softwoods in different areas of the world. In total, hardwoods are estimated to exist in volumes almost double those of softwoods.

Table 2.1 Areas of Forestland in the World, by Geographic Location and Species Group - 1980 [78]

Area	Total	Softwoods (thousand ha)	Hardwoods
North America	807,092	533,075	274,017
Latin America	915,019	20,474	894,545
Europe	158,902	97,989	60,913
Africa	743,713	13,891	729,822
Asia	468,230	102,238	365,992
USSR	928,600	679,900	248,700
Pacific area	298,947	15,995	282,952
World	4,320,503	1,463,562	2,856,941

The elemental constituents of wood are primarily of cellulose, hemicellulose, lignin, and extractives. Softwoods and hardwoods are slightly different in chemical composition and react differently with certain chemicals. Table 2.2 shows approximate per-

cent of dry weight of cellulose, hemicellulose and lignin in hardwood and softwood. Cellulose is a crystalline linear polymer of glucose. The glucose units are interconnected through linkages involving a β -special arrangement of chemical bonds that tend to lie parallel to one another in a regular array. Hemicellulose is the branched chain polymer of wood, other than cellulose. Lignin is an amorphous polymer, consisting of aromatic units (benzene rings), that serves to cement the fibers of wood together.

Wood pH can vary from 3.2 to 8.2 and can also affect wood-cement compatibility. The broad variation in wood constituents and pH among species is largely responsible for the differences in wood-cement compatibility.

Wood cells are formed in the cambia layer, a very narrow layer which separates wood and bark. The first layer of the cell wall is reinforced with a more or less random network of microfibrils, which are complex chains of cellulose molecules, and is called the primary wall. Inside this is the secondary wall, which may be divided into three separate layers: the outer layer, referred to as S-1; the middle layer, S-2; and the inner layer, S-3. The S-2 layer is usually much thicker than the others. The microfibrils in the secondary wall occur in ordered patterns (Figure 2.2). It should be noted that in the S-2 layer the microfibrils are aligned at a much smaller angle to the longitudinal axis of the fiber. The membrane at the outside of these layers which separates the cells from each other is called the middle lamella. When the formation of the cell wall is complete, impregnation with lignin begins in the middle lamella and gradually extends through the cell wall.

Table 2.2 Organic Constituents of Wood [79]

Type	Cellulose	Hemicellulose (% dry weight)	Lignin
Hardwood	40 - 44	15 - 35	18 - 25
Softwood	40 - 44	20 - 32	25 - 35

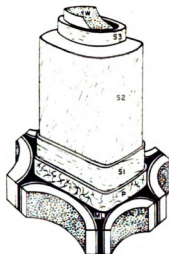


Figure 2.2 Organization of the Wood Cell Wall. P=primary wall; ML=middle lamella or intercellular layer; S1, S2, and S3 refer to the outer, middle, and inner layers of the secondary wall, respectively; W=warty layer [80]

In hardwoods, a newly formed cell on the inner side of the cambium may become one of four types of wood tissue: parenchyma cell, fiber, tracheid, or vessel. Each type of tissue serves one or more special functions: the parenchyma cells conduct and store food and water; the fiber's main role is to provide mechanical support. Tracheas and vessels conduct water and dissolved mineral salts from the roots to the leaves; they also provide mechanical support. Vessels (or pores) occur only in hardwoods and are their main distinguishing feature (see Figure 2.3a).

In softwoods, the structure is much less complex than hardwoods and their cells are of simpler form (Figure 2.3b). Parenchyma cells are rectangular with thin walls. Tracheas are elongated cells with rounded ends and walls, whereas fibers are long pointed cells. Tracheas, which are not common in hardwoods, will be referred to simply as 'fibers'. The rate of increase in size of a tree varies with the seasons and climate conditions. During late fall and winter, there is little or no growth, but growth is at a maximum in spring. The spring or early wood usually has wood cells with larger diameter and thinner wall than those cells formed during periods of slow growth - summer wood or late wood (see Figure 2.3b) [38].

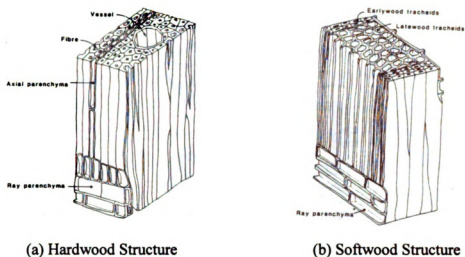


Figure 2.3 Hardwood and Softwood Structure [38]

Some type of cutting or milling is needed for preparing of the wood particles. Chips cut down into flakes or smaller and fine particles. Roundwood bolts are usually debarked and then cut into shorter lengths before being reduced to flakes, wafers, or strands. Lumber trim and other types of solid wood materials are often chipped prior to the final breakdown into particles. Even planer shavings may have to be milled further to obtain the size of particle desired and to reduce size variation.

A variety of machines including refiners, hammermills, flakes, and waferizers can be used to produce the type of furnish desired. These machines grind, cut or tear the wood into a range of particle sizes. Figure 2.4 illustrates the operation of a ring flake. This machine has knives that cut thin particles from whatever kind of wood is fed to it. A disk refiner of the general type shown in Figure 2.5 is sometimes used to prepare small fiberlike particles. The rotating disk plates are grooved. As wood particles move from the center to the outer edges of the disk, they are ground to fiber bundles. The closer the disk are set together, the finer would be the particles produced.

Once particles are dried, they are often screened to remove fine, dustlike materials (fines). Fines contribute little to the properties of a board but weight. Screening of particles may also be used to separate finer components from the coarser ones.

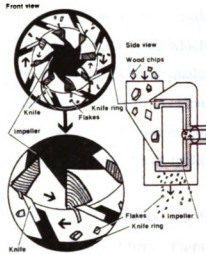


Figure 2.4 Elements of a Knife-Ring Flaker [81]

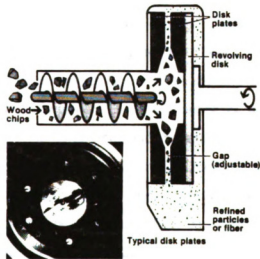


Figure 2.5 Main Components and Plates of a Disk Refiner [81]

2.2.2. Cellulose Fibers

Wood or plants are composites built up of a variety of organic matter and materials. Cellulose constitutes chemically the bulk of many naturally occurring fibrous substances, including wood, leaf, seed, and grass fibers. The discrete cellulose fibers are embedded in, bonded and held together in different ways by a continuous organic matrix, the lignin.

The wood fibers may be used either as milled, single fibers, or in the form of pulp or paper. The dimension of the individual fibers vary considerably from type to type and depend on the origin of the fiber source, on the method which is used to remove the fiber, and on the pulping process. Thus, different paper pulp qualities are available worldwide. The price of the paper pulp cellulose is also very low compared with most man-made fiber materials, but the low modulus of elasticity and the durability of the natural celluloses are two main factors which cast doubt on their direct application as a reinforcement of cement matrices.

The method of removal of the fibers from wood and the grade of the refining has a profound effect on the properties of cellulose fibers. Pulping is the process by which wood is reduced to a fibrous mass. The commercial pulping processes are generally classified as mechanical, thermomechanical, semi-chemical, and chemical. Most pulp is made from wood fibers, but a large number of other fibers do find their way into pulp production, including both vegetable and man-made fibers.

Mechanical pulping is frequently called the groundwood process, because in its original form it entails literally grinding the fibers out of the wood. Refiner groundwood is generally preferred over stone groundwood, because it contains more long fibers and yields a strong end-product. Sometimes the wood is thermally or chemically pre-softened to reduce the power needed for grinding. In mechanical separation of fibers, the proportion of wood raw material that become usable fiber is commonly on the order of 95 to 99 percent, producing an inferior product because of the high lignin content.

The thermo-mechanical process, conducted at temperatures greater than the glass transition temperature of the lignin binder, gives a high yield of lignin coated, uncollapsed fiber. The fibers may be further refined to produce paper pulps with partially collapsed lignin-coated fibers. Thermomechanical pulp is commonly referred to as TMP.

Chemical pulping is a process in which the lignin in wood can be degraded and dissolved by various chemical reagents, leaving most of the cellulose and hemicellulose in the form of fibers. The two main methods of chemical pulping are the kraft or sulphate process and the sulphite process. Because lignin has an adverse effect on cellulose strength and color, this rather stiff macromolecular material is removed to a greater or

lesser extent in all chemical pulping processes. The kraft process involves cooking the wood chips in a solution of sodium hydroxide, sodium carbonate and sodium sulphite. Several different grades of kraft pulp are made for different end-products. Unbleached grades contain more lignin and have a higher yield from wood than pulps destined to be bleached into grades that can be made into white paper. Kraft pulps yield strong fibers. In the alternative sulphite process, an acidic mixture of sulphur dioxide, water and a chemical base material is the means of attacking and dissolving the lignin. Here the mechanisms of chemical attack removes the lignin as salts of lignosulphonic acid, and the aromatic ring structure is left largely intact. The chemical base can be ionic calcium, magnesium, sodium or ammonium. Sulphite pulps are fairly light in color and can be bleached easily. The sulphite pulps are weaker than the equivalent sheets of kraft pulp.

The semichemical pulp combines the high-yield advantages of mechanical processing and some of the high quality features of chemical processing. The most important high-yield semi-chemical pulping processes are the cold caustic process and the neutral-sulphite process. All cold caustic pulps are inferior to kraft pulps in physical properties, but are stronger than softwood groundwood pulps. In the neutral-sulphite process, the most successful of the semi-chemical pulping operations, hardwood chips are impregnated under pressure with the cooking liquor. The cooked pulp is defibreized mechanically with refiners.

2.3 SPECIAL PROBLEMS OF WOOD PARTICLES AND FIBERS IN CEMENTITIOUS MATERIALS

The industries which use wood particles and fibers in cement-based composites are growing in importance. There are different considerations to be taken into account before selection of the 'right fiber' for production of natural fiber cement based composites. These include the many different particle or fiber types to chose from, wood types, mechanical or chemical treatments, pulping processes and possible after-treatments of the pulp.

2.3.1 Setting and Curing of Wood-Cement Composites

It's well known that wood inhibits the curing (setting) of cement, and hardwoods are generally more inhibitory to cement setting than softwoods. Weatherwax and Tarkow found that the hemicellulose in hardwood had a pronounced inhibitory effect on the setting of cement [18]. Sandermann [72] found starches, sugars, tannins, and certain phenols to be inhibitory: Lignicellulosic and hydroxylated carboxylic are used commercially as retarder of cement setting, and various sugars have an inhibitory effect on cement. The kraft process produces a low yield of partially collapsed, delignified fibers. These fibers will have little effect on the setting and curing of the cement. Unbleached fibers in every case contain various amounts of lignin, and can therefore inhibit the setting and curing of cement. In some cases, it may be necessary to pretreat the pulp, because it may contain leachable matter which may retard the setting and hardening of the cement.

Techniques for overcoming the wood-cement incompatibility and the set inhibitory effects of wood on the setting of cement are based on the removal of water- and sodium hydroxide-soluble wood chemical constituents, or on the chemical modification of the mixture by using admixtures such as calcium chloride, calcium hydroxide, sodium hydroxide, sodium silicate, fly ash, etc [56, 57, 65, 73]. Partial or complete removal of extractable from wood prior to fabrication may help improve the properties of wood-cement composites and maintain long-term serviceability.

2.3.2. Treatment of Fibers / Particles

It has been pointed out earlier that the method of removal of the cellulose fiber from wood has important effects on both the mechanical and chemical properties of the fibers. Mechanical treatment of wood, for example with disc refining, mainly influences the physical dimensions and form of the fibers, and has only little influence on the chemical composition of the fiber. After this treatment the fibers will be partially collapsed but unalignified.

On the other hand, chemical treatments may influence both the fiber (particle) form and its chemical composition, as the chemical treatment mostly reduces the lignin and also the hemicellulose content of the fibers (particles).

The uncollapsed, lignified cellulose fibers might be expected to give fiber reinforced cement-based composites a lower density, strength, and elastic modulus than composites containing delignified fibers, but having greater water resistance and toughness, as cellulose fibers are hollow.

2.3.3 Mechanical Properties

The tensile strength of fibers or particles appears to have considerable influence on strength development in wood-cement composite. The elastic modulus and tensile strength of the wood particles and pulp fibers show considerable variations as they depend on fiber/particle angle and the extent and type of defects. If a cellulose fiber is collapsed on drying, as do most delignified pulp fibers, the area of cell wall will closely approximate the overall fiber area.

Values for the strength and elastic modulus of unclaspfed linefeed wood fibers are not available. Such fibers are relatively thin-walled and do not collapse on drying; therefore these fibers are considered from the point of view of fiber reinforcement of composites. Their relative strength may be lower than those of delignified fibers. Bleaching the fibers increases both the elastic modulus and flexural strength but reduces the specific work of fracture. Kraft fibers are always stronger than acid sulphite and sulphite-bisulphite fibers.

2.3.4. Seasoning Effects on Fiber / Particle Properties

The springwood fibers (particles) have a thin-walled structure compared with thick-walled summerwood fibers (particles). The superior strength of summerwood fibers (particles) of various species has been reported by McIntosh [20]. Also, the different constituents of wood vary with the season.

2.3.5. Attack by Micro-Organisms

The action of common fungi increases the permeability of wood, and also lowers the degree of polymerization of wood constituents, thereby increasing the amounts of

carbohydrate and lignin soluble in alkalis. The growth of fungi depends on suitably mild temperatures, moisture, and air (oxygen).

Toughness is affected by decay. This is generally followed by reductions in strength values. Eventually, cell strength properties are seriously reduced; the loss of strength during early stages of decay can be considerable. The reduction in toughness has ranged from six percent to more than fifty percent, by the time a one percent weight loss had occurred in the wood as a result of fungal attack. By the time weight losses due to decay have reached ten percent most strength losses may be expected to exceed fifty percent.

2.3.6. Humidity Condition

Water has a dramatic adverse effect on the elastic modulus and flexural strength of wood particles and fibers. The unclapsed, linefeed cellulose fibers retain their strength better than delignified fibers when exposed to moisture.

Wet summerwood fibers (particles) show a distinctly higher breaking load than the corresponding dry fibers (particles), but this is not the case for springwood fibers (particles).

2.3.7. Temperature

Wood strength is reduced by increasing temperature at a given level of wood moisture below the fiber saturation point. The thermal degradation (pyrolysis) of wood substances is affected by chemical break down of the various constituents of solid wood. The degree to which thermal degradation affects wood and the rate at which it occurs depend mainly on the temperature at which the reaction takes place, the amount of air present, and the time the reactions proceed [21]

The most obvious result of the thermal degradation of wood is weight loss. As Figure 2.6 shows, the weight loss of wood and its major components is relatively minor at temperatures which do not exceed 300°C (572°F). Hemicellulose, as represented by xylan, is the least stable wood component, whereas cellulose is practically unaffected. Lignin decomposes gradually at temperatures below 149°C (300°F).

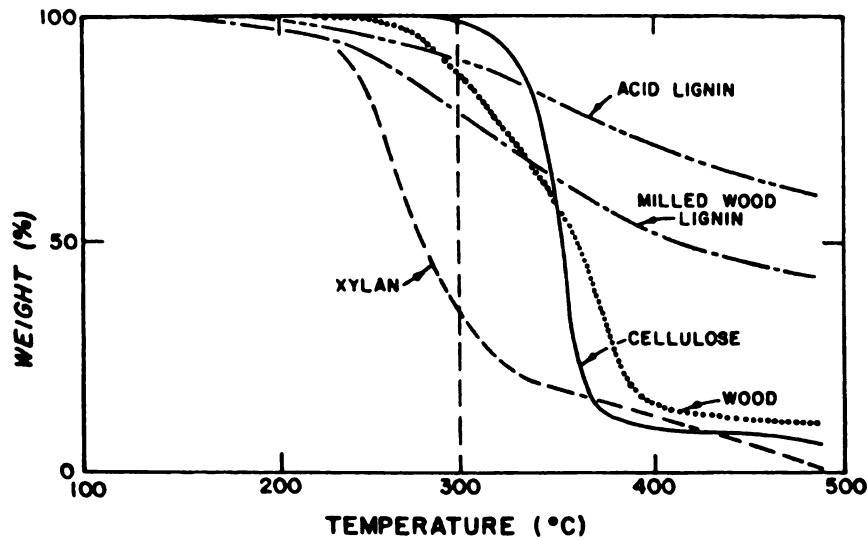


Figure 2.6 Weight loss of Wood and Wood Components as a Function of Temperature [22]

The adhesion between two cellulose chains is believed to be due to hydrogen bonding, the attractive forces developing between the positively charged hydrogen atom and any negatively charged atom such as oxygen (Figure 2.7). If water evaporates, the close contact between fibers is brought about by the lost surface tension of water; this pulls fibers together (see Figure 2.8). The addition of water or heat also will destroy the cohesive strength of the matrix.

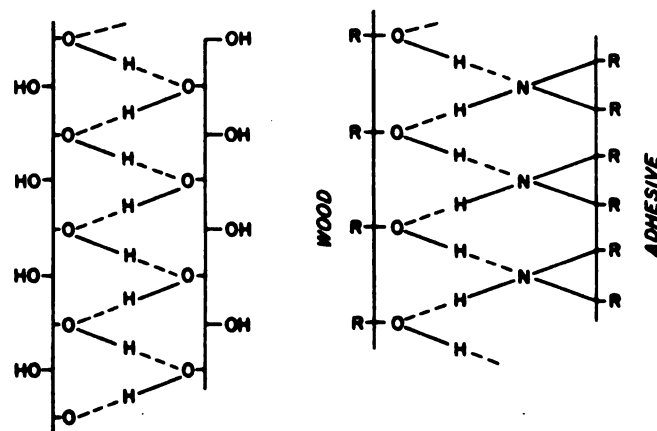


Figure 2.7 Hydrogen Bonds between two Cellulose Chains. The Bond Develops between Hydroxyl Groups (-OH) of the Cellulose Molecules and is Indicated by Dotted Lines. [23]

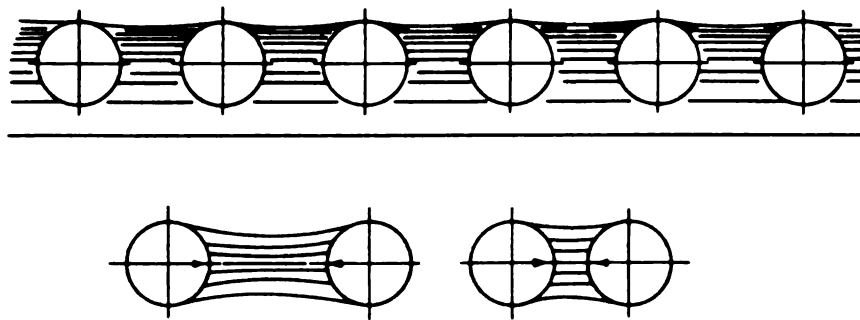


Figure 2.8 Attractive Forces between Fibers due to Surface Tension of Evaporating Water [23, 82]

In the upper portion of the picture, fibers are shown (in cross section) in suspension in water. The lower portion shows the attractive forces developing between drying fibers as the water is being removed. This will lead to fiber contact and the formation of hydrogen bonds [23].

CHAPTER 3

LITERATURE REVIEW

3.1 INTRODUCTION

The asbestos free wood-cement composites industry emerged in the late 1970s and early 1980s. The potential and feasibility of using wood particles and fibers as reinforcement in cement-based composites was identified and investigated by different researchers; their efforts resulted in a series of commercial products destined to replace asbestos cement [34, 35, 36, 37, 38, 39]. The literature review presented in this chapter emphasizes CO₂ curing of cement-bonded wood particleboard as well as the general engineering characteristics of fiber reinforced cement composites.

3.2 HISTORY AND DEVELOPMENT OF WOOD-CEMENT COMPOSITES

3.2.1 Cement-Bonded Wood Particleboard

The concept of combining inorganic binders with wood or agricultural biomass is ancient. Incorporating wheat or rice straw with mud to produce bricks has its roots in prehistory. Such inorganic-bonded composites are still used in many parts of the world. Mixing straw with mud improves workability, impact resistance and reduces fracture development by providing a reinforcing fiber. Table 3.1 traces the development of inorganic-bonded wood composites. The early magnesite-bonded boards were generally of low quality because the magnesite matrix was very sensitive to moisture. Cement-bonded excelsior boards, which were developed later, had better water resistance. The industrial application of pressure to produce wood-cement panels did not occur until about mid-1930's. With the gradual evolution of resin-bonded particleboard technology, much was learned that is also applicable to cement-bonded wood composite panels. A considerable amount of research and development was carried out by Elmendorf Research, Inc. (ERI) on cement-bonded panel products in the United States [25].

Early industrial production of wood-cement panels was based on ERI patents. In 1965, panels were produced in Japan based on these patent. There appears to be little doubt that inorganic-bonded wood composite technology is taking hold around the world, and significant expansions are anticipated.

Table 3.1 Industrial Production of Inorganic-bonded Wood Composites [24]

Year	Production
1900	Magnesite-bonded boards
1905	Gypsum-bonded excelsior board
1915	Magnesite-bonded excelsior board
1915	Cement-bonded excelsior boards
1927	Molded wood-cement products
1937	Resin-bonded particleboards
1942	Cement-bonded wood composite panels
1965	Gypsum fiberboards (shredded paper)
1972	Magnesite-bonded wood composite panels
1982	Gypsum particleboard

3.2.2 Cellulose Fiber Reinforced Cement Composites

As an economic asbestos substitute, cellulose fibers were considered for use in fiber reinforced cement in the early to mid-1940's. This work was intensified during the post-world war II years when there was a worldwide shortage of asbestos fiber. An investigation was conducted to discover whether paper pulp could be used to replace asbestos completely or partially in asbestos cement sheets. Fibers studied include bagasse, groundwood, wheat straw, and those derived from cement bags and brown paper. The experimental autoclaved sheets showed that brown paper (kraft) was the best of the pulp sources, giving the greatest strength to the composite material. However, when asbestos supply was reinstated, this work was discontinued.

Renewed interest in wood fibers began almost inadvertently in 1960. In those days, the asbestos fiber board, containing 15% asbestos, was made between steel interleaves. To make a cheap board as an alternative interleaf, boards were made up with half the asbestos replaced by wood fibers. It was found, however, that this material was a better product than the material they were selling, and full production started in 1964 in Australia. From the 1960s onwards such products have contained no more than 8% asbestos, which was about half the amount the rest of the industry was using. By 1981 the new generation of asbestos free autoclaved cement products was being commercially manufactured. This autoclaved product was totally reinforced by refined kraft wood fibers. At the present time there is considerable activity in the patent literature concerning the use of wood fibers or mixture of wood fibers with other synthetic fibers.

3.3 WOOD-CEMENT COMPATIBILITY

Portland cement is a mixture of different inorganic compounds. Table 3.2 shows the typical composition of a type I Portland cement. Cement hydration in water produces large amounts of calcium hydroxide that raises the pH of the water-cement solution to 12 or more. The hydration of type I cement is a very slow process that takes not less than one hour and not more than twelve hours in the first stage (setting) where the reaction liberates heat and the temperature rises. The second stage (hardening) is completed in 28 days, although it may take years to reach maximum strength. The hydration of cement is a complicated process, especially if it is used as binder in composites containing lignocellulosics or compounds which become soluble under the influence of water and could inhibit the setting or hardening of cement. The exothermic reaction characteristics are used to indicate compatibility between cement and other materials like wood.

Wood consists of large amounts of carbohydrates and phenolic compounds. These compounds have detrimental effects on the cure and strength of wood-cement mixtures. Miller [26] studied the effects of pure carbohydrates and tannin on the tensile strength and hydration characteristics of Portland cement. He concluded that glucose decreased cement tensile strength by over 40%, and hemicellulose, tannin, and acetic acid

Table 3.2 Chemical Composition of Type I Portland Cement [41]

Name	Formula	Abbreviation	Percent
Tricalcium silicate	3CaO SiO_2	C_3S	25-60
Dicalcium silicate	2CaO SiO_2	C_2S	15-20
Tricalcium aluminate	$3\text{CaO Al}_2\text{O}_3$	C_3A	4-12
Tetracalcium aluminoferrite	$4\text{CaO Al}_2\text{O}_3 \text{Fe}_2\text{O}_3$	C_4AF	8-12
Minor constituents			5-8

decreased it by lesser amounts. Though these results do not exactly reflect the performance in the real environment of wood-cement composites, they point out problems relating to hemicellulose which can be broken into simple sugars in the presence of an alkaline solution. Hemicellulose, a heteropolysaccharide, is an amorphous, branched polymer and is a major wood constituents (25% or more). It presents a low degree of polymerization (around 300 or less). In an alkaline solution, hemicellulose may be reduced to simple sugars such as glucose, mannose, xylose, galactose, and some acids such as glucuronic acid and galacturonic acid. These simple sugars and other compounds of wood detrimentally affect cement hydration and strength (a tea spoon of sugar in a barrow of concrete is sufficient to prevent hardening). When wood is mixed with cement, this interference may be manifested by a reduction in the exothermic hydration temperature, an increase in the setting time and decrease in strength. In extreme cases it can lead to total inhibition of cement curing. The mechanism of interference is not well understood. Hachimi [27] proposed that wood probably mineralizes, thereby reducing the amount of cations available for the crystallization of cement. The degree of interference caused by a given wood species varies, because the amount and type of hemicellulose and extractives vary from one wood species to another. In general, softwoods are more suitable than hardwoods because the latter contains more extractives and hemicellulose.

Figure 3.1 shows heat of hydration of cement and wood-cement composites. This graph can be divided into several stages. Over the first 15 to 30 minutes, there is an initial rapid hydration followed by a dormant period which lasts 2 to 4 hours. Subsequently,

the rate of heat evolution accelerates (setting phase) for several hours, and then slows down (hardening phase) within 24 hours. The cement continues to harden in a steady phase over several weeks. During the early stages of cement hydration, the dicalcium and tricalcium silicates are hydrated to form tobermorite gel and calcium hydroxide. Approximately 25 percent by weight of the cement is converted to calcium hydroxide. This calcium hydroxide increases the pH of the cement paste to approximately 12.5, producing a highly alkaline paste which can swell, dissolve, and degrade wood. Cement strength depends mainly on the ratios of the dicalcium and tricalcium silicates. The addition of any other materials to the cement-water mixture, such as wood particles and chemical additives (pure organic and inorganic compounds), will affect the magnitude of the hydration reaction, the time for the stages, and the cement strength.

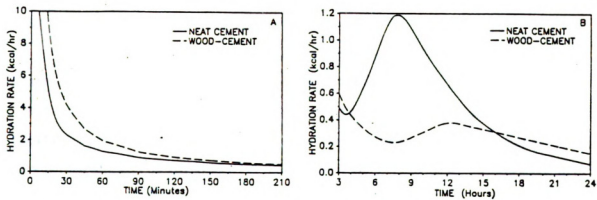


Figure 3.1 Hydration Rate of Cement and Wood-Cement Mixtures in the Early Stages (A) and the Setting and Hardening Stages (B) [41]

The long setting time required by cement is undesirable in manufacturing wood-cement composites. Several different techniques have been developed to overcome the problems caused by the inherently slow setting of cement and the retarding/inhibitory effects of wood. The common techniques are:

1. Controlled seasoning or fermentation of wood;
2. Addition of Pozzolans;
3. Addition of additives such as calcium chloride (CaCl_2), aluminum sulfate ($\text{Al}_2(\text{SO}_4)_3$), and sodium silicate (Na_2SiO_3) [23];

4. Altering cement composition (e.g. use of high-alumina cement or cements forming ettringite);
5. Addition of carbonates (e.g. potassium carbonate, ammonium carbonate, or sodium carbonate);
6. Water extraction to remove water soluble extractives that cause cement setting problems [16, 28], and
7. Use of carbon dioxide gas injection during pressing [12, 13, 23].

These processes are being applied industrially, though most of them are still in the developing stage.

3.4 OVERVIEW OF EARLIER CARBONATION STUDIES

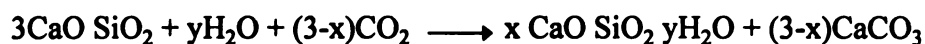
3.4.1 Influence of Carbon Dioxide

The setting and hardening of cement-based composite boards is a slow process. In the wood-cement composite case, the retarding effects of some wood species on the hydration process of cement further slow down the process [5]. This necessitates pressing and clamping of conventional cement-bonded particleboards for several hours before they harden and can be removed from the press without spring-back. Wet processing of cellulose fiber reinforced cement board also needs several hours of high-pressure steam curing to achieve high early strength. The result is reduced productivity and increased initial cost. Conventional pressing techniques in the manufacturing of cement-bonded wood particleboard require 8 to 24 hours of clamp time. Efforts toward reducing this initial curing time by substantially increasing the setting and hardening rate of cement should still provide sufficient “open time” during which the wood-cement-water furnish stays plastic to be mixed, formed and pressed. Developments in the area of rapid-setting boards have generally focused on altering the chemical composition of cement through the use of special cements and accelerating admixtures [29]. Retarding admixtures are also used to maximize the a workable “open time” [42].

Several different approaches to accelerating the slow manufacturing process of cement-based composites have been investigated. This section briefly reviews the ap-

proaches relying on carbonation to accelerate the process of strength development in cement paste.

Tremendous reduction in the setting time of cement-based binders, from few hours to few minutes, can be achieved through the addition of carbon dioxide [6, 7, 30, 31, 32]. The predominant chemical reaction occurring on carbonation has been defined by Berger et al. [33]:



Carbon dioxide lowers the pH value by forming carbonic acid. It is neutralized by calcium silicates, resulting in highly insoluble calcium carbonate. Calcium carbonate can appear as a mixture of vaterite, calcite, and aragonite.

Calcium carbonate provides the initial strength necessary for early release of the board from the press. The carbon dioxide can be obtained from the decomposition of a carbonate or introduced as a gas. In conventional use of cement, this reaction is very slow because the carbon dioxide content in air is extremely low. However, it is possible to make the reaction faster by blowing CO₂ gas into the formed cement particleboard mat at the pressing stage. The mat is porous enough to enable gas to be blown into it, and thus the free lime reacts with the CO₂, producing limestone. Because of this bonding, the product can be handled after a few minutes of pressing. It has, at this point in time, about half of its final strength. In the subsequent 2 weeks of storage, the normal cement setting reaction takes place which gives the 100 percent bondage. The carbonizing reaction is exothermal and the temperature of the product reaches 100°C (212°F) in less than 1 minute. Certain wood species, especially hardwoods, contain large amounts of sugars and tannins that decisively retard the setting of cement. This means that special attention must be paid to the choice of suitable wood species when cement bonded particleboard is manufactured with the conventional method. Some species cannot be used at all. The new carbonizing method has the solution to this problem (Table 3.3). All tested wood species are suitable for the CO₂ method.

Table 3.3 The New Carbonizing Technology [43]

Wood Species	Bending Strength			
	CO ₂ method		Conventional method	
	(psi)	(MPa)	(psi)	(Mpa)
Spruce	1,421	9.8	1,334	9.2
Red beech	1,262	8.7	*	*
Horn beam	1,407	9.7	*	*
Poplar	1,871	12.9	1,668	11.5
Dak	1,334	9.2	*	*
Acacia	1,117	7.7	*	*
Birch	1,262	8.7	*	*

* not suitable with the conventional method

By the injection of CO₂ into a cement-bonded particleboard, board compaction pressure can be released in 4-1/2 minutes [44]. The carbon dioxide treatment also reduces the inhibiting effect that many species have on cement hydration. Carbon dioxide has been used in some manufacturing plants to accelerate the setting of cement in wood wool boards [45]; the coarse porous nature of wood wool boards allows easy access of the gas to cement paste. These plants used exhaust gases from boilers and engines as the source of carbon dioxide. According to a British patent, carbon dioxide is used to make calcium carbonate (CaCO₃) in cement bonded fiberboard with good mechanical properties [46]. The green boards, made on a hatscheck machine, were heated to 60°C and subsequently treated with carbon dioxide. A Japanese patent describes the application of carbon dioxide to accelerate the hardening of cement-bonded fiber boards [47]. In this process, the green boards are heated to lower the moisture content and improve the porosity. According to a new process developed in Hungary [43], carbon dioxide is injected during the pressing of Portland cement-bonded particleboards. The process resembles the injection of saturated steam during the pressing of phenol formaldehyde-bonded particleboard.

Simatupang et al made experimental boards using a press with plates that enables the injection of carbon dioxide during pressing [48]. Introduction of carbon dioxide prior to pressing the furnish led to non-uniform carbonation due to pre-setting of surface layers which prevented thorough penetration of the gas. The distribution was also poor with CO₂ injection after pressing as evidenced by the appearance of air pockets. Injection of nitrogen prior to pressing followed by CO₂ injection after pressing, or the application of a vacuum-CO₂ injection-vacuum cycle after pressing were required to ensure uniform distribution of carbon dioxide and acceptable board properties. A comparison of board properties pressed according to various method is shown in Table 3.4 [92].

Table 3.4 Influence of Carbon Dioxide Injection on Cement-Bonded Particleboards [92]

Mode of injection	Setting time (min.)	Maximum hydration temperature (°C)	Density-ovendry (kg/m ³)	Modulus of rupture (MPa)	Carbon dioxide distribution
<i>Preinjection</i>					
Carbon dioxide	1.2	95	1,050	8.0	Satisfactory
Nitrogen	1.5	79	1,090	12.5	Satisfactory
<i>After closing</i>					
Direct	1.1	82	1,090	12.7	Unsatisfactory
After vacuum	1.2	88	1,125	12.5	Good

Geimer et al. studied two press schedules (unsealed and sealed), both of which yielded satisfactory results [44]. The sealed system provided slightly better gas utilization but produced boards that were slightly inferior in bending properties compared to boards made in the unsealed system. The boards pressed in the sealed system absorbed more CO₂ than did those in the unsealed system. Increases in either water or wood cement tended to reduce gas permeability and consequently reduced the CO₂ absorption, resulting in lower weight gain (Figure 3.2). An increase in board density decreased the percentage of weight gain. Board temperature was also affected by the gas temperature, which tended to decrease with increased usage, by changes in board mass, and by evapo-

ration of the water. Total CO_2 consumption is compared to weight gain in Figure 3.3. Weight gain was highly dependent on gas penetration and was decreased with increasing wood compaction.

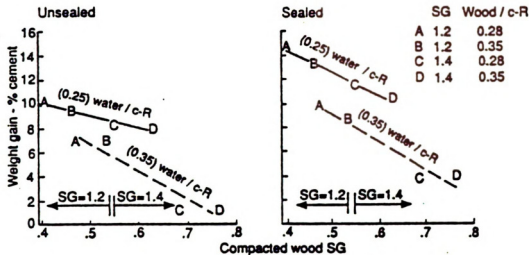


Figure 3.2 Weight Gain vs. Compacted Wood Specific Gravity and Water/Cement Ratio

[44]

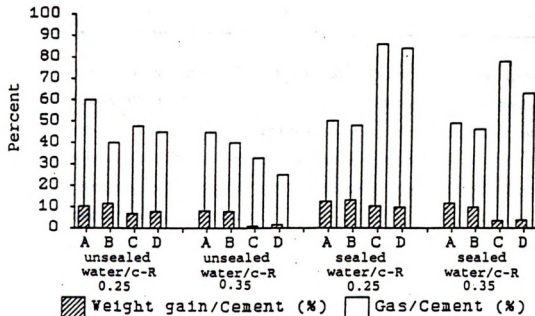


Figure 3.3 Gas Consumption and Board Weight Gain by Board Type. Specific Gravity and Wood/Cement Ratio, respectively: A, 1.2 and 0.28; B, 1.2 and 0.35; C, 1.4 and 0.28; D, 1.4 and 0.35 (water/cement ratio is water/c-R) [44]

The influence of the carbon dioxide pressure on the properties of the boards is shown in Table 3.5 and Figure 3.4. Under increasing carbon dioxide pressure, the setting time of cement was shorter, and the maximum temperature was higher. Gas flow rate should normally decrease after hydration temperature peaks because of the decreased chemical reaction as the available Ca(OH)_2 diminishes and permeability decreases due to the deposition of water formed during the reaction.

Table 3.5 Influence of Carbon Dioxide Pressure on Cement-Bonded Particleboards [92]

Carbon dioxide pressure (bar)	Setting time (min.)	Maximum hydra- tion temperature (°C)	Density- ovendry (kg/m^3)	Modulus of rupture (MPa)
1.5	2.6	61.0	*	*
3	1.8	66.6	*	*
5	1.2	67.1	1,130	13.8
7	1.2	88.4	1,130	12.5
9	1.1	102.4	1,140	12.6

However, once the system became charged, flow rate was nearly linear throughout the exposure time even after the board reached maximum temperature. This indicated a constant leakage of gas. Gas usage was dependent on the extent to which gas loss could be restrained, whereas gas efficiency depended on obtaining gas penetration of the board. The greatest weight gain, between four and five times that accounted for by the added Ca(OH)_2 , occurred in low density boards

For different water-cement ratios, the maximum temperature and setting time are shown in Figure 3.5 [6]. The shortest setting time and the highest temperature were reached at a water-cement ratio of 0.2. The curing time may be reduced to 7 days, as already about 80 percent of strength properties have been obtained. The calcium hydroxide content of specimens made by carbon dioxide injection is negligible as shown in Figure 3.6 [6]. The addition of about 5 to 10% of Ca(OH)_2 is advantageous [6, 44].

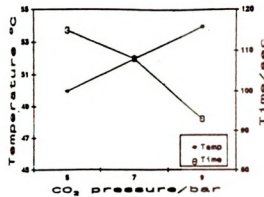


Figure 3.4 Influence of Various Carbon Dioxide Pressures on Maximum Hydration Temperature and Setting Time of Cement in Wood/Cement Specimens [6]

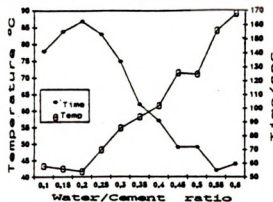


Figure 3.5 Influence of Water-Cement Ratio on Maximum Hydration Temperature and Setting Time of Cement in Wood/Cement Specimens [6]

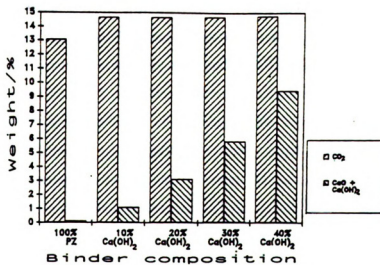


Figure 3.6 Influence of Binder Composition on Carbon Dioxide Content and Calcium Hydroxide Content of Specimens by the Carbon Dioxide Injection Process [6]

The CO₂ injected boards were up to 1.9 times greater in bending modulus of elasticity (MOE) and up to 2.5 times greater in bending modulus of rupture (MOR) than were similar boards pressed in conventional manner [44]. The initial stiffness values measured directly after pressing increased with board specific gravity. Initial MOE values for the sealed and unsealed boards are combined and averaged in Figure 3.7. MOE did not respond to the board variables in the same manner as weight gain.

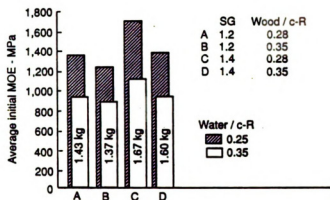


Figure 3.7 Initial Modulus of Elasticity (MOE) (average of sealed and unsealed system boards) is Highly Dependent on Total Weight of Cement (values shown in bars) [44]

The bending MOE value ascends with increasing weight of cement. Increasing water-cement ratio decreased initial MOE values. This reduction of initial stiffness was attributed to a diminished reaction between the CO₂ and Ca(OH)₂, as indicated by less weight gain. The bending stiffness was considered to be adequate even in those boards that had relatively low weight gains. Modulus of elasticity values increased with an increase in specific gravity but decreased with increases in wood-cement ratio (Figure 3.8). MOE values are highly dependent on the amount of cement. Modulus of rupture (MOR) values were maintained or increased with an increase in both specific gravity and wood-cement ratio (Figure 3.9).

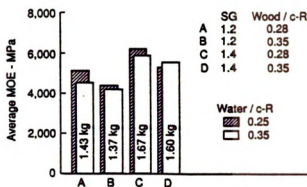


Figure 3.8 Modulus of Elasticity (MOE) (average of sealed and sealed system boards) of Fully Hydrated Board is Highly Dependent on Total Weight of Cement (values shown in bars) [44]

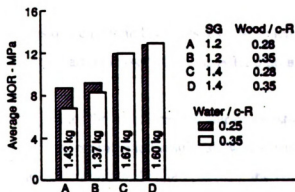


Figure 3.9 Modulus of Rupture (MOR) (average of sealed and unsealed system boards) of Fully Hydrated Board is Dependent on Specific Gravity of Compacted Wood (weight of cement shown in bars) [44]

Internal bond is also higher when compared with conventional board. Compared to boards bonded with thermosetting resin, the 24-hour value for inorganic bonded boards is quite low. Increasing swell was highly dependent on both the amount of wood and the degree of compaction. Water absorption was influenced by board SG but showed no consistent relation to either wood-cement ratio or water-cement ratio. The relation be-

tween thickness swelling (TS) and water absorption (WA) was not as direct as normally experienced with organic resin bonded boards. [44] The result x-ray diffraction (Figure 3.10) indicated that carbonized specimens do not contain calcium hydroxide, but calcium carbonate. Specimens made according to conventional methods show on increasing amount of calcium hydroxide with time.

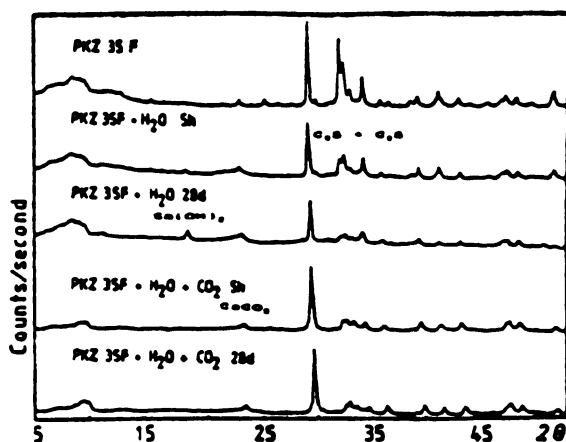


Figure 3.10 X-Ray Patterns of Cement and Various Wood-Cement Specimens Fabricated by Conventional Method and Carbon Dioxide Process After 5 hours or 28 days [6]

The length swelling under the influence of water or moisture is a critical property of cement particleboards. The experimental results show that carbonization causes a reduction of length swelling. According to Lange et al [85], the length swelling of cement bonded particleboards are influenced by the nature of the matrix. They reported length swelling from 0.396 to 0.508 percent for cement-wood particleboards made with four kinds of cement. The required swelling value of less than two percent can be obtained by using a cement of higher strength class. With gas mixtures containing only about 30 percent of carbon dioxide, the fabricated boards showed comparable properties with those made with pure carbon dioxide. Gases enriched with carbon dioxide are emitted in many processes, e.g. calcination plants, fermentation plants, and cement plants. In the manufacture of Portland cement about 136 kg of carbon dioxide is emitted for each 1,000 kg of produced cement. This amount is nearly equal to the amount bounded by cement in the carbon dioxide processes.

In glass fiber reinforced cement (GRC), the effective water/cement ratio of the 24 hours dried specimens was in the range of 0.08 to 0.140 [10]. This is close to the water/cement ratios which Klemn and Berger reported to be the optimal ones for efficient CO_2 curing [90]. The effect of drying time on the work to fracture (WF) of the composite before and after CO_2 curing is shown in Figures 3.11 and 3.12. The curves prior to CO_2 curing (no CO_2) indicate that increased drying time is associated with reduction in WF. The reduction is greater for longer periods of drying. The CO_2 curing, following the initial heat treatment, is accompanied by additional reduction in WF in this case and a slight increase in the case of the compacted specimens.

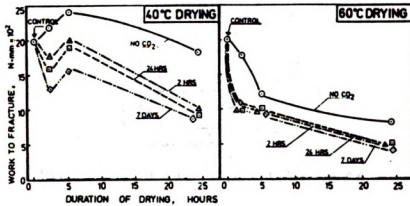


Figure 3.11 Effect of Heat Treatment at 40 and 60°C (curves marked as “no CO_2 ”) and Subsequent CO_2 Curing for 2 and 24 Hours and 7 Days, in CO_2 (curves marked by 2 hours, 24 hours, 7 days) on WF Values of Cast Specimens [10]

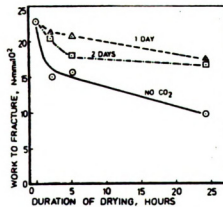


Figure 3.12 Effect of Heat Treatment (curves marked as “no CO_2 ”) and subsequent CO_2 Curing for 1 and 2 Days on the WF Values of Compacted Specimens [10].

Figure 3.13 showed the effect of drying time prior to CO_2 curing and the length of CO_2 treatment on the WF after exposed to different conditions. It can be seen that the carbonation resulted in some improvement over uncarbonated control specimens. The optimal improvement was obtained at specimens that were dried for 2 and 5 hours [10].

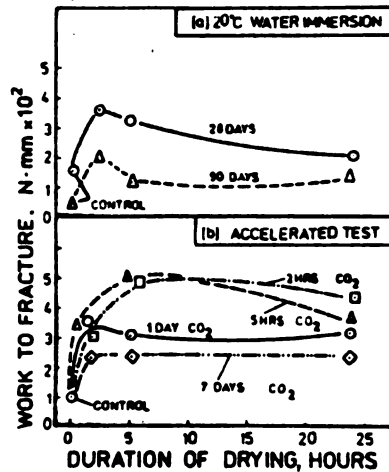


Figure 3.13 Effect of Drying Time and Length of CO_2 Treatment on the WF after Exposure to Different Conditions [10]

Goodbrake et al investigated the influence of water-solid ratio, humidity condition and the pressure of CO_2 in wetted powder of beta-dicalcium silicate ($\beta\text{-2CaO SiO}_2$) and tricalcium silicate (3CaO SiO_2) [9]. They concluded that water-solid ratio plays an important role in CO_2 dissolution, and relatively humidities in the range of 0 to 50% strongly affect the rate of carbonation as does a change of the CO_2 partial pressure in the range from 0.05 to 0.15 atm.

In the case of hardened cellulose and asbestos-fiber reinforced cement composites subjected to carbonation, Sharman and Vautier [87] concluded that the maximum amount of carbonation obtained is of the order of 35% CaCO_3 by weight level; absorption of further CO_2 was extremely slow. The asbestos cement sheet showed increase in the modulus of rupture and tensile strength, and decreased in moisture movement (see Figure 3.14)

[87]. The significant changes noted in the properties of carbonated wood-fiber reinforced cement sheet were increases in tensile strength, internal bond and moisture movement (Figure 3.15) [87]. Exposure of fully carbonated wood fiber cement sheet in a fungal cellar generally confirmed literature projections of fungal resistance, although a moderate decline in mechanical properties was observed [87]. The mode of fiber failure was “brittle-petrified”, and brittle-hollow failure was less frequently observed. The filling of the core of the fiber and possibly its cell wall with hydration is expected to result in an increase in its strength and stiffness. The ‘petrified’ fibers are more stable dimensionally; no separation and debonding between them and the matrix could be observed. Due to the increase in the density of the matrix around the fibers and the reduction in the tendency of the fiber to shrink away from the matrix, the bond between the two becomes greater. The increase in fiber-matrix bond, and the increase in fiber strength and stiffness may account for the marked increase in the strength and E-modulus of the composite and in its reduced toughness upon carbonation after hardening.

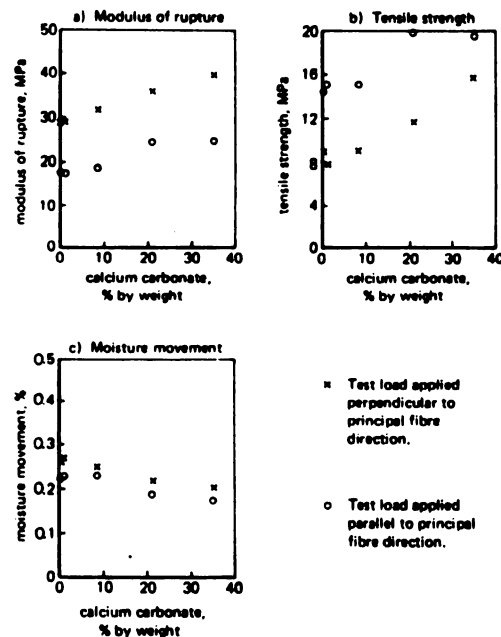


Figure 3.14 Effect of Carbonation on Mechanical Properties of Asbestos-Cement Sheet [87]

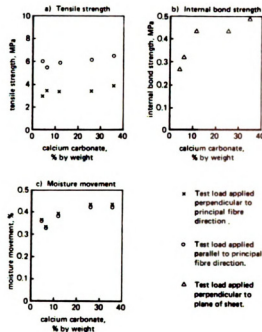


Figure 3.15 Effect of Carbonation on Mechanical Properties of Cellulose- Fiber Cement Sheet [87]

3.4.2 Durability Characteristics

According to the examinations of Dinwoodie and Paxton, and Lamper and Sattler, conventional cement-bonded wood particleboards can be considered as durable materials [1,10, 54, 91]. The boards reportedly show an increase wet strength properties with aging. Efflorescence of cement-bonded composites can be presented through carbon dioxide curing. The increase in tensile strength, internal bond strength, and moisture movement of cellulose-fiber reinforced cement composites with carbonation under aging effects are shown in Figure 3.15 [87, 88, 89]. The changes in mechanical properties when compared with uncarbonated, unexposed cellulose-fiber cement composites are summarized in Table 3.6 for carbonated, fungal cellar exposed composites [87]. The complete carbonation (elimination of all the calcium hydroxide) has also led to significant improvements in durability characteristics in GRC [10].

Table 3.6 Summary of Comparison Between Carbonated, Fungal Cellar-Exposed and Uncarbonated, Unexposed Cellulose Fiber-Cement Composites (differences significant at the 95% confidence level) [87]

Comparison between	Mechanical test method	Modulus of rupture	tensile strength	Internal bond strength	Impact strength	moisture movement	modulus of elasticity
uc, ue	prep.	-	0	0	-	+	0
versus c, e	para.	0	-		0	+	-

uc = not carbonated

c = carbonated

ue = not exposed in fungal cellar

e = exposed in fungal cellar

perp. = test load applied perpendicular to principal direction

para. = test load applied parallel to principal fiber direction

0 = no change

- = decrease after carbonation and exposure in fungal cellar

+= increase after carbonation and exposure in fungal cellar

Durability of conventional and rapidly curing (using CO₂) cement-bonded wood particleboard was studied by Simatupang [6]. He concluded that conventionally made cement-bonded wood particleboards have higher bending strength properties and are also more durable. However, the properties of the rapidly setting boards fulfill the requirements of existing standards. After 64 weeks of weathering no substantial loss of bending strength was observed. The results of the durability tests are presented in Table 3.7.

Table 3.7 Comparative Durability of Conventionally and Rapidly Setting Cement-Bonded Wood Particleboard from Spruce [6]

Cement	Bending strength (BS) and Density (D)							
	28 days		32 weeks		64 weeks (outdoor)		64 weeks (indoor)	
	BS (MPa)	D (kg/m ³)	BS (MPa)	D (kg/m ³)	BS (MPa)	D (kg/m ³)	BS (MPa)	D (kg/m ³)
<i>Press time 8 hours: *</i>								
PZ 35F	14.38	1,117	17.92	1,189	22.19	1,207	16.85	1,141
Trass	16.30	1,128	18.35	1,184	19.62	1,184	11.16	1,109
Highfurnace slag	11.55	1,049	13.52	1,122	15.70	1,159	10.79	1,079
<i>Press time 18 minutes: **</i>								
PZ 35F	11.84	1,089	10.18	1,157	12.98	1,154	12.01	1,155
Trass	11.56	1,092	8.58	1,069	9.25	1,054	17.14	1,150
Highfurnace slag	11.03	1,039	8.67	1,076	10.04	1,079	11.45	1,107

**) Accelerator: 3 wt% CaCl₂, Press time : 8 hours at 40°C*

****) Additive: 13 wt% K₂CO₃ + 1.5 wt% waterglass, Press time: 18 minutes at 85°C*

The embrittlement of wood (wood particle and cellulose fiber) in cement based matrices is a degradation of the wood in the alkalinity environment of the cement matrix. This gradation of the fiber (particle) can be avoid by a reduction of the alkalinity of the cement matrix.

Gram [103, 104] was well describe the mechanisms of decomposition in case of sisal fiber and cellulose. Generally held that the decomposition of cellulose in an alkaline environment can take place in accordance with two different mechanisms. One is the peeling-off mechanisms which occurs at the end of the molecular chain. The end group, which is reductive, reacts with OH⁻ and forms isosaccharin acid (CH₂OH) which is unhooked from the molecular chain. End groups are liberated in this way all the times. The probability of the group forming metasaccharin acid instead, which is not unhooked and which is stable in an alkaline solution, is 1:50. Since the degree polymerization is high, about 25000, the peeling-off mechanism is fairly harmless in itself. Peeling off is said to

occur within a wide temperature interval but the rate does not become markedly high until a temperature of about 75°C or above. The other form of cellulose decomposition consists of alkaline hydrolysis. This cause the molecular chain to devide and the degree of polymerization decreases. Since the division of the molecular chain entails the exposure of new reductive end groups, the peeling-off mechanisms can be started. Alkaline hydrolysis does not take place at a high rate until the temperature is in excess of 100°C. The decomposition of hemicellulose in an alkaline environment follows the same pattern. The degree of polymerization lies between 50 and 200. Consequently, the peeling-off mechanism becomes the dominating decomposition mechanism. Lignin is composed of large 3-dimensional molecules. The structure of these molecules is not known. Lignin consists of aromatic substances, is easily broken down in an alkaline environment and is colored yellow and brown when oxidized. Lignin begins to soften at 70°C-80°C. At 120°C it is partly liquid. The primary cause of the change in the characteristics of sisal fiber in the alkaline environment of the cement matrix is assumed consist of a chemical decomposition of the lignin and the hemicellulose in the middle lamellae. The alkaline pore water in the concrete dissolves the lignin and the hemicellulose and thus breaks the link between the individual fiber cells. [103, 104]

Under natural weathering, wood fibers may be exposed to moisture cycling and fungal effects. The behavior of wood-cement composites has been investigated.

3.4.3 Economy

In the manufacturing of cement-bonded wood particleboard with accelerated (CO₂) curing, several remarkable advantage can be gained when compared to the conventional manufacturing system [43]. Table 3.8 shows the consumption of raw materials and energy for accelerated versus conventional manufacturing of cement-bonded wood particleboard.

Table 3.8 Comparison of Raw Materials and Energy [43]

Material or energy per cubic foot of panel	CO ₂ system	Conventional system
Wood	19.56 lb.	26.49 lb.
Cement	54.57 lb.	57.39 lb.
CO ₂	4.36 lb.	--
H ₂ O	22.24 lb.	34.20 lb.
Waterglass	--	0.87 lb.
Compressed air	1,085 N-gal./ft. ³	2,275 N-gal./ft. ³
Electric energy	10.6 kWh	7.48 kWh
Heat energy	30.6 BTU	90.2 BTU

3.5 DESIGN OF NATURAL FIBER REINFORCED CEMENT COMPOSITES

Although interest in natural fiber reinforced cement composite materials has grown at a greatly accelerating pace in the last few years, composites as such are not new. The main factors controlling the performance of composite materials are the physical properties of the fibers and the matrix, and of the strength of the bond between the two.

The important factors in the design of fiber reinforced cement composites are:

1. Fiber volume fraction
2. Fiber orientation
3. The form of reinforcement (fiber dimensions: aligned short fiber, continuous, combined)
4. Fiber distribution

3.5.1 Volume Fraction of Fiber and Particle

It is typical of composite materials, where the matrix is normally organic (polymeric), to have quite a high fiber content ($V_f = 0.2$ to 0.7). On the other hand, composite materials with an inorganic cement matrix usually have a quite low fiber content

($V_f = 0.01$ to 0.3). Figure 3.16 shows various composite stress-strain curves for fiber-reinforced brittle materials with different fiber volume fractions.

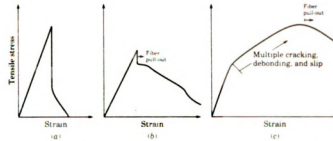


Figure 3.16 The Composite Stress-Strain Curves for Fiber-Reinforced Brittle Matrices: (a) Low fiber volume fractions; (b) Intermediate fiber volume fractions; (c) High fiber volume fractions [113]

Figure 3.17a and 3.17b show typical effects of kraft pulp fiber weight fraction on the flexural strength and toughness (area under neath the flexural load-deflection curve) of cementitious materials with different with proportions which have been cured in different conditions.

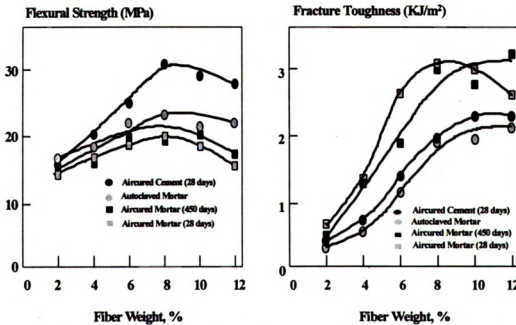


Figure 3.17 Flexural Strength and Toughness verses Fiber Weight Fraction for Cements and Mortars Reinforced with Wood Fiber (kraft pulp) [66]

The gains in tensile (flexural) strength with the addition of discrete reinforcing inclusions are, however, accompanied with losses of compressive strength. In cement bonded wood particleboard, the compressive strength of red maple wood-cement composites with different wood particle weight fractions (Figure 3.18) tends to decrease as the amount of wood is increased (Figure 3.18).

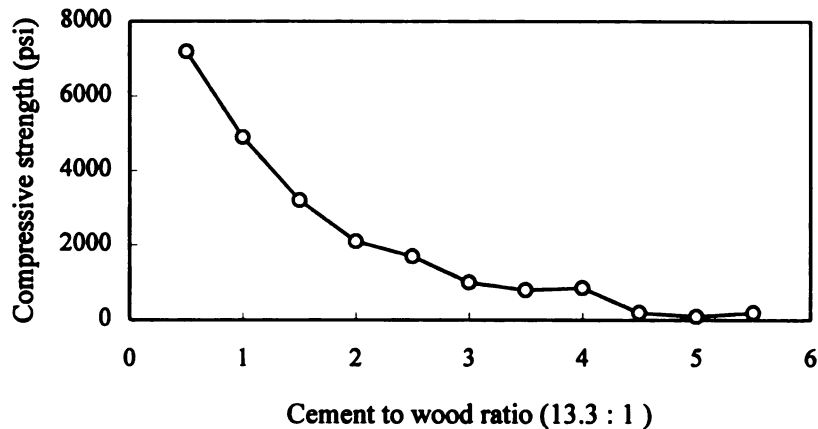


Figure 3.18 Compressive Strength of Red Maple Wood-Cement Composites after 28 Days of Curing as a Function of Wood-Cement Ratio [65]

3.5.2 Fiber and Particle Forms

Forms in which fibers can be embedded in a matrix are varied. In many ways, the simplest form is short, randomly distribute fibers. An example of the particle form for developing strength and dimensional stability is a thin flake of uniform thickness with a high length to thickness ratio. Most equipment designed to make thin flakes actually produce a variety of particles, including some ideal flakes but also considerable amounts of finer, more granular material. In practice, the industry starts with whichever form of raw material is most economically applicable to the type of cement-bonded particle board. The dimensional relationships are more significant in the development of composite properties than are the actual mechanical properties of the fiber.

3.5.3 Fiber/Particle Length and Aspect Ratio

Fiber length can be used to classify fibers for use in composite materials. The fibers can be continuous, discontinuous or both within a given composite material. There is not a fiber length which is constant for all materials and below which the fibers may be termed 'short'. However, the fiber length or the aspect ratio can have a significant effect on the properties and on the failure modes of composite materials. The effect of the aspect ratio and the fiber volume fraction on composite tensile strength is illustrated in Figure 3.19. The behavior of very short fibers is dominated by end effects and they do not therefore act as good reinforcing agents. Reinforcing fibers with lengths less than the critical length l_c will tend to pull out. On the other hand, when the fiber length is greater than l_c , the fibers will fracture, rather than pull out. In the region before the matrix failure strain is reached, the length efficiency factor for an aligned short fiber composite with frictional bond at the fiber interface is nearly unity for practical composites.

Fiber length also affects the ease with which the fibers can be aligned and packed. In general, short fibers are more difficult to align and to pack densely than the continuous fibers. On the other hand, in the case of cement-base matrices, excess fiber lengths and aspect ratios require the use of excess efforts for achieving satisfactory compaction of the composite.

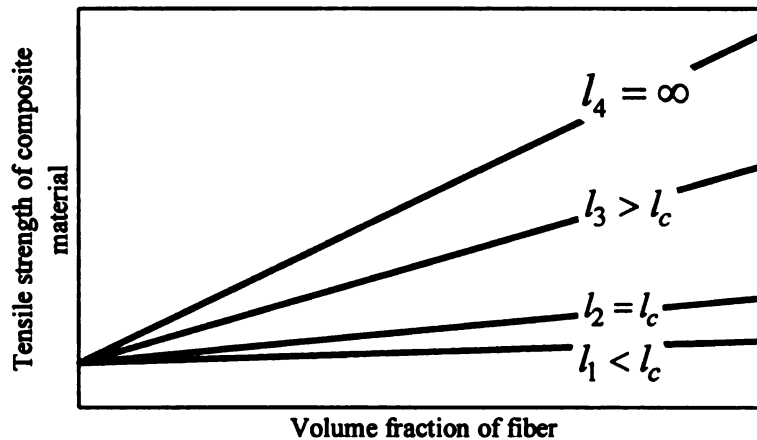


Figure 3.19 Effect of the Fiber Aspect Ratio on the Tensile Strength of Fiber Reinforced Composites [12]

3.5.4 Fiber Orientation

The orientation of fibers has a decisive influence on the mechanical properties and the behavior of the composite material. The fiber orientation depends on the processing route. Maximum loading of the fibers and maximum composite strength occurs when all the fibers are aligned parallel to a uniaxial tensile load. The theoretical effect of fiber orientation on the strength of a composite is shown in Table 3.9.

Table 3.9 The Effect of Fiber Orientation on Strength of Composite, for a given fiber orientation relative to the direction of stress [49]

Fiber orientation	Efficiency factors
1-D aligned	1
2-D random in plane	1/3
3-D random	1/6

3.5.5 Fiber Shape

Fiber shape can have an effect on the maximum obtainable fiber volume fraction, and can also affect composite properties.

Cellulose fibers, being hollow, can in some cases confer benefits in terms of reduced composite density and increased strength-density ratios.

3.5.6 Effect of Voids

Voids in composites may be formed in a number of ways. The presence of voids is detrimental to composite integrity and strength. Bond strength is weakened by the presence of voids.

Figure 3.20 shows that the increase fiber content is offset by the increase in void content; beyond the optimum fiber content (8 to 12% by mass fraction), the detrimental effect due to the porosity increase is greater than the reinforcing influence of the added fiber.

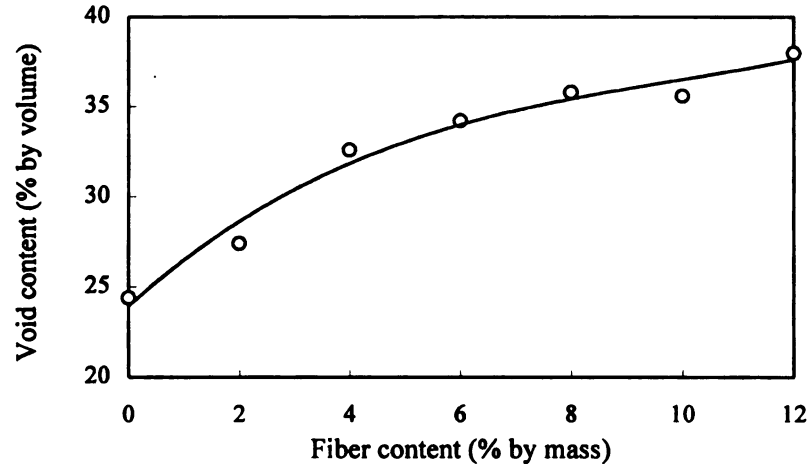


Figure 3.20 Effect of Cellulose Pulp Fiber Content and Void Content of Air Cured Composites [67]

3.5.7 Constituent Behavior

Whether the constituents are brittle or ductile, they affect composite properties. If fibers are brittle, the composite will tend to fracture in the linear portion of a stress-strain curve, even when the matrix is ductile. If ductile fibers are reinforcing a ductile matrix, the composite will show plastic deformation prior to fracture. On the other hand, if ductile fibers are reinforcing a brittle matrix, the composite will exhibit linear behavior until the first crack, and after that, ductile behavior (considerable elongations or deflections) may occur over a period of time.

Studies of natural fibers and of reinforcing and pulping technologies, have lead our interest into different pulp qualities, and it has become clear that fibers could have functions other than load-bearing, and that the matrix not only holds the fibers together but also plays a significant role in composite behavior. A third consideration - the interface between fiber and matrix - plays a very important role in the fracture behavior of composite materials.

3.6. THEORETICAL PRINCIPLES

If the maximum benefits of composites as engineering materials is to be achieved, it is necessary to understand their load-bearing potential. Linear elastic fracture mechanics (LEFM), the discipline concerned with failure by crack initiation and propagation, is often used to assess the suitability of conventional engineering materials such as concrete and ceramics in load-bearing situations. Failure in a fiber composite emanates from defects in the material. These may be broken fibers, flaws in the matrix and debonded fiber/matrix interfaces. Figure 3.21 shows a schematic representation of a cross-section through a fiber reinforced matrix. The diagram shows several possible local failure events occurring before fracture of the composite. At some distance ahead of the crack that is traveling through the composite, fibers begin to be influenced. In the high stress region near the crack tip, fibers may debond from the matrix (e.g. fiber 1). This rupture of chemical bonds at the interface uses up energy from the stressed system. Also, sufficient stress may be transferred to a fiber (e.g. fiber 2) to enable the fiber to be ultimately fractured (as in fiber 4). When total debonding occurs, the debonded fiber can then be pulled out from the matrix and considerable energy lost from the system in the form of frictional energy (e.g. fiber 3). It is also possible for a fiber to be left intact as the crack propagates. This process is called crack bridging. The net effect of the interaction of fibers with cracks in cement composites is the improvement of ductility and tensile strength of the resulting cement-based composite material. From this simplistic approach we are immediately made aware of the importance of fiber to matrix bond strength, frictional stress opposing pull out, tensile strength of the fiber, fiber length and fiber content.



Figure 3.21 Schematic Representation of Crack Traveling Through a Fiber Reinforced Matrix [8]

Information concerning theoretical treatment of cement-bonded wood composite board is very limited. Different efforts have been made to predict the strength of cement-bonded particleboard and isolate the major parameters affecting it. Dinwoodie, Paxton and Sorfa qualitatively related strength to density [54, 55, 56, 57]. Lee and Hong [58] studied the effect of the hydration temperature on strength. Higher temperatures gave higher strengths. They also investigated the effects of wood species on strength. Sorfa [55] generated empirical formula by multiple linear regression analysis over different parameters such as wood/cement and water/cement ratios to predict the density and the bending strength of cement-bonded particleboard. His correlation varies from 80 to 95% over cement-bonded particleboard densities ranging from 480.6 to 1296 kg/m³ (30 to 80 pcf). A more recent work by Sarja [59] presents empirical formulas for the modulus of elasticity modulus of rupture and compressive strength of cement-bonded particleboard as a function of density; these formulas are given below:

$$f_c = 4.5(\rho / 1000)$$

$$f_{ct} = \rho / 500$$

$$E_c = 1500(\rho / 1000)^4$$

where ρ is the density at 40% humidity in kg/m³

f_c is the compressive strength in MPa

f_{ct} is the tensile strength in MPa

E_c is the modulus of elasticity in Mpa

The composite material approach has been used by several researchers in the form of 'rule of mixtures' to predict strength behavior of cellulose fiber reinforced cement composite [50]. The rule of mixtures stated in its most general form can be given as:

$$\sigma_c = \sigma_m \nu_m + \sigma_f \nu_f$$

where σ_c is the strength of composite, σ_m is the strength of the matrix, σ_f the strength of the fibers, η is the efficiency factor, ν_o is the void fraction and ν_m and ν_f are the volume fractions of the matrix and the fibers respectively. When the matrix cracks, the composite may carry a lesser or greater load than the matrix, depending on fiber content.

Figure 3.22 shows load-deflection curves for a range of fiber composites tested in flexure. The 'critical volume' of fiber needed to exceed matrix strength is much lower in the flexural case than for tensile strength tests, but it does indicate the ability of fibers to carry the load after the matrix has cracked. Theoretical calculations often show that very low values of v_f are needed to achieve strengthening; however, factors such as poor bonding or fiber orientation make higher values necessary for practical applications. When the critical volume of fiber is exceeded it is possible to achieve multiple cracking, and the brittle matrix can respond as a pseudo-ductile material (see Figure 3.22).

Similarly, for the modulus of elasticity in tension, E_c , the rule of mixture is written as :

$$E_c = E_m(1 - V_o)V_m + \eta E_f V_f$$

where E_c , E_m and E_f are the elastic module of composite, matrix and fiber, respectively.

The rule of mixtures assumes that there is no effect from Poisson's ratio and, before cracking of the composite, fibers are fully bonded to matrix, i.e. equal strains in fiber and matrix. However, cement matrix has a strain at failure between 50 and 500×10^{-6} where as cellulose fiber has a strain at failure $>20,000 \times 10^{-6}$. Andonian et al. attempted the first theoretical analysis of the mechanical properties of cellulose fiber reinforced cement composites using the rule of mixtures for random fiber reinforced composites, on the basis that fiber pull-out is the principal mechanism of failure. The model gave close predictions of strength and modulus values in flexure and tension for the experimental results they obtained [51].

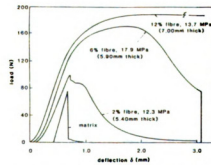


Figure 3.22 Load-Deflection Curves for a Range of Cellulose Fiber Reinforced Cement Composites Tested in Flexure [64]

Das Gupta et al. included in the rule of mixtures the effects of orientation and length, and developed different relations for fibers with lengths greater than, and shorter than critical length. Their model was used to analyze pastes reinforced with short, randomly distributed coir fibers [60].

Laws [105] questions the use of the rule of mixtures for predicting the tensile strength of fiber reinforced brittle matrices; the matrix is brittle and fails at a strain very much lower than the failure strain of fibers, and it is suggested that the tensile strength should depend on the fiber contribution alone and is given simply by

$$\sigma_c = \eta_1 \eta_2 \sigma_{fu} v_f$$

Swift and Smith have used this equation to explain flexural strength for sisal reinforced cement [61]. The basic rule of mixtures assumes that fibers are aligned in the direction of the stress, and although η_1 tries to compensate for a degree of randomness, it cannot be determined as a precise value. Likewise, η_2 is determined by the length of fiber in relation to the critical length (l_c). The critical length is defined as twice the length of fiber embedment which will cause fiber failure during pullout:

$$\eta_2 = \frac{l}{2l_c} \text{ when } l < l_c$$

or

$$\eta_2 = l - \frac{l_c}{2l} \text{ when } l > l_c$$

Again, in practical terms the precise value of η_2 is rarely known, because the determination of l_c with any accuracy is very difficult.

The critical fiber length as stated above can be obtained as follows if the shear stress (τ_s) developed at the interface is uniform

$$l_c = \frac{\sigma_{fu} \cdot r}{\tau_s} \text{ (where } r \text{ is fiber radius)}$$

Andonian et al. calculated the critical length of cellulose fiber reinforced cement composites to be about 20 mm, and as the measured length of the fiber is about 3.5 mm, fiber fracture was not possible [50]. Coutts et al. had observed fiber fracture during wood fiber reinforced cement composite failure and concluded that the “apparent critical fiber

length" must be less than 3.5 mm. The conflicting reports on the predominance of fracture or pull-out of wood fibers from a cement matrix prompted Morrissey et al. [53] to study a model system consisting of sisal slivers embedded in cement and protruding from one end of the cement matrix. About 200 such samples were tested under tension. It was found that the slivers did not behave in the manner predicted for uniform cylindrical fibers. After a break of the elastic bond between the fiber and the matrix, the fiber started to pull out. The force resisting pullout was not proportional to the length of embedment but was dominated by the highest local resistances present due to fiber shape. As pullout proceeded, anchor spots developed and the force required rose or fell in an apparently random manner. When the anchorage was too strong to be dislodged by the maximum force the fiber could carry, tensile fracture of the fiber occurred (Figure 3.23). There was a 'critical length' of embedment, which for the sisal slivers was approximately 30 mm. When the embedment length was shorter, fibers tended to be pulled out (Figure 3.23), and when it was longer they tended to break. This 'critical length' is not the length for which a uniformly distributed frictional stress reaches its critical value under the maximum sustainable tensile load, as is commonly assumed, but it corresponds to the length around which the probability of a local strong anchorage becomes high. The 'critical length' of 30 mm for sisal slivers corresponds to an aspect ratio of 110 ± 50 , which is comparable with the aspect ratio of *P. radiata* fibers. This would support the observation that *P. radiata* woodpulp fiber cement composites frequently experience fiber fracture during failure.

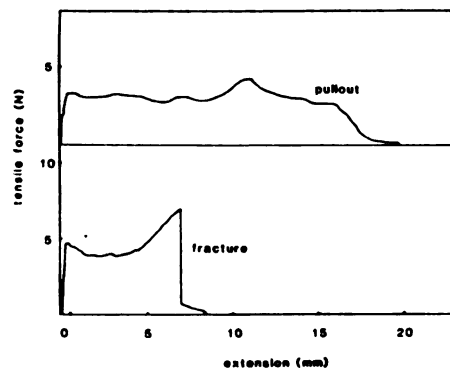


Figure 3.23 Tensile Load-Extension Curves for Different Failure Modes of Sisal Slives Embedded in Cement [15]

Numerous studies of steel fiber and glass fiber reinforced cements and concretes have indicated that the major factors affecting flexural strength are the volume and aspect ratio of fibers. Higher values of either lead to higher values of flexural strength. Without considering the theoretical equations leading to the above conclusions, it is interesting to note that in cellulose fiber reinforced cement composites an increase of fiber volume leads to increased flexural strength up to about 8% by mass or fiber, at which stage efficient packing of the fibers becomes difficult and strength starts to drop (Table 3.10). With respect to the aspect ratio of fibers, it has been noted by Coutts and Warden that air-cured wood fiber-cement composite samples reinforced with softwood fibers ($l/d = 80-100$), when compared to similar samples reinforced with hardwood fibers ($l/d = 50-60$), displayed higher flexural strength at the same fiber content by mass (see Table 3.10). Conflicting with this observation is the fact that autoclaved samples of mortars reinforced with softwood fibers and New Zealand flax ($l/d=200$) show very similar flexural strength, but, more importantly, lower fracture toughness. The reason that NZ flax composites do not produce higher strength properties is related to the fact that most of the fibers (with tensile strength approximately 300 MPa) are broken, and so σ_{fu} is a limiting factor and not l/d . When tested wet, the longer NZ flax fibers produce stronger samples than the short *P. Radiata* fibers, due to the fact that more of the long fibers can be loaded up to failure. In keeping with this, we find the very short *E. regnans* fiber reinforced materials are weak when tested wet or at RH test conditions ($50 \pm 5\%$ relative humidity, $22 \pm 2^\circ\text{C}$), because the short fibers cannot be loaded to failure. In the above argument it is proposed that the interfacial bond is constant, as all fibers were prepared by the kraft pulping method.

As seen in Figure 3.22 the post-cracking ductility imparted to the composite by fiber addition can be considerable. The origin of fracture toughness in wood fiber reinforced cement composites was claimed to come mainly from fiber pullout (85% to 90%). Toughness measurements can be conducted in several ways, including: impact tests such as Charpy or Izod (which involve stored energy in a pendulum), calculating the area un-

der stress strain curves, the use of fracture mechanics involving stress intensity or similar parameters, or more practical tests such as dropped balls or weights, etc.

Table 3.10 Effect of Aspect Ratio and Fiber Content [67, 68, 69, 70]

Fiber content (% by mass)	Flexural Strength (MPa)				Flexural Toughness (KJ/m ²)			
	P.radiata		NZ flax		P.radiata		NZ flax	
	RH	Wet	RH	Wet	RH	Wet	RH	Wet
2*	15.6	11.5	17.4	12.8	0.31	0.37	0.19	0.24
4*	16.6	11.7	20.5	16.9	0.57	0.88	0.34	0.71
6*	19.9	12.4	21.4	16.6	1.15	1.81	0.48	0.94
8*	23.1	14.8	23.2	18.0	1.86	3.15	0.84	1.74
10*	21.3	12.9	23.4	17.3	1.92	2.97	1.19	2.15
12*	21.7	10.5	17.7	-	2.09	2.88	2.59	-
	P. radiata		E. regnans		P. radiata		E. regnans	
2**	14.9	10.1	10.6	8.6	0.41	0.64	0.25	0.33
4**	20.2	11.9	14.2	10.5	0.64	1.52	0.51	1.00
6**	25.1	13.3	20.9	10.4	1.40	3.72	1.06	1.61
8**	30.3	14.8	20.3	8.4	1.93	4.51	1.37	1.49
10**	29.2	13.1	20.1	9.6	2.28	4.60	1.46	1.83
12**	27.6	10.4	20.6	9.3	2.25	3.60	1.68	1.79

*Autoclaved mortar

**Air-cured cement

Some of these techniques are more suited to particular composites, but all have limitations which render elusive the well-defined material properties useful to engineers and material scientists. Mindess and Bentur studied the fracture of wood fiber reinforced cement products and found that saturated samples were weaker and more compliant than

air-dried specimens [52]. It was found that the wet samples were completely notch-insensitive, while the air-dried specimens could be slightly notch-sensitive. Notch sensitivity is a requirement for the application of linear elastic fracture mechanics to cement composites, and so these workers concluded that the application of LEFM to this system is inappropriate. Mai and Hakeem have studied the slow crack growth of bleached and unbleached cellulose fiber reinforced cement composites for both dry and wet materials, using a double-cantilever beam system [62]. The results were analyzed using K-solutions and compliance measurements within the framework of LEFM. It was concluded that LEFM concepts can be used for wood fiber reinforced cement products. The use of LEFM requires a linear elastic homogeneous matrix. The introduction of fibers into a matrix, to achieve ductility, must by their very nature result in a heterogeneous material with a non-linear stress-strain curve after matrix cracking. The fracture toughness results given in Table 3.10 for a range of wood fiber reinforced cement composites have all been obtained by the method of measuring the area under the load/deflection curve. As the materials are non-linear and non-elastic, this approach is useful in that the total recorded energy will include the contributions of the work of fracture of the matrix, the debonding and frictional slipping of the reinforcement, and any strain energy released by fiber fracture. For fiber cements and concretes the matrix work of fracture is virtually that of the unreinforced cement or concrete and is less than 50 J/m^2 . Therefore, it is assumed that any improvement in composite toughness will depend on whether the fibers bridging the crack are able to support the load previously carried by the matrix, and on whether the fibers break or pull out of the matrix. Fiber pullout is the most common mode of failure for steel and glass fiber cements and concretes. This is because, to incorporate sufficient fiber into the formulations without fiber tangling, the fiber aspect ratio cannot be high enough to exceed the critical fiber length. It has been recorded that wood fibers can be loaded into the matrix material with fiber volumes in excess of $v_{f \text{ crit}}$ (Figure 3.22), and can be fractured during failure; hence, the “apparent critical length” would be exceeded. This behavior does result in relatively high levels of fracture toughness (Table 3.10) but does not lend itself to a conventional form of theoretical analysis. Hughes and Hannant

have studied the reinforcement of Griffith flaws in wood fiber reinforced cement composite in an attempt to explain their behavior, and concluded that stresses developed are significantly higher than would be expected using the rule of mixtures theory [63].

CHAPTER 4

MANUFACTURING AND EARLY AGE CHARACTERISTICS UNDER CARBONATION EFFECTS

4.1 INTRODUCTION

The manufacturing of cement-bonded wood particleboard is somewhat similar to that of concrete masonry units. In the case of cellulose fiber reinforced cement composites, mix proportioning and processing methods are quite different from normal concrete or mortar. The process includes refining of fibers in a slurry and mixing of all constituents in a slurry. The slurry has a low solid content (20%) in order to uniformly disperse the fibers; vacuum is then applied as the sheet is built-up in laminates to extract the excess water. The composite may then be compacted under a press, and curing is usually achieved using high-pressure steam (about 8 to 12 hours) for accelerated strength gain in prefabrication facilities.

The current processing technologies of these two categories of wood-cement composites present some important problems. The long curing time of cement-bonded particleboard under the press reduces the productivity of plant and adds to the initial cost of the end product. In the case of cellulose fiber reinforced cement also, the need for elongated high-pressure steam curing adds to the capital investment on the plant, slows down the manufacturing process, and adds to the process energy consumption and cost.

The main thrust of this work is to accelerate the process of manufacturing cement-bonded particleboard and cellulose fiber reinforced cement through early exposure to CO_2 . The end products of cement curing in the presence of CO_2 are also potentially more stable and compatible with wood than conventional cement hydration products. Furthermore, the accelerated reactions in the presence of CO_2 would allow for the use of lower-value wood species which would otherwise, in slow hydration conditions, have inhibitory effects on the hydration of cement.

4.2 OBJECTIVES

The main thrust of this phase of research was to develop efficient processing systems for wood-cement composites which utilize the advantages of CO₂. Different sequences of processing cement-bonded wood particleboard and cellulose fiber reinforced cement were evaluated. The effects of CO₂ concentration on the end product quality were also investigated in the case of cement-bonded wood particleboard.

The performance characteristics were evaluated through flexural testing of composites. In the case of cement-bonded wood particleboard, tests were conducted immediately after accelerated processing with CO₂. For cellulose fiber reinforced cement, the specimens were air-cured for seven more days and then tested after two days of immersion in water. The test results obtained in this study were analyzed statistically using the analysis of variance technique in order to derive statistically reliable conclusions.

4.3 CEMENT HYDRATION CHARACTERISTICS IN THE PRESENCE OF WOOD PARTICLES

The nature and quality of the wood component critically affect the cement hydration reactions and consequently the composite strength. This is more so in the case of cement-bonded wood particleboard which uses less processed wood. Cellulose fiber reinforced cement, on the other hand, typically uses Kraft pulp, which is highly processed and contains less extractives and cement hydration inhibitors. This section focuses on the use of less processed wood particles in cement-bonded wood particleboard. CO₂ curing is expected to accelerate the processing of cement-bonded wood particleboard to the point that the inhibitors in wood can not be extracted to damage the curing process. Hence, with CO₂ curing the sensitivity to wood species will be reduced. The exact causes of hydration inhibition by wood is difficult to ascertain since a number of complex chemical and physical processes occur and interact in the process. A wood-portland cement-water system is highly species-sensitive as determined by hydration temperature data. The considerable influence of species on hardening of cement can constitute a significant problem for the wood-cement composite board industry where residues from a variety of

species may have to be accepted as raw material. In this study four different species (southern pine, aspen, red oak, and maple) were examined.

In prior research, different investigators had concluded that the differences in behavior of species when mixed with cement are due primarily to water soluble substances present in the cell walls of wood [18, 28, 71, 72].

The wood from different species was collected by the Michigan State University Forest Experimental Station in Kalamazoo, Michigan. A hammermill was used to produce the needed wood particles which passed through a 20-mesh (0.85 mm) screen and remained on a 40-mesh (0.425 mm) screen. Wood particles of each species were dried for 24 hours in an oven at 103°C. To obtain data on the heat of hydration of wood-portland cement-water system, 200 grams of cement and 15 grams of wood particles (based on oven-dried weight) were dry-mixed in a polystyrene cup. The mixture was blended with 90.5 ml of distilled water (2.7 ml of water per gram of oven-dried wood and an additional 0.25 ml of water per gram of cement) [18, 72, 73, 74]. The polystyrene cup containing the wood-cement-water mixture was wrapped with aluminum foil and placed into a 2-liter Dewar flask. An aluminum- wrapped Type J thermocouple was inserted into the approximate center of the mixture. The flask was then promptly insulated by placing several layers of fiberglass insulation on its top and sides, and it was then wrapped with mastering tape. Figure 4.1 shows the design used to determine the heat of hydration of wood-cement-water systems.

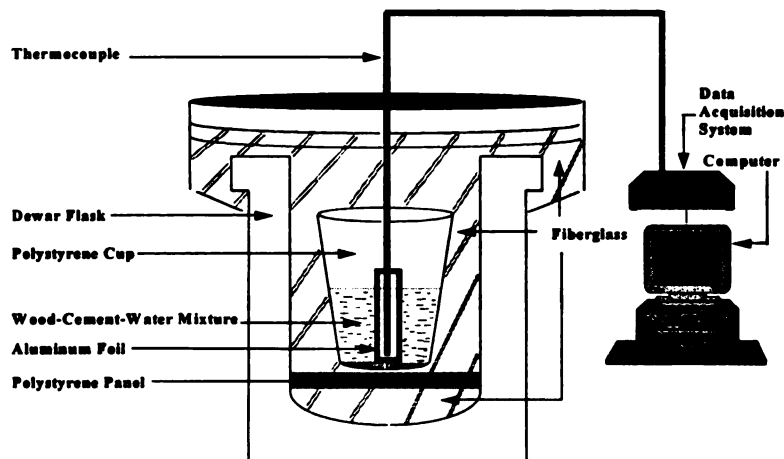


Figure 4.1 Experimental Set-Up to Determine the Heat of Hydration of Wood-Cement-Water systems.

All experiments were carried out at ambient room temperature between 21 to 23°C. The temperature of the mix was measured at 1-minute intervals. Three replications for each species were performed. The average heat of hydration curves for neat cement paste and wood-cement-water systems with the four species are compared in Figure 4.2.

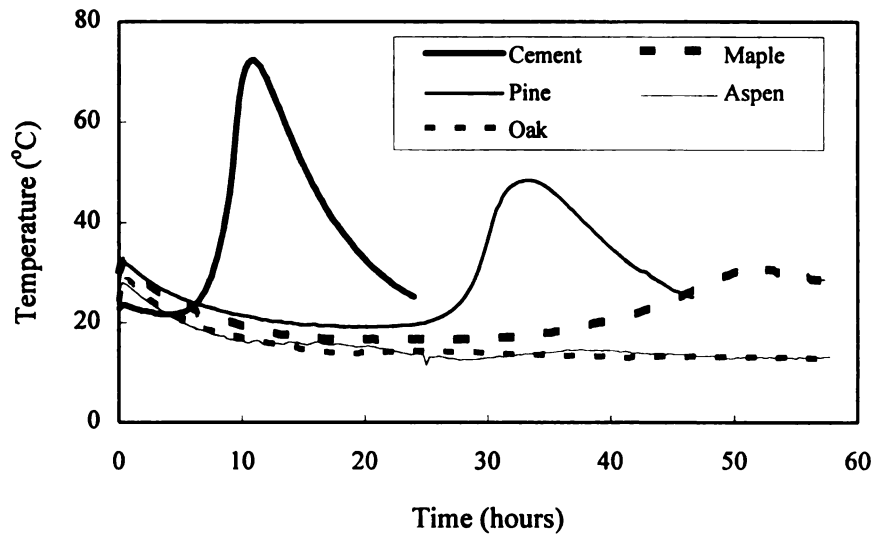


Figure 4.2 The Heat of Hydration Test Results

The test results with aspen and oak species are dramatically different from those for neat cement paste and southern pine as seen in Figure 4.2. The data indicate that hardwood species (aspen, maple and oak) react differently but generally slow down the hydration process. Maple showed an average maximum hydration temperature of 31.1°C occurring in 51.75 hours; aspen and oak, on the other hand, failed to set and exhibited low temperatures. While southern pine (a softwood) performed better than hardwoods, it still had some inhibitory effects. One may conclude from Figure 4.2 that the inhibitory effects of hardwoods complicates their use in cement-bonded particleboard following conventional techniques.

4.4 CEMENT-BONDED PARTICLEBOARD

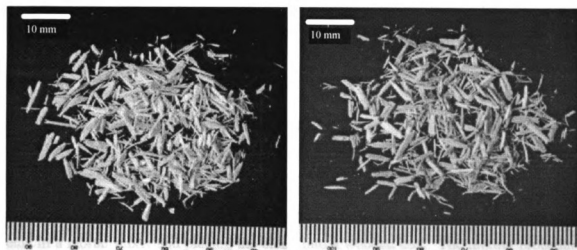
4.4.1 Materials and Manufacturing Procedures

Wood particles were derived from various wood pieces by dry mechanical processing. Softwood (southern pine) and hardwood (aspen) species were chosen for this research. A hammermill used to make the particles, and screened the resulting particles to a final 6 to 20 mesh (3.35 to 0.85 mm) particle size (pass through No. 6 sieve staying on No. 20 sieve). The average moisture content of these particles was about 5% (oven-dried basis). Figure 4.3a shows pictures of the wood particles. An image analysis equipment (SONY CCD camera connected with computer analysis system) was used to measure average particle dimensions. The average length, width, and thickness of wood particle were shown in Table 4.1. The gradation of final particles is shown in Figure 4.3.

Table 4.1 Wood Particle Dimension

	Southern Pine	Aspen
Length (St. Dev.)	5.32 mm (1.73)	4.97 mm (1.66)
Width (St. Dev.)	1.20 mm (0.67)	1.25 mm (0.47)
Thickness (St. Dev.)	0.40 mm (0.15)	0.50 mm (0.22)

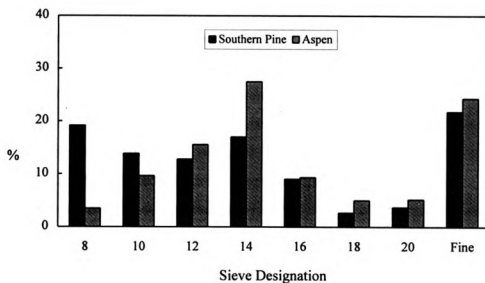
Type I Portland cement was used. The chemical composition of the cement is shown in Table 4.2. Agricultural grade of calcium hydroxide (Ca(OH)_2) at 7.5% by weight of cement was used when curing was accomplished using CO_2 gas. In this case, calcium hydroxide replaced an equivalent weight of cement. Different carbon dioxide (CO_2) gas concentrations (25, 50, 75, 100%) were used.



Southern Pine

Aspen

(a) Picture of Wood Particles



(b) Gradation

Figure 4.3 Wood Particles

Table 4.2 Chemical Composition of the Type I Portland Cement used in this Investigation

Chemical Composition	Percent by weight
Tricalcium Silicate (C_3S)	43.3
Dicalcium Silicate (C_2S)	26.3
Tricalcium Aluminate (C_3A)	11.0
Tetracalcium Aluminoferrite (C_4AF)	8.6
Insoluble Residue	0.12

Manufacturing of cement-bonded particleboard involved mixing of the constituents in a mortar mixer and placing the blend into a wooden box. The mixing procedure for the manufacturing of cement-bonded wood particleboard in a regular mortar mixer was as follow: (1) add wood particles and 70% of water while mixer operating at low speed (140 rpm) for about 1 minute or until a uniform distribution of water in wood particles is reached; $Ca(OH)_2$ was dispersed in the water; (2) add cement and the remainder of water and mix for 2 minutes at low speed; (3) stop the mixer and wait for 1 minute, and then finalize the process by mixing at medium speed (285 rpm) for 2 minutes. The mat was hand made in a wooden box of 12 in. (305 mm) by 12 in. (305 mm) planar dimensions. As caul plate, a fine screen (with mild tampering) was assembled in a steel frame. The mat was allowed to rest for 5 minutes prior to processing. This time was established as a standard for all boards for two reasons: (1) some time is typically needed to prepare the press system, and (b) a consistent plan needs to be developed for the board processing since hydration reactions initial upon contact of cement with water.

Figure 4.4 shows the cement-bonded wood particleboard processing system which incorporates CO_2 curing. To produce various concentration of CO_2 gas mixture, as seen in Figure 4.4, two gas cylinders (one CO_2 and the other air) were used. Each cylinder was connected with a flowmeter which controlled the CO_2 concentration and the gas flow level. A CO_2 gas heating element was used in the CO_2 pressure supply line to prevent the gas from freezing. Pressure was applied on boards using a 50-ton capacity press. In the unsealed press, the platens were perforated with 2.38 mm (3/32 in.) diameter holes drilled

in a 13 x 51 mm (0.5 x 2 in.) spacing pattern which covered an area of 305 x 305 mm (12 x 12 in.). The top and bottom perforated plate were connected to the CO₂, air and vacuum lines. The set-up is capable of applying any combination of CO₂, air and vacuum on either side of the board. The temperature of the cement-bonded wood particleboard was also measured during gas injection using a thermocouple connected to a data acquisition system. A metal screen was used above the bottom plate. Moisture traps were used to prevent possible damage to the vacuum pump by small particles and water.

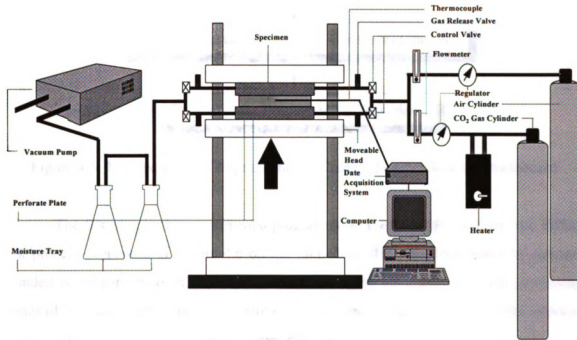


Figure 4.4 Processing System Incorporating CO₂ Curing

The next section describes various press programs which were investigated along with other processing variables and different concentrations of the CO₂ gas.

4.4.2 Experimental Design

The main emphasis in this phase of research was to establish the effects of various processing and mix proportioning variables on the immediate flexural characteristics of

CO₂-cured cement-bonded particleboard. The experimental program comprised these sequential steps (Figure 4.5) concerned with the effects of the processing sequence, CO₂ concentration, and mix proportioning variables. These replicated test specimens were manufactured for each condition in order to derive reliable conclusions through statistical analysis of results.

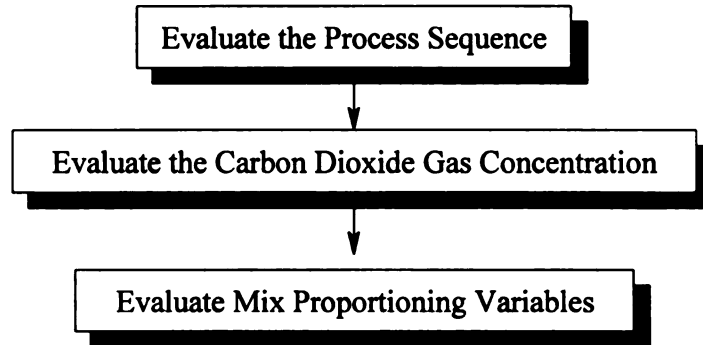


Figure 4.5 The Sequence of Experiments on Cement-Bonded Wood Particleboard

The first step in the experimental program concerned the effects of the two different process sequences of Figure 4.6 on the immediate flexural performance of cement-bonded wood particleboard. Methods I and II in Figure 4.6 comprised total processing times of 3.50 and 4.50 minutes, respectively. The steps in method I involve the application of: (1) 100 psi gas pressure on upper plate and 381 mm (15 in.) Hg of vacuum on bottom plate for 1 minute; (2) 100 psi gas pressure on both top and bottom plates for 2 minutes; and (3) 381 mm (15 in.) Hg of vacuum on both top and bottom plates for 30 seconds. The steps in method II involved the application of: (1) 100 psi gas pressure on the top plate and 381 mm (15 in.) Hg of vacuum on the bottom plate for 1 minute; (2) 50 psi gas pressure on the bottom plate and 381 mm (15 in.) Hg of vacuum on the top plate for 1 minute; (3) 100 psi of gas pressure on both top and bottom plates for 2 minutes; and (4) 381 mm (15 in.) Hg of vacuum on both top and bottom plate for 30 seconds. Softwood (southern pine) was used to evaluate these two process sequences.

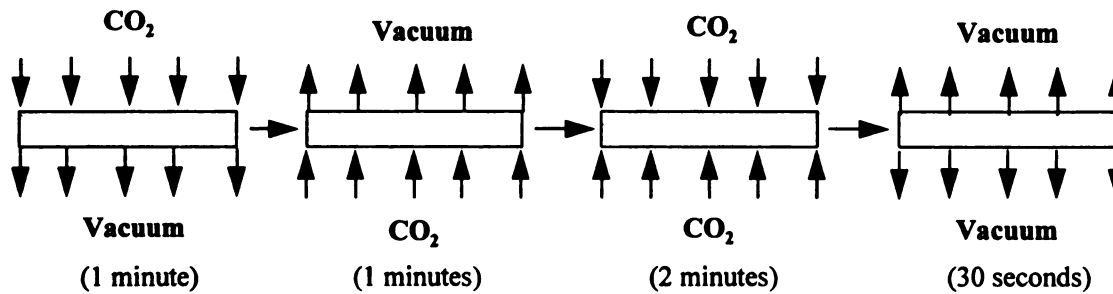
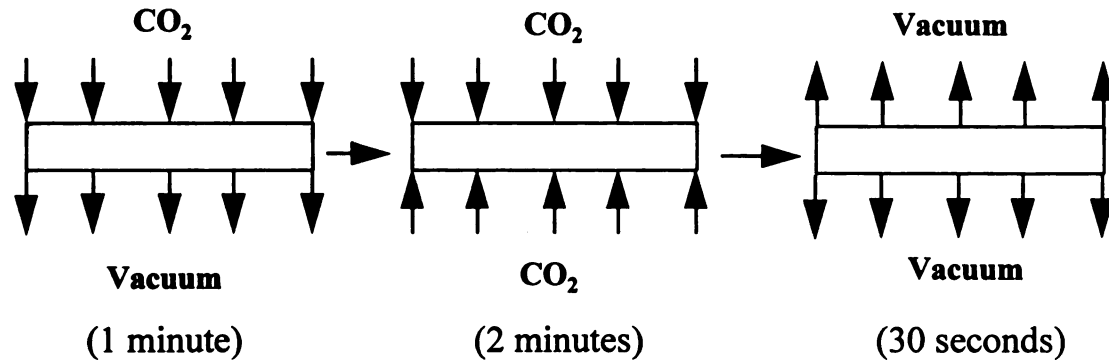


Figure 4.6 The Two Alternative Processing Sequences

Evaluation of the processing sequences of Figure 4.6 would yield the preferable sequence for the remainder of the research investigation. Subsequently, using the preferred processing condition, the effect of CO₂ gas concentration was evaluated through the experimental program of Table 4.3

Table 4.3 Experimental Program to Evaluate Various CO₂ Concentrations

Wood Species	CO ₂ Concentration			
	25 %	50 %	75 %	100 %
Softwood	*	*	*	*
Hardwood	*	*	*	*

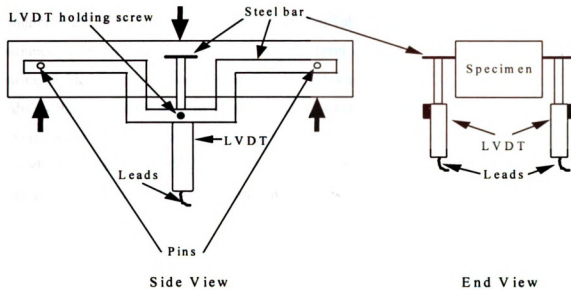
The two earlier steps in this experimental program were conducted with mixes having a wood-cement ratio of 0.28 and a water-cement ratio of 0.25. The last step in this phase of the experimental program concerns the effects of the mix proportioning variables with the process sequence and the CO₂ gas concentration established in the earlier steps. A 2 x 2 x 2 x 2 factorial design of experiments (Table 4.4) was followed in this phase of research.

Table 4.4 Experimental Program for the Evaluation of Various Mix Compositions

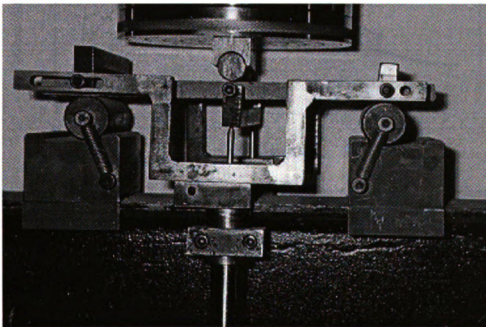
Wood Species	Wood-Cement ratio (by weight)			
	0.28		0.35	
	CO ₂ Concentration		CO ₂ Concentration	
	Low (based on earlier steps)	100%	Low (based on earlier steps)	100%
Softwood	*	*	*	*
Hardwood	*	*	*	*

The flexural test procedure and sample preparation followed the guidelines recommended by ISO 8335 (International Standard) for cement-bonded wood particleboard [77]. The flexural test set-up was a slight modification of that in ISO; a “yoke” (Figure 4.7) was used for accurate measurements of the mid-span deflection under three-point loading where extraneous deformations (e.g. due to penetration into the specimen at supports and load points) are excluded. The flexural test samples had a clear span of 20 cm (7.87 in.), a width of 10 cm (3.94 in.), and a thickness of 1.2 cm (0.47 in.). The photograph of test set-up is shown in Figure 4.7b. A displacement rate of 2.8 mm per minute was used in flexural tests which were conducted in a displacement-controlled mode. A computer controlled data acquisition system was used to record the test data and plot the flexural load-deflection curve. The load-deflection curves are characterized by flexural strength, toughness (area under neath the load-deflection curve), and initial stiffness (defined here as the stiffness obtained through linear regression analysis of the load-

deflection points for loads below 15% of maximum load). The target density of CO₂-cured cement-bonded particleboard was 1.2 g/cm³. All samples were tested immediately after processing CO₂ injection.



(a) Test Set-Up Scale



(b) Photograph of Flexural Test Set-Up

Figure 4.7 The Three-Point Flexural Test Set-Up

4.4.3 Test Results and Statistical Analysis

Processing sequences

Typical load-deflection curves (see Figure 4.8) of cement-bonded particleboards subjected to the two CO₂-curing sequences (see Figure 4.6). The flexural strength, toughness and stiffness test results are presented in Table 4.5 and Figure 4.9. Analysis of variance of test results confirmed that, at 95% level of confidence, method II of CO₂-curing yielded improved flexural performance. This sequence of CO₂-curing essentially reduces the processing time of cement-bonded wood particleboard (under press) from several hours to 4.5 minutes. The board temperature variations with time (covering the periods before and after CO₂ injection) are shown in Figure 4.10. Method II of CO₂-curing is observed to yield higher board temperatures.

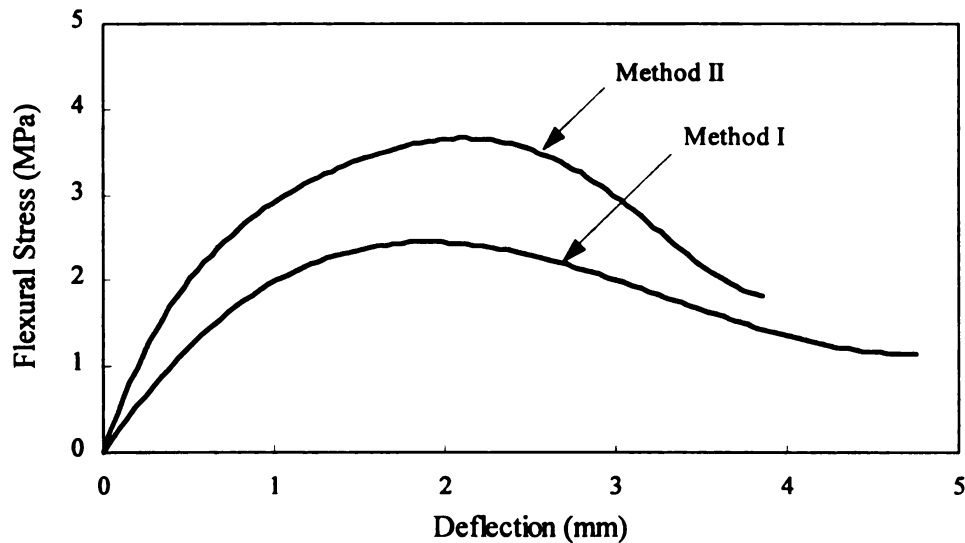
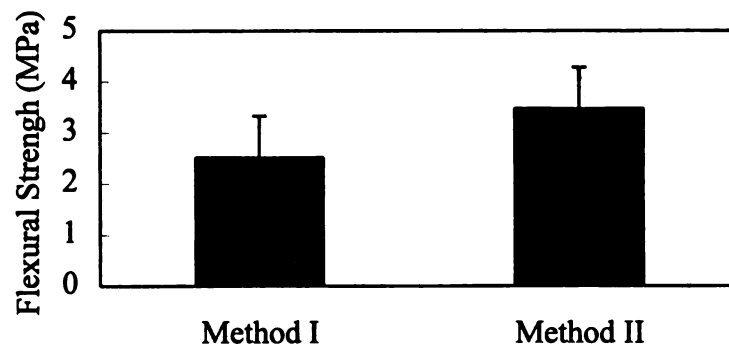


Figure 4.8 Typical Flexural Load-Deflection curves obtained with the Two Process Sequence

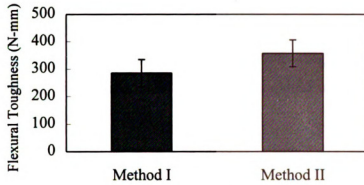
Table 4.5 Flexural Performance of Cement-Bonded Wood Particleboards Subjected to Methods I and II of CO₂-Curing

Processing Sequence	Flexural Strength (MPa)	Flexural Toughness (N-mm)	Initial Stiffness (N/mm)
Method I	2.04	279.180	72.986
	2.88	283.427	103.216
	2.62	293.882	141.029
Mean (St. Dev.)	2.51 (0.43)	285.496 (7.566)	105.744 (34.092)
Method II	3.72	321.901	195.555
	3.67	358.995	249.643
	3.01	391.157	374.275
Mean (St. Dev.)	3.47 (0.39)	357.351 (34.657)	273.158 (91.651)

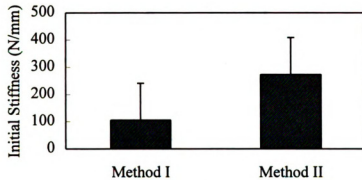


(a) Flexural Strength

Figure 4.9 Effects of the Processing Sequence on Flexural Performance: mean and 95% confidence interval



(b) Flexural Toughness



(c) Initial Stiffness

Figure 4.9 (Cont'd) Effects of the Processing Sequence on Flexural Performance: mean and 95% confidence interval

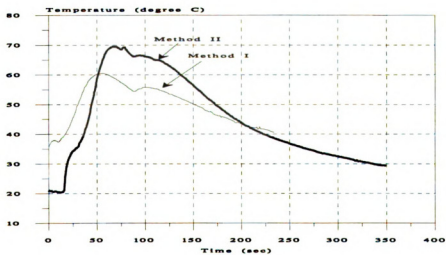
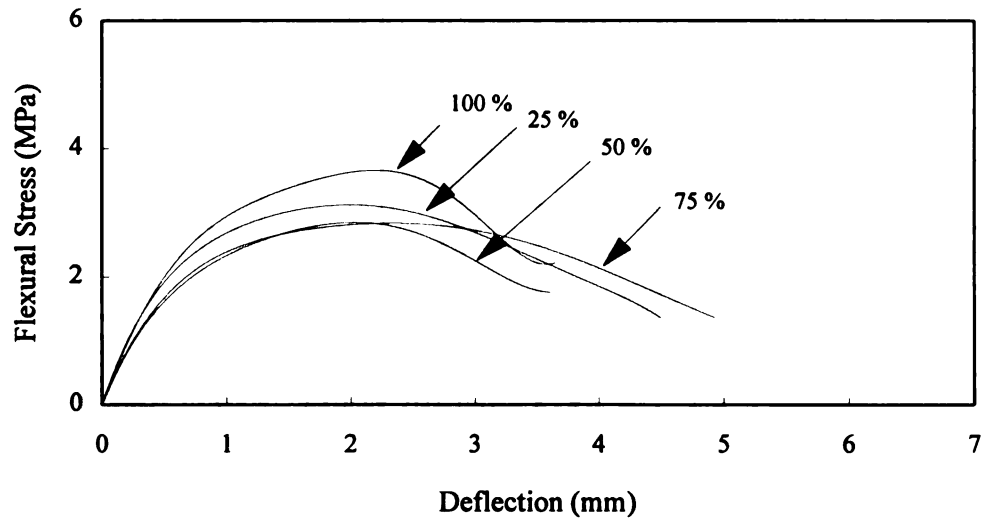


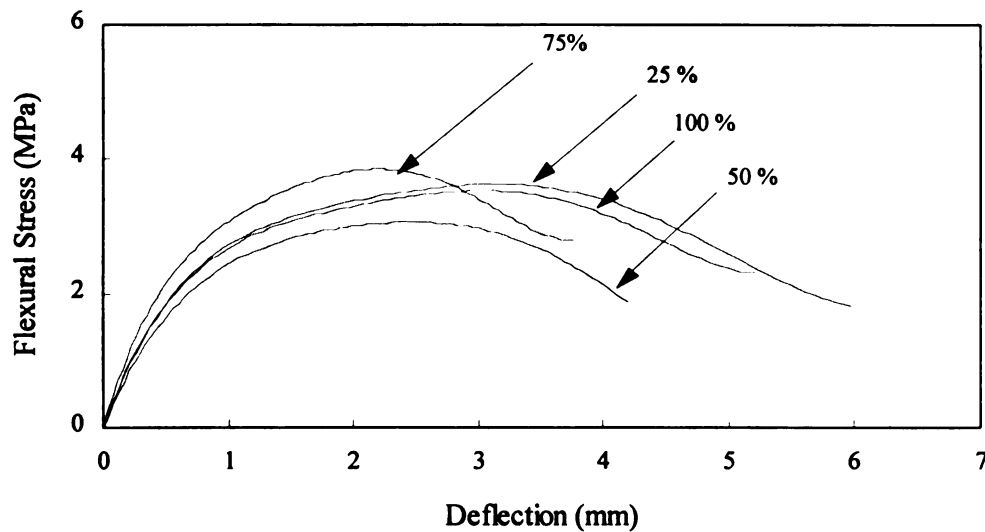
Figure 4.10 Board Temperatures under Method I and II of CO₂-Curing

CO₂ Concentration

Following the preferred sequence (Method II) of CO₂-curing, the effects of CO₂ concentration were evaluated. Typical load-deflection curves (Figure 4.11) obtained with different CO₂ concentrations. The flexural strength, toughness and stiffness test results are shown in Table 4.6 and Figure 4.12.



(a) Softwood

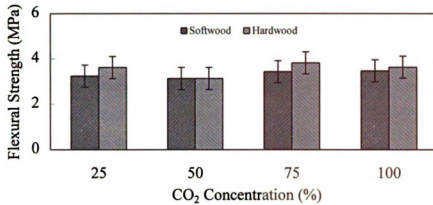


(b) Hardwood

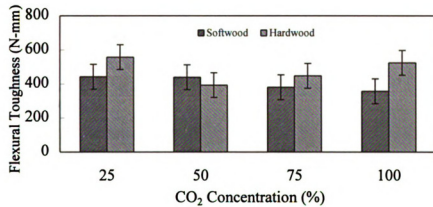
Figure 4.11 Effects of CO₂ Concentration of Flexural Load-Deflection Curves

Table 4.6 Effects of Various CO₂ Concentrations on the Flexural Performance of Cement-Bonded Wood Particleboard

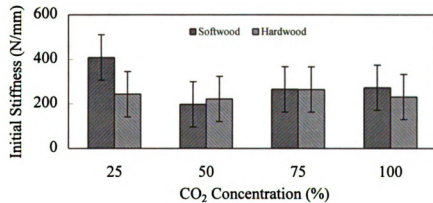
Wood	CO ₂ condition (%)	Weight Gain (g)	Flexural Strength (MPa)	Mean (St. Dev.)	Flexural Toughness (N-mm)	Mean (St. Dev.)	Initial Stiffness (N/mm)	Mean (St. Dev.)
Soft wood	100	42	3.72	3.47 (0.39)	321.901	357.351 (34.657)	195.555	273.158 (91.651)
			3.67		358.995		249.643	
			3.01		391.157		374.275	
	75	49.5	3.47	3.43 (0.24)	471.230	380.754 (107.373)	269.821	265.818 (48.852)
			3.65		408.93		312.546	
			3.18		262.103		215.088	
	50	39	3.06	3.13 (0.09)	442.948	439.942 (4.250)	189.677	198.056 (11.843)
			3.20		436.937		206.436	
	25	18	3.24	3.24 (0.05)	476.143	442.417 (29.668)	410.047	408.616 (2.092)
			3.19		420.343		406.215	
			3.30		430.767		409.586	
Hard wood	100	39.3	4.38	3.63 (0.69)	503.076	524.635 (23.313)	315.867	231.621 (79.678)
			3.52		521.453		221.524	
			3.01		549.376		157.472	
	75	46.7	3.84	3.82 (0.01)	429.558	447.985 (26.362)	364.874	264.943 (94.625)
			3.82		436.215		253.246	
			3.82		478.181		176.711	
	50	32.9	2.96	3.13 (0.23)	369.380	393.338 (29.437)	225.810	222.370 (3.178)
			3.06		384.436		219.542	
	25	11.3	3.39		426.199		221.760	
			3.83	3.62 (0.18)	605.085	557.762 (42.353)	334.874	243.551 (89.756)
			3.47		523.413		240.326	
			3.58		544.789		155.449	



(a) Flexural Strength



(b) Flexural Toughness



(c) Initial Stiffness

Figure 4.12 Effects of Various CO₂ Concentrations on the Flexural Performance of Cement-Bonded Wood Particleboard: mean and 95% confidence interval

The following conclusions could be derived from the data regarding the effects on CO₂ concentration on flexural performance.

A lower concentration of CO₂ concentration observed comparable to those obtained at 100% CO₂ on flexural strength and toughness. Initial stiffness case 25% CO₂ concentration softwood board better property than other (50%, 75%, 100%) concentration. Overall hardwood properties were slightly better than softwood. These observations were confirmed through 95% level of confidence.

Block analysis of variance of the flexural test results indicated, at 95% level of confidence, that flexural strength, toughness and stiffness values were comparable at different CO₂ concentrations ranging from 25 to 100%. Economic criteria encourage the use of low CO₂ concentrations.

Effect of Mix proportions

The complete flexure test results for this phase of the experimental program is shown in Table 4.7. The methodology adopted for the analysis of data is illustrated in Figure 4.13. Only two factor interactions were considered to be of significance and three factor interactions were used as part of the error term. The results of statistical analysis are presented in Table 4.8. The trends of in the effects of different variables obtained by analysis of variance of results are shown in Figure 4.14 to 4.16. The cube plots resulting from statistical analysis of the flexure test results are shown in Figure 4.17. A review of Table 4.8 indicated that only wood-cement ratio has any statistically significant effect on flexural strength. The two CO₂ concentrations (25% and 100%) as well as the two wood species (softwood and hardwood) yielded comparable flexural strength. The trend in the effect of wood-cement ratio on flexural strength is shown in Figure 4.14. The cube plot of Figure 4.17a further demonstrates the effects of different variables on flexural strength. Increasing the wood-cement ration for 0.28 to 0.35 led to an average reduction of 18% in flexural strength.

Table 4.8 suggests that more of the variables canceled had any statistical significant effect, at 95% level of confidence on the flexural toughness of cement-bonded parti-

cleboard. At 90% level of confidence, however, wood species and CO₂ concentration started to have statistically significant effects. Hardwood, when compared to softwood, yielded higher flexural toughness, and 25% of CO₂ concentration performed better in this regard. The trends and cube plot relevant to flexural toughness are shown in Figure 4.15 and 4.17b. On the average, flexural toughness with hardwood was 15% higher than with softwood. At 25% CO₂ concentration, flexural toughness values gained which were 16% higher than those of 100% CO₂.

As far as the initial stiffness is concerned, as shown in Table 4.8, all three factors (wood-cement ratio, CO₂ concentration and wood species) had statistically significant effect at 95% level of confidence. The trends shown in Figure 4.16 and the cube plot of Figure 4.17c further clarify the results. At 0.28 wood-cement ratio, flexural stiffness was with average, 39% more than that of 0.35 wood-cement ratio. The 25% CO₂ concentration yielded average initial stiffness which were 40% higher than that of 100% CO₂ concentration. The softwood also produced initial stiffness which were on the average 23% higher than that with hardwood.

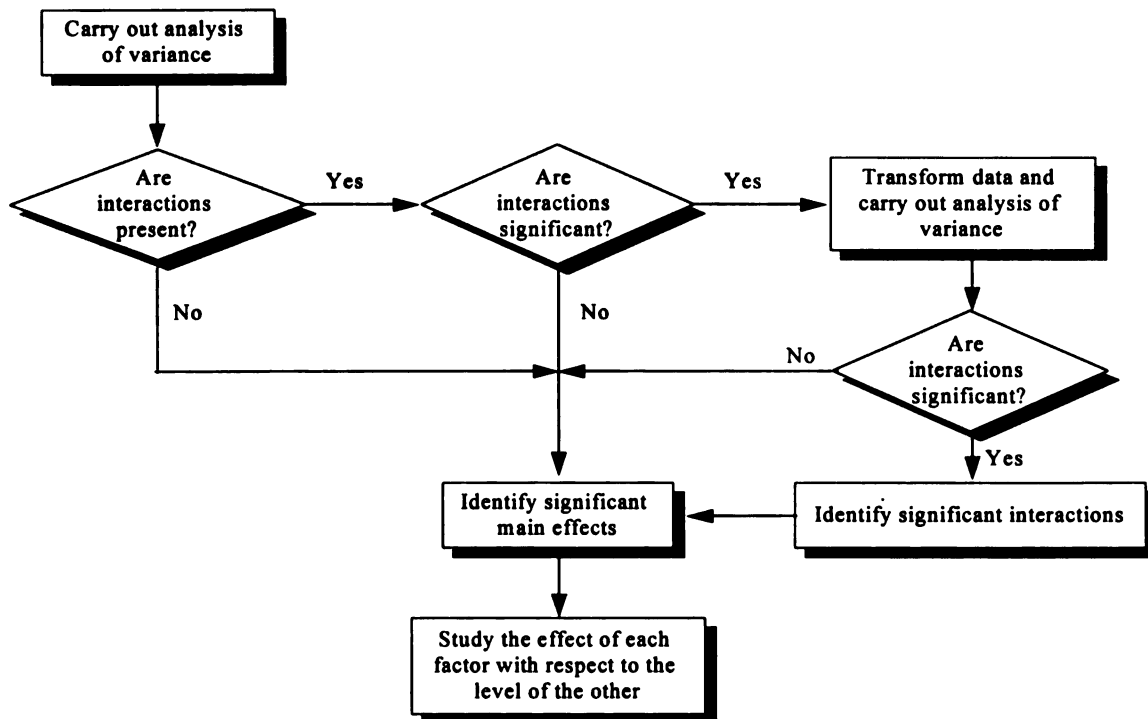


Figure 4.13 Methodology of Analysis [86]

Table 4.7 Flexure Test Results

	Wood-Cement ratio							
	0.28				0.35			
	CO ₂ concentration				CO ₂ concentration			
	25		100		25		100	
	Wood Species		Wood Species		Wood Species		Wood Species	
	Softwood	Hardwood	Softwood	Hardwood	Softwood	Hardwood	Softwood	Hardwood
Flexural Strength (MPa)	3.24 3.19 3.30	3.83 3.47 3.58	3.72 3.67 3.01	4.38 3.52 3.01	3.73 2.25 2.56	3.68 3.15 2.89	2.60 2.25 3.02	3.39 2.08 2.73
Mean (St. Dev.)	3.24 (0.05)	3.62 (0.18)	3.47 (0.39)	3.63 (0.69)	2.85 (0.78)	3.24 (0.40)	2.62 (0.38)	2.73 (0.65)
Flexural Toughness (N-mm)	476.143 420.343 430.767	605.085 523.413 544.789	321.901 358.995 391.157	503.076 521.453 549.376	661.279 343.652 437.263	670.329 588.999 321.624	330.915 390.543 501.891	549.339 302.260 360.276
Mean (St. Dev.)	442.417 (29.668)	557.762 (42.353)	357.351 (34.657)	524.635 (23.313)	480.731 (163.214)	526.984 (182.437)	407.783 (86.782)	403.358 (129.202)
Initial Stiffness (N/mm)	410.047 406.215 409.586	334.874 240.326 155.449	195.555 249.643 374.275	315.867 221.524 157.472	294.624 283.784 272.656	351.066 143.232 204.627	117.124 114.684 96.532	59.266 108.098 98.496
Mean (St. Dev.)	408.616 (2.092)	243.551 (89.756)	273.158 (91.651)	231.621 (79.678)	283.688 (10.984)	232.975 (106.777)	109.447 (11.251)	88.62 (25.871)

Table 4.8 The Results of the Analysis of Variance (Flexural strength, Toughness, and Initial Stiffness)

	Source	Sum-of-Squares	DF	Mean-Square	F-Ratio	P
Flexural Strength	A*	2.400	1	2.400	10.083	0.006
	B	0.093	1	0.093	0.389	0.541
	C	0.419	1	0.419	1.759	0.202
	AxB	0.348	1	0.348	1.462	0.243
	BxC	0.093	1	0.093	0.389	0.541
	AxC	0.001	1	0.001	0.004	0.951
	Residual**	4.047	17	0.238		
Flexural Toughness	A	1474.673	1	1474.673	0.138	0.714
	B	37013.075	1	37013.075	3.476	0.080
	C	39623.189	1	39623.189	3.721	0.071
	AxB	2268.648	1	2268.648	0.213	0.650
	BxC	1.300	1	1.300	0.000	0.991
	AxC	21636.135	1	21636.135	2.032	0.172
	Residual**	181032.641	17	10648.979		
Initial Stiffness	A*	73332.679	1	73332.679	16.951	0.001
	B*	81427.675	1	81427.675	18.823	0.000
	C*	29011.254	1	29011.254	6.706	0.019
	AxB	10992.238	1	10992.238	2.541	0.129
	BxC	8826.176	1	8826.176	2.040	1.171
	AxC	6840.789	1	6840.789	1.581	0.226
	Residual**	73542.605	17	4326.036		

*: statistically significant at the 5% level

**: Residual estimated using three way interaction

A: Wood/Cement ratio; B: CO₂ concentration; C: Wood species

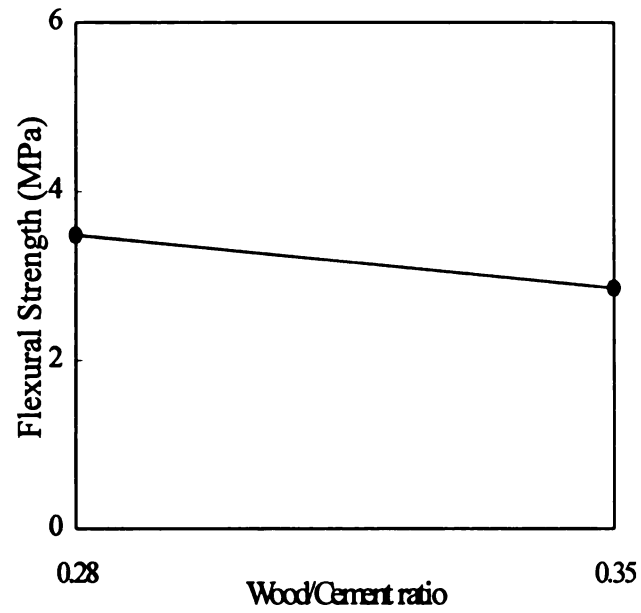


Figure 4.14 The Trends in Flexural Strength

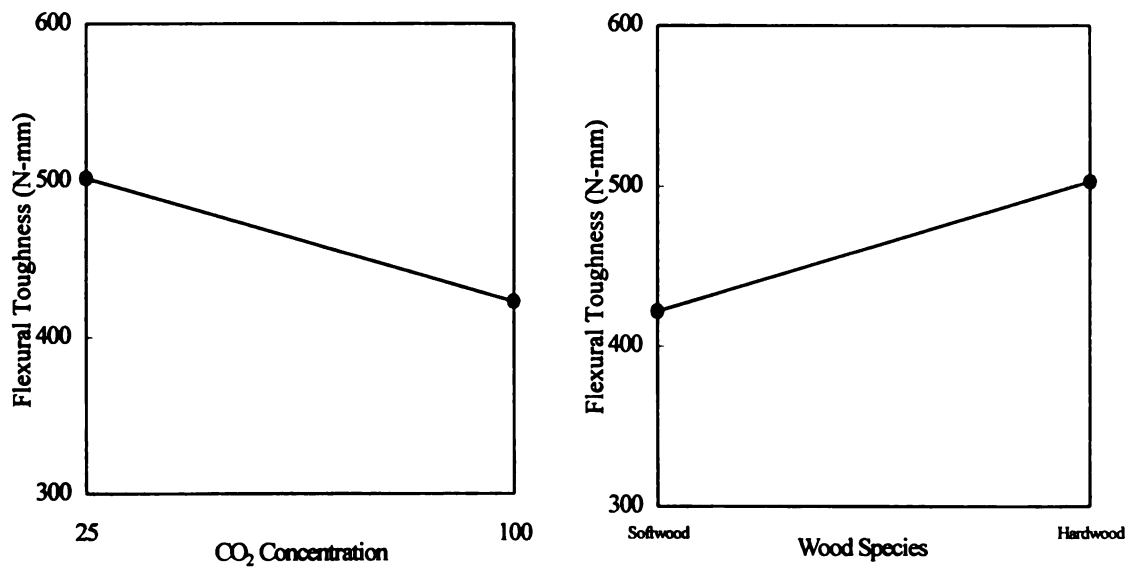


Figure 4.15 The Trends in Flexural Toughness

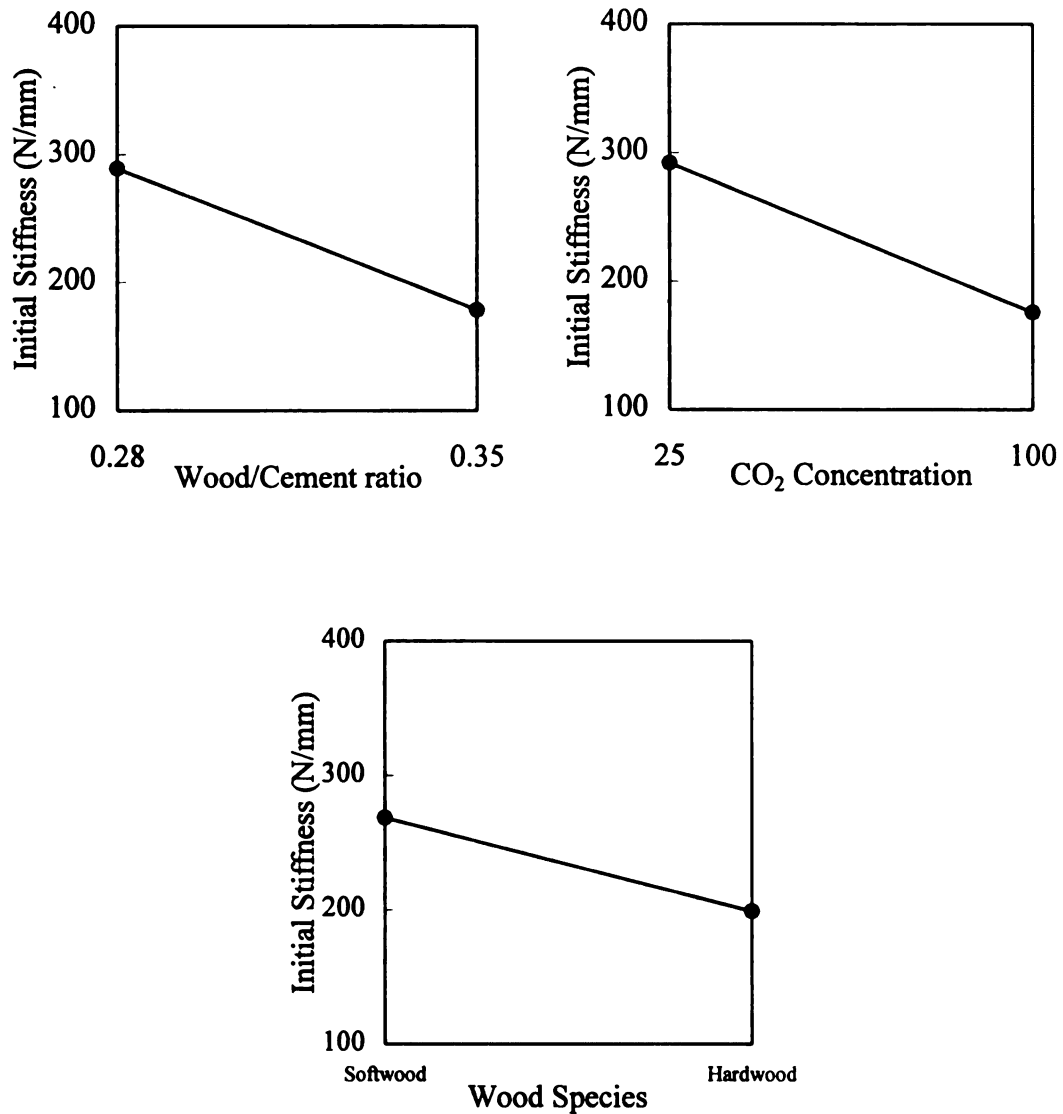
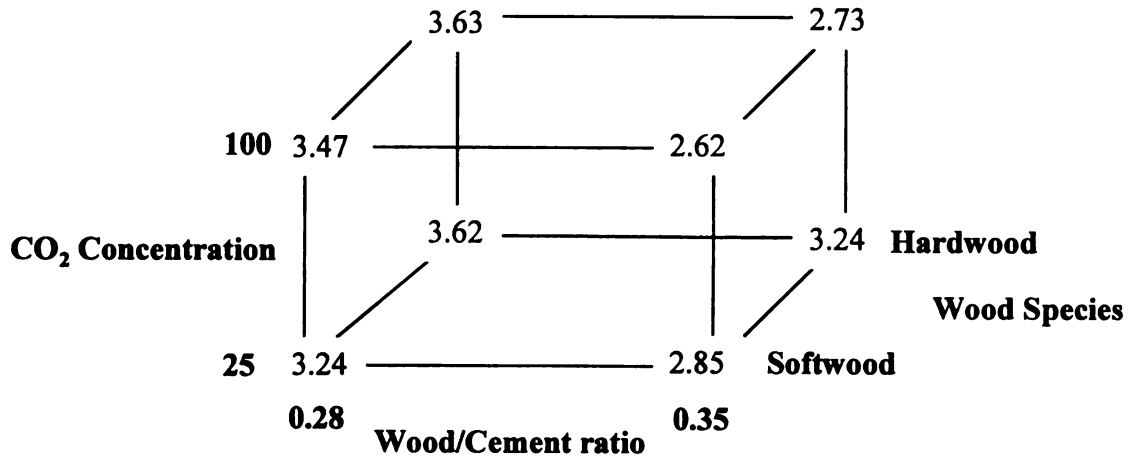
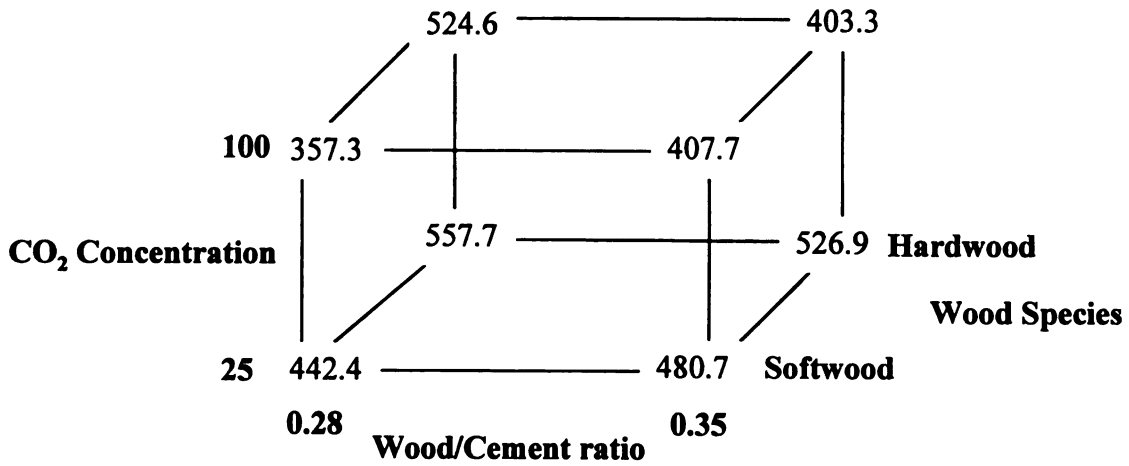


Figure 4.16 The Trends in Initial Stiffness

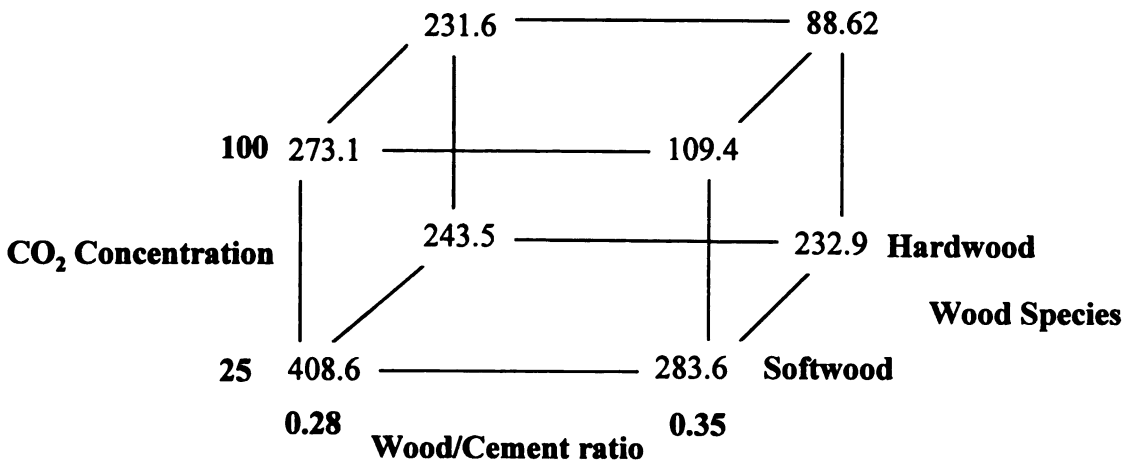
The statistical analysis and discussion presented above suggest that a wood-cement ratio of 0.28 and CO₂ concentration of 25% yield cement-bonded wood particle-board with desirable performance and cost position.



(a) Flexural Strength (MPa)



(b) Flexural Toughness (N-mm)



(c) Initial Stiffness (N/mm)

Figure 4.17 Cube Plot of Flexure Test Results

4.5 CELLULOSE FIBER REINFORCED CEMENT COMPOSITES

The main thrust of this phase of research was to determine the effects of processing variables on cellulose fiber reinforced cement boards subjected to CO₂ pre-curing followed by autoclave curing.

4.5.1 Materials, Manufacturing Procedures and Experimental Program

The cellulose fiber selected for this investigation was Southern Softwood Kraft (SSK) pulp [83]. Average length of this fiber is 3.0 mm. The fiber mass fraction and matrix mix proportions used in this phase of the study are introduced in Table 4.9. In the slurry-dewatering method of manufacture, thin-sheet specimens were formed from a dilute slurry of approximately 20% solids. A relatively small dosage of diluted flocculent [84] (flocculent/cement = 0.001 by weight) was added to achieve agglomeration of cement particles in order to prevent passing of particles through the filtering screens during dewatering. Fiber mass fraction, in the slurry-dewatering method of manufacturing, is generally defined as the ratio of fibers to the dry constituents of the matrix by weight. The gradation of the silica sand used in this investigation is illustrated in Figure 4.18 (ASTM E-11).

Table 4.9 The Composition of Cellulose Fiber Reinforced Cement Composite

Fiber Type	Fiber Mass Fraction (%)	Sand-Binder ratio (by weight)	Flocculent-Cement ratio (by weight)	Silica Fume-Cement ratio (by weight)
Softwood Kraft Pulp (SSK)	8	0.75	0.001	0.75

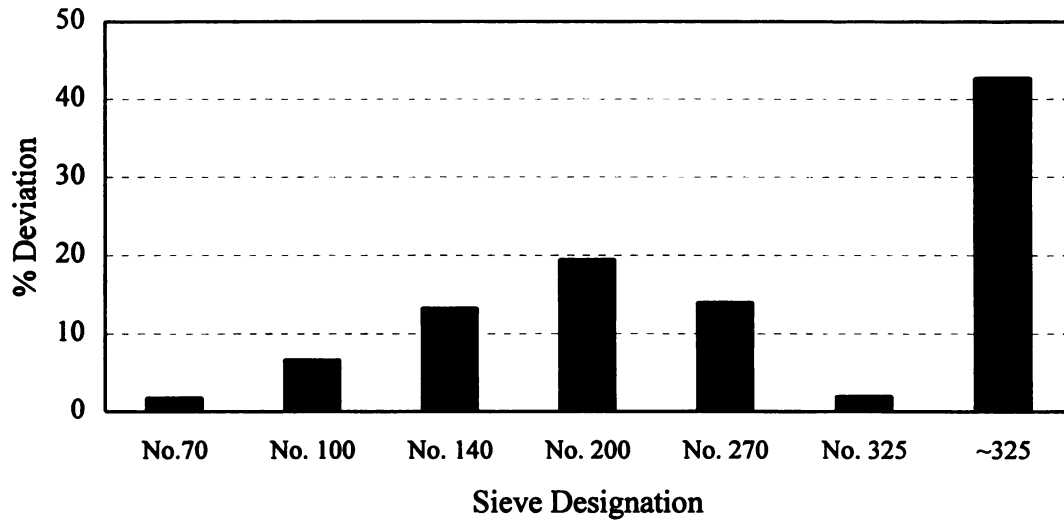


Figure 4.18 Gradation of Silica Sand (typical mean % deviation on individual sieves)

Thin-sheet cellulose fiber reinforced cement composites were manufactured as follows: (1) a weighted dry lap of cellulose fiber was soaked in water for a minimum period of 4 hours; (2) a laboratory-scale pulp disintegrator (TMI refiner) was used at a speed of 3,000 rpm. The beating time used in this study was 10 minutes (yielding refined cellulose fibers with Canadian Standard Freeness of 500 ± 50); (3) The fibers, sand, flocculating agent and cement were proportioned; (4) The ingredients were mixed in water to produce a slurry of 20% solids by weight; a high-speed mixer was used to achieve a uniform dispersion of cellulose fibers and other mix ingredients in the slurry. Flocculating agent is the last solid constituent to be added, which improves the binding of cement particles to cellulose fibers and controls the escape of cement particles during vacuum-dewatering of the slurry (when the excess water is extracted). The extraction of water is actually performed in two stages. First, the excess water on top of the settled slurry is removed, and then the settled slurry is put in a vacuum box 305 mm by 305 mm (12 in. by 12 in.) in planer dimensions. The slurry is evenly spread onto the screen of the vacuum box, and then vacuum is applied at 381 mm (15 in.) Hg of mercury. The sheet is then removed on the filter screen. The sheet together with the screen are stored between two steel plates. Two sheets were made in this manner, with the first one being stored temporarily with its

screen between steel plates in a sealed plastic bag. The screen was then removed and the bottom face of the second sheet was placed against the top face of the first sheet, as shown in Figure 4.19. The sheets are then slightly pressed for 5 minutes at a pressure of 0.24 MPa (35 psi) and 32 MPa (464 psi) simulating unpressed and pressed production conditions, respectively. The preparation is completed within one hour of starting the mix. After the completion of processing the screen is carefully removed from the sheets which are then stacked flat in a pre-curing oven or carbonation chamber. After pre-curing, the sheets are autoclaved.



Figure 4.19 Schematic of Formation of Two-Ply Cellulose Fiber Reinforced Cement Composite Sheet

There are several reasons for using an autoclave in the curing of cellulose fiber reinforced cement composites [85]. Autoclave curing changes the chemistry of hydration and results in a product that has substantially different properties from products cured below 100°C. The most important improvements are:

1. Products are ready for use within 24 hours; the early age strength is generally equivalent to 28-day strength under ambient curing
2. Substantially less creep and shrinkage
3. Better sulfate resistance
4. Elimination of efflorescence
5. Lower moisture content after curing

High pressure steam curing can only be used for precast concrete products. It can be used to advantage in the manufacture of specialty products, such as lightweight cellular concrete and calcium silicate (sand-lime) bricks. The curing cycle is similar to that

used in low-pressure steam curing and consists of a “presteaming” period, a “soaking” period, and controlled rates of heating and cooling. The rate of pressure release at the end of the soaking period should also be controlled. The autoclave time-pressure cycles pattern used in this study is shown in Figure 4.20.

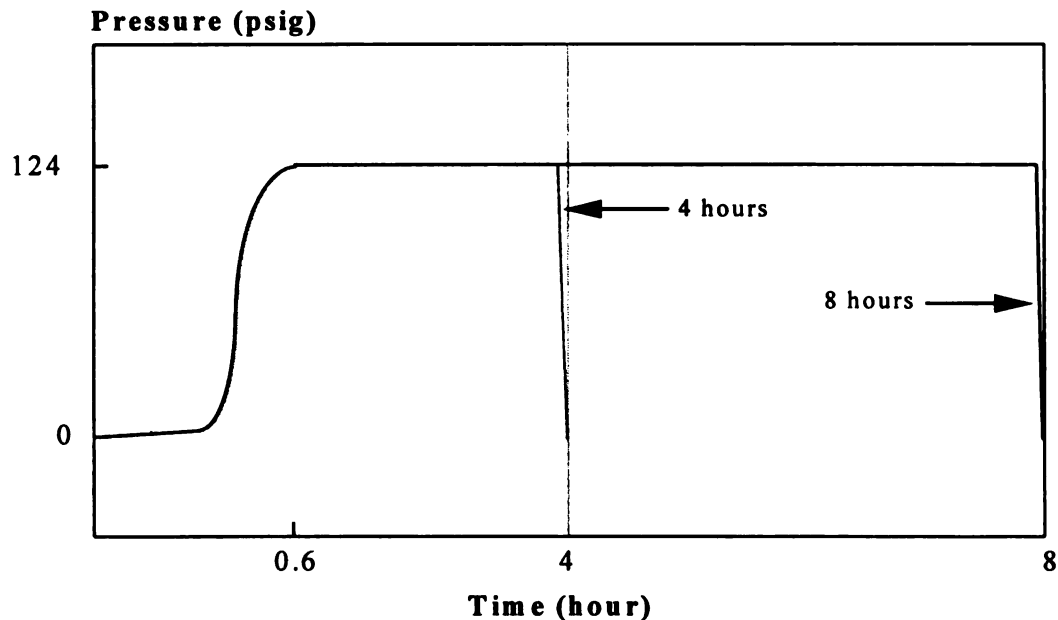


Figure 4.20 Time-Pressure Cycles in Autoclave

The laboratory-scale manufacturing and curing facilities used in this investigation are presented in Figure 4.21. The full factorial experimental program followed in this phase of the studying is in Table 4.10a (pressed board) and Table 4.10b (unpressed board). Each case (pressed or unpressed) has two different control conditions. In the pressed case, one control condition involves: (1) making of the board; (2) storing for one day in plastic bag and then removing from the plastic bag; and (3) autoclave curing for 8 hours. The second control condition of pressed case was similar to the first except the 24 hours of storage in plastic bag was in placed with one hour of storage in oven at 50°C followed by one hour of steam curing at 50°C and 95% relative humidity. For the unpressed case, the two control conditions are introduced in Table 4.10b.

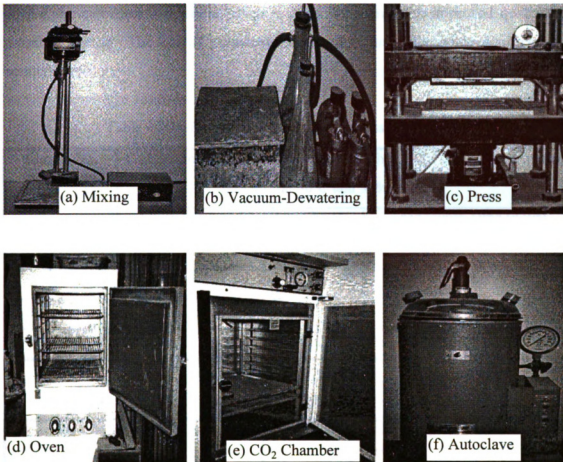


Figure 4.21 Carbonation Curing Facilities for Cellulose Fiber Reinforced Cement Composites

The experimental design for the pressed and unpressed boards are presented in Table 4.10a and b, respectively. The variables in the pressed case were the oven temperature used for pre-drying of young sheets prior to CO₂ pre-curing and the autoclave duration. This research investigated the effects of these variables through a full factorial experimental design implemented with the following variables: oven temperature, oven duration, CO₂ chamber duration and autoclave duration. In both pressed and unpressed cases, oven-drying is used to lower the moisture content of board to the point where CO₂ penetration and reaction would be facilitated. After drying, in the humid environment of CO₂ chamber the penetration of CO₂ (possibly with water vapor) into the board accom-

plishes the carbonation reaction, which provide the board with improved qualities for autoclave curing. The low CO₂ concentration used in this study yields significant economic benefition.

Table 4.10a Design of Experimental (Pressed Composite)

Sample No.	Carbonation Chamber Storage Time: 1 hour (20% CO ₂ concentration) at 50°C and 95% RH	
	Oven Temperature (°C): 1 hour	Autoclave Time (hour)
1	50	4
2	50	8
3	100	4
4	100	8

Table 4.10b Design of Experimental (Unpressed Composite)

Factor	Code	Factor Level		Control 1	Control 2
		-	+		
Oven temperature (°C)	A	50	100	50	
Duration in oven (hours)	B	1	2	1	
Duration in CO ₂ chamber: @20% CO ₂ concentration (hours) (50°C and 95% RH)	C	1	4	1 (0% CO ₂)	
Autoclaved duration (hour)	D	4	8	4	8

4.5.2 Experimental Set-Up

Flexural tests were performed according to the ASTM C 1185. The test set-up is similar to that described earlier for cement-bonded particleboard, except for the dimensions which are different. The flexural test samples have a clear span of 254 mm (10 in.), a width of 152.4 mm (6 in.), and a thickness 10 mm (0.4 in.) for unpressed boards and 7 mm (0.3 in.) for pressed boards. Figure 4.22 shows photograph of the 3-point flexural

test set-up used for cellulose fiber reinforced cement composites. The flexural performance was evaluated in wet condition. The specimens were immersed in water at a temperature of $23 \pm 4^{\circ}\text{C}$ ($73 \pm 7^{\circ}\text{F}$) for a period of 48 hours minimum. The specimens were tested immediately upon removal from the water.

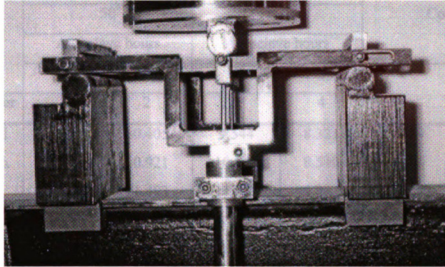


Figure 4.22 Photograph of the Flexural Test Set-Up for Cellulose Fiber-Cement Composite

4.5.3 Test Results and Statistical Analysis

The flexural test results are shown in Table 4.11a and Figure 4.23a (pressed) and a Table 4.11b and Figure 4.23b (in the case of unpressed). The methodology for statistical analysis of data was described earlier and the results are given in Figure 4.13. In pressed boards, the variables considered were: oven temperature and autoclave time. In unpressed boards, only two-factor interactions were considered to be of significance (and three and four factor interactions were used the error term). The result of analysis of variance for pressed and unpressed case are shown in Table 4.12 and 4.13, respectively. Trends caused by the main effects and interactions are in Figure 4.24 to 4.26. Due to the significance of interaction in the initial analysis of variance, the data were transformed (by log) then re-analysis of variance. The results of transformed analysis of variance (Tables 4.14 and 4.15) are almost same.

Table 4.11a Flexural Performance of Cellulose Fiber Reinforced Cement Composites (pressed)

	Duration of CO ₂ chamber: 1 hour (20% CO ₂ concentration)				Control	
	Oven temperature (1 hour)					
	50		100			
	Autoclave hours		Autoclave hours			
	4	8	4	8	1*	2**
Run Order	1	2	3	4		
Flexural	9.579	10.405	9.544	8.321	9.069	8.301
Strength	10.526	10.921	10.523	8.540	9.826	7.720
(MPa)	10.878	11.493	11.082	8.070	10.75	7.936
Mean	10.328	10.940	10.383	8.31	9.882	7.986
(St. Dev.)	(0.672)	(0.544)	(0.778)	(0.235)	(0.842)	(0.294)
Flexural	2282.875	2824.791	1976.035	1621.520	2763.849	2320.836
Toughness	2293.417	2432.216	2343.211	1687.707	2936.193	1953.452
(N-mm)	2339.175	2091.657	2931.211	1651.460	3224.134	2056.126
Mean	2305.156	2449.522	2417.024	1653.562	2974.725	2110.138
(St. Dev.)	(29.926)	(366.874)	(482.151)	(33.144)	(232.549)	(189.554)
Initial	109.760	161.390	98.777	100.521	119.062	116.018
Stiffness	102.488	132.390	111.203	148.833	121.549	116.464
(N/mm)	93.488	108.135	128.203	85.831	134.767	113.626
Mean	101.861	134.053	112.740	111.728	125.126	115.369
(St. Dev.)	(8.146)	(26.656)	(14.792)	(32.962)	(8.441)	(1.526)

*Control 1: 1 hour in oven at 50°C, then 1 hour in steam box at 50°C and 95% RH, and finally 8 hours autoclave

**Control 2: 24 hours inside plastic bag, and then 8 hours in autoclave

Table 4.11b Flexural Performance of Cellulose Fiber Reinforced Cement Composite (upressed)

Run order	A	B	C	D	Strength (MPa)	Mean (St. Dev.)	Toughness (N-mm)	Mean (St. Dev.)	Stiffness (N/mm)	Mean (St. Dev.)
1	-	-	-	-	5.135 5.866 5.538	5.513 (0.366)	3002.119 2329.511 2629.431	2653.687 (336.959)	137.632 141.769 140.167	139.856 (2.086)
2	+	-	-	-	5.432 5.918 4.918	5.423 (0.5)	1999.263 2007.884 1922.771	1976.639 (46.850)	157.213 176.426 107.288	146.976 (35.688)
3	-	+	-	-	5.723 5.331 4.935	5.330 (0.394)	1966.347 1843.331 1808.799	1872.826 (82.812)	81.642 80.342 79.621	80.535 (1.024)
4	+	+	-	-	3.084 5.461 4.321	4.289 (1.189)	670.425 1180.216 869.211	906.617 (256.946)	31.089 45.042 40.568	38.900 (7.125)
5	-	-	+	-	7.079 7.035 7.055	7.056 (0.022)	2554.452 2401.637 2429.364	2461.818 (81.413)	116.016 111.432 113.214	113.554 (2.311)
6	+	-	+	-	7.406 5.785 6.993	6.728 (0.842)	2793.201 2624.798 2683.703	2700.567 (85.459)	166.653 159.653 163.213	162.983 (3.791)
7	-	+	+	-	2.529 2.556 2.490	2.525 (0.033)	838.152 829.555 814.732	827.480 (11.847)	51.678 53.216 59.598	54.831 (4.200)
8	+	+	+	-	2.437 2.005 2.236	2.226 (0.216)	954.226 609.203 782.214	781.881 (172.512)	54.432 20.490 40.316	38.413 (17.051)
9	-	-	-	+	5.327 5.183 5.695	5.402 (0.264)	2183.562 1966.189 2314.418	2154.723 (175.897)	105.221 104.215 108.184	105.873 (2.063)
10	+	-	-	+	3.106 3.187 3.099	3.131 (0.049)	885.823 737.394 799.921	807.713 (74.521)	46.102 39.990 43.210	43.101 (3.057)
11	-	+	-	+	3.963 3.503 3.713	3.726 (0.230)	1916.395 1545.357 1721.334	1727.695 (185.601)	120.150 110.003 115.412	115.188 (5.077)
12	+	+	-	+	3.821 4.260 3.578	3.886 (0.346)	1510.313 1419.553 1642.057	1523.974 (111.879)	89.216 84.958 92.232	88.802 (3.655)
13	-	-	+	+	4.678 5.216 6.125	5.340 (0.731)	2515.911 2843.524 3223.308	2860.914 (354.019)	141.786 146.219 154.340	147.448 (6.367)
14	+	-	+	+	6.326 6.471 6.080	6.292 (0.198)	2721.226 2632.058 2972.258	2775.181 (176.401)	139.213 165.021 133.073	145.769 (16.953)
15	-	+	+	+	5.810 4.323 4.826	5.320 (± 0.863)	3204.346 2217.397 2823.421	2748.388 (497.734)	206.071 135.995 170.221	170.762 (35.041)
16	+	+	+	+	3.820 3.530 4.486	3.945 (0.490)	1526.931 1380.532 1813.403	1573.622 (220.180)	92.624 71.170 113.059	92.284 (20.947)
Control 1					3.200 4.438 3.284	3.641 (0.692)	1596.002 2173.015 1349.216	1706.078 (422.787)	105.400 108.416 96.915	103.577 (5.963)
Control 2					4.225 5.499 5.392	5.039 (0.707)	1956.227 2345.003 2004.321	2101.850 (211.945)	159.526 142.926 150.338	150.930 (8.316)

A: Oven Temperature; B: Oven duration; C: Autoclave duration; D: CO₂ chamber duration

Table 4.12 Analysis of Variance of the Flexural Test Results for Cellulose Fiber Reinforced Cement Composites (pressed)

	Source	Sum-of-Squares	DF	Mean-Square	F-Ratio	P
Flexural Strength	A*	4.969	1	4.969	14.108	0.006
	B	1.600	1	1.600	4.543	0.066
	AxB*	5.406	1	5.406	15.347	0.004
	Error	2.818	8	0.352		
Flexural Toughness	A	351229.635	1	351229.635	3.810	0.087
	B	287238.609	1	287238.609	3.116	0.116
	AxB*	617879.107	1	617879.107	6.703	0.032
	Error	737490.006	8	92186.251		
Initial Stiffness	A	97.944	1	97.944	0.188	0.676
	B	723.558	1	723.558	1.390	0.272
	AxB	819.673	1	819.673	1.575	0.245
	Error	4164.151	8	520.519		

***: statistically significant at the 95% level of confidence**

A: Oven temperature; B: Autoclave duration

Table 4.13 Analysis of Variance of the Flexural Test Result for Cellulose Fiber Reinforced Cement Composites (unpressed)

	Source	Sum-of-Squares	DF	Mean-Square	F-Ratio	P
Flexural Strength	A*	2.937	1	2.937	4.572	0.039
	B*	36.596	1	36.596	56.968	0.000
	C	1.080	1	1.080	1.691	0.203
	D	1.063	1	1.063	1.654	0.206
	AxB	0.044	1	0.044	0.068	0.795
	AxC	1.197	1	1.197	1.863	0.180
	AxD	0.036	1	0.036	0.057	0.813
	BxC*	16.910	1	16.910	26.323	0.000
	BxD*	8.494	1	8.494	13.223	0.001
	CxD*	7.770	1	7.770	12.095	0.001
	Error	23.769	37	0.642		
Flexural Toughness	A*	3404809.595	1	3404809.595	32.057	0.000
	B*	7749175.874	1	7749175.874	72.960	0.000
	C*	1808828.796	1	1808828.796	17.030	0.000
	D*	743037.733	1	743037.733	6.996	0.012
	AxB	50554.245	1	50554.245	0.476	0.495
	AxC*	847986.003	1	847986.003	7.984	0.008
	AxD	347374.498	1	347374.498	3.271	0.079
	BxC*	2048637.340	1	2048637.340	19.288	0.000
	BxD*	3595525.742	1	3595525.742	33.852	0.000
	CxD*	3600399.093	1	3600399.093	33.898	0.000
	Error	3929843.933	37	106211.998		
Initial Stiffness	A*	5459.051	1	5459.051	13.555	0.001
	B*	19931.029	1	19931.029	49.489	0.000
	C*	5229.417	1	5229.417	12.985	0.001
	D*	3316.272	1	3316.272	8.234	0.007
	AxB*	4516.572	1	4516.572	11.215	0.002
	AxC	1103.569	1	1103.569	2.740	0.106
	AxD*	5292.105	1	5292.105	13.140	0.001
	BxC*	1923.067	1	1923.067	4.775	0.035
	BxD*	26469.427	1	26469.427	65.724	0.000
	CxD*	10763.641	1	10763.641	26.726	0.000
	Error	14901.173	37			

*: statistically significant at 95% level of confidence

A: Oven temperature; B: Oven duration; C: Autoclave duration; D: CO₂ chamber duration

Table 4.14 Results of Analysis of Variance after Transformation (pressed)

	Source	Sum-of-Squares	DF	Mean-Square	F-Ratio	P
Flexural Strength	A*	0.054	1	0.054	16.269	0.004
	B	0.020	1	0.020	5.942	0.041
	AxB*	0.058	1	0.058	17.468	0.003
	Error	0.027	8	0.003		
Flexural Toughness	A*	0.093	1	0.093	5.949	0.041
	B	0.074	1	0.074	4.729	0.061
	AxB*	0.132	1	0.132	8.495	0.019
	Error	0.125	8	0.016		
Initial Stiffness	A	0.007	1	0.007	0.202	0.665
	B	0.040	1	0.040	1.118	0.321
	AxB	0.064	1	0.064	1.791	0.218
	Error	0.288	8	0.036		

*: statistically significant at 95% level of confidence

A: Oven temperature; B: Autoclave duration

Table 4.15 Results of Analysis of Variance after Transformation (unpressed)

	Source	Sum-of-Squares	DF	Mean-Square	F-Ratio	P
Flexural Strength	A*	0.191	1	0.191	5.704	0.022
	B*	1.830	1	1.830	54.753	0.000
	C	0.001	1	0.001	0.022	0.883
	D	0.002	1	0.002	0.057	0.812
	AxB	0.003	1	0.003	0.076	0.784
	AxC	0.051	1	0.051	1.519	0.225
	AxD	0.003	1	0.003	0.085	0.772
	BxC*	0.926	1	0.926	27.705	0.000
	BxD*	0.558	1	0.558	16.696	0.000
	CxD*	0.673	1	0.673	20.141	0.000
	Error	1.236	37	0.033		
Flexural Toughness	A*	1.373	1	1.373	33.930	0.000
	B*	2.568	1	2.568	63.466	0.000
	C*	0.311	1	0.311	7.689	0.009
	D*	0.382	1	0.382	9.450	0.004
	AxB	0.016	1	0.016	0.405	0.528
	AxC*	0.472	1	0.472	11.658	0.002
	AxD	0.082	1	0.082	2.036	0.162
	BxC*	0.931	1	0.931	23.008	0.000
	BxD*	2.030	1	2.030	50.159	0.000
	CxD*	1.380	1	1.380	34.099	0.000
	Error	1.497	37	0.040		
Initial Stiffness	A*	1.243	1	1.243	21.521	0.000
	B*	2.504	1	2.504	43.365	0.000
	C*	0.368	1	0.368	6.377	0.016
	D*	0.685	1	0.685	11.873	0.001
	AxB*	0.436	1	0.436	7.549	0.009
	AxC*	0.256	1	0.256	4.439	0.042
	AxD	0.193	1	0.193	3.342	0.076
	BxC*	0.437	1	0.437	7.572	0.009
	BxD*	0.359	1	3.959	68.570	0.000
	CxD*	1.167	1	1.167	20.209	0.000
	Error	2.136	37	0.058		

*: statistically significant at 95% level of confidence

A: Oven temperature; B: Oven duration; C: Autoclave duration; D: CO₂ chamber duration

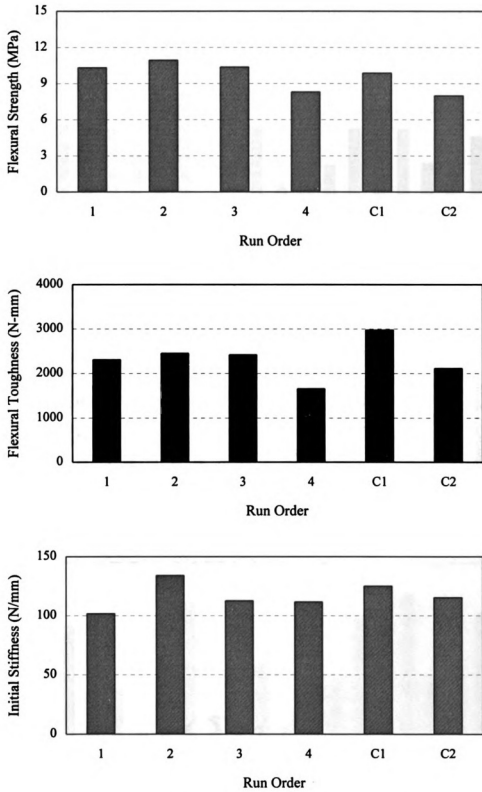


Figure 4.23a Flexural Test Results (pressed); C1: control 1, C2: Control 2

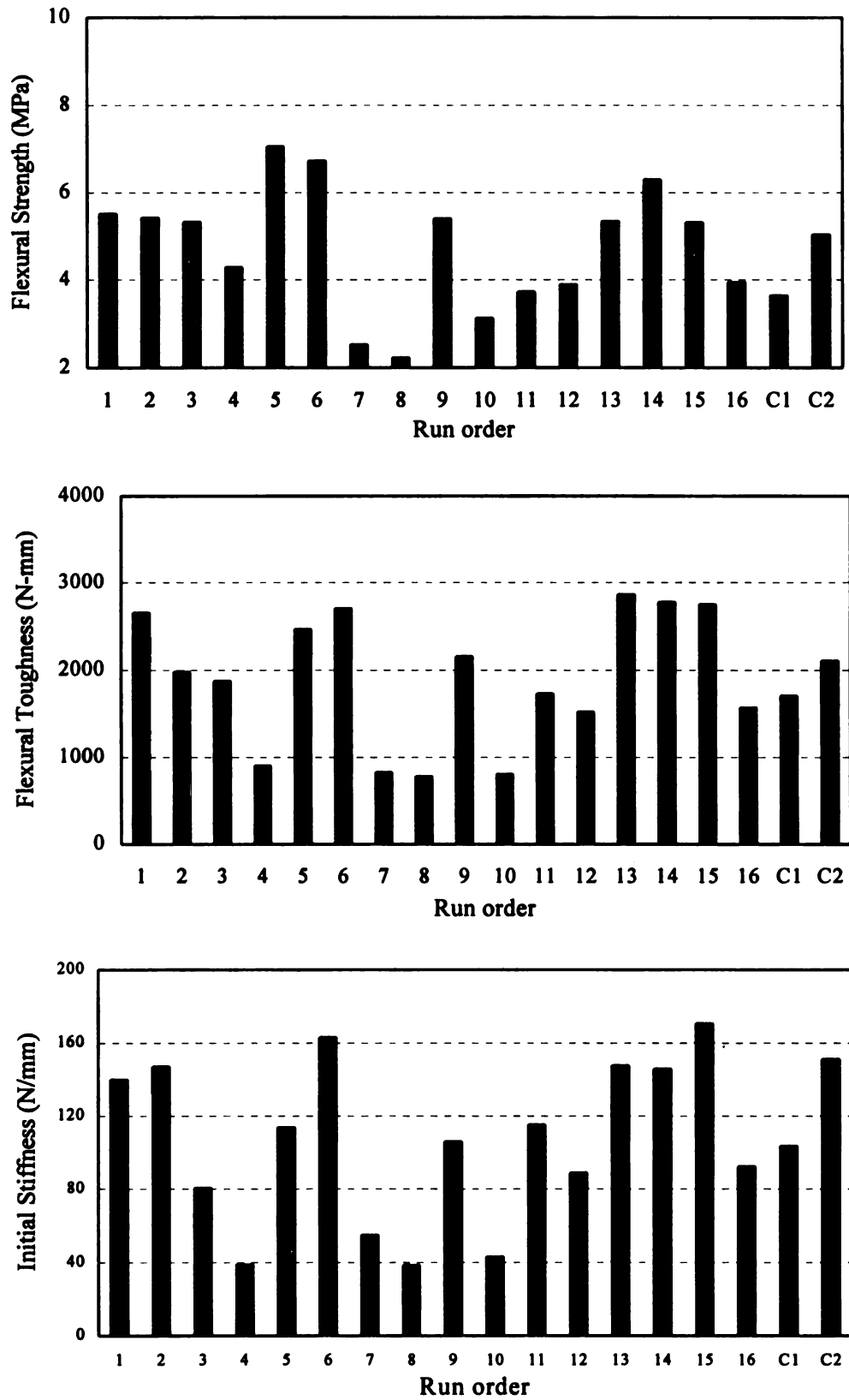
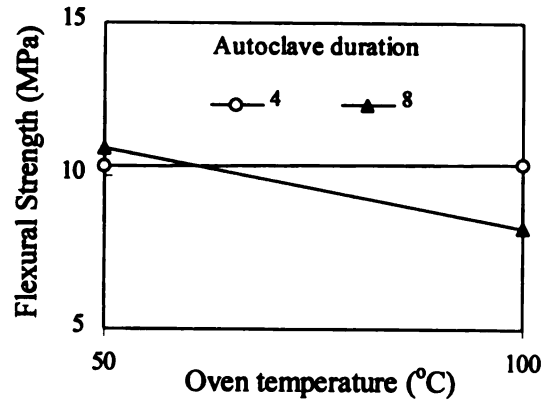
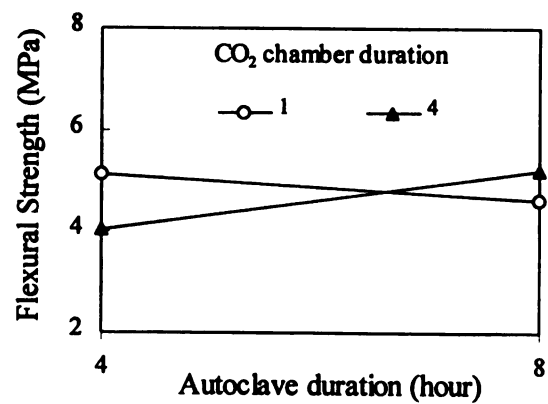
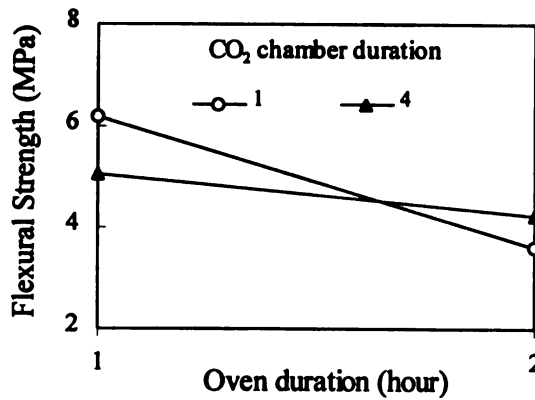
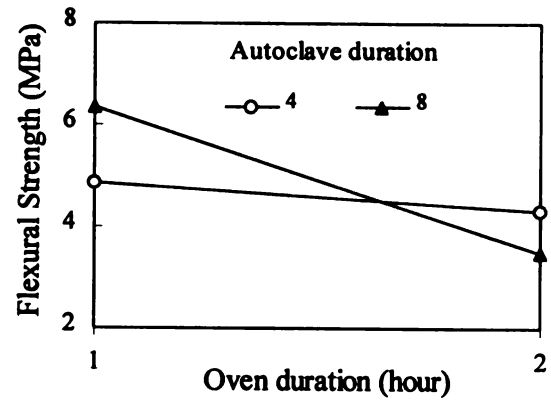
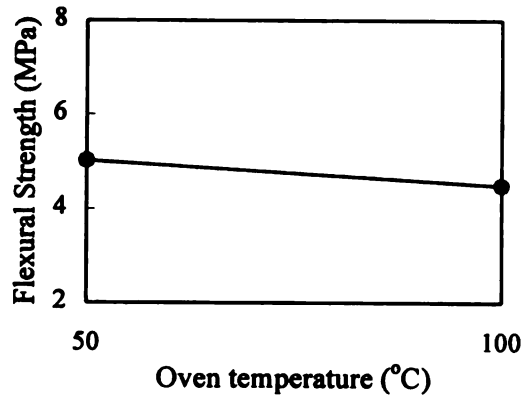


Figure 4.23b Flexural Test Results (unpressed); C1: control 1, C2: Control 2

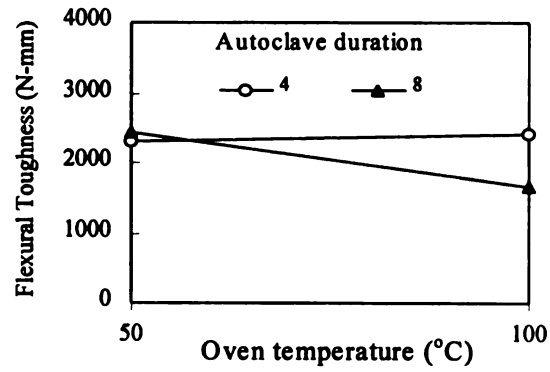


(a) Pressed

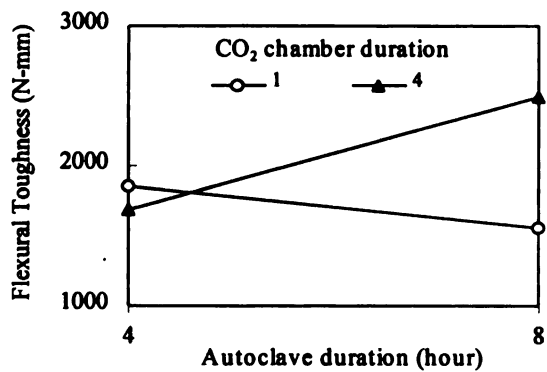
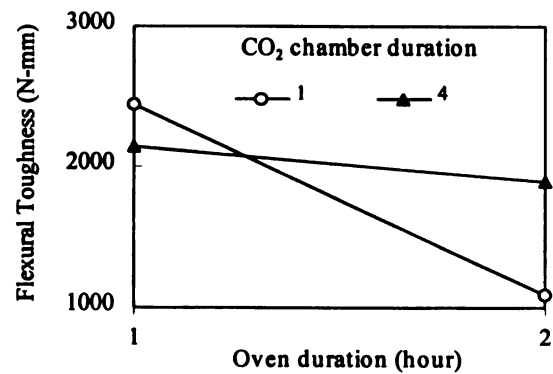
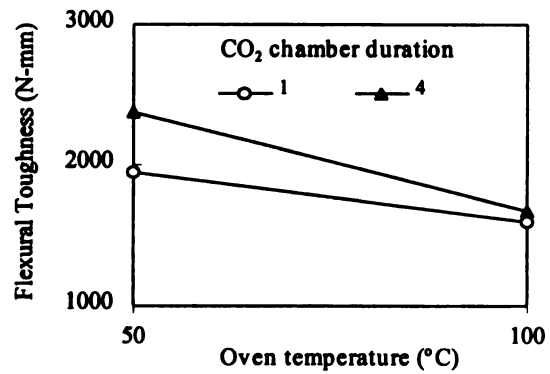
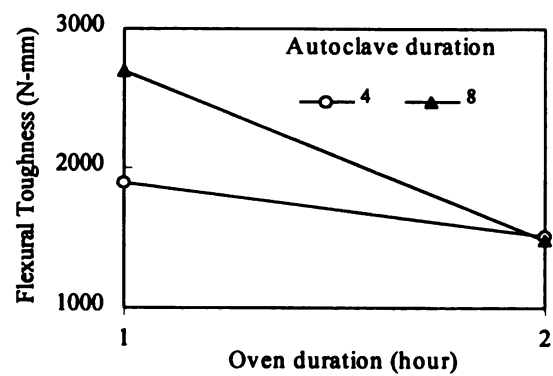
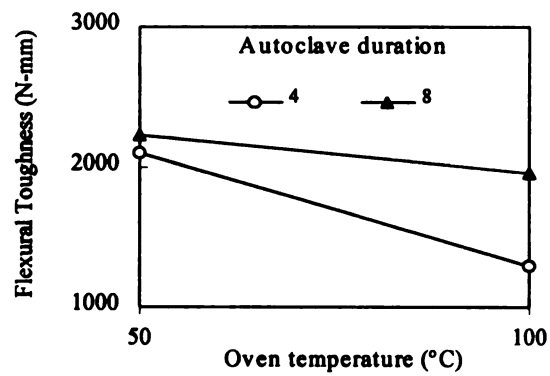


(b) Unpressed

Figure 4.24 The Trends in Flexural Strength



(a) Pressed



(b) Unpressed

Figure 4.25 The Trends in Flexural Toughness

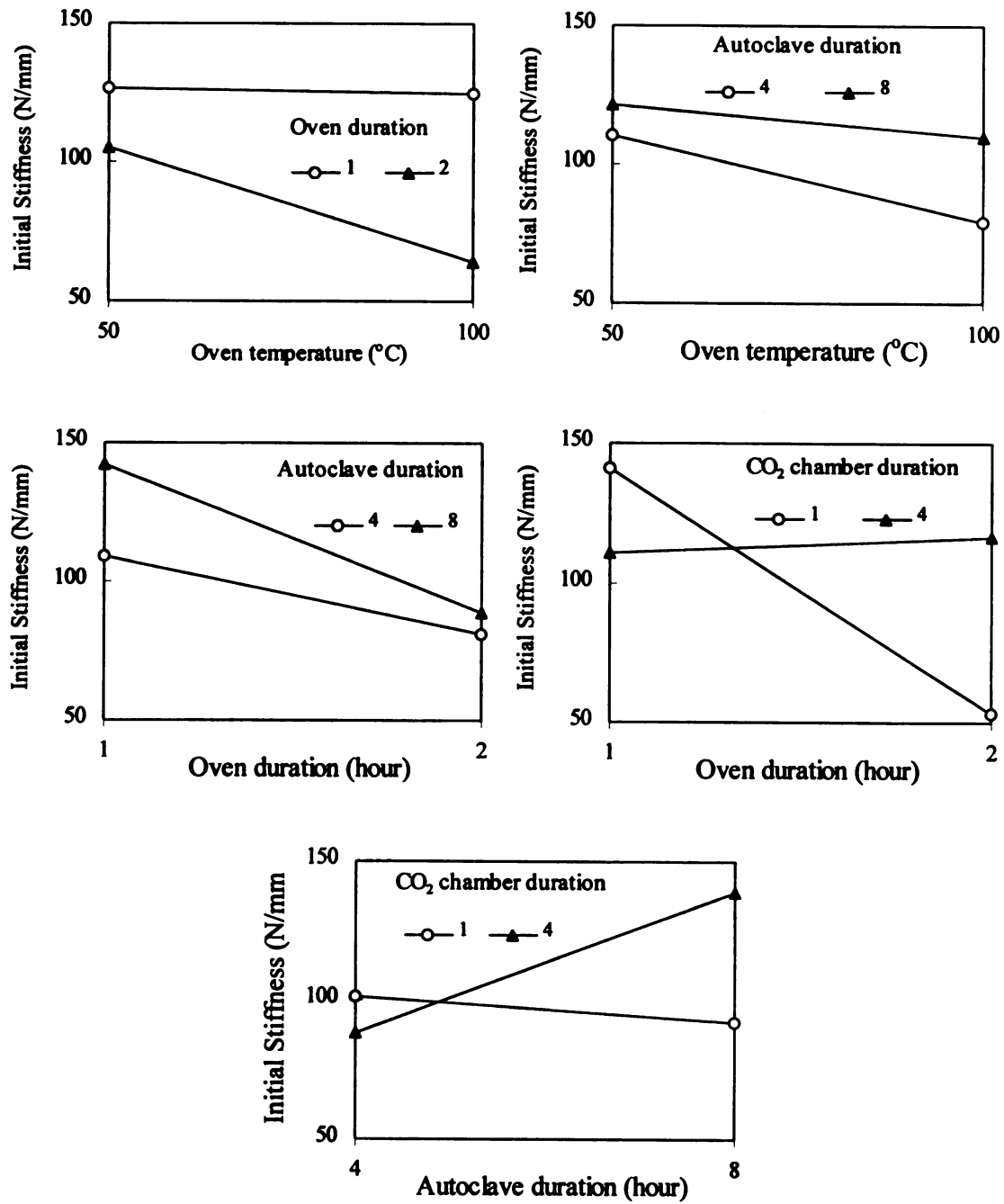


Figure 4.26 The Trends in Initial Stiffness (Unpressed)

Based on the statistical analyses, discussed above, all variables (A, B, C, and D) in the unpressed case are statistically significant at the 95% level of confidence, and there effects should be considered in the optimization process at next phase of the project. However, in order to reduce the size of optimization test program, we decided to keep the less in flexural factor of oven temperature constant. In order to select this temperature, experimental conducted a series of tests at different oven temperatures (20, 35, 50, and 100°C). The fixed variables used were oven duration of 1 hour, CO₂ chamber duration of 1 hour and autoclave duration of 8 hour which yielded the highest flexural strength.

Table 4.16 Test Results of Evaluated Oven Temperature (unpressed)

	Oven Temperature (°C)			
	20	35	50	100
Flexural strength (MPa)	4.416	5.687	7.079	7.406
	4.985	5.524	7.035	5.785
	4.699	5.643	7.055	6.993
Mean (St. Dev.)	4.700 (0.285)	5.618 (0.084)	7.056 (0.022)	6.728 (0.842)
Flexural Toughness (N-mm)	1994.499	2459.219	2554.452	2793.201
	2154.903	2227.633	2401.637	2624.798
	2105.116	2392.514	2429.364	2683.703
Mean (St. Dev.)	2084.839 (82.102)	2359.789 (119.211)	2461.818 (81.413)	2700.567 (85.459)
Initial Stiffness (N/mm)	130.714	124.806	116.016	166.653
	133.860	126.914	111.432	159.653
	132.211	125.212	113.214	163.213
Mean (St. Dev.)	132.262 (1.574)	125.644 (1.118)	113.554 (2.311)	162.983 (3.791)

The Figure 4.27 shows the flexural performance obtained at different oven temperatures in unpressed cellulose fiber reinforced cement composites. Among the four temperatures considered (20, 35, 50 and 100°C), 50°C yielded a better balance of properties..

Since a limited number of variables were investigated in the pressed case, base on the results produced, selected the processing condition with 1 hour of oven-drying of 50°C, 1 hour of CO₂ curing and 4 hour of autoclave curing as the preferred one.

4.6 SUMMARY AND DISCUSSION

An experimental study was conducted to access the effects of the CO₂ curing process variables on wood-cement composites.

4.6.1 Cement -Bonded Wood Particleboard

Hydration Characteristics of Cement in the Presence of Wood

A variety of wood species were selected and characterized based on their interaction with cement. The wood species were: southern pine, red oak, maple, and aspen. The test results indicated that:

- The presence of wood causes delays in the development of heat of hydration and reduces the peak temperature
- Hardwoods are generally more inhibitory than softwood

CO₂ Curing Process

Alternative sequences of applying CO₂ and vacuum on faces of the board were investigated and the preferred sequence was selected. The judgments was based on the flexural performance immediately after CO₂ curing.

Effects CO₂ Concentration

A lower CO₂ concentration (25%) yielded immediate flexural performance characteristics which were generally comparable to those obtained at 100% CO₂ concentration. Initial stiffness was actually higher at the lower CO₂ concentration.

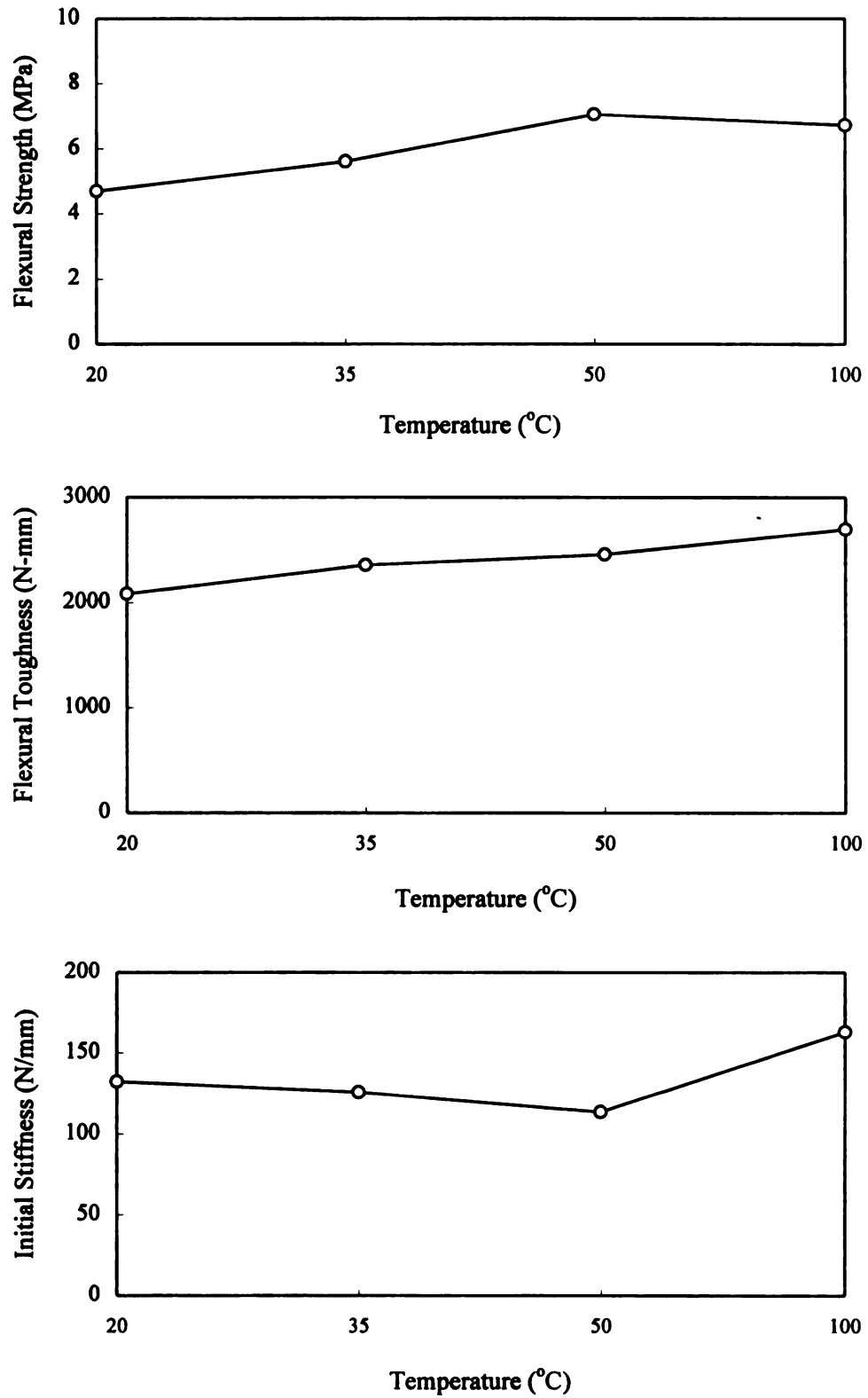


Figure 4.27 Flexural Performance at the Different Oven Temperatures (unpressed)

Effects of Mix Composition

A factorial design of the experiments was conducted to investigate the effects of wood-cement ratio (0.28 vs. 0.35), CO₂ concentration (25% vs. 100%) and wood species (softwood vs. Hardwood) on the immediate flexural performance. The results suggested that the preferred condition involved the case of a wood-cement ratio of 0.28 and 25% CO₂ concentration.

4.6.2 Cellulose Fiber Reinforced Cement Composites

An experimental study was conducted to assess the effects of CO₂ curing on the flexural performance of autoclaved cellulose fiber reinforced cement composites. The processing parameters investigated were the oven temperature and autoclaved duration for pressed board; and the oven temperature, oven duration, CO₂ chamber duration, and autoclave duration for unpressed boards. The test results indicated that:

- In pressed boards, all variables (oven temperature and autoclave duration) were statistically significant at 95% level of confidence. CO₂ curing in some condition yielded better results than conventional curing process even at half the autoclave duration.
- In the case of unpressed boards, oven duration had statistically significant effects at 95% level of confidence on flexural strength. In the case of toughness, oven temperature, oven duration, oven duration-CO₂ chamber duration interaction, and CO₂ chamber duration-autoclaved duration interaction were statistically significant at the 95% level of confidence. In the case of stiffness, oven duration, oven duration-CO₂ chamber duration interaction, and CO₂ chamber duration-autoclave duration interaction were statistically significant at 95% level of confidence.
- In both pressed and unpressed cases, an oven temperature of 50°C was chosen as the preferred one. The results yielded preferred processing conditions of pressed board. For unpressed boards, the oven duration, CO₂ curing duration and autoclave duration are to be optimized.

CHAPTER 5

OPTIMIZATION AND ASSESSMENT OF MECHANICAL AND PHYSICAL PROPERTIES

5.1 INTRODUCTION

The experimental studies of chapter 4 revealed the influential variables determining the performance characteristics of wood-cement composites and also suggested preferred levels for some variables. The optimum carbonation of all key variables should now be selected to achieve the best balance between technical performance and cost.

5.2 OBJECTIVE

The main thrust of this phase of the research was to optimize the production conditions of wood-cement composites for achieving the best performance characteristics at reasonable cost.

5.3 CELLULOSE FIBER REINFORCED CEMENT COMPOSITES

5.3.1 Optimization of the Manufacturing Variables of Cellulose Fiber Reinforced Cement Composites by CO₂ Curing: Unpressed Case

Three influential variables identified in the previous phase of the study (oven duration, CO₂ chamber duration, and autoclaved duration) were selected to be optimized initial phase based on performance and cost consideration. The optimization experimental design was formulated based on the statistical theory of response surface analysis. The objective of the optimization process was to maximize flexural performance (strength, toughness and stiffness) and minimize cost.

Once the optimized manufacturing variables were identified, the mechanical and physical performance of CO₂ cured composites were compared with those of conventional composites made without CO₂ curing. Table 5.1 shows the experimental program for optimization through response surface analysis. Various combinations of the three

statistically influential variables are considered in this experimental program. The background (fixed) variable was oven temperature (50°C).

The boards were air cured for seven days. Flexural specimens (152.4 x 254 x 10 mm, 6 x 10 x 0.4 in.) were cut from each sample using a diamond saw, and an average of 3 specimens were tested for flexural performance. The specimens were tested after two days of immersion in water at room temperature following ASTM C 1185.

5.3.2 Test Results and Analysis

Typical flexural load-deflection curves obtained for the composites of Table 5.1 are presented in Figure 5.1. A summary of all flexural test results is presented in Table 5.1. The Figure 5.2 presents the response surface contour plots based on flexural performance (flexural strength, toughness, and stiffness). The response surface contours of Figure 5.2 can be interpreted to understand the effects of variables on response. Increasing flexural strength and toughness values were obtained by increasing oven, CO₂ chamber and autoclaved duration. In stiffness, decreasing the oven time increased the stiffness values while increasing CO₂ chamber and autoclave duration produced better stiffness performance.

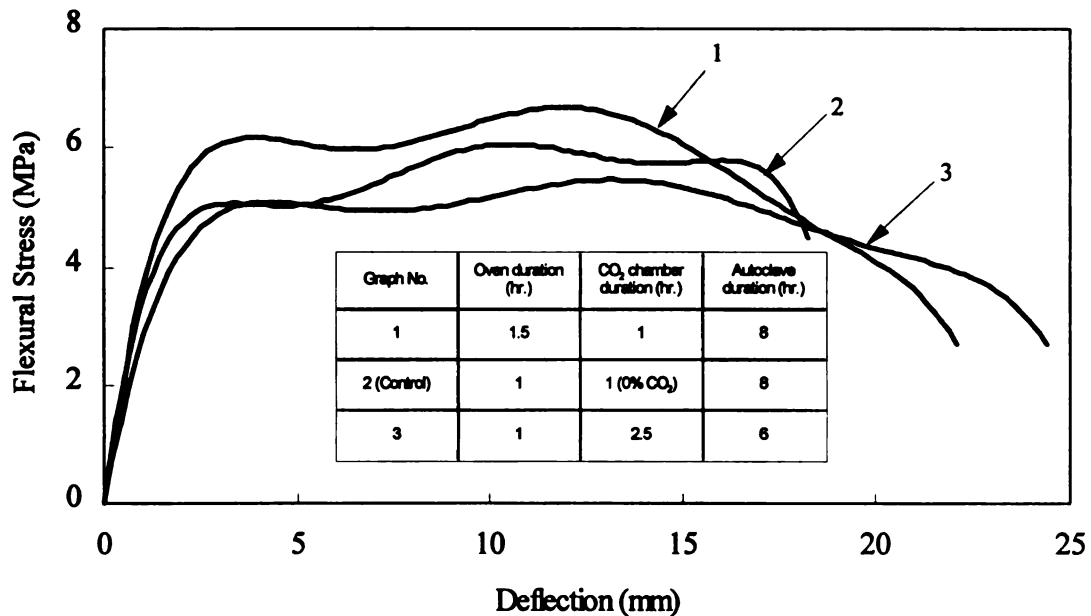


Figure 5.1 Typical Load-Deflection Curves with CO₂ Curing for Unpressed Cellulose Fiber Reinforced Cement Composites

Optimization plots were then generated (see Figure 5.3) for achieving maximum flexural strength , toughness and stiffness of lowest possible manufacturing cost. In Figure 5.3, the non-shaded region corresponds to optimum conditions for manufacturing of unpressed cellulose fiber reinforced cement composites using CO₂ curing.

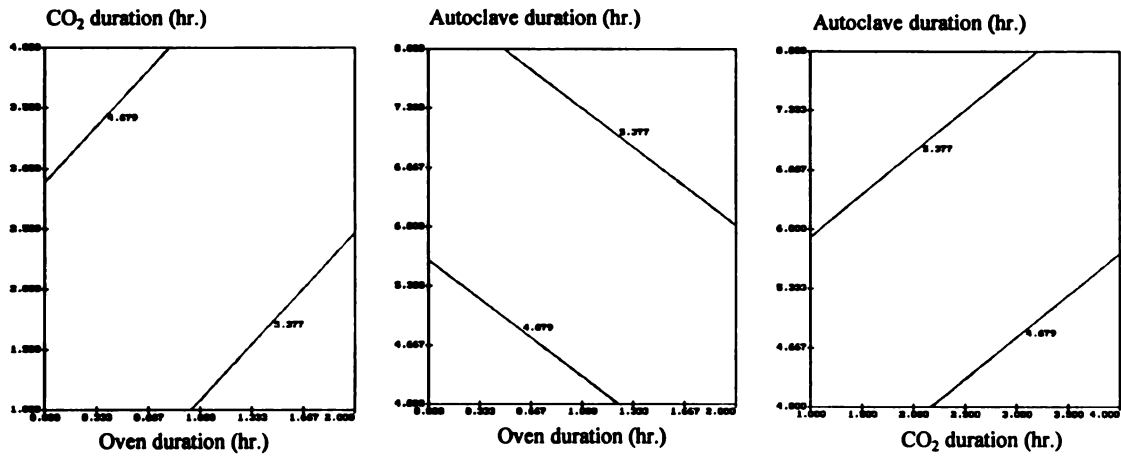
The optimum level of the variables derived from the above process are as follow:

- Oven Temperature: 50°C
- Oven Duration: 1 hour
- CO₂ Chamber Duration: 1 hour
- Autoclaved Duration: 6 hours

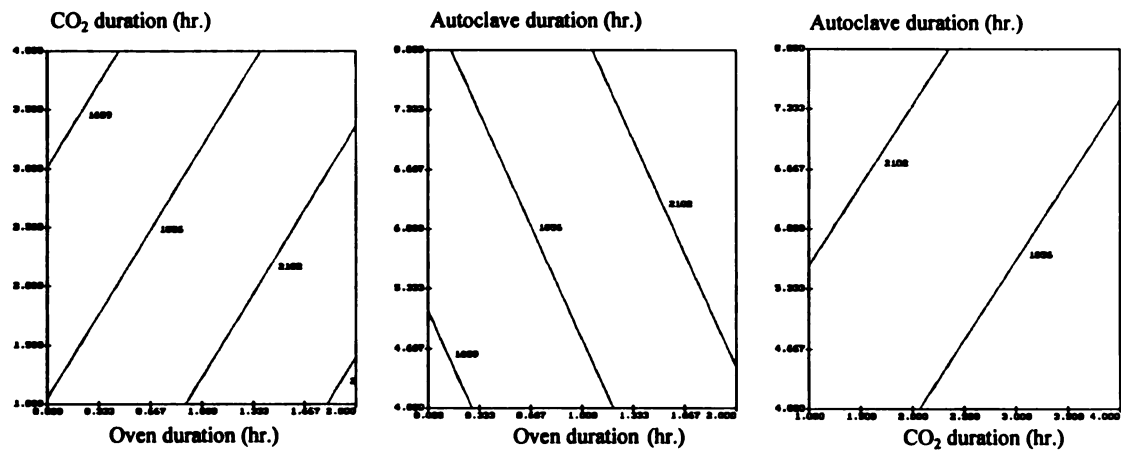
Table 5.1 Optimization Experimental Design and Test Results

Run order	A*	B*	C*	Strength (MPa) Mean (St. Dev.)	Toughness (N-mm) Mean (St. Dev.)	Stiffness (N/mm) Mean (St. Dev.)
1	0.5	4	4	4.246 4.013 <u>3.797</u> 4.019 (0.225)	1425.917 1621.500 <u>1779.600</u> 1609.006 (177.172)	112.134 120.376 <u>118.542</u> 117.017 (4.327)
2	1	2.5	6	5.653 5.522 <u>5.511</u> 5.562 (0.079)	2435.489 1885.827 <u>1921.531</u> 2080.949 (307.559)	157.210 72.698 <u>121.214</u> 117.041 (4.2410)
3	1.5	1	4	3.889 3.660 <u>4.397</u> 3.982 (0.377)	2001.224 1963.115 <u>1841.763</u> 1935.367 (83.273)	77.645 85.065 <u>69.452</u> 77.387 (7.810)
4	1	2.5	6	5.159 5.037 <u>5.110</u> 5.102 (0.062)	1799.249 1505.522 <u>1621.554</u> 1642.108 (147.938)	96.546 191.886 <u>132.621</u> 140.351 (4.8.138)
5	0.5	1	4	5.145 5.200 <u>5.250</u> 5.198 (0.053)	2462.260 1924.521 <u>1725.402</u> 2037.394 (381.176)	213.402 153.211 <u>95.638</u> 154.084 (58.887)
6	0.5	1	8	5.214 5.896 <u>4.107</u> 5.072 (0.903)	2019.346 2219.677 <u>1968.917</u> 2069.313 (132.637)	142.169 134.985 <u>153.683</u> 143.612 (9.432)
7	1.5	1	8	6.769 6.772 <u>6.774</u> 6.772 (0.003)	2928.741 2543.263 <u>2315.729</u> 2595.911 (309.879)	158.996 139.211 <u>124.919</u> 141.042 (17.112)
8	1	2.5	6	5.650 5.421 <u>5.368</u> 5.480 (0.150)	2399.291 1898.541 <u>1821.699</u> 2039.844 (313.653)	150.624 129.553 <u>132.626</u> 137.601 (11.382)
9	1.5	4	4	4.736 4.686 <u>4.589</u> 4.670 (0.075)	1824.316 1644.419 <u>1743.216</u> 1737.317 (90.093)	110.624 104.421 <u>108.523</u> 107.856 (3.155)
10	1.5	4	8	4.899 4.767 <u>5.027</u> 4.898 (0.130)	2100.913 2098.820 <u>2260.309</u> 2153.347 (92.637)	159.523 155.791 <u>168.041</u> 161.118 (6.279)
11	1	2.5	6	5.160 5.038 <u>5.529</u> 5.242 (0.256)	1821.215 1621.213 <u>1892.321</u> 1778.250 (140.568)	100.548 188.521 <u>100.629</u> 129.899 (50.768)
12	0.5	4	8	4.826 4.709 <u>4.920</u> 4.818 (0.106)	1621.523 1502.582 <u>1770.075</u> 1631.393 (134.019)	116.435 110.928 <u>119.919</u> 115.761 (4.533)

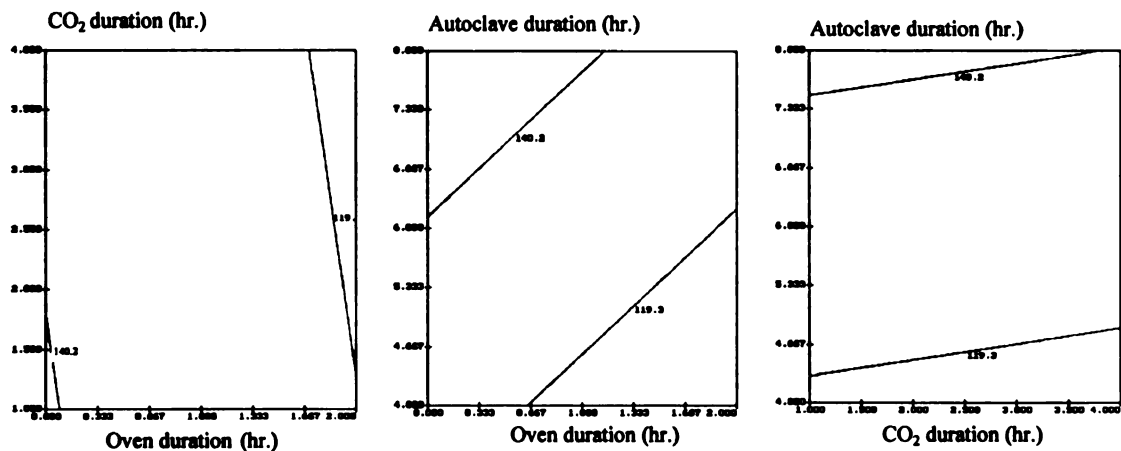
*A: Oven duration; B: CO₂ Chamber duration; C: Autoclaved duration, All units for A, B, and C are in hours



(a) Flexural Strength



(b) Flexural Toughness



(c) Initial Stiffness

Figure 5.2 Response Surface of Flexural Performance for Unpressed Cellulose Fiber Reinforced Cement Composites

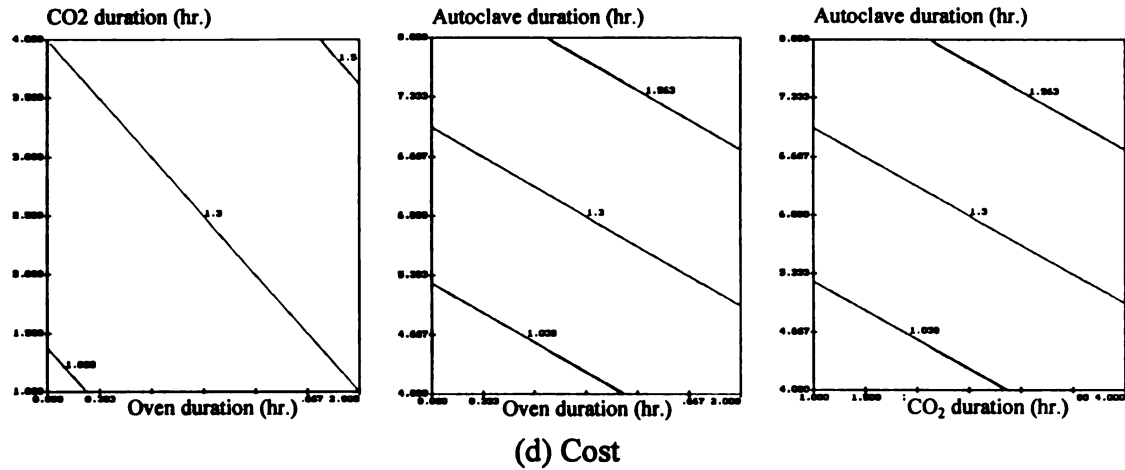


Figure 5.2 (Cont'd) Response Surface of Flexural Performance for Unpressed Cellulose Fiber Reinforced Cement Composites

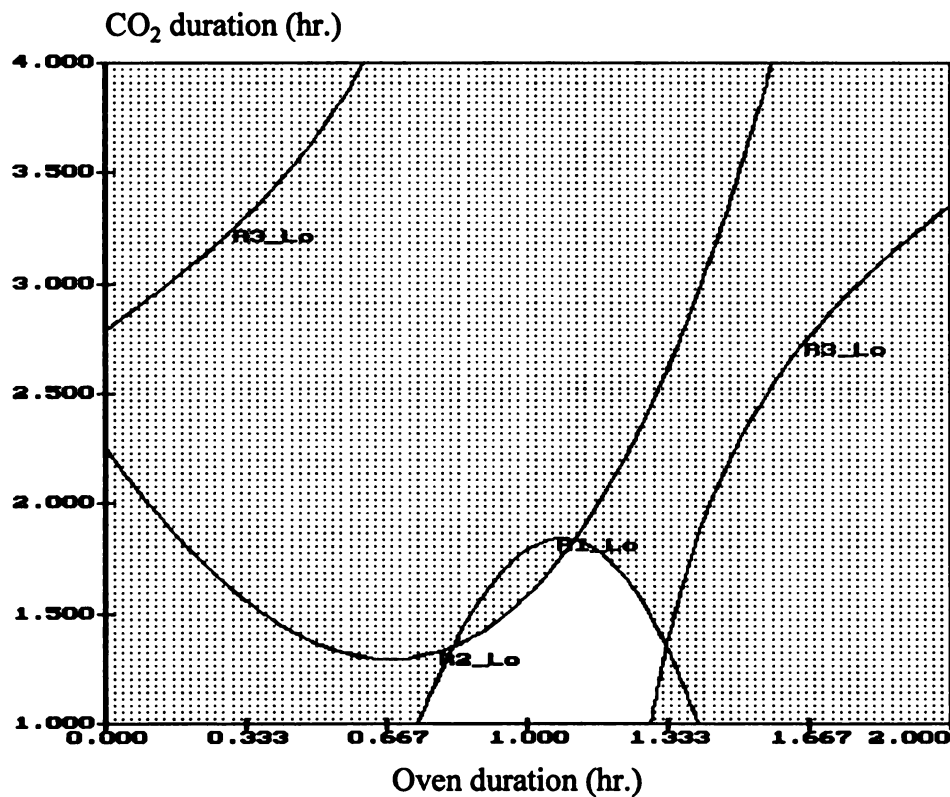


Figure 5.3 Optimum Manufacturing Conditions of Unpressed Cellulose Fiber Reinforced Cement Composites (based on 6 hours of autoclave duration)

5.3.3 Mechanical and Physical Properties of Cellulose Fiber Reinforced Cement Composites

5.3.3.1 Mechanical Properties of Unpressed Boards

The flexural performance of the optimized unpressed composite produced through CO₂ curing is compared in Figure 5.4 and Table 5.2 with the one of two control boards manufactured without CO₂ curing. All tests were conducted in equilibrium condition. Strength of CO₂ cured composite was higher than those of control boards at 95% level of confidence. Table 5.3 shows percentage difference in flexural properties of the CO₂-cured composite versus those of the control boards.

Table 5.2 Flexural Performance of Optimized CO₂-Cured Unpressed Cellulose Fiber Reinforced Cement Composites Versus Those of Controls

Type of Composite	Strength (MPa) Mean (St. Dev.)	Toughness (N-mm) Mean (St. Dev.)	Stiffness (N/mm) Mean (St. Dev.)
CO ₂ -cured (1-1-6)*	11.72	2281.792	191.313
	11.61	1660.080	194.831
	11.64	1721.514	187.215
	<u>11.14</u>	<u>1834.543</u>	<u>190.216</u>
	11.528 (0.262)	1874.482 (280.989)	190.894 (3.145)
Control 1 (1-1-6)**	7.66	1767.638	122.327
	7.60	1984.112	141.628
	7.58	1824.312	131.219
	<u>7.68</u>	<u>1722.558</u>	<u>129.214</u>
	7.63 (0.048)	1824.655 (114.166)	161.348 (19.755)
Control 2 (1-1-8)**	8.92	2622.431	177.170
	8.39	2100.280	132.792
	8.42	2522.521	149.215
	<u>8.36</u>	<u>2213.216</u>	<u>139.228</u>
	8.523 (0.266)	2364.612 (247.789)	149.601 (19.582)

* : 1-1-6 means 1 hour in oven at 50°C, 1 hour in CO₂ chamber and 6 hours in autoclave

** : 1-1-6 or 1-1-8 means 1 hour in oven at 50°C, 1 hour in CO₂ chamber but with 0% CO₂ and 6 or 8 hours in autoclave

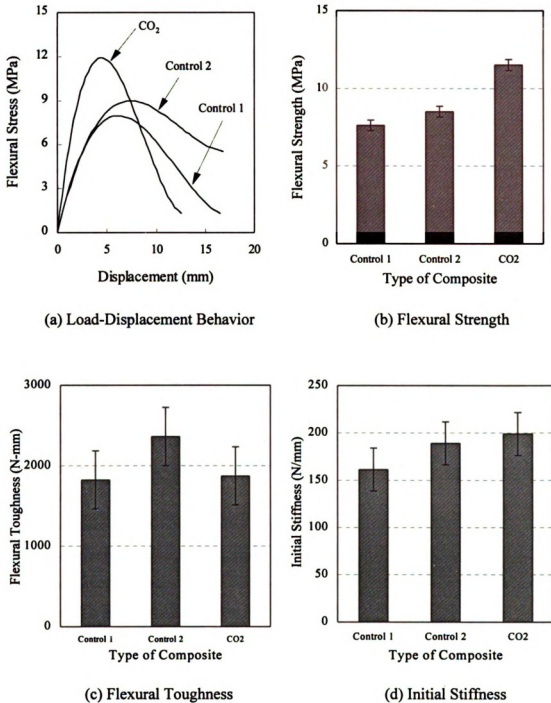


Figure 5.4 Flexural Performance of Optimized CO₂ Cured Unpressed Cellulose Fiber Reinforced Cement Composite (Equilibrium condition) Versus Those of Controls: Control 1 (1-1-6); Control 2 (1-1-8); CO₂ (1-1-6)

Table 5.3 The Percentage Difference in Flexural Performance of CO₂-Cured Boards Versus Controls

	Control 1	Control 2
Flexural Strength	+51%	+35.1%
Flexural Toughness	+2.7%	-20.7%
Initial Stiffness	+18.3%	+29.4%

CO₂-curing seems to have yielded better matrix and board qualities. Unpressed board seems to have some negative effects on initial toughness. After aging, however, toughness may also be improve with CO₂-curing.

5.3.3.2 Mechanical Properties of Pressed Boards

The pressed boards considered were CO₂-cured with 1 hour oven-drying at 50°C, 1 hour in CO₂ chamber and 4 hours in autoclave. Two control conditions were also considered with 1 hour of oven-drying at 50°C, 1 hour in CO₂ chamber but with 0% CO₂, and 4 and 8 hours in autoclave. Flexural tests were conducted were in equilibrium condition at room temperature of 22±2°C (72±3°F) and 50±10% RH. The results are presented in Table 5.4 and Figure 5.5.

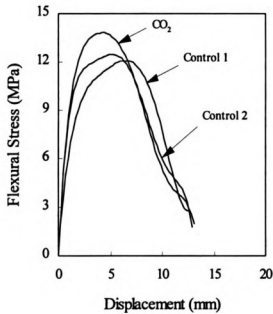
The effects of CO₂-curing were significant at 95% level of confidence. Compressed boards associated with CO₂-curing seems to have some negative effects on early use toughness characteristics. Table 5.5 show percentage differences in the flexural performance of CO₂-cured versus control pressed cellulose fiber reinforced cement composites.

Table 5.4 Flexural Performance of CO₂-Cured Pressed Cellulose Fiber Reinforced Cement Composites Versus Those of Controls

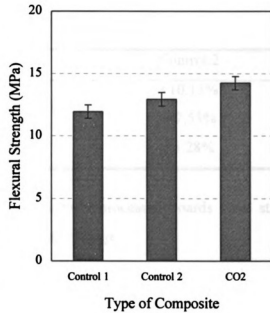
	<u>Strength (MPa)</u>	<u>Toughness(N-mm)</u>	<u>Stiffness (N/mm)</u>
	Mean (St. Dev.)	Mean (St. Dev.)	Mean (St. Dev.)
CO ₂ -cured	14.24	2275.274	204.420
(1-1-4)*	14.42	1863.887	192.206
	14.32	1869.213	199.214
	<u>13.99</u>	<u>1922.432</u>	<u>200.513</u>
	14.243 (0.184)	1982.702 (196.831)	199.088 (5.094)
Control 1	11.49	2995.953	184.204
(1-1-4)**	12.39	2877.625	140.094
	11.55	2855.579	150.662
	<u>12.33</u>	<u>2938.243</u>	<u>170.432</u>
	11.94 (0.486)	2928.100 (71.768)	161.348 (19.755)
Control 2	12.61	2616.021	172.843
(1-1-8)**	13.12	2122.374	200.157
	12.88	2243.215	200.221
	<u>13.11</u>	<u>2634.562</u>	<u>183.215</u>
	12.93 (0.24)	2404.043 (260.305)	189.109 (13.477)

* : 1-1-4 means 1 hour in oven at 50°C, 1 hour in CO₂ chamber and 4 hours in autoclave

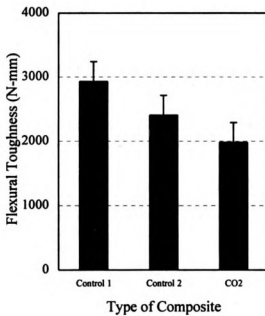
** : 1-1-4 or 1-1-8 means 1 hour in oven at 50°C, 1 hour in CO₂ chamber but with 0% CO₂ and 4 or 8 hours in autoclave



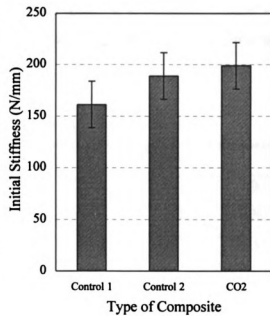
(a) Load-Displacement Behavior



(b) Flexural Strength



(c) Flexural Toughness



(d) Initial Stiffness

Figure 5.5 Flexural Performance of Pressed Cellulose Fiber Reinforced Cement Composites (Equilibrium Condition): Control 1 (1-1-4); Control 2 (1-1-8); CO₂ (1-1-4)

Table 5.5 The Percentage Difference of Flexural Performance of CO₂-Cured Boards Versus Controls (pressed)

	Control 1	Control 2
Flexural Strength	+19.29%	+10.15%
Flexural Toughness	-32.29%	-17.53%
Initial Stiffness	+23.39%	+5.28%

Two hours after mixing, while the conventionally processed boards were still plastic, the CO₂-cured ones could be hardened without breakage.

5.3.3.3 Physical Properties

Water absorption and specific gravity is indirectly related to density in that both are dependent upon the void volume of the sample. The water absorption capacities are presented in Table 5.6 and Figure 5.6 for CO₂-cured and control boards. The CO₂ curing on unpressed and pressed composite are observed in Figure 5.6 show reduced water absorption when compared with control (non-CO₂) curing composite. The dense structure could be responsible for this phenomenon.

Table 5.6 Water Absorption and Specific Gravity Test Results

	Unpressed			Pressed		
	Control 1	Control 2	CO ₂	Control 1	Control 2	CO ₂
Specific Gravity	1.11	1.18	1.11	1.18	1.22	1.26
Water absorption (%)	51.42	48.39	45.04	32.8	33.06	31.55

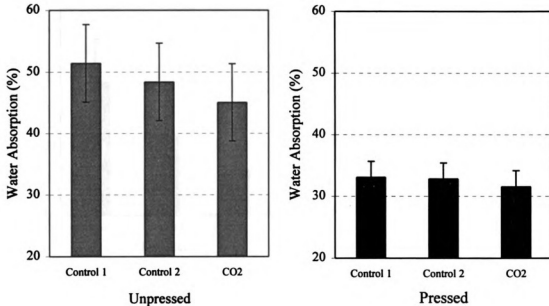


Figure 5.6 Water Absorption of Cellulose Fiber Reinforced Cement Composite

Wood fiber consists of long chains of glucose molecules attracted to each other by hydrogen bonds. They contain voids in excess of 50% of their total volume. When these voids are filled with moisture, the dimensional stability of the material is affected. The diameter change of cellulose is large, and can affect the bonding of the fiber to the matrix. Dimensional stability is measured in terms of dimensional movements expressed as the percentage changes in length, thickness, and mass as relative humidity is increased from 30% to 90%. Figure 5.7 shows the results of tests on dimensional stability of CO₂-cured and conventional composites. CO₂-curing is observed to yield major improvements in the dimensional stability of boards.

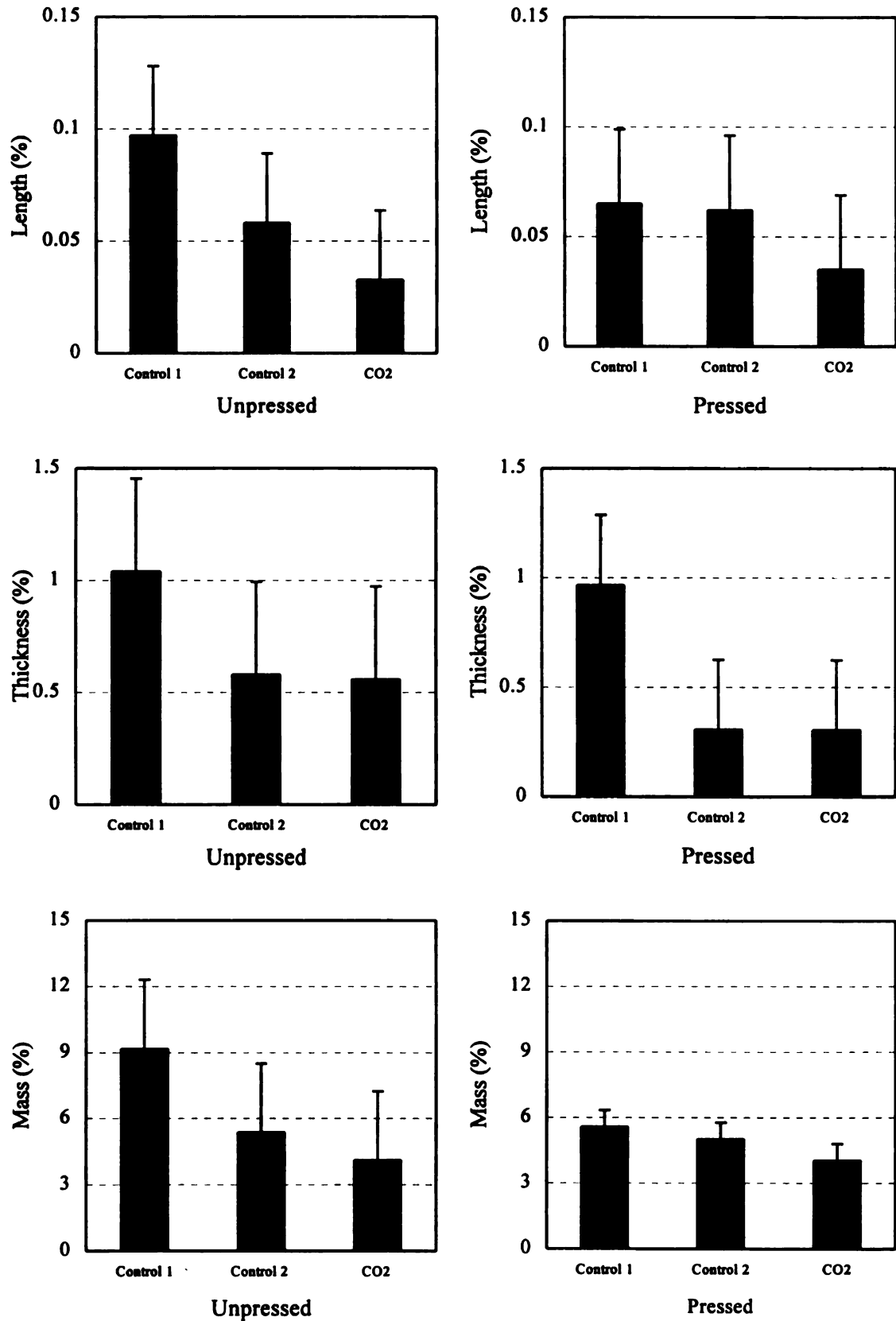


Figure 5.7 Dimensional Stability Test Results

5.4 CEMENT-BONDED PARTICLEBOARD

The main thrust of this phase of research on cement-bonded particleboard was to provide further insight into effects of wood-cement ratio and wood species on various aspects of board performance characteristics. This phase is also concerned with the comparison of curing processes involving CO₂ with the conventional curing process. In this phase 100 and 25% CO₂ concentration and method II of CO₂ curing (see Figure 4.6 of chapter 4). The experimental program followed in this phase of research is shown in Table 5.7. The control process of curing cement-bonded particleboard is schematically depicted in Figure 5.8.

The cement-bonded wood particleboards were evaluated based on flexural performance development over time, internal bond strength at 28 days (ASTM D 1037), and moisture movements, swelling at moisture content (BS 5669).

5.4.1 Mechanical Properties

Typical flexural load-deflection curves for the boards prepared following the experimental program of Table 5.8 are presented in Figure 5.9. Unless stated, all mechanical test results were generated after 28 days of storage in plastic bag (following the curing process). The 28 days flexural test results are depicted in Table 5.8 and Figure 5.10. Statistically analysis (factorial analysis of variance) of flexural strength results are shown in Table 5.9 and 5.10. The trends in the effects of various factors shown in Figure 5.11 and Figure 5.12. The development of flexural strength with time is shown in Figure 5.13.

The 28 days flexural performance of CO₂-cured cement-bonded particleboard wood particleboard was generally improved as wood-cement ratio increased from 0.28 to 0.35. The results were better with aspen when compared with southern pine. Control specimens (without CO₂-curing) clearly inferior to CO₂-cured cement-bonded wood particleboards in all aspects of 28-days flexural performance.

Table 5.7 The Experimental Program

Carbonated Composite				Control	
Wood/Cement ratio				Wood/Cement ratio	
0.28		0.35		0.28	0.35
Southern Pine	Aspen	Southern Pine	Aspen	Southern Pine	Southern Pine
*	*	*	*	*	*

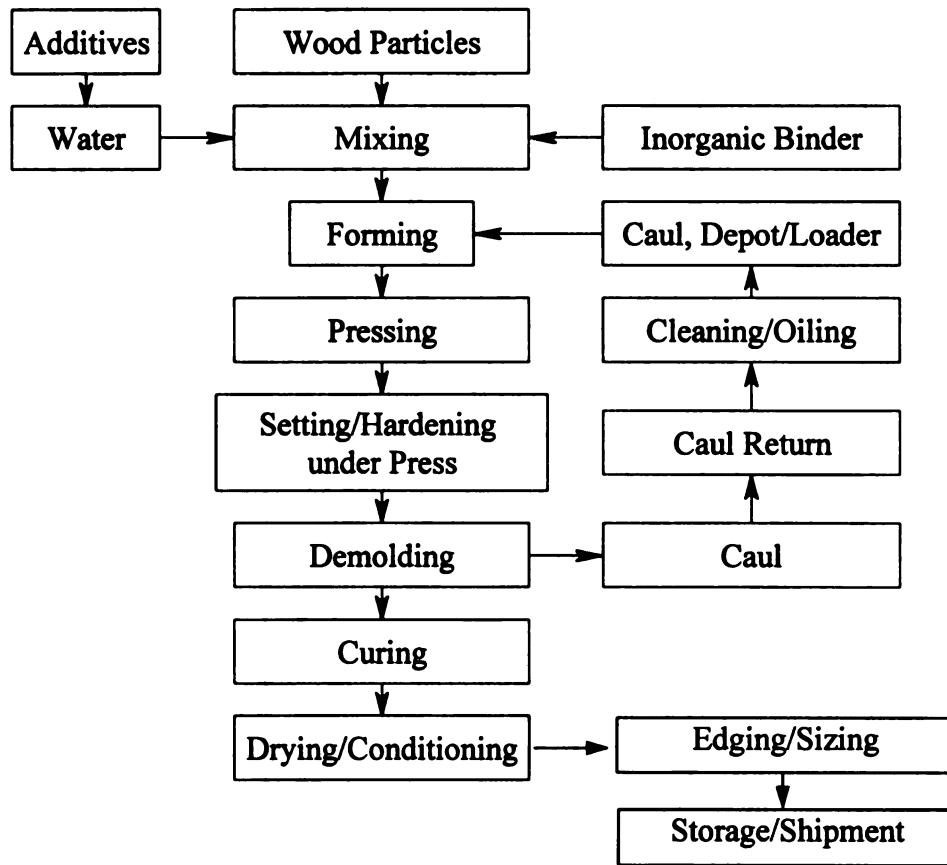
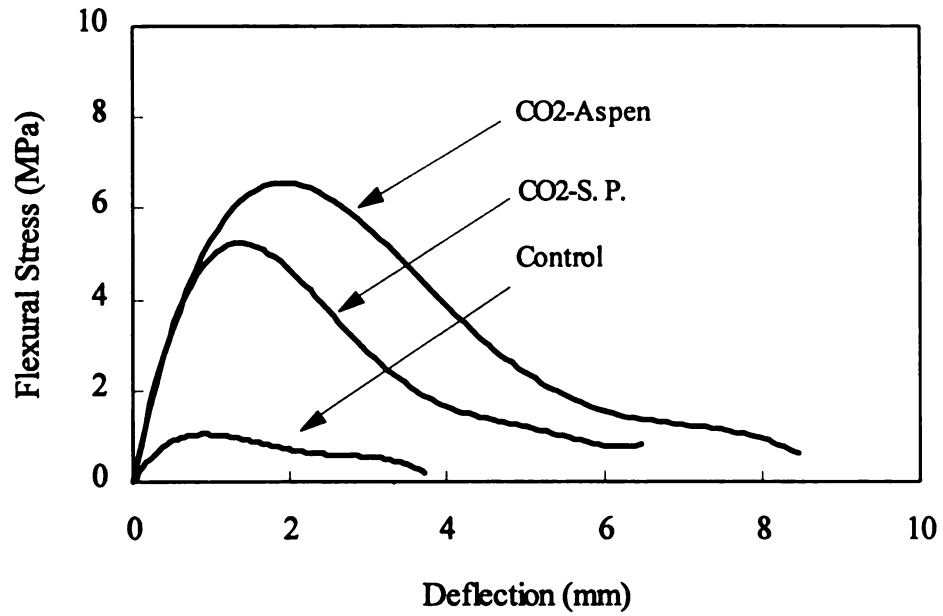


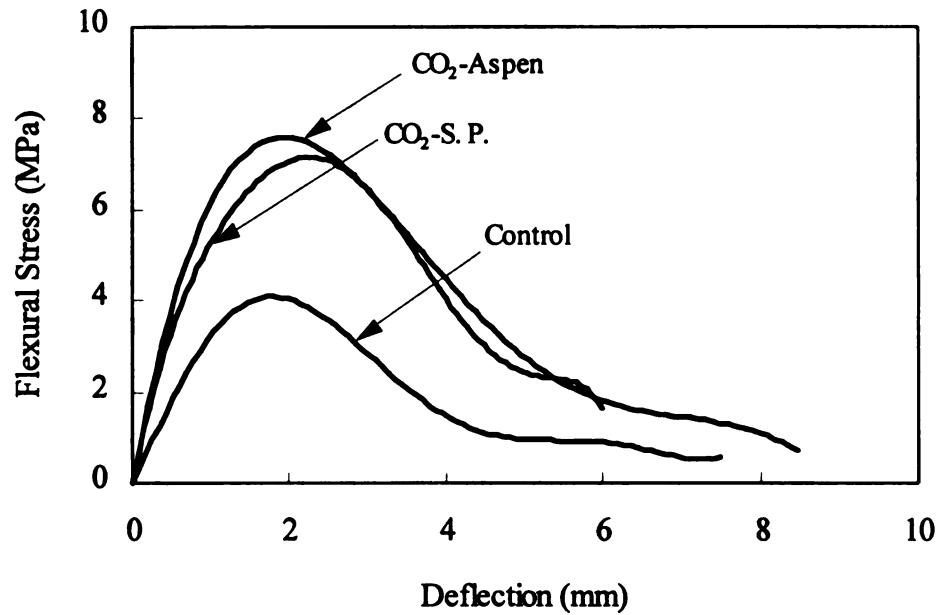
Figure 5.8 Schematic Diagram of Cement-Bonded Particleboard Manufacturing by Conventional Method [17, 25]

Table 5.8 Flexural Test Results at 28 Days of Age

	CO ₂ -Curing				Control	
	Wood/Cement Ratio				Wood/Cement Ratio	
	0.28		0.35		0.28	0.35
	Wood Species		Wood Species		Wood Species	
	Southern Pine	Aspen	Southern Pine	Aspen	Southern Pine	Southern Pine
Flexural Strength (MPa)	5.23	6.36	7.02	6.77	1.08	4.32
	5.37	6.45	7.39	8.27	1.45	3.99
	5.56	5.39	7.42	8.53	1.96	4.83
	5.42	6.92	6.99	7.58	2.23	4.59
Mean (St. Dev.)	5.395 (0.136)	6.28 (0.642)	7.205 (0.232)	7.788 (0.788)	1.680 (0.514)	4.433 (0.361)
Flexural Toughness (N-mm)	541.934	920.432	900.551	890.510	89.818	452.643
	520.632	839.411	907.825	870.832	114.700	483.219
	533.526	880.559	910.515	732.499	132.624	488.553
	500.693	859.299	827.704	719.918	149.954	462.434
Mean (St. Dev.)	524.196 (17.952)	874.925 (34.880)	886.649 (39.521)	803.440 (89.687)	121.774 (25.710)	471.712 (16.988)
Initial Stiffness (N/mm)	170.216	221.551	246.663	243.164	140.316	135.211
	183.214	243.164	274.315	272.119	138.677	130.554
	149.226	239.255	209.551	213.516	123.611	140-.221
	183.214	255.194	232.646	250.551	128.769	139.551
Mean (St. Dev.)	171.468 (16.044)	239.791 (13.924)	240.794 (27.084)	244.838 (24.226)	132.843 (7.994)	136.384 (4.477)



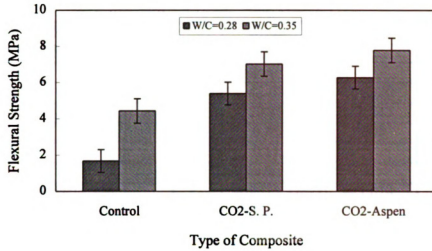
(a) Wood/Cement Ratio = 0.28



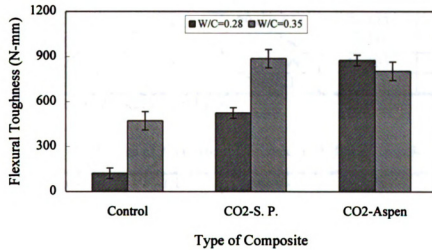
(b) Wood/Cement Ratio = 0.35

Figure 5.9 Typical 28 Days Flexural Load-Deflection Behavior of Cement-Bonded Particleboard

(a)



(b)



(c)

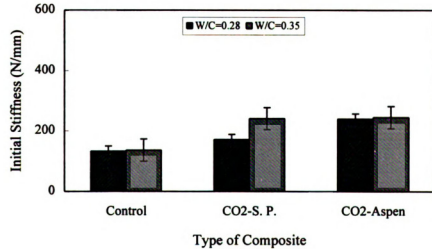


Figure 5.10 28 Days Flexural Performance of Cement-Bonded Particleboard: (a) Flexural Strength; (b) Flexural Toughness; (c) Initial Stiffness

Table 5.9 Results of Analysis of Variance: CO₂ Versus Conventionally Cured Boards

Source	Sun-of-Squares	DF	Mean-Square	F-Ratio	P
Flexural Strength					
A**	42.088	1	42.088	360.320	0.000
B**	20.816	1	20.816	178.213	0.000
AxB*	0.888	1	0.888	7.605	0.017
Error	1.402	12	0.117		
Flexural Toughness					
A**	668075.326	1	668075.326	943.014	0.000
B**	507500.581	1	507500.581	716.356	0.000
AxB	156.606	1	156.606	0.221	0.647
Error	8501.367	12	708.447		
Initial Stiffness					
A**	20458.654	1	20458.654	76.133	0.000
B**	5309.636	1	5309.636	19.759	0.001
AxB**	4327.699	1	4327.699	16.105	0.002
Error	3224.655	12	268.721		

A: Curing Conditions; B: Wood/Cement Ratio

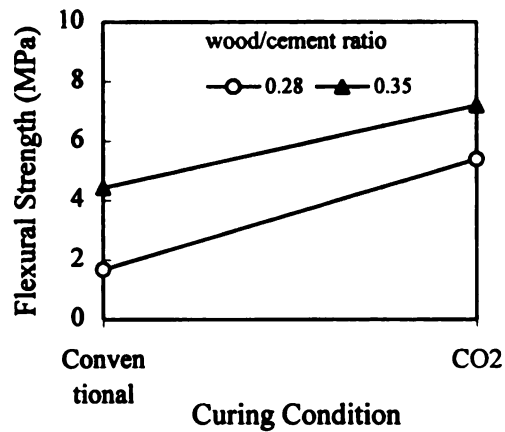
Table 5.10 Results of Analysis of Variance: CO₂ Cured Boards

Source	Sun-of-Squares	DF	Mean-Square	F-Ratio	P
Flexural Strength					
A*	2.154	1	2.154	7.793	0.016
B**	11.006	1	11.006	39.827	0.000
AxB	0.092	1	0.092	0.331	0.576
Error	3.316	12	0.276		
Flexural Toughness					
A**	71566.950	1	71566.950	25.719	0.000
B**	84661.795	1	84661.795	30.425	0.000
AxB**	188302.188	1	188302.188	67.670	0.000
Error	33392.028	12	2782.669		
Initial Stiffness					
A**	5237.019	1	5237.019	11.823	0.005
B**	5531.306	1	5531.306	12.488	0.004
AxB*	4131.886	1	4131.886	9.328	0.010
Error	5315.204	12	442.934		

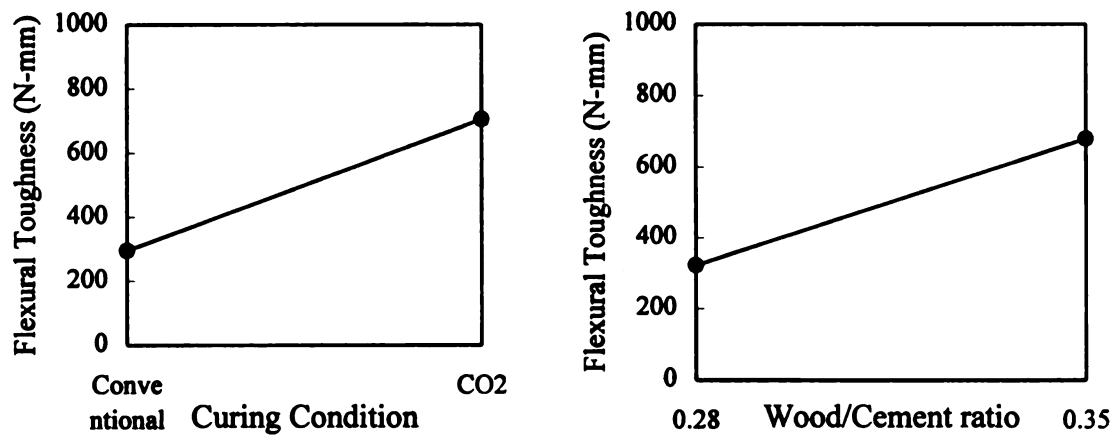
A: Wood Species; B: Wood/Cement Ratio

*: Statistically significant at 95% level of confidence

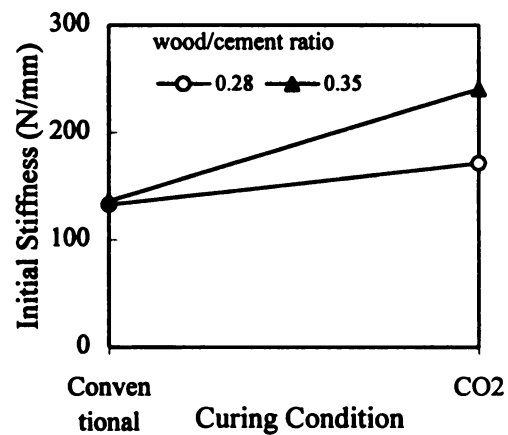
**: Statistically significant at 99% level of confidence



(a) Flexural Strength



(b) Flexural Toughness



(c) Initial Stiffness

Figure 5.11 The Trends in Flexural Performance: CO₂ Versus Conventionally Cured Boards

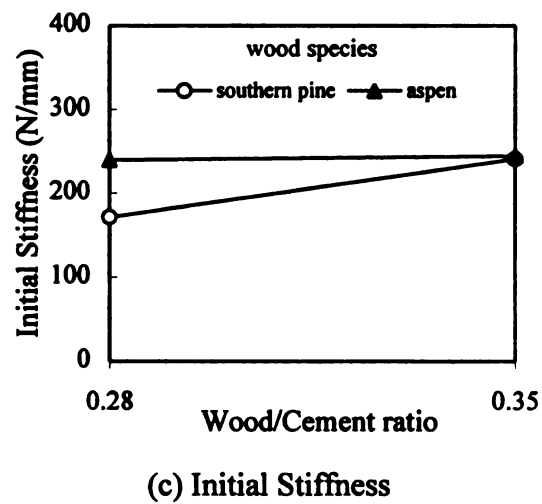
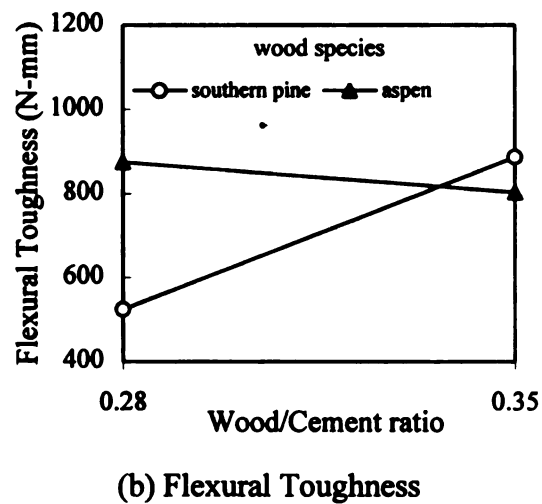
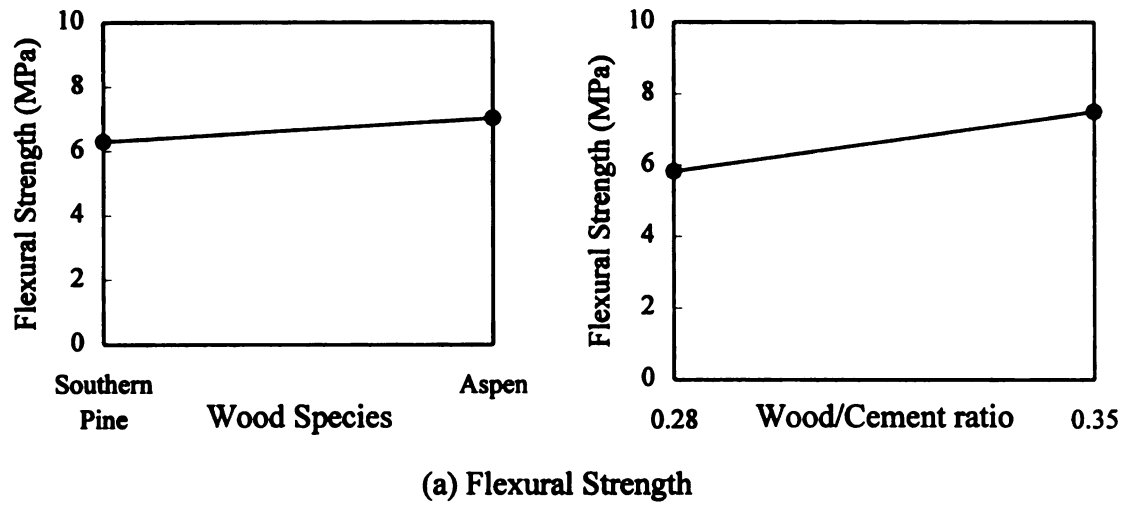
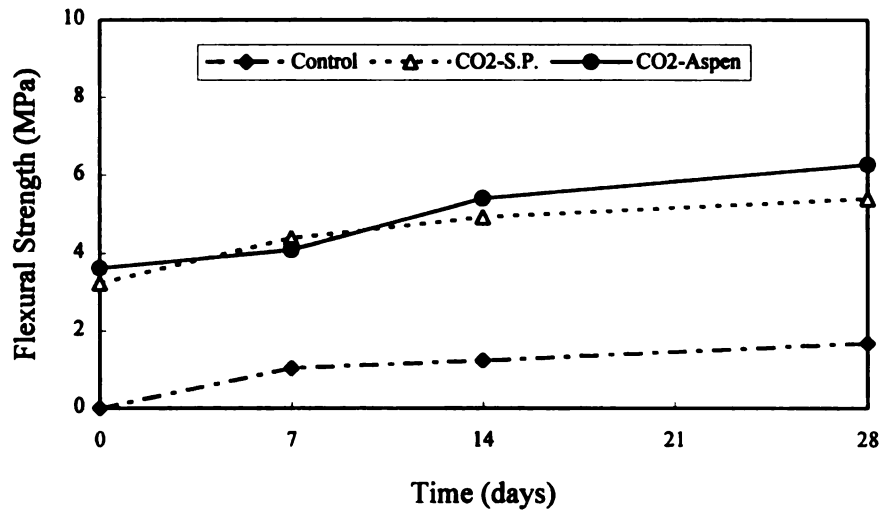
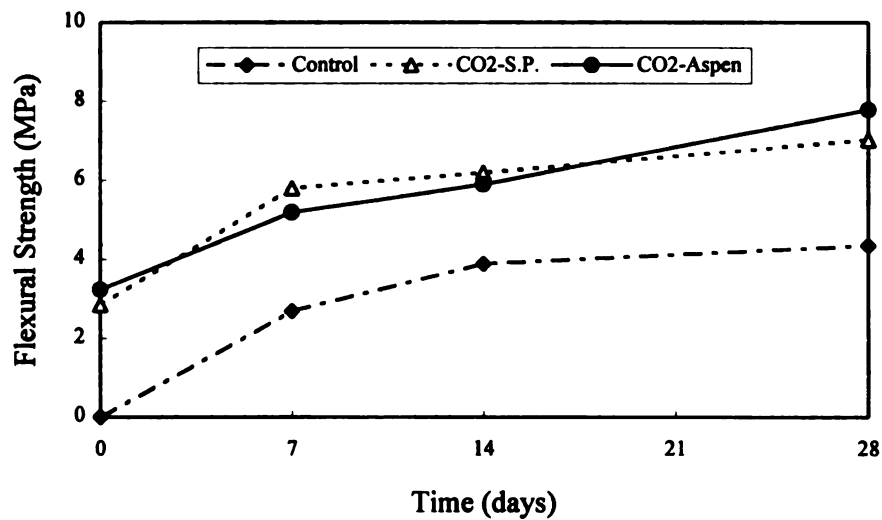


Figure 5.12 The Trends in Flexural Performance: CO₂ Cured Boards



(a) Wood/Cement Ratio = 0.28



(b) Wood/Cement Ratio = 0.35

Figure 5.13 Time-Property Relationship of CO₂ and Conventionally Cured Cement-Bonded Particleboard

Test results on the development of flexural strength over time (Figure 5.13) suggest that immediate strength is highest for the 0.28 wood-cement ratio but 28-day strengths are higher at 0.35 wood-cement ratio. At 0.28 wood-cement ratio, CO₂-curing

yielded an immediate strength approximately 60% of that achieved at 28 days of age. At 0.35 wood-cement ratio, however, CO₂-curing was less effective and yielded an immediate flexural strength which was less than 45% of the 28-days strength.

Another important strength property of cement-bonded particleboard is internal bond (IB), which is the strength in tension perpendicular to the plane of the composite. To determine internal bond, a 50.8 mm (2 in.) square sample of board is glued between two steel blocks. The blocks are then pulled apart, and the load to failure is recorded. The load to failure divided by the area gives the internal bond strength (IB) in MPa (psi). A board with inferior IB could delaminate in service when swelling stresses occur. IB is the best single measure of the quality of manufacture of a board because it indicates the strength of the board between particles. It is an important test for quality control because it indicates the adequacy of the blending, forming and pressing processes. Figure 5.14 shows the specimen and blocks for conducting an IB test. Table 5.11 and Figure 5.15 show results of internal bond tests. All internal bond tests were conducted at 28-days of age. Statistical analysis of internal bond strength are shown in Table 5.12. The trends of internal bond test results are shown in Figures 5.16 and 5.17.

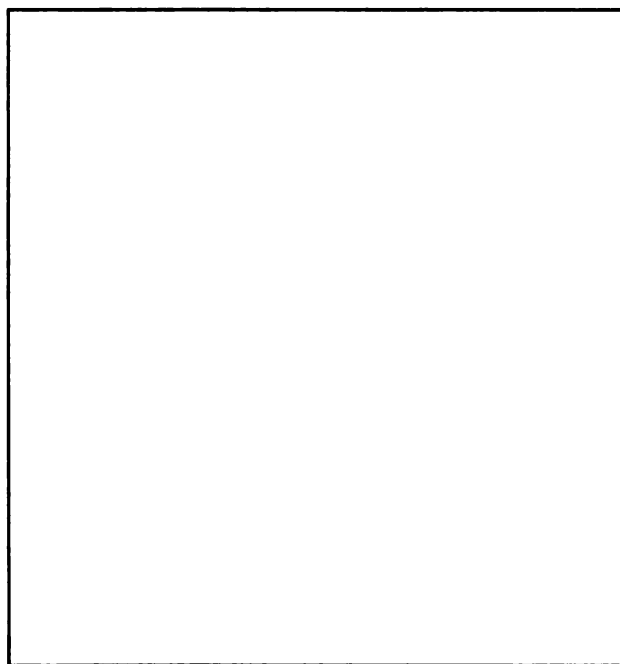


Figure 5.14 Internal Bond Test Set-Up for Cement-Bonded Particleboard

Table 5.11 Internal Bond Test Results

	CO ₂ -Cured Boards				Control	
	Wood/Cement Ratio				Wood/Cement Ratio	
	0.28		0.35		0.28	0.35
	Southern Pine	Aspen	Southern Pine	Aspen	Southern Pine	
IB (KPa)	985.785	791.369	638.123	659.390	62.357	96.071
	1031.003	843.652	811.345	579.996	82.325	284.090
	1409.857	810.634	743.824	517.787	79.541	152.263
Mean	1142.215	815.218	731.097	585.724	74.741	177.475
(St. Dev.)	(232.885)	(26.441)	(87.309)	(70.975)	(10.815)	(96.512)

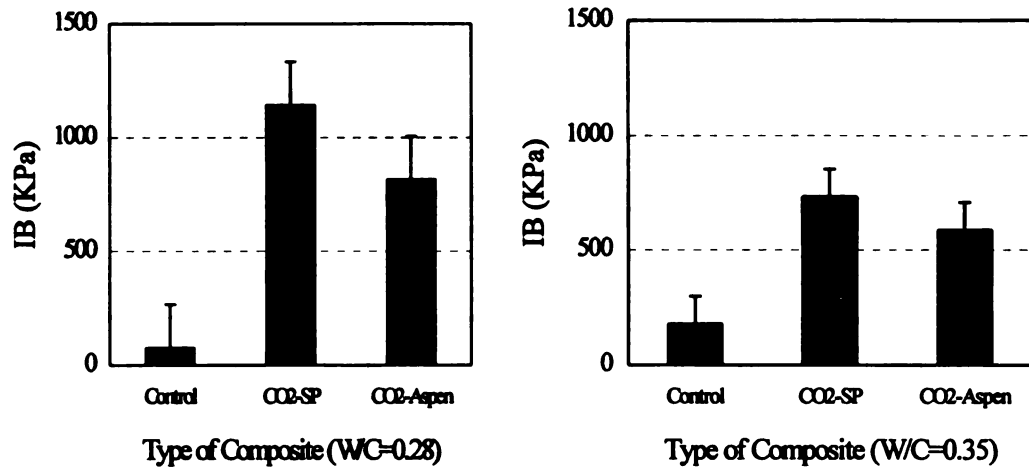


Figure 5.15 Internal Bond Test Results (means and 95% confidence interval)

Table 5.12 Results of Analysis of Variance for IB: CO₂ Versus Conventionally Cured Boards

Source	Sum-of-Squares	DF	Mean-Square	F-Ratio	P
A**	1970965.802	1	1970965.802	110.589	0.000
B	71325.519	1	71325.519	4.002	0.080
AxB*	198032.395	1	198032.395	11.111	0.010
Error	142579.512	8	17822.439		

A: Curing Conditions; B: Wood/Cement Ratio

*: Statistically significant at 95% level of confidence

**: Statistically significant at 99% level of confidence

Table 5.13 Results of Analysis of Variance for IB: CO₂ Cured Boards

Source	Sum-of-Squares	DF	Mean-Square	F-Ratio	P
A*	167349.826	1	167349.826	9.903	0.014
B**	307787.481	1	307787.481	18.214	0.003
AxB	24740.367	1	24740.367	1.464	0.261
Error	135189.782	8	16898.723		

A: Wood Species; B: Wood/Cement Ratio

*: Statistically significant at 95% level of confidence

**: Statistically significant at 99% level of confidence

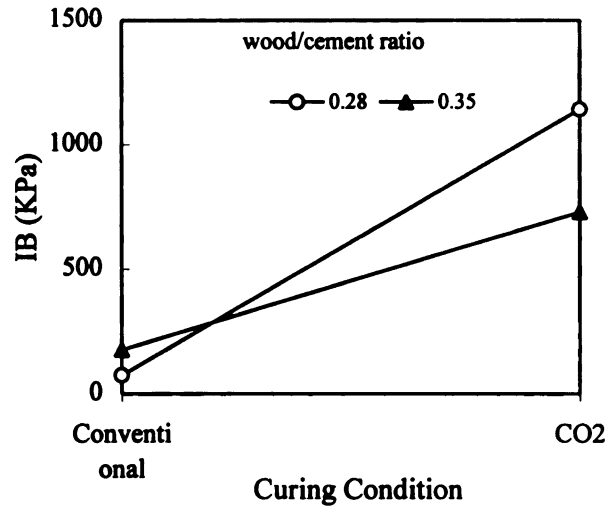


Figure 5.16 The Trends in Internal Bond Strength: CO₂ Versus Conventionally Cured Boards

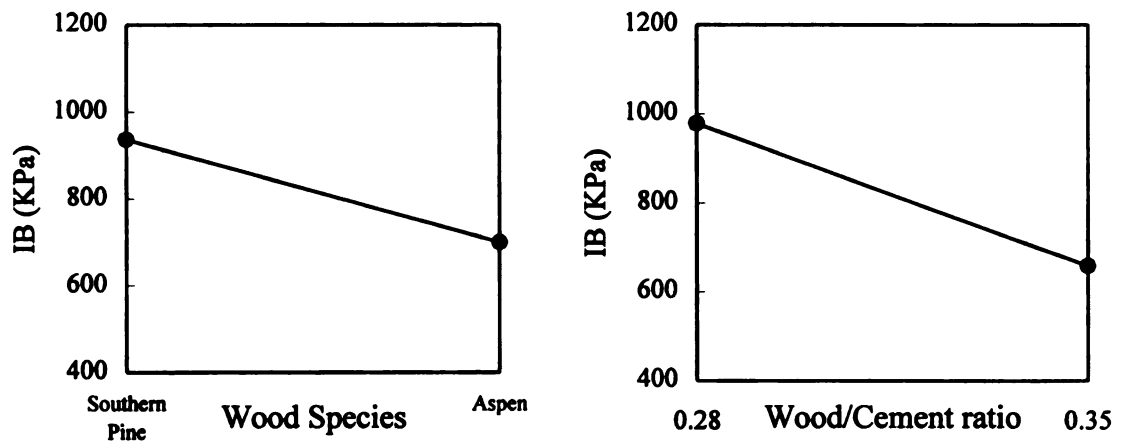


Figure 5.17 The Trends in Internal Bond Strength: CO₂ Cured Boards

The internal bond strength values were higher at 0.28 wood-cement ratio when compared with those of 0.35 wood-cement ratio. Higher binder seems to have provided for better bonding condition to wood particles. CO₂-curing provides for substantial increase in bond strength compared to control (non-CO₂-cured) specimens, CO₂-curing could improve bonding through partially petrifying wood particles near their surfaces.

5.4.2 Physical Properties

The physical properties investigated in this phase of research was dimensional stability, moisture content and swelling in water , following the BS 5669 test procedures.

The length, thickness and mass of the specimens are determined after conditioning at 25°C and 65% relative humidity, and following reconditioning at 25°C and 85% relative humidity. The results are expressed as a percentage increase of the original value. The test specimens are 200 mm x 13 mm x board thickness (7.874 in. x 0.512 in. x board thickness). The test results are shown in Figure 5.18. Length, thickness swelling and mass gain of cement-bonded wood particleboard with increasing moisture content (from 65% to 85%) were reduced as a result of CO₂ curing.

Moisture content represents the loss in mass of a test specimen dried to constant mass at 103± 2°C. Test specimens are 100 mm square x board thickness (3.937 in. square x board thickness) according to BS5669. Figure 5.19 shows moisture content test results.

CO₂-curing, particularly at a wood-cement ratio of 0.28 where CO₂ reactions seems to have been more through, led to increased moisture content of cement-bonded particleboard. This could result forth fact that CO₂ reaction make generation of water which, due to storage in plastic bag, could not evaporate.

Swelling in water is determined by the measurement of thickness swelling resulting from immersion in clean water at ambient temperature. The specimens shall be placed vertically and be separated by at least 10 mm from each other and from the bottom and sides of the container, and should be covered with an approximate depth of 25 mm of water. After 24 hours, each specimen is withdrawn from water and allowed to stand under normal room conditions for 2 hours with the bottom edges on a non-absorbent surface. The thickness is then remeasured at the same points. Figure 5.20 shows the thickness swelling test results.

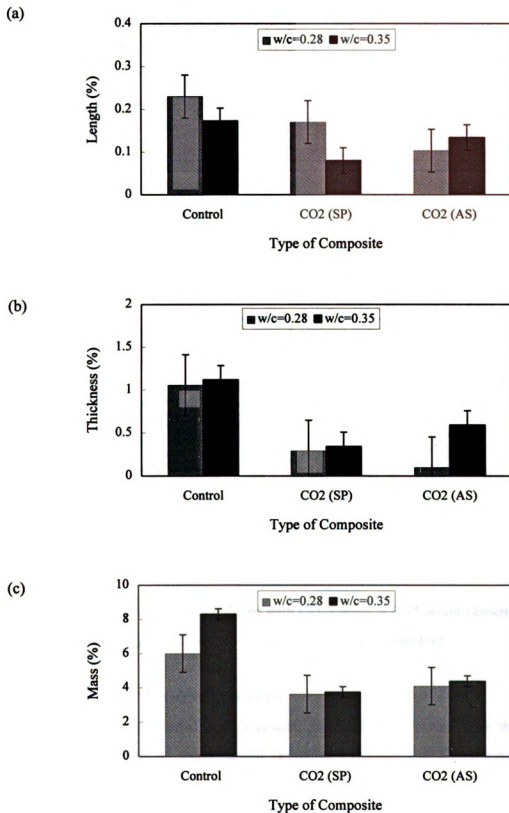


Figure 5.18 Dimensional Stability: (a) Length; (b) Thickness; (c) Mass

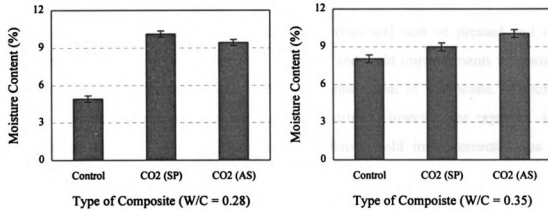


Figure 5.19 Moisture Content

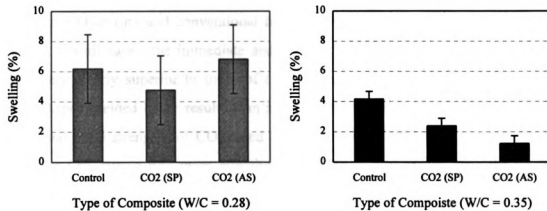


Figure 5.20 Swelling in Water of Cement-Bonded Particleboard

Thickness swelling was reduced with CO₂-curing at 0.35 wood-cement ratio. The effects of CO₂-curing at 0.28 wood-cement ratio were not consistent.

5.5 SUMMARY AND CONCLUSIONS

The results presented in this chapter provided more insight into the optimum processing conditions of wood-cement composites subjected to CO₂-curing. A more comprehensive view was also provided with effects of CO₂-curing in various aspects of composite board performance characteristics.

5.5.1 Cellulose Fiber Reinforced Cement Composite

CO₂-curing helps reduce the manufacturing time and cost of pressed and unpressed cellulose fiber reinforced cement composites, and yield improvements in flexural strength, stiffness, dimensional stability and water absorption of composite. Flexural toughness tends to be somewhat reduced with CO₂-curing. However, the expected improvements in resistance to aging (carbonation) effects yield improvements even in toughness after aging.

5.5.2 Cement-Bonded Particleboard

CO₂-curing at 25% CO₂ concentration seemed to be more effective at the lower wood-cement ratio of 0.25. At the higher wood-cement ratio of 0.35, however, the combination of CO₂-curing and conventional hydration yielded better 28 day flexural performance. In all cases, the immediate and 28-day flexural performance of CO₂-cured boards were clearly superior to those of conventional boards processed without CO₂-curing. Aspen yielded better results than southern pine when subjected to CO₂ curing. The internal bond strength of CO₂-cured boards, particularly at wood-cement ratio of 0.28 where CO₂-curing was more effective, was substantially greater than the internal bond strength values obtained through conventional processing without CO₂ curing. As far as moisture movements are concerned, CO₂-curing generally enhanced the dimensional stability of the board, or did not markedly influence it.

MICHIGAN STATE UNIV. LIBRARIES



31293014000578

THESIS

4



**PLACE IN RETURN BOX to remove this checkout from your record.
TO AVOID FINES return on or before date due.**

DATE DUE	DATE DUE	DATE DUE
DEC 28 2003		
AUG 31 2004		
AUG 26 11		

MSU is An Affirmative Action/Equal Opportunity Institution

c:\crl\data\due.pm3-p.1

CHAPTER 6

DURABILITY CHARACTERISTICS OF CARBONATED WOOD-CEMENT COMPOSITES

6.1 INTRODUCTION

As with any other material, concrete durability is governed by the material's quality and the severity of the environmental conditions to which it is exposed over its service life. Temperature and the presence of water may be considered the two most important factors, which affect the durability of wood-cement composites. A great deal of interest is expressed in the long-term performance of wood-cement composites under service conditions. Consequently, methods have been developed, or adopted from other materials where they have been thought to be appropriate, to predict such performance from some form of short-term test.

The utilization of carbon dioxide gas in curing of concrete transforms calcium hydroxide to calcium carbonate. Calcium carbonate is less soluble in water than calcium hydroxide and there is a small decrease in porosity associated with the formation of calcium carbonate (calcite) from calcium hydroxide. Table 6.1 compares molecular weight, molar volumes, density, and solubility of calcium hydroxide and calcium carbonate.

Table 6.1 The Properties of Cement Phases [93]

Compound	Molecular weight	Density (g/cm ³)	Molar volume (cm ³ /mol)	Solubility (mol/l)
Ca(OH) ₂	74	2.24	33.2	2.02x10 ⁻²
CaCO ₃	100.1	2.71	36.9	1.4 x10 ⁻⁴

During carbonation, the deposition of CaCO₃ in the pores makes the carbonated concrete layer denser and improves the pore structure. This change of composition enhances the performance of concrete under freezing and thawing, and in sulphate attack. Besides reducing the permeability of concrete, the surface hardness, modules of elasticity

and density of concrete are also improved. CO₂ curing also reduces the alkalinity of concrete pore water. The possibility of improving the durability of wood-cement composite was explored by reducing the alkalinity of the cement matrix [73].

6.2 TEST PROCEDURES

In this phase of the research, the long-term durability characteristics of cement-bonded wood particleboard and cellulose fiber reinforced cement composites were assessed. The cement-bonded particleboard specimens were subjected to repeated cycles of freezing-thawing and wetting-drying. After aging, the specimens were tested for mechanical and physical performance. The dimensions and the number of specimens depend on the specific test performed. All tests adopted in this study follow BS 5669 [94], ASTM C1185 [96]. In cellulose fiber reinforced cement composites, the effects of moisture and accelerated aging on the flexural performance of the carbonated and control composites were investigated. Tests generally followed ASTM C1185 [96]. One non-standard condition was used where wetting-drying cycles was accompanied with artificial carbonation.

6.2.1 Accelerated Wetting and Drying

Repeated wetting and drying cycles simulated repeated rain-heat conditions in natural weathering. This aging condition promotes some key chemical and physical mechanisms of deterioration in wood-cement composites. These conditions accelerate the alkaline pore water attack on wood particles/fibers; they also promote migration (through dissolution and re-precipitation) of some cement hydration products from the matrix into the wood particle/fiber cores and their interface zones. These microstructural changes would reflect in the engineering properties of aged composites. Cyclic drying and wetting effects on strength and shrinkage of asbestos cement indicate that susceptibility to shrinkage cracking is highest during the first cycle. However, drying and wetting of elements whose shrinkage was restrained generally resulted in no visible cracking [109]. A wetting-drying test chamber was used in this investigation (Figure 6.1). The specimens in this climate cubicle are subjected to moistening and cooling by spraying

them with water from the sprinkler nozzles. The water, which is sprayed for 3 hours at 30°C (86°F) until the capillary pores are filled with pore water, and then dried to reach 60°C (140°F) where this temperature is maintained 3 hours to dry out the capillary pore system. Under these conditions, the fibers come in contact with the alkaline pore water of the concrete during the moistening phase, and then any decomposition products formed as a result of the reaction between the fiber components and the pore water transported away from the fibers during the drying phase. New alkaline pore solution is introduced during next cycle. A total 25 cycles were used. These wetting-drying cycles follow the requirements of ASTM C1185 [96].

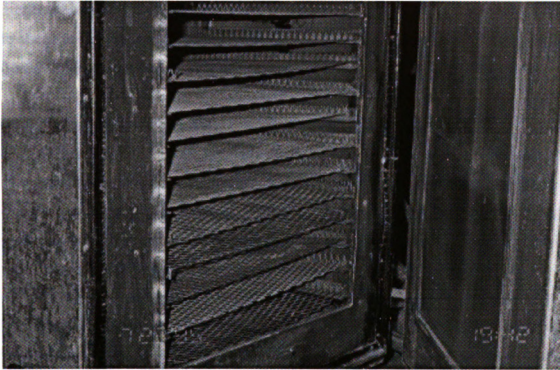


Figure 6.1 Test Set-Up for Wetting and Drying

6.2.2 Accelerated Freezing and Thawing

This test investigates possible degradation of the product due to exposure to repeated freeze-thaw cycles. Freezing of water in the cement paste capillary pores, due to the volume increase of water upon turning to ice, would produce internal pressures which

lead to cracking and deterioration of the composite. In cellulose fiber reinforced cement composites, total of 50 cycles are applied as required by ASTM C1185 [96]. The specimens are proposed by immersing in water at a temperature greater than 5°C (41°F) for a minimum of 48 hours. Each specimen is then sealed separately in a plastic bag. The freeze-thaw cycle should have a minimum cycle time of four hours; it consists of cooling at $-20\pm 2^{\circ}\text{C}$ ($-4\pm 4^{\circ}\text{F}$) over a period of an hour, holding the specimens at $-20\pm 2^{\circ}\text{C}$ ($-4\pm 4^{\circ}\text{F}$) for one hour, thawing to $20\pm 2^{\circ}\text{C}$ ($68\pm 4^{\circ}\text{F}$) over a period of one hour, and maintaining the specimens at $20\pm 2^{\circ}\text{C}$ ($68\pm 4^{\circ}\text{F}$) for one hour before proceeding with freezing. The time for the application of one cycle was 6 hours. In cement-bonded particleboard, total of 25 cycles are applied following BS 4624 [97]. Before the test cycle, the sample is immersed in water (not less than 5°C, 41°F) for 48 hours. The specimen is then subjected to alternate freezing and thawing between temperature of $-20\pm 3^{\circ}\text{C}$ ($68\pm 5^{\circ}\text{F}$) and $-20\pm 3^{\circ}\text{C}$ ($-68\pm 5^{\circ}\text{F}$) (each cycle consisting of 12 hours of freezing and 12 hours of thawing).

6.2.3 Warm Water Immersion

Chemical reactions are normally accelerated at elevated temperatures in the presence of moisture. Alkaline hydrolysis of cellulose tend to be accelerated of 100°C; decomposition of hemicellulose in an alkaline environment in similar to that of cellulose. Lignin consists of aromatic substances and begins to soften at 70°C - 80°C, and it is partly liquid at 120°C [103].

This test investigates the long-term chemical interactions of cellulose fiber in cement-based matrices following ASTM C1185 procedures [96]. Wet and elevated temperature conditions are used to accelerate the aging process. The test specimens are saturated in water with an excess of lime and maintained at $60\pm 2^{\circ}\text{C}$ ($140\pm 4^{\circ}\text{F}$) for 56 ± 2 days. At the end of the period, the specimens are placed in a conditioning chamber at $23\pm 2^{\circ}\text{C}$ ($73\pm 4^{\circ}\text{F}$) and 50±5% relative humidity for 48 ± 2 hours. Two replicated specimens were soaked in warm water. Flexural tests were performed before and after this aging process.

6.2.4 Repeated Wetting-Drying-Carbonation

In the case of asbestos cement, carbonation of the cement matrix by atmospheric carbon dioxide has been implicated in the embrittlement and loss of strength, and in 'corrosion' of the asbestos fibers in asbestos cement. Since cellulose fiber cement composites will also undergo carbonation in everyday use, it was thought desirable to accelerate this process and measure any corresponding changes in properties. Carbonation of cellulose fiber reinforced cement composites leads to petrification of the cellulose fiber, which fills the fiber cavity with reaction products and probably impregnates the fiber cell wall. This process can lead to an increase of the bond between the fibers and the matrix. Petrification of the fiber apparently increases its strength and rigidity, and in turns leads to increased strength, modulus of elasticity and moisture movement of the composite. The increase in strength was accompanied by a decrease in toughness, which could be due to densening of the matrix-fiber interfaces.

The test cycle chosen were optimized by trial and error experiments based on the degree of carbonation and water penetration into the products [89]. The test cycle used this study was [89]: (1) 8 hours submerged under water at 20°C; (2) 1 hour in oven at 80°C; (3) 5 hours at 20°C in a CO₂ environment at ~95% relative humidity; (4) 9 hours in oven at 80°C; and (5) 1 hour cooling down from 80°C to 20°C. In CO₂ chamber, 10% concentration of carbon dioxide was used.

6.2.5 Moisture Sensitivity

Cellulose fiber reinforced cement composites are sensitive to moisture variations. Considerable differences in flexural performances are observed when the specimens are tested at different moisture contents. There is a general tendency in flexural strength to decrease and flexural toughness to increase with increasing moisture content in cellulose fiber reinforced cement composites. This has been attributed to moisture effects on the interface zones and wood fibers.

Three different moisture conditions were selected: the specimen after storage for 7 days in the laboratory were air-dried, oven-dried, or saturated before being tested for flexural performance. These moisture conditions are described below.

- **Air-drying:** Place the test specimens for 4 days in a controlled atmosphere of 23°C (73°F) and 50% relative humidity and in such a manner that all faces are adequately ventilated.
- **Oven-drying:** Dry out the test specimen in an oven at 102°C (216°F) until the difference between two consecutive weightings, at intervals not less than two hours, does not exceed 0.1% of mass.
- **Saturation:** Immerse specimens in water at a temperature of 23°C (73°F) for a period of 48 hours. Test the specimens immediately upon removal from water.

Rapid drying of cement-based materials may induce tensile cracks due to non-uniform drying (and hence differences in drying shrinkage) of the specimen. The cracks do not have much effects on compressive strength but will lower the flexural and tensile strengths [40]. If drying takes place very slowly, so that internal stresses can be redistributed and alleviated by creep, an increase in strength may result from drying.

Wetting of concrete may lead to losses in compressive strength as a result of the dilation of cement gel by absorbed water and also breaking of Si-O-Si bonds, which leads to reduction of the cohesion between solid particles. Conversely, when the wedge-action of water upon drying ceases, an apparent increase in strength of the specimen is recorded. Resoaking of oven-dried specimens in water reduces their strength to the value of continuously wet-cured specimens, provided they have been hydrated to the same degree. The variation in strength due to drying is thus a reversible phenomenon.

In the case of cellulose fiber reinforced cement, however, moisture effects on cellulose fibers and their bond to matrix seems to be dominated. Moisture reduces hydrogen bonding of the fibers to matrix, reduces the elastic modulus of fibers and causes a radial expansion of fibers which produces compressive stresses at the interface.

6.3 TEST RESULTS

This section presents the test results on long-term durability of wood-cement composites. Repeated cycles of wetting-drying and freezing-thawing were applied on cement-bonded particleboard specimens. Wetting-drying, freezing-thawing, warm water immersion and wetting-drying-carbonation accelerated aging conditions were applied on cellulose fiber reinforced cement composite.

6.3.1 Cement-Bonded Particleboard

6.3.1.1 Repeated Wetting-Drying Cycles

Accelerated wetting-drying tests were performed to study the aging behavior of cement-bonded particleboard. Flexural tests were conducted on composites subjected to 25 cycles of accelerated wetting-drying. The effects of repeated wetting-drying on flexural load-deflection behavior are shown in Figure 6.2. Figure 6.3 shows the mean values and 95% confidence intervals of the flexural test results for control and carbonated composites before and after wetting-drying. Flexural test results are shown in Tables 6.2 to 6.4, and the outcomes of statistic analysis (analysis of variance) of results are shown in Table 6.5 and 6.6. In general, repeated wetting-drying cycles lead to increased stiffness and reduced toughness values. The effects on flexural strength are mixed.

Statistical Analysis - CO₂ Cured Boards

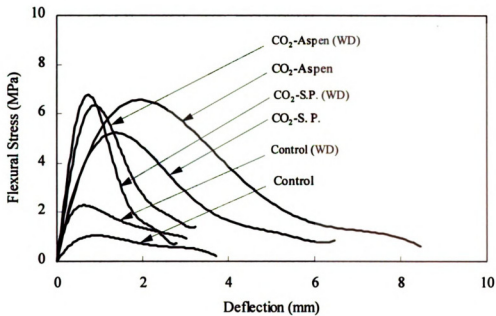
Statistical analyses of the flexural strength test results (see Table 6.5) suggest that wood species (aspen versus southern pine) and wood-cement ratios had statistically significant interactions with the aging effects on the flexural strength of cement-bonded particleboard. The trends in the effects of various factors on flexural strength (Figure 6.4a) suggest that, from a practical point of view, the effects and interactions of wood species, wood-cement ratio and aging on flexural strength are relatively small.

In the case of toughness (Table 6.5 and Figure 6.4b), aging has a definite adverse effect. Other effects and interactions in relation toughness seem to be of little practical significance.

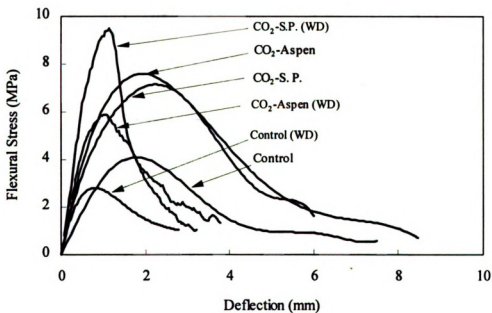
In the case of initial stiffness (Table 6.5 and Figure 6.4c), wood-cement ratio had a relatively small but statistically significant effect on stiffness. Aging leads to significant gains in stiffness; the interaction of aging with wood species in relation to stiffness, while statistically significant, seems to be rather small from a practical point of view.

Statistical Analysis - CO₂ Versus Conventional Curing

Statistical analysis of the flexural strength test results (see Table 6.6) suggests that curing conditions (CO₂ vs. conventional) and wood-cement ratio (0.28 vs. 0.35) had statistically significant interactions with the aging effect on flexural strength. The trends in the effects of various factors on flexural strength (Figure 6.5a) suggest that, CO₂ curing not only enhanced the initial flexural strength of cement-bonded particleboard, but also improved the resistance to aging effects on the flexural strength. The effects and interaction of wood-cement ratio and aging in regard to flexural strength were relatively small. In the case of flexural toughness (Table 6.6 and Figure 6.5b), the effects and interactions of curing condition and aging were statistically significant. Flexural toughness was higher with CO₂-curing; aging caused embrittlement in both CO₂ and conventionally cured boards but flexural toughness after aging remained higher in CO₂ cured boards. The adverse effects of aging on toughness were more pronounced at the higher wood-cement ratio of 0.35. In the case of initial stiffness (Table 6.6 and Figure 6.5c), aging leads to significant gains in stiffness; the interaction of aging with curing condition in relation to stiffness was statistically significant; the CO₂-cured boards showed more gain in stiffness upon aging than the conventionally cured boards.



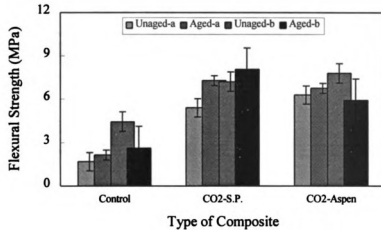
(a) Wood/Cement=0.28



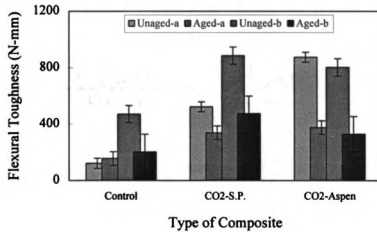
(b) Wood/Cement=0.35

Figure 6.2 Effects of Repeated Wetting-Drying on the Flexural Load-Deflection Behavior of Cement-Bonded Particleboard (S.P.= Southern Pine; WD= After wetting-drying)

(a)



(b)



(c)

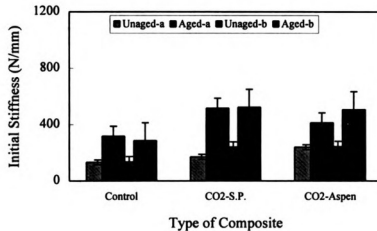


Figure 6.3 Effects of Repeated Wetting-Drying Cycles on Flexural Behavior (means and 95% confidence interval): (a) Flexural Strength; (b) Flexural Toughness; (c) Initial Stiffness (a-wood/cement=0.28; b-wood/cement=0.35)

Table 6.2 Repeated Wetting-Drying Effects on Flexural Strength of Cement-Bonded Particleboard (MPa)

Type of Composite		After W-D	Unaged
Wood/Cement=0.28	CO ₂ -S. P.	7.43	5.23
		7.22	5.37
		7.34	5.56
		7.11	5.42
	Mean (St. Dev.)	7.275 (0.140)	5.395 (0.136)
	CO ₂ -Aspen	6.53	6.36
		6.96	6.45
		6.65	5.39
		6.83	6.92
	Mean (St. Dev.)	6.743 (0.190)	6.28 (0.642)
	Control	1.89	1.08
		2.58	1.45
		1.99	1.96
		2.12	2.23
	Mean (St. Dev.)	2.145 (0.305)	1.680 (0.514)
Wood/Cement=0.35	CO ₂ -S. P.	6.66	7.02
		9.82	7.39
		8.54	7.42
		7.22	6.99
	Mean (St. Dev.)	8.060 (1.413)	7.205 (0.232)
	CO ₂ -Aspen	5.57	6.77
		6.18	8.27
		5.89	8.53
		6.03	7.58
	Mean (St. Dev.)	5.918 (0.260)	7.788 (0.788)
	Control	1.63	4.32
		3.26	3.99
		3.06	4.83
		2.54	4.59
	Mean (St. Dev.)	2.623 (0.728)	4.433 (0.361)

Table 6.3 Repeated Wetting-Drying Effects on Flexural Toughness of Cement-Bonded Particleboard (N-mm)

Type of Composite		After W-D	Control
Wood/Cement=0.28	CO ₂ -S. P.	346.743 338.393 340.557 329.558	541.934 520.632 533.526 500.693
	Mean (St. Dev.)	338.813 (7.112)	524.196 (17.952)
	CO ₂ -Aspen	328.875 414.939 377.265 383.541	920.432 839.411 880.559 859.299
	Mean (St. Dev.)	376.155 (35.569)	874.925 (34.880)
	Control	103.920 187.794 155.219 176.554	89.818 114.700 132.624 149.954
	Mean (St. Dev.)	155.872 (37.176)	121.774 (25.710)
Wood/Cement=0.35	CO ₂ -S. P.	367.851 647.435 399.513 485.416	900.551 907.825 910.515 827.704
	Mean (St. Dev.)	475.054 (125.195)	886.649 (39.521)
	CO ₂ -Aspen	285.616 384.052 337.736 350.694	890.510 870.832 732.499 719.918
	Mean (St. Dev.)	329.525 (40.893)	803.440 (89.687)
	Control	244.645 212.216 184.554 170.567	452.643 483.219 488.553 462.434
	Mean (St. Dev.)	202.996 (32.718)	471.712 (16.988)

Table 6.4 Repeated Wetting-Drying Effects on Initial Stiffness of Cement-Bonded Particleboard (N/mm)

Type of Composite		After W-D	Control
Wood/Cement=0.28	CO ₂ -S. P.	507.329 533.091 520.551 503.113	170.216 183.214 149.226 183.214
	Mean (St. Dev.)	516.021 (13.590)	171.468 (16.044)
	CO ₂ -Aspen	394.314 436.567 409.586 411.584	221.551 243.164 239.255 255.194
	Mean (St. Dev.)	413.038 (17.489)	239.791 (13.924)
	Control	212.278 376.535 339.261 345.589	140.316 138.677 123.611 128.769
	Mean (St. Dev.)	318.416 (72.608)	132.843 (7.994)
Wood/Cement=0.35	CO ₂ -S. P.	510.009 505.276 521.559 554.316	246.663 274.315 209.551 232.646
	Mean (St. Dev.)	522.790 (22.102)	240.794 (27.084)
	CO ₂ -Aspen	511.349 499.943 513.504 500.332	243.164 272.119 213.516 250.551
	Mean (St. Dev.)	506.282 (7.151)	244.838 (24.226)
	Control	195.732 327.802 304.593 316.663	135.211 130.554 140.221 139.551
	Mean (St. Dev.)	286.198 (61.050)	136.384 (4.477)

Table 6.5 Results of Analysis of Variance After Wetting-Drying: CO₂ Cured Boards

Source	Sum-of - Squares	DF	Mean-Square	F-Ratio	P
Flexural Strength					
A	0.729	1	0.729	1.730	0.200
B	0.881	1	0.881	2.091	0.161
C**	5.371	1	5.371	12.746	0.001
AxB**	8.580	1	8.580	20.362	0.000
AxC**	1.829	1	1.829	4.340	0.048
BxC**	5.636	1	5.636	13.376	0.001
Error	10.535	25	0.421		
Flexural Toughness					
A	14336.832	1	14336.832	2.903	0.101
B**	1216275.896	1	1216275.896	246.299	0.000
C**	76275.392	1	76275.392	15.446	0.001
AxB**	66870.805	1	66870.805	13.541	0.001
AxC**	184108.885	1	184108.885	37.282	0.000
BxC	18308.655	1	18308.655	3.708	0.066
Error	123455.314	25	4938.213		
Initial Stiffness					
A	1111.514	1	1111.514	1.405	0.247
B**	563089.699	1	563089.699	711.916	0.000
C**	15209.598	1	15209.598	19.230	0.000
AxB**	18409.639	1	18409.639	23.275	0.000
AxC	246.875	1	246.875	0.312	0.581
BxC	329.359	1	329.359	0.416	0.525
Error	19773.727	25	790.949		

A: Wood Species; B: Aging(WD) Conditions; C: Wood/Cement Ratio

*: Statistically significant at 95% level of confidence

**: Statistically significant at 99% level of confidence

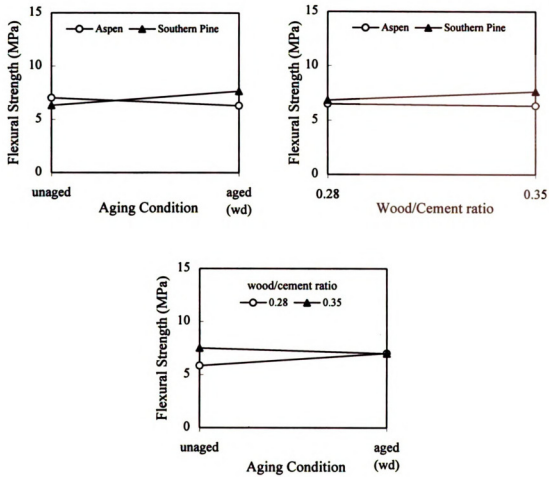
Table 6.6 Results of Analysis of Variance After Wetting-Drying: CO₂ Versus Conventionally Cured Boards

Source	Sum-of - Squares	DF	Mean-Square	F-Ratio	P
Flexural Strength					
A**	145.437	1	145.437	359.863	0.000
B	0.966	1	0.966	2.390	0.135
C**	16.965	1	16.965	41.978	0.000
AxB**	8.323	1	8.323	20.595	0.000
BxC**	5.445	1	5.445	13.473	0.001
AxC	0.202	1	0.202	0.499	0.487
Error	10.104	25	0.404		
Flexural Toughness					
A**	809447.440	1	809447.440	306.766	0.000
B**	345777.201	1	345777.201	131.043	0.000
C**	401188.958	1	401188.958	152.043	0.000
AxB**	65652.204	1	65652.204	24.881	0.000
BxC**	139934.254	1	139934.254	53.033	0.000
AxC	5164.481	1	5164.481	1.957	0.174
Error	65966.232	25	2638.649		
Initial Stiffness					
A**	166598.102	1	166598.102	127.756	0.000
B**	462659.953	1	462659.953	354.792	0.000
C	1124.233	1	1124.233	0.862	0.362
AxB**	42388.237	1	42388.237	32.506	0.000
BxC	4833.067	1	4833.067	3.706	0.066
AxC	5488.638	1	5488.638	4.209	0.051
Error	32600.754	25	1304.030		

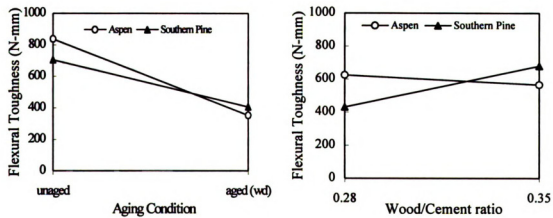
A: Curing Conditions; B: Aging (WD) Conditions; C: Wood/Cement Ratio

*: Statistically significant at 95% level of confidence

**: Statistically significant at 99% level of confidence

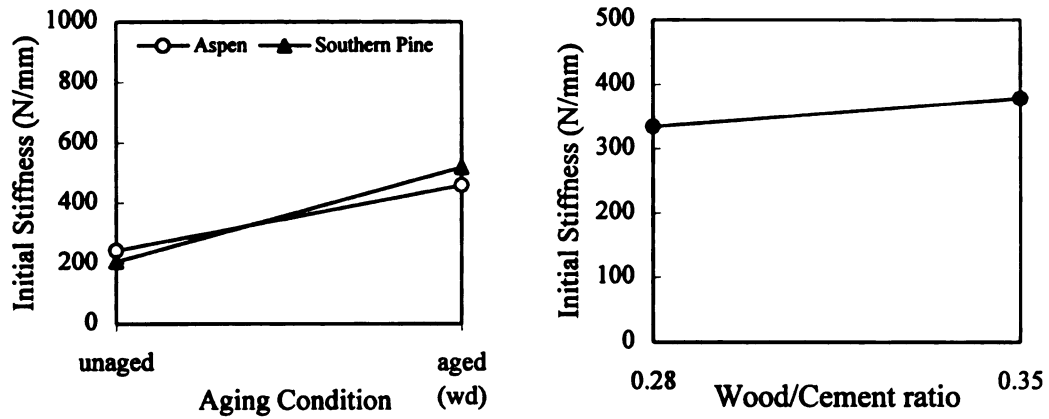


(a) Flexural Strength

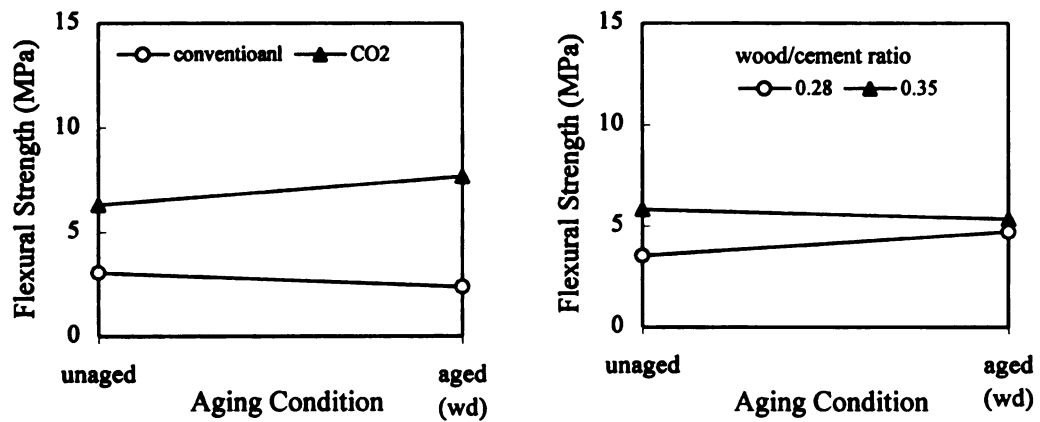


(b) Flexural Toughness

Figure 6.4 The Trends in Flexural Performance: CO₂ Cured Boards

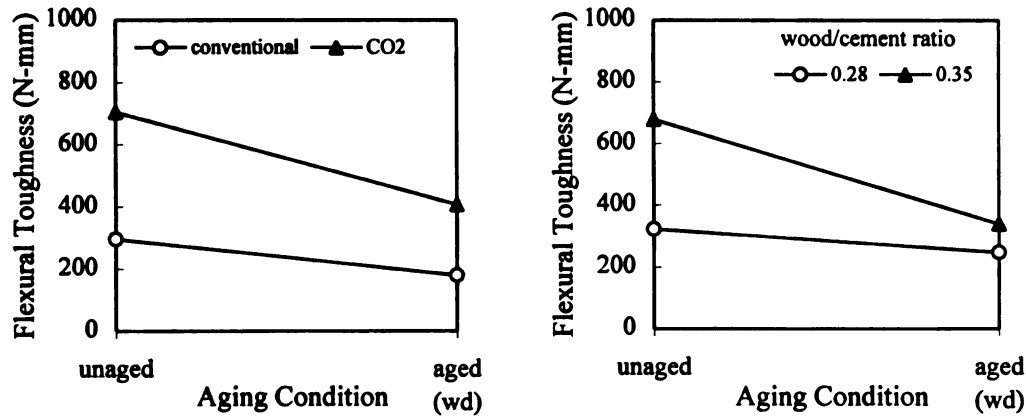


(c) Initial Stiffness

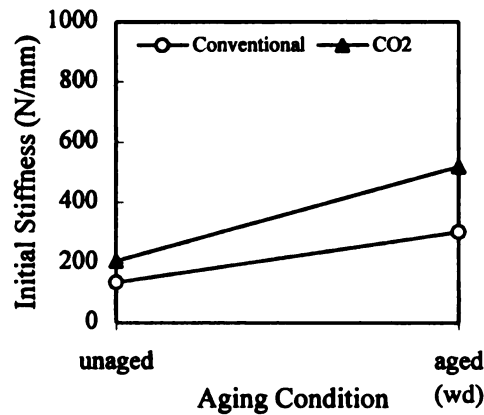
Figure 6.4 (Cont'd) The Trends in Flexural Performance: CO₂ Cured Boards

(a) Flexural Strength

Figure 6.5 The Trends in Flexural Performance: CO₂ Versus Conventionally Cured Boards



(b) Flexural Toughness



(c) Initial Stiffness

Figure 6.5 (Cont'd) The Trends in Flexural Performance: CO₂ Versus Conventionally Cured Boards

6.3.1.2 Repeated Freezing-Thawing Cycles

The boards were tested for flexural performance before and after exposure to freeze-thaw cycles. The effects of repeated freeze-thaw cycles on flexural load-deflection behavior are presented in Figure 6.6. Figure 6.7 and Tables 6.7 to 6.9 show the freeze-thaw effects on flexural strength, toughness and stiffness of carbonated and non-carbonated composites. No cracks were observed in the specimens subjected to repeated freeze-thaw cycles. Tables 6.10 and 6.11 show the results of statistical analysis of vari-

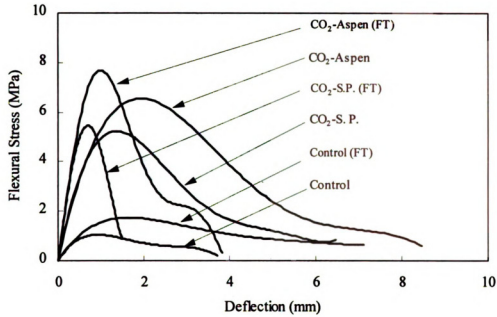
ance of test result. In general, repeated freezing-thawing cycles led to increased stiffness and reduced toughness of cement-bonded wood particleboard. The effects on flexural strength were mixed but generally negative.

Statistical Analysis - CO₂ Cured Boards

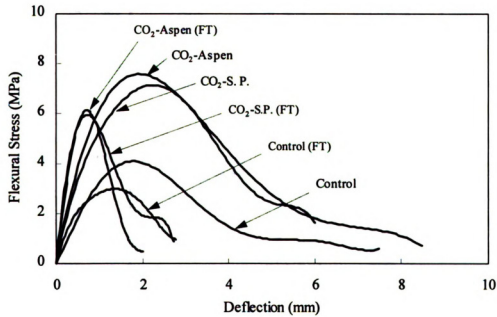
Statistical analysis of the flexural strength test results (Table 6.10 and Figure 6.8a) suggests that the effects and interactions of various variables, although statistically significant, are relatively small and of little practical significance. Flexural strength tends to be rather stable under repeated freeze-thaw cycles. As shown in Figure 6.8b and Table 6.10, flexural toughness seriously drops with aging under freeze-thaw effect. This adverse effect of repeated freeze-thaw cycles was more pronounced at the higher wood-cement ratio of 0.35. Figure 6.8c and Table 6.10 indicate that repeated freeze-thaw cycles substantially increase the stiffness of cement-bonded wood particleboard.

Statistical Analysis - CO₂ Versus Conventional Curing

Statistical analysis of the flexural strength test results (Table 6.11 and Figure 6.9a) confirms that flexural strength was rather stable under repeated freeze-thaw cycles. CO₂-curing produces substantially improved flexural strengths before and after the application of freeze-thaw cycles. As shown in Figure 6.9b and Table 6.11, flexural toughness seriously drops with aging. There was a strong interaction of curing condition and wood-cement ratio with aging. The freeze-thaw effects on toughness were more pronounced at the higher wood-cement ratio and in the case of CO₂-cured boards. Figure 6.9c and Table 6.11 confirm that repeated freeze-thaw cycles substantially increased the stiffness of cement-bonded wood particleboard; the effects and interactions of curing conditions and wood-cement ratio with aging were statistically significant. The increase in the stiffness of cement-bonded wood particleboard was more pronounced when the boards were subjected to CO₂-curing.



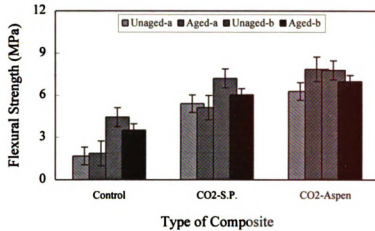
(a) Wood/Cement=0.28



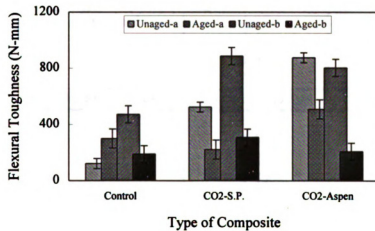
(b) Wood/Cement=0.35

Figure 6.6 Effects of Repeated Freezing-Thawing Cycles on the Flexural Load-Deflection Behavior of Cement-Bonded Particleboard (S.P.= Southern Pine; FT= After freezing-thawing)

(a)



(b)



(c)

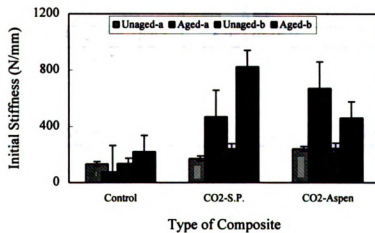


Figure 6.7 Effects of Repeated Freezing-Thawing Cycles on Flexural Behavior (means and 95% confidence intervals): (a) Flexural Strength; (b) Flexural Toughness; (c) Initial Stiffness; (a-wood/cement=0.28, b-wood/cement=0.35)

Table 6.7 Repeated Freezing-Thawing Effects on Flexural Strength of Cement-Bonded Particleboard (MPa)

Type of Composite		After F-T	Control
Wood/Cement=0.28	CO ₂ -S. P.	4.35	5.23
		5.74	5.37
		5.51	5.56
		4.86	5.42
	Mean (St. Dev.)	5.115 (0.632)	5.395 (0.136)
	CO ₂ -Aspen	8.49	6.36
		7.48	6.45
		7.22	5.39
		8.25	6.92
	Mean (St. Dev.)	7.860 (0.606)	6.28 (0.642)
	Control	1.88	1.08
		1.92	1.45
		1.93	1.96
		1.72	2.23
	Mean (St. Dev.)	1.863 (0.097)	1.680 (0.514)
Wood/Cement=0.35	CO ₂ -S. P.	6.43	7.02
		5.54	7.39
		6.28	7.42
		5.88	6.99
	Mean (St. Dev.)	6.033 (0.402)	7.205 (0.232)
	CO ₂ -Aspen	7.02	6.77
		7.11	8.27
		6.86	8.53
		6.94	7.58
	Mean (St. Dev.)	6.983 (0.107)	7.788 (0.788)
	Control	3.28	4.32
		3.81	3.99
		3.55	4.83
		3.42	4.59
	Mean (St. Dev.)	3.515 (0.225)	4.433 (0.361)

Table 6.8 Repeated Freezing-Thawing Effects on Flexural Toughness of Cement-Bonded Particleboard (N-mm)

Type of Composite		After F-T	Unaged
Wood/Cement=0.28	CO ₂ -S. P.	224.763	541.934
		217.322	520.632
		226.853	533.526
		218.774	500.693
	Mean (St. Dev.)	221.928 (4.599)	524.196 (17.952)
	CO ₂ -Aspen	589.824	920.432
		429.895	839.411
		488.661	880.559
		527.891	859.299
	Mean (St. Dev.)	509.068 (67.233)	874.925 (34.880)
	Control	286.241	89.818
		308.543	114.700
		298.845	132.624
		306.144	149.954
	Mean (St. Dev.)	299.943 (10.023)	121.774 (25.710)
Wood/Cement=0.35	CO ₂ -S. P.	373.711	900.551
		236.715	907.825
		288.437	910.515
		335.129	827.704
	Mean (St. Dev.)	308.498 (59.209)	886.649 (39.521)
	CO ₂ -Aspen	217.040	890.510
		210.556	870.832
		199.994	732.499
		206.557	719.918
	Mean (St. Dev.)	208.537 (7.148)	803.440 (89.687)
	Control	192.698	452.643
		189.653	483.219
		190.472	488.553
		185.865	462.434
	Mean (St. Dev.)	189.672 (2.845)	471.712 (16.988)

Table 6.9 Repeated Freezing-Thawing Effects on Initial Stiffness of Cement-Bonded Particleboard (N/mm)

Type of Composite		After F-T	Unaged
Wood/Cement=0.28	CO ₂ -S. P.	364.655	170.216
		530.616	183.214
		500.073	149.226
		485.778	183.214
	Mean (St. Dev.)	470.281 (72.858)	171.468 (16.044)
	CO ₂ -Aspen	565.814	221.551
		928.235	243.164
		588.521	239.255
		603.951	255.194
	Mean (St. Dev.)	671.630 (171.785)	239.791 (13.924)
	Control	56.063	140.316
		93.173	138.677
		90.238	123.611
		65.387	128.769
	Mean (St. Dev.)	76.215 (18.326)	132.843 (7.994)
Wood/Cement=0.35	CO ₂ -S. P.	921.185	246.663
		713.087	274.315
		900.663	209.551
		793.628	232.646
	Mean (St. Dev.)	824. 641 (102.090)	240.794 (27.084)
	CO ₂ -Aspen	441.863	243.164
		480.767	272.119
		502.115	213.516
		420.894	250.551
	Mean (St. Dev.)	461.410 (36.766)	244.838 (24.226)
	Control	171.178	135.211
		288.305	130.554
		190.682	140.221
		230.404	139.551
	Mean (St. Dev.)	220.142 (51.694)	136.384 (4.477)

Table 6.10 Results of Analysis of Variance After Repeated Freezing-Thawing: CO₂ Cured Boards

Source	Sum-of - Squares	DF	Mean-Square	F-Ratio	P
Flexural Strength					
A**	13.326	1	13.326	45.955	0.000
B	0.230	1	0.230	0.791	0.382
C**	5.636	1	5.636	19.438	0.000
AxB**	2.481	1	2.481	8.556	0.007
AxC*	2.200	1	2.200	7.586	0.011
BxC**	5.371	1	5.371	18.522	0.000
Error	7.249	25	0.290		
Flexural Toughness					
A**	103375.363	1	103375.363	43.964	0.000
B**	1694970.976	1	1694970.976	720.854	0.000
C	2964.962	1	2964.962	1.261	0.272
AxB	3227.378	1	3227.378	1.373	0.252
AxC**	337052.520	1	337052.520	143.345	0.000
BxC**	127476.143	1	127476.143	54.214	0.000
Error	58783.451	25	2351.338		
Initial Stiffness					
A	4705.858	1	4705.858	0.434	0.516
B**	1183601.130	1	1183601.130	109.173	0.000
C	25540.825	1	25540.825	2.356	0.137
AxB	29221.169	1	29221.169	2.695	0.113
AxC**	202477.343	1	202477.343	18.676	0.000
BxC	2985.095	1	2985.095	0.275	0.604
Error	271038.148	25	10841.526		

A: Wood Species; B: Aging(WD) Conditions; C:Wood/Cement Ratio

*: Statistically significant at 95% level of confidence

**: Statistically significant at 99% level of confidence

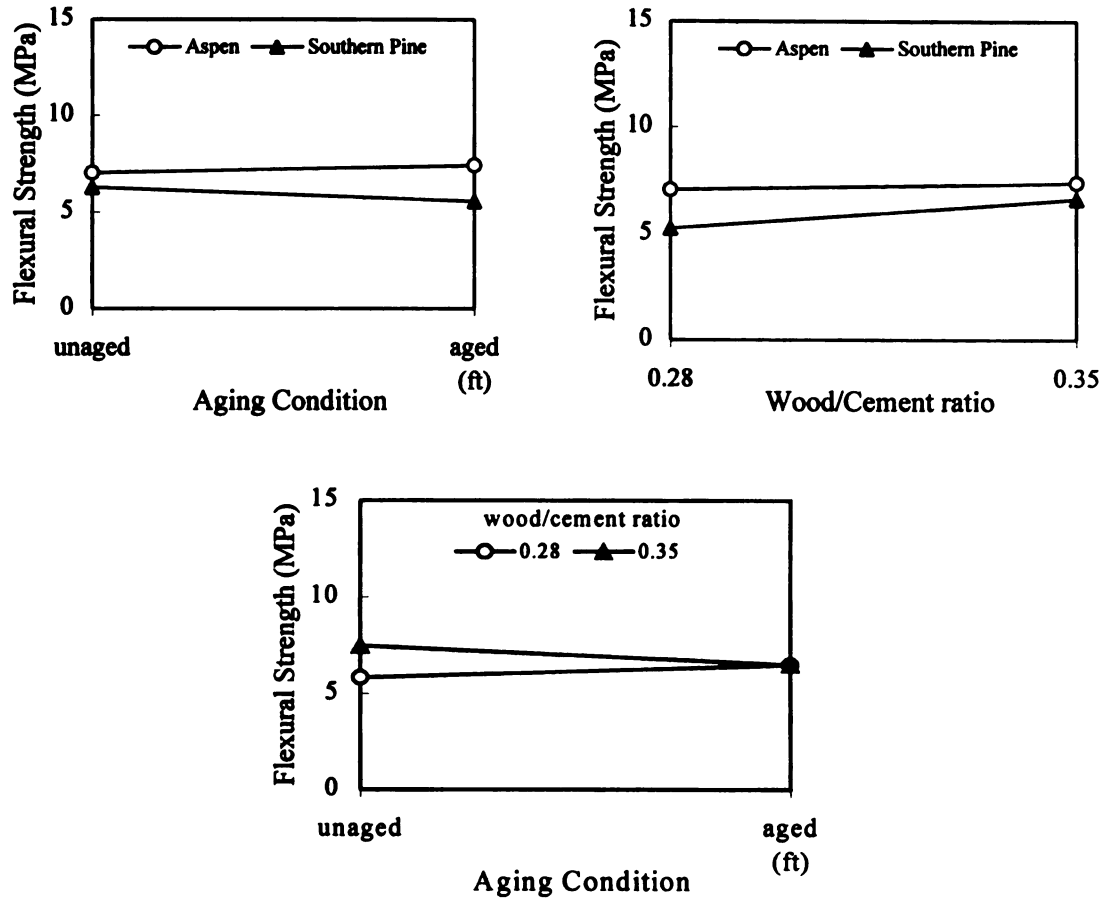
Table 6.11 Results of Analysis of Variance After Freezing-Thawing: CO₂ Versus Conventionally Cured Boards

Source	Sum-of - Squares	DF	Mean-Square	F-Ratio	P
Flexural Strength					
A**	82.786	1	82.786	350.322	0.000
B**	3.913	1	3.913	16.558	0.000
C**	17.746	1	17.746	75.094	0.000
AxB	0.006	1	0.006	0.024	0.877
BxC**	5.017	1	5.017	21.228	0.000
AxC	0.126	1	0.126	0.534	0.472
Error	5.908	25	0.236		
Flexural Toughness					
A**	488978.911	1	488978.911	456.098	0.000
B**	621654.871	1	621654.871	579.853	0.000
C**	357929.491	1	357929.491	333.861	0.000
AxB**	208528.820	1	208528.820	194.507	0.000
BxC**	167445.109	1	167445.109	156.186	0.000
AxC	1349.947	1	1349.947	1.259	0.272
Error	26802.268	25	1072.091		
Initial Stiffness					
A**	353507.424	1	353507.424	68.874	0.000
B**	750981.193	1	750981.193	146.314	0.000
C**	81006.848	1	81006.848	15.783	0.001
AxB**	153887.234	1	153887.234	29.982	0.000
BxC*	32966.636	1	32966.636	6.423	0.018
AxC**	105737.334	1	105737.334	20.601	0.000
Error	128316.434	25	5132.657		

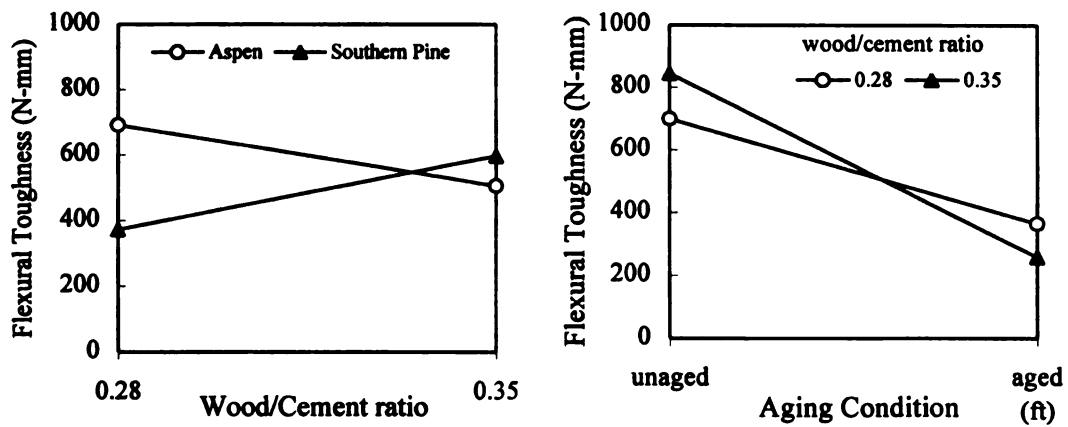
A: Curing Conditions; B: Aging(FT) Conditions; C:Wood/Cement Ratio

*: Statistically significant at 95% level of confidence

** : Statistically significant at 99% level of confidence

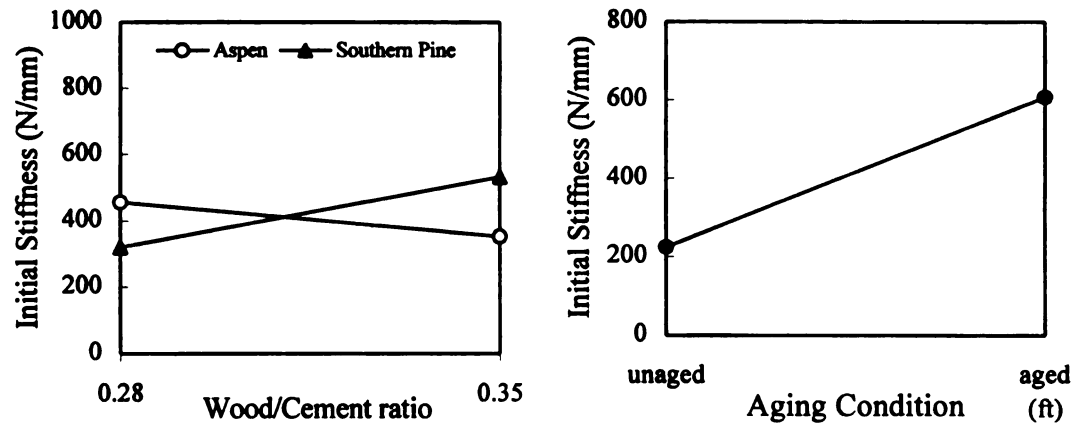


(a) Flexural Strength

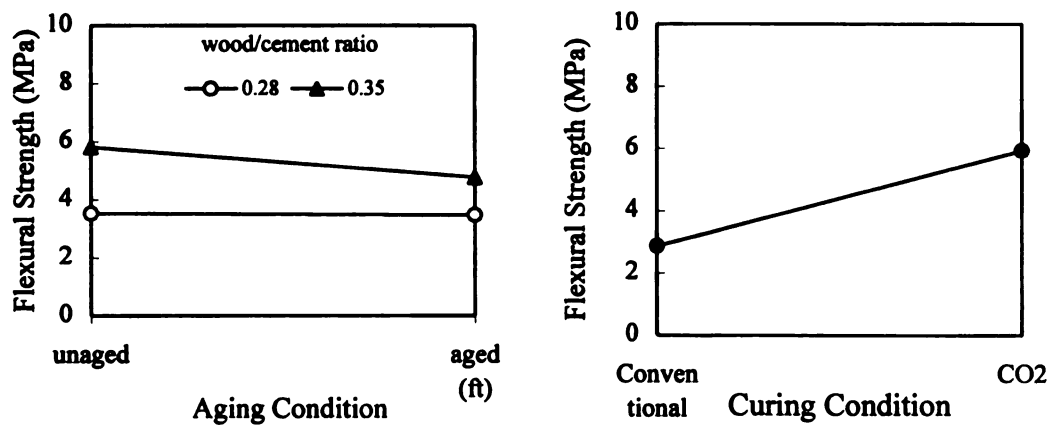


(b) Flexural Toughness

Figure 6.8 The Trends in Flexural Performance: CO₂ Cured Boards

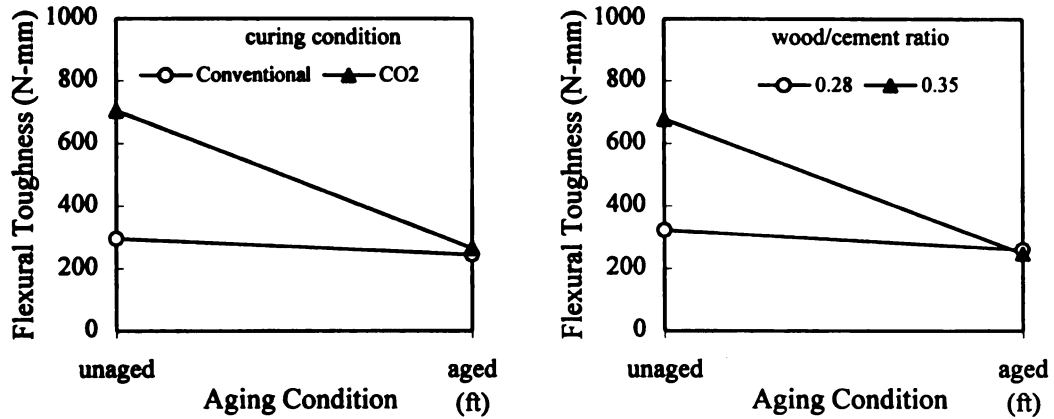


(c) Initial Stiffness

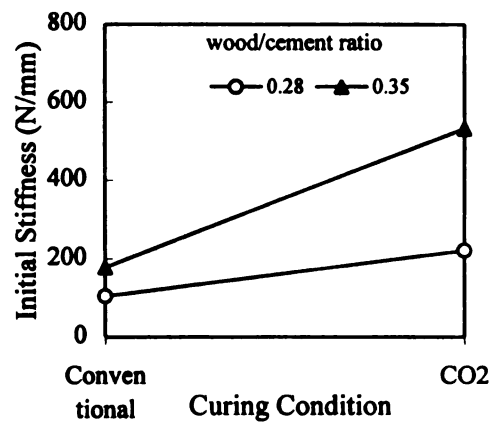
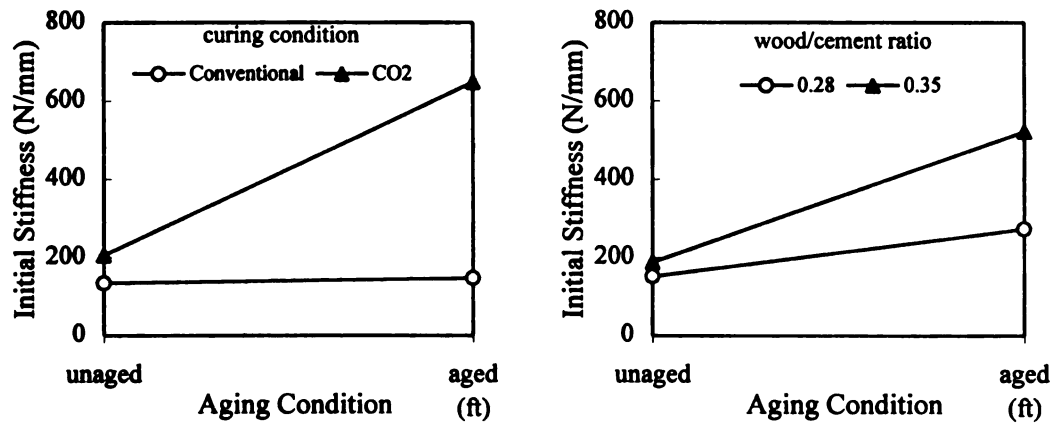
Figure 6.8 (Cont'd) The Trends in Flexural Performance: CO₂ Cured Boards

(a) Flexural Strength

Figure 6.9 The Trends in Flexural Performance: CO₂ Versus Conventionally Cured Boards



(b) Flexural Toughness



(c) Initial Stiffness

Figure 6.9 (Cont'd) The Trends in Flexural Performance: CO₂ Versus Conventionally Cured Boards

6.3.2 Cellulose Fiber Reinforced Cement Composite

Figures 5.4 and 5.5 for unpressed and pressed boards, respectively, show the flexural performance of unaged panel, cured under two control conditions and also under CO₂ exposure. Table 6.12 shows the results of statistical analysis of variance of test data when considering unaged panels which have been cured by conventional method 1 and 2 (control condition) and through CO₂ exposure. Tables 6.13 and 6.14 present the results of multiple comparison of test data.

The improved flexural strength of boards with CO₂ curing was observed to be statistically significant at 99% level of confidence. Control curing conditions produced flexural toughnesses which were higher than those obtained through CO₂-curing. The improved stiffness with CO₂ curing was statistically significant at 99% level of confidence for unpressed boards; in the case of pressed boards the stiffness obtained with CO₂-curing was statistically comparable to that product by the longer curing period but, at 95% level of confidence, superior to the stiffness of boards subjected to a similar autoclave curing period without CO₂-curing.

Table 6.12 Results of the Statistical Analysis of Test Data: Unaged Cases

Source	Sum-of-Squares	DF	Mean-Square	F-Ratio	P
Flexural Strength (Unpressed)					
Curing**	33.356	2	16.678	352.395	0.000
Error	0.426	9	0.047		
Flexural Toughness (Unpressed)					
Curing**	712353.960	2	356176.980	6.966	0.015
Error	460164.138	9	51129.349		
Initial Stiffness (Unpressed)					
Curing**	7497.506	2	3748.753	24.602	0.000
Error	1371.386	9	152.376		
Flexural Strength (Pressed)					
Curing**	10.672	2	5.336	48.813	0.000
Error	0.984	9	0.109		
Flexural Toughness (Pressed)					
Curing**	1750844.132	2	875422.066	23.766	0.000
Error	331512.040	9	36834.671		
Initial Stiffness (Pressed)					
Curing*	3059.447	2	1529.723	7.676	0.011
Error	1793.534	9	199.282		

*: Statistically significant at 95% level of confidence

**: Statistically significant at 99% level of confidence

Table 6.13 Statistical Analysis of Test Results: Unaged Cases (Unpressed)

	Flexural Strength			Flexural Toughness			Initial Stiffness		
	C1	C2	CO ₂	C1	C2	CO ₂	C1	C2	CO ₂
C1	-			-			-		
C2	**	-		*	-		-	-	
CO ₂	**	**	-	-	-	-	**	**	-

-: Statistically insignificant difference

*: Statistically significant difference at 95% level of confidence

**: Statistically significant difference at 99% level of confidence

C1: Control 1; C2: Control 2

Table 6.14 Statistical Analysis of Test Results: Unaged Cases (Pressed)

	Flexural Strength			Flexural Toughness			Initial Stiffness		
	C1	C2	CO ₂	C1	C2	CO ₂	C1	C2	CO ₂
C1	-			-			-		
C2	**	-		*	-		-	-	
CO ₂	**	**	-	**	*	-	*	-	-

-: Statistically insignificant difference

*: Statistically significant difference at 95% level of confidence

**: Statistically significant difference at 99% level of confidence

C1: Control 1; C2: Control 2

6.3.2.1 Repeated Wetting-Drying Cycles

Figure 6.10 presents the effects of repeated wetting-drying cycles on the flexural load-deflection behavior of cellulose fiber reinforced cement composites. The effects of repeated wetting-drying cycles on flexural performance are presented in Table 6.15, and in Figures 6.11 and 6.12. These results suggest that repeated wetting-drying cycles caused an increase in the flexural stiffness and a drop in the flexural toughness of composites, without significantly affecting their flexural strength. In the case of unpressed boards, analysis of variance of flexure test results (Table 6.16) suggests that repeated wetting-drying cycles had statistically significant effects, at 99% level of confidence, on flexural strength, toughness and stiffness. In the case of pressed boards (Table 6.17), the effects of repeated wetting-drying cycles were statistically significant, at 95% level of confidence, only for flexural toughness. CO₂-curing led to higher original strength and stiffness values but did not seem to change the general trends in the effects of wetting-drying cycles. Results of the statistical analysis of the test data are shown in Tables 6.18 and 6.19. Results of the multiple comparisons of the test data are shown in Tables 6.16, 6.17 and 6.20 to 6.23.

Table 6.20 which reflects the outcomes of statistical analysis of unpressed boards indicated that, after aging, the CO₂-cured boards were still superior to conventionally cured ones in all aspects of flexural performance (strength, toughness and stiffness) at 99% level of confidence. It is interesting to notice that, as shown in Table 6.21, after ag-

ing the differences in flexural performance under different curing condition disappear. Table 6.22 suggest that CO_2 -curing helped control the aging effects on the toughness of unpressed boards. With CO_2 -curing, the increase in stiffness with aging was also more pronounced than that for the control curing condition 2. Otherwise, Tables 6.22 and 6.23 indicate similar trends were observed in aging effects on CO_2 -cured and conventionally cured composites.

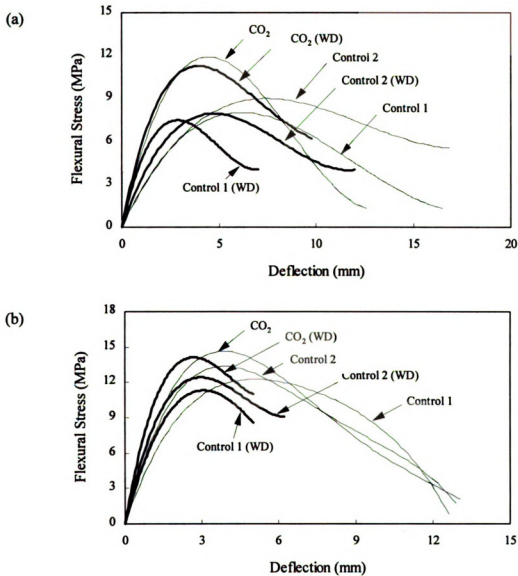


Figure 6.10 Typical Flexural Load-Deflection Behavior After Repeated Wetting-Drying Cycles of Cellulose Fiber Reinforced Cement Composites: (a) unpressed; (b) pressed

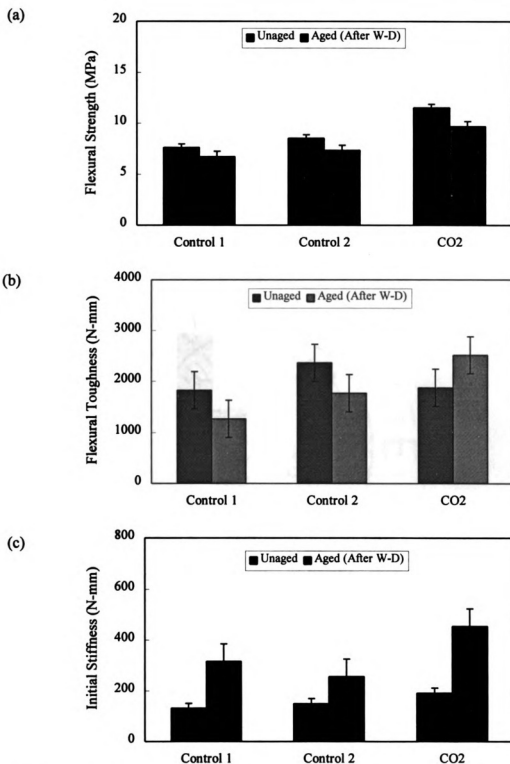


Figure 6.11 Flexural Performance After Wetting-Drying of Unpressed Cellulose Fiber-Reinforced Cement Composites: (a) Flexural Strength; (b) Flexural Toughness; (c) Initial Stiffness

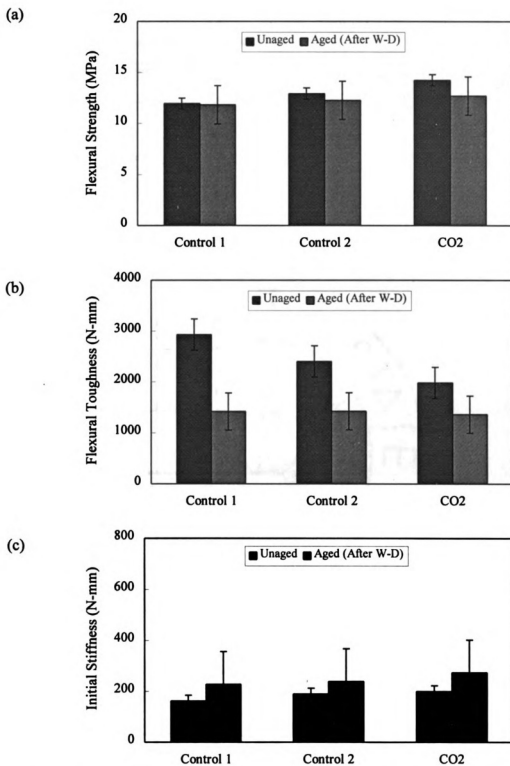


Figure 6.12 Flexural Performance After Wetting-Drying of Pressed Cellulose Fiber-Reinforced Cement Composites: (a) Flexural Strength; (b) Flexural Toughness; (c) Initial Stiffness

Table 6.15 Effects of Repeated Wetting-Drying on the Flexural Performance of Cellulose Fiber Reinforced Cement Composites

Type of Composite			After Wetting-Drying		
			Strength (MPa) Mean (St. Dev.)	Toughness (N-mm) Mean (St. Dev.)	Stiffness (N/mm) Mean (St. Dev.)
Control	Unpressed	1-1-6	6.96	854.148	306.809
			6.49	1484.665	378.185
			6.62	1529.301	300.162
			6.80	1200.619	281.134
			6.718 (0.206)	1267.183 (311.466)	316.573 (42.492)
	1-1-8	7.19	7.19	1957.345	296.726
			7.92	1596.309	268.143
			7.21	1662.005	220.777
			6.98	1853.110	239.539
CO ₂	Unpressed	1-1-4	7.325 (0.410)	1767.192 (167.138)	256.296 (33.253)
			10.99	1440.357	113.297
			12.01	1437.712	395.066
			11.88	1380.552	200.652
	Pressed	1-1-8	12.42	1402.439	199.632
			11.825 (0.602)	1415.265 (28.885)	227.162 (119.188)
			13.40	1707.389	165.289
			10.04	1057.497	322.712
Unaged	Unpressed	1-1-6	12.88	1532.993	263.662
			12.72	1390.274	200.598
			12.260 (1.508)	1422.038 (275.460)	238.065 (69.065)
			9.22	2494.970	459.135
	Pressed	1-1-4	9.90	2723.672	521.533
			9.84	2536.748	439.732
			9.79	2300.535	397.572
			9.688 (0.315)	2513.981 (173.598)	454.493 (51.555)
Control	Unpressed	1-1-6	11.00	951.151	258.128
			13.21	1471.159	289.638
			13.83	1493.768	266.637
			12.77	1550.618	277.358
	Pressed	1-1-4	12.703 (1.215)	1361.674 (276.153)	272.940 (13.632)
			7.66	1767.638	122.327
			7.60	1984.112	141.628
			7.58	1824.312	131.219
CO ₂	Unpressed	1-1-6	7.68	1722.558	129.214
			7.63 (0.048)	1824.655 (114.166)	131.097 (7.987)
	1-1-8	8.92	8.92	2622.431	177.170
			8.39	2100.280	132.792
			8.42	2522.521	149.215
			8.36	2213.216	139.228
	Pressed	1-1-4	8.523 (0.266)	2364.612 (247.789)	149.601 (19.582)
			11.49	2995.953	184.204
Unaged	Unpressed	1-1-6	12.39	2877.625	140.094
			11.55	2855.579	150.662
			12.33	2938.243	170.432
			11.94 (0.486)	2928.100 (71.768)	161.348 (19.755)
	Pressed	1-1-8	12.61	2616.021	172.843
			13.12	2122.374	200.157
			12.88	2243.215	200.221
			13.11	2634.562	183.215
CO ₂	Unpressed	1-1-6	12.93 (0.24)	2404.043 (260.305)	189.109 (13.477)
			11.72	2281.792	191.313
			11.61	1660.080	194.831
			11.64	1721.514	187.215
	Pressed	1-1-4	11.14	1834.543	190.216
			11.528 (0.262)	1874.482 (280.989)	190.894 (3.145)
			14.24	2275.274	204.420
			14.42	1863.887	192.206
Control	Unpressed	1-1-6	14.32	1869.213	199.214
			13.99	1922.432	200.513
			14.243 (0.184)	1982.702 (196.831)	199.088 (5.094)
	Pressed	1-1-8	11.72	2281.792	191.313
			11.61	1660.080	194.831
			11.64	1721.514	187.215
			11.14	1834.543	190.216
	Unpressed	1-1-4	11.528 (0.262)	1874.482 (280.989)	190.894 (3.145)
			14.24	2275.274	204.420
			14.42	1863.887	192.206
			14.32	1869.213	199.214
CO ₂	Unpressed	1-1-6	13.99	1922.432	200.513
			14.243 (0.184)	1982.702 (196.831)	199.088 (5.094)
	Pressed	1-1-8	11.72	2281.792	191.313
			11.61	1660.080	194.831
			11.64	1721.514	187.215
			11.14	1834.543	190.216
	Unpressed	1-1-4	11.528 (0.262)	1874.482 (280.989)	190.894 (3.145)
			14.24	2275.274	204.420
			14.42	1863.887	192.206
			14.32	1869.213	199.214

Table 6.16 Results of the Analysis of Test Data (Unpressed)

		Unaged								
		Flexural Strength			Flexural Toughness			Initial Stiffness		
		C1	C2	CO ₂	C1	C2	CO ₂	C1	C2	CO ₂
Aged	C1	**			**			**		
	C2		**			**			**	
	CO ₂			**			**			**

:- Statistically insignificant difference

*: Statistically significant difference at 95% level of confidence

**: Statistically significant difference at 99% level of confidence

C1: Control 1; C2: Control 2

Table 6.17 Results of the Analysis of Test Data (Pressed)

		Unaged								
		Flexural Strength			Flexural Toughness			Initial Stiffness		
		C1	C2	CO ₂	C1	C2	CO ₂	C1	C2	CO ₂
Aged	C1	-			*			-		
	C2		-			*			-	
	CO ₂			-			**			-

:- Statistically insignificant difference

*: Statistically significant difference at 95% level of confidence

**: Statistically significant difference at 99% level of confidence

C1: Control 1; C2: Control 2

Table 6.18 Results of the Analysis of Test Data: Aged Cases

Source	Sum-of-Squares	DF	Mean-Square	F-Ratio	P
Flexural Strength (Unpressed)					
Curing**	19.695	2	9.848	95.417	0.000
Error	0.929	9	0.103		
Flexural Toughness (Unpressed)					
Curing**	3149610.751	2	1574805.376	30.464	0.000
Error	465247.579	9	51694.175		
Initial Stiffness (Unpressed)					
Curing**	82582.990	2	41291.495	22.243	0.000
Error	16707.748	9	1856.416		
Flexural Strength (Pressed)					
Curing	1.540	2	0.770	0.561	0.589
Error	12.344	9	1.372		
Flexural Toughness (Pressed)					
Curing	7296.216	2	3648.108	0.071	0.932
Error	463703.031	9	51522.559		
Initial Stiffness (Pressed)					
Curing	4574.431	2	2287.215	0.357	0.709
Error	57695.581	9	6410.620		

*: Statistically significant at 95% level of confidence

**: Statistically significant at 99% level of confidence

Table 6.19 Results of the Analysis of Test Data: Unaged/Aged Ratio

Source	Sum-of-Squares	DF	Mean-Square	F-Ratio	P
Flexural Strength (Unpressed)					
Curing*	0.006	2	0.003	4.266	0.050
Error	0.006	9	0.001		
Flexural Toughness (Unpressed)					
Curing**	1.124	2	0.562	41.724	0.000
Error	0.121	9	0.013		
Initial Stiffness (Unpressed)					
Curing**	0.074	2	0.037	17.040	0.001
Error	0.020	9	0.002		
Flexural Strength (Pressed)					
Curing**	0.026	2	0.013	16.548	0.001
Error	0.007	9	0.001		
Flexural Toughness (Pressed)					
Curing**	0.790	2	0.395	20.992	0.000
Error	0.169	9	0.019		
Initial Stiffness (Pressed)					
Curing	0.016	2	0.008	2.105	0.178
Error	0.033	9	0.004		

*: Statistically significant at 95% level of confidence

**: Statistically significant at 99% level of confidence

Table 6.20 Statistical Analysis of Test Results: Aged Cases (Unpressed)

	Flexural Strength			Flexural Toughness			Initial Stiffness		
	C1	C2	CO ₂	C1	C2	CO ₂	C1	C2	CO ₂
C1	-			-			-		
C2	-	-		*	-		-	-	
CO ₂	**	**	-	**	**	-	**	**	-

Table 6.21 Statistical Analysis of Test Results: Aged Cases (Pressed)

	Flexural Strength			Flexural Toughness			Initial Stiffness		
	C1	C2	CO ₂	C1	C2	CO ₂	C1	C2	CO ₂
C1	-			-			-		
C2	-	-		-	-		-	-	
CO ₂	-	-	-	-	-	-	-	-	-

Table 6.22 Statistical Analysis of Test Results: Unaged/Aged Ratio (Unpressed)

	Flexural Strength			Flexural Toughness			Initial Stiffness		
	C1	C2	CO ₂	C1	C2	CO ₂	C1	C2	CO ₂
C1	-			-			-		
C2	-	-		-	-		**	-	
CO ₂	*	-	-	**	**	-	-	**	-

Table 6.23 Statistical Analysis of Test Results: Unaged/Aged Ratio (Pressed)

	Flexural Strength			Flexural Toughness			Initial Stiffness		
	C1	C2	CO ₂	C1	C2	CO ₂	C1	C2	CO ₂
C1	-			-			-		
C2	-	-		**	-		-	-	
CO ₂	**	*	-	**	-	-	-	-	-

-: Statistically insignificant difference

*: Statistically significant difference at 95% level of confidence

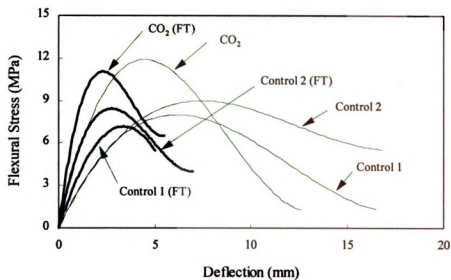
**: Statistically significant difference at 99% level of confidence

C1: Control 1; C2: Control 2

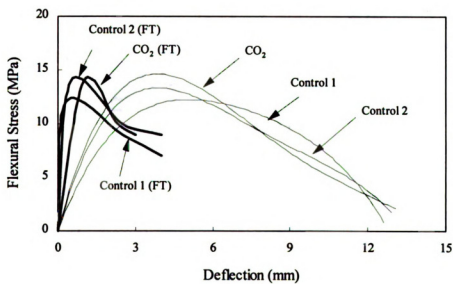
6.3.2.2 Repeated Freezing-Thawing Cycles

Figure 6.13 presents the effects of repeated freezing-thawing cycles on the flexural load-deflection behavior of carbonated cellulose fiber reinforced cement composites. The effects of repeated freezing-thawing cycles on flexural performance are presented in Table 6.24, Figure 6.14 and 6.15. The effects of freeze-thaw cycles on flexural strength were mixed, but flexural stiffness generally increased and toughness decreased after exposure to repeated freeze-thaw cycles. In the case of unpressed boards, analysis of variance of the flexure test data (Table 6.25) indicates that freeze-thaw cycles generally had statistically significant effects, at 99% level of confidence, on flexural strength, stiffness and toughness. In the case of pressed boards, effects on flexural strength were not statistically significant, but those on stiffness and toughness were. Results of the statistical analysis of the test data are shown on Tables 6.27 and 6.28 outcomes of the multiple comparisons of the test data are shown in Tables 6.25, 6.26 and 6.29 to 6.32.

Table 6.30 suggest that pressed boards, after exposure to repeated freeze-thaw cycles, all performed rather similarly in flexure irrespective of the curing condition. Table 6.29 suggests that aged unpressed boards subjected to CO₂-curing possessed strength, toughness and stiffness characteristics which, at 95% level of confidence, were superior to those obtained with the control curing condition at similar autoclave curing period and comparable to those obtained with the other control curing condition at elongated autoclave curing period. As far as the aging effects are concerned, Table 6.31 and Figure 6.14 suggest that CO₂-curing controlled the adverse aging-effects on the flexural toughness of unpressed boards and pronounced the positive effects of aging on initial stiffness. For pressed boards, CO₂-curing did not render improved control over the aging effects on toughness.



(a) Unpressed



(b) Pressed

Figure 6.13 Typical Flexural Load-Deflection Behavior After Repeated Freezing-Thawing Cycles of Cellulose Fiber Reinforced Cement Composites

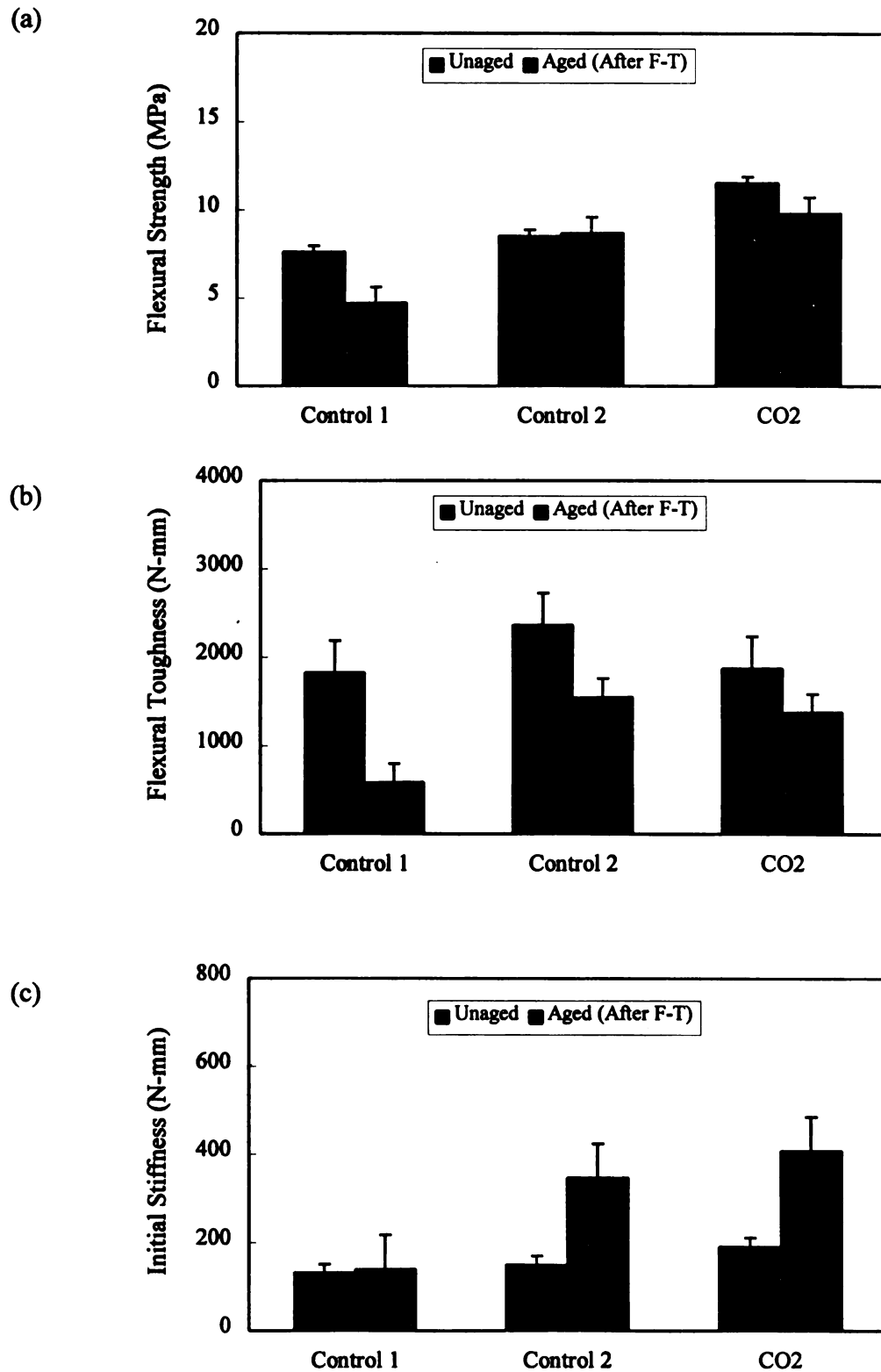


Figure 6.14 Effects of Repeated Freezing-Thawing on the Flexural Performance of Unpressed Cellulose Fiber-Reinforced Cement Composites: (a) Flexural Strength; (b) Flexural Toughness; (c) Initial Stiffness

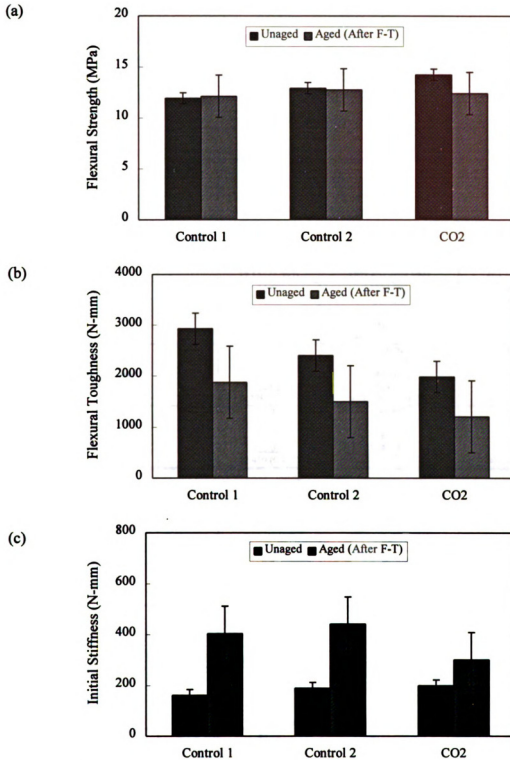


Figure 6.15 Effects of Repeated Freezing-Thawing on the Flexural Performance of Pressed Cellulose Fiber-Reinforced Cement Composites: (a) Flexural Strength; (b) Flexural Toughness; (c) Initial Stiffness

Table 6.24 Effects of Repeated Freeze-Thaw on the Flexural Performance of Cellulose Fiber Reinforced Cement Composites

Type of Composite			After Freeze-Thaw		
			Strength (MPa) Mean (St. Dev.)	Toughness (N-mm) Mean (St. Dev.)	Stiffness (N/mm) Mean (St. Dev.)
Control	Unpressed	1-1-6	4.38	518.499	122.526
			4.66	589.970	129.532
			4.92	642.631	159.638
			4.81	592.916	144.732
			4.693 (0.234)	586.004 (51.079)	139.107 (16.531)
		1-1-8	9.73	1762.133	342.241
			8.45	1315.677	413.952
			8.31	1434.721	331.946
			8.54	1693.668	296.742
			8.683 (0.501)	1551.550 (211.209)	346.220 (49.177)
	Pressed	1-1-4	14.06	2280.621	378.022
			11.98	1334.249	461.480
			11.63	2000.742	382.663
			10.83	1894.993	395.283
			12.125 (1.377)	1877.651 (397.124)	404.362 (38.771)
		1-1-8	14.60	1134.960	436.443
			10.99	814.433	380.237
			12.73	2086.383	548.239
			12.73	1953.628	399.995
			12.763 (1.474)	1497.351 (619.906)	441.229 (75.043)
CO ₂	Unpressed	1-1-6	10.27	1418.006	479.266
			8.75	1291.535	321.461
			10.16	1401.116	400.618
			10.01	1404.527	429.538
			9.798 (0.706)	1378.796 (58.629)	407.721 (66.045)
	Pressed	1-1-4	11.33	931.943	190.927
			13.36	1227.341	296.356
			11.90	1367.157	362.291
			13.05	1295.996	355.629
			12.410 (0.955)	1205.609 (191.166)	301.301 (79.327)
Unaged					
Control	Unpressed	1-1-6	7.66	1767.638	122.327
			7.60	1984.112	141.628
			7.58	1824.312	131.219
			7.68	1722.558	129.214
			7.63 (0.048)	1824.655 (114.166)	131.097 (7.987)
		1-1-8	8.92	2622.431	177.170
			8.39	2100.280	132.792
			8.42	2522.521	149.215
			8.36	2213.216	139.228
			8.523 (0.266)	2364.612 (247.789)	149.601 (19.582)
	Pressed	1-1-4	11.49	2995.953	184.204
			12.39	2877.625	140.094
			11.55	2855.579	150.662
			12.33	2938.243	170.432
			11.94 (0.486)	2928.100 (71.768)	161.348 (19.755)
		1-1-8	12.61	2616.021	172.843
			13.12	2122.374	200.157
			12.88	2243.215	200.221
			13.11	2634.562	183.215
			12.93 (0.24)	2404.043 (260.305)	189.109 (13.477)
CO ₂	Unpressed	1-1-6	11.72	2281.792	191.313
			11.61	1660.080	194.831
			11.64	1721.514	187.215
			11.14	1834.543	190.216
			11.528 (0.262)	1874.482 (280.989)	190.894 (3.145)
	Pressed	1-1-4	14.24	2275.274	204.420
			14.42	1863.887	192.206
			14.32	1869.213	199.214
			13.99	1922.432	200.513
			14.243 (0.184)	1982.702 (196.831)	199.088 (5.094)

Table 6.25 Results of the Analysis of Test Data (Unpressed)

		Unaged								
		Flexural Strength			Flexural Toughness			Initial Stiffness		
		C1	C2	CO ₂	C1	C2	CO ₂	C1	C2	CO ₂
Aged	C1	**			**			-		
	C2		**			**			**	
	CO ₂			**			*			**

-: Statistically insignificant difference

*: Statistically significant difference at 95% level of confidence

*: Statistically significant difference at 99% level of confidence

C1: Control 1; C2: Control 2

Table 6.26 Results of the Analysis of Test Data (Pressed)

		Unaged								
		Flexural Strength			Flexural Toughness			Initial Stiffness		
		C1	C2	CO ₂	C1	C2	CO ₂	C1	C2	CO ₂
Aged	C1	-			**			**		
	C2		-			*			**	
	CO ₂			-			*			-

-: Statistically insignificant difference

*: Statistically significant difference at 95% level of confidence

*: Statistically significant difference at 99% level of confidence

C1: Control 1; C2: Control 2

Table 6.27 Results of the Analysis of Test Data: Aged Cases

Source	Sum-of-Squares	DF	Mean-Square	F-Ratio	P
Flexural Strength (Unpressed)					
Curing**	58.222	2	29.111	88.837	0.000
Error	2.949	9	0.328		
Flexural Toughness (Unpressed)					
Curing**	2120855.478	2	1060427.739	62.802	0.000
Error	151967.033	9	16885.226		
Initial Stiffness (Unpressed)					
Curing**	158442.075	2	79221.038	33.694	0.000
Error	21160.957	9	2351.217		
Flexural Strength (Pressed)					
Curing	0.816	2	0.408	0.246	0.787
Error	14.946	9	1.661		
Flexural Toughness (Pressed)					
Curing	908509.305	2	454254.652	2.356	0.150
Error	1735607.249	9	192845.250		
Initial Stiffness (Pressed)					
Curing*	42080.714	2	21040.357	4.701	0.040
Error	40282.034	9	4475.782		

*: Statistically significant at 95% level of confidence

**: Statistically significant at 99% level of confidence

Table 6.28 Results of the Analysis of Test Data: Unaged/Aged Ratio

Source	Sum-of-Squares	DF	Mean-Square	F-Ratio	P
Flexural Strength (Unpressed)					
Curing**	0.875	2	0.438	726.138	0.000
Error	0.005	9	0.001		
Flexural Toughness (Unpressed)					
Curing**	7.498	2	3.749	103.362	0.000
Error	0.326	9	0.036		
Initial Stiffness (Unpressed)					
Curing**	0.650	2	0.325	145.707	0.000
Error	0.020	9	0.002		
Flexural Strength (Pressed)					
Curing**	0.059	2	0.030	38.858	0.000
Error	0.007	9	0.001		
Flexural Toughness (Pressed)					
Curing	0.017	2	0.009	0.445	0.654
Error	0.175	9	0.019		
Initial Stiffness (Pressed)					
Curing**	0.167	2	0.083	69.705	0.000
Error	0.011	9	0.001		

*: Statistically significant at 95% level of confidence

**: Statistically significant at 99% level of confidence

Table 6.29 Statistical Analysis of Test Results: Aged Cases (Unpressed)

	Flexural Strength			Flexural Toughness			Initial Stiffness		
	C1	C2	CO ₂	C1	C2	CO ₂	C1	C2	CO ₂
C1	-			-			-		
C2	**	-		**	-		**	-	
CO ₂	**	-	-	**	-	-	**	-	-

Table 6.30 Statistical Analysis of Test Results: Aged Cases (Pressed)

	Flexural Strength			Flexural Toughness			Initial Stiffness		
	C1	C2	CO ₂	C1	C2	CO ₂	C1	C2	CO ₂
C1	-			-			-		
C2	-	-		-	-		-	-	
CO ₂	-	-	-	-	-	-	-	*	-

Table 6.31 Statistical Analysis of Test Results: Unaged/Aged Ratio (Unpressed)

	Flexural Strength			Flexural Toughness			Initial Stiffness		
	C1	C2	CO ₂	C1	C2	CO ₂	C1	C2	CO ₂
C1	-			-			-		
C2	**	-		**	-		**	-	
CO ₂	**	**	-	**	-	-	**	-	-

Table 6.32 Statistical Analysis of Test Results: Unaged/Aged Ratio (Pressed)

	Flexural Strength			Flexural Toughness			Initial Stiffness		
	C1	C2	CO ₂	C1	C2	CO ₂	C1	C2	CO ₂
C1	-			-			-		
C2	-	-		-	-		-	-	
CO ₂	**	**	-	-	-	-	**	**	-

-: Statistically insignificant difference

*: Statistically significant difference at 95% level of confidence

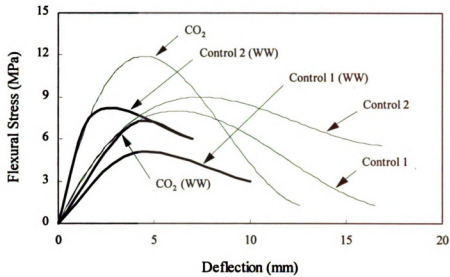
**: Statistically significant difference at 99% level of confidence

C1: Control 1; C2: Control 2

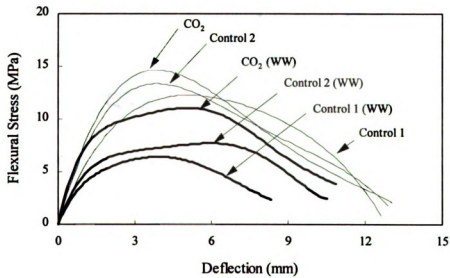
6.3.2.3 Immersion in Warm Water

Figure 6.16 presents the effects of immersion in warm water on the flexural load-deflection behavior of carbonated cellulose fiber reinforced cement composites. The effects of warm water immersion on flexural performance are presented in Table 6.33, and Figure 6.17 and 6.18. Warm water immersion had generally adverse effects on flexural strength, toughness and stiffness. Analysis of variance of the test data suggests that the warm water immersion effects on flexural performance were generally statistically significant for both unpressed and pressed boards as shown in Table 6.34 and 6.35, respectively. The results of analysis of variance with effects of curing are shown in Tables 6.36 and 6.37. The results of multiple comparison of means are presented in Tables 6.34, 6.35 and 6.38 to 6.41.

Table 6.36 and 6.38 together with Figure 6.17 indicate that after aging the unpressed CO₂-cured boards, performed better than boards subjected to the control curing at similar autoclave period. Elongated autoclave curing (without CO₂ exposure), however, generally produced better aged results. In the case of pressed boards (see Figure 6.18 and Table 6.36 and 6.39), the aged CO₂-cured boards presented better flexural strength and stiffness and comparable flexural toughness when compared with the aged boards subjected to control curing conditions. The results of statistical analysis presented in Tables 6.37, 6.40 and 6.41, together with the test data of Figure 6.17 and 6.18 suggest that the influence of CO₂ curing on the consequence of warm water immersion were mixed.



(a) Unpressed



(b) Pressed

Figure 6.16 Typical Flexural Load-Deflection Behavior Before and After Warm Water Immersion of Cellulose Fiber Reinforced Cement Composites

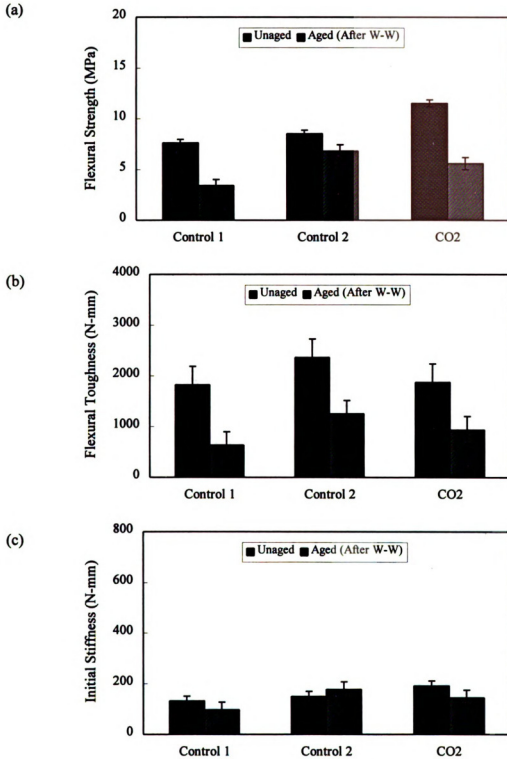


Figure 6.17 Flexural Performance Before and After Warm Water Immersion of Unpressed Cellulose Fiber-Reinforced Cement Composites: (a) Flexural Strength; (b) Flexural Toughness; (c) Initial Stiffness

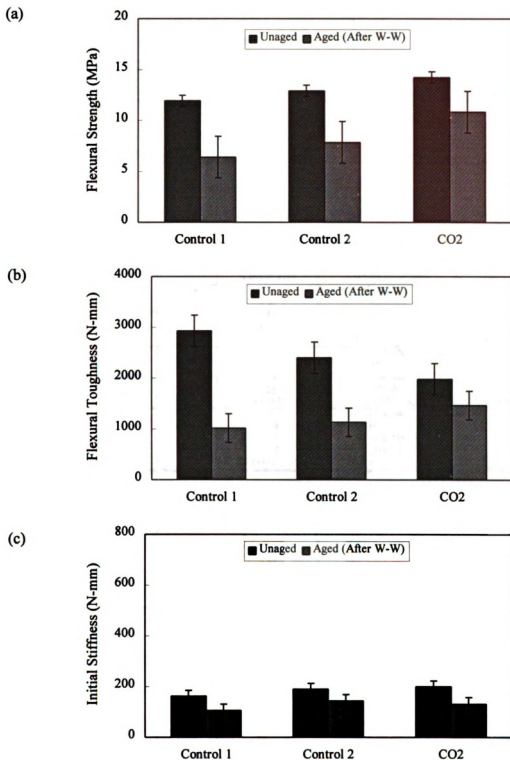


Figure 6.18 Flexural Performance Before and After Warm-Water of Pressed Cellulose Fiber-Reinforced Cement Composites: (a) Flexural Strength; (b) Flexural Toughness; (c) Initial Stiffness

Table 6.33 Effects of Warm Water Immersion on the Flexural Performance of Cellulose Fiber Reinforced Cement Composites

Type of Composite			After Warm Water		
			Strength (MPa) Mean (St. Dev.)	Toughness (N-mm) Mean (St. Dev.)	Stiffness (N/mm) Mean (St. Dev.)
Control	Unpressed	1-1-6	2.86	523.920	90.447
			3.16	666.822	99.036
			3.97	690.310	93.631
			<u>3.62</u>	<u>653.552</u>	<u>105.448</u>
			3.403 (0.491)	633.651 (74.716)	97.141 (6.576)
	1-1-8	6.90	1310.649	129.031	
		7.08	1096.315	191.168	
		6.77	1298.646	190.935	
		<u>6.51</u>	<u>1300.711</u>	<u>195.375</u>	
		6.815 (0.240)	1251.580 (103.643)	176.627 (31.796)	
Pressed	1-1-4	5.82	1164.411	118.779	
		6.74	661.208	78.742	
		6.63	1042.782	115.583	
		<u>6.43</u>	<u>1190.639</u>	<u>107.548</u>	
		6.405 (0.411)	1014.760 (244.345)	105.163 (18.237)	
1-1-8	6.86	1155.394	155.975		
	8.50	1085.247	113.371		
	7.89	1184.448	152.648		
	<u>8.15</u>	<u>1098.783</u>	<u>148.548</u>		
	7.85 (0.706)	1131.968 (48.383)	142.636 (19.745)		
CO ₂	Unpressed	1-1-6	5.75	1075.976	143.342
			5.07	555.532	147.169
			5.64	1000.649	144.853
			<u>5.88</u>	<u>1110.040</u>	<u>140.632</u>
			5.585 (0.357)	935.549 (257.435)	143.999 (2.741)
	Pressed	1-1-4	7.95	1258.290	121.272
			12.44	1626.752	135.235
			10.77	1600.746	136.842
			<u>12.17</u>	<u>1389.655</u>	<u>130.735</u>
			10.833 (2.056)	1468.861 (176.008)	131.021 (6.994)
Unaged					
Control	Unpressed	1-1-6	7.66	1767.638	122.327
			7.60	1984.112	141.628
			7.58	1824.312	131.219
			<u>7.68</u>	<u>1722.558</u>	<u>129.214</u>
			7.63 (0.048)	1824.655 (114.166)	131.097 (7.987)
		1-1-8	8.92	2622.431	177.170
			8.39	2100.280	132.792
			8.42	2522.521	149.215
			<u>8.36</u>	<u>2213.216</u>	<u>139.228</u>
			8.523 (0.266)	2364.612 (247.789)	149.601 (19.582)
	Pressed	1-1-4	11.49	2995.953	184.204
			12.39	2877.625	140.094
			11.55	2855.579	150.662
			<u>12.33</u>	<u>2938.243</u>	<u>170.432</u>
			11.94 (0.486)	2928.100 (71.768)	161.348 (19.755)
1-1-8	12.61	2616.021	172.843		
	13.12	2122.374	200.157		
	12.88	2243.215	200.221		
	<u>13.11</u>	<u>2634.562</u>	<u>183.215</u>		
	12.93 (0.24)	2404.043 (260.305)	189.109 (13.477)		
CO ₂	Unpressed	1-1-6	11.72	2281.792	191.313
			11.61	1660.080	194.831
			11.64	1721.514	187.215
			<u>11.14</u>	<u>1834.543</u>	<u>190.216</u>
			11.528 (0.262)	1874.482 (280.989)	190.894 (3.145)
	Pressed	1-1-4	14.24	2275.274	204.420
			14.42	1863.887	192.206
			14.32	1869.213	199.214
			<u>13.99</u>	<u>1922.432</u>	<u>200.513</u>
			14.243 (0.184)	1982.702 (196.831)	199.088 (5.094)

Table 6.34 Results of the Analysis of Variance of Test Data (Unpressed)

		Unaged								
		Flexural Strength			Flexural Toughness			Initial Stiffness		
		C1	C2	CO ₂	C1	C2	CO ₂	C1	C2	CO ₂
Aged	C1	**			**			*		
	C2		**			**			-	
	CO ₂			**			**			**

∴ Statistically insignificant difference

*: Statistically significant difference at 95% level of confidence

*: Statistically significant difference at 99% level of confidence

C1: Control 1; C2: Control 2

Table 6.35 Results of the Analysis of Variance of Test Data (Pressed)

		Unaged								
		Flexural Strength			Flexural Toughness			Initial Stiffness		
		C1	C2	CO ₂	C1	C2	CO ₂	C1	C2	CO ₂
Aged	C1	**			**			**		
	C2		**			**			-	
	CO ₂			**			**			**

∴ Statistically insignificant difference

*: Statistically significant difference at 95% level of confidence

*: Statistically significant difference at 99% level of confidence

C1: Control 1; C2: Control 2

Table 6.36 Results of the Analysis of Variance of Test Data: Aged Cases

Source	Sum-of-Squares	DF	Mean-Square	F-Ratio	P
Flexural Strength (Unpressed)					
Curing**	23.895	2	11.948	84.172	0.000
Error	1.277	9	0.142		
Flexural Toughness (Unpressed)					
Curing**	763806.272	2	381903.136	13.871	0.002
Error	247790.712	9	27532.301		
Initial Stiffness (Unpressed)					
Curing **	12603.493	2	6301.747	17.605	0.001
Error	3221.530	9	357.948		
Flexural Strength (Pressed)					
Curing **	40.781	2	20.391	12.496	0.003
Error	14.686	9	1.632		
Flexural Toughness (Pressed)					
Curing *	445177.735	2	222588.867	7.190	0.014
Error	278633.075	9	30959.231		
Initial Stiffness (Pressed)					
Curing *	2943.628	2	1471.814	5.724	0.025
Error	2314.057	9	257.117		

*: Statistically significant at 95% level of confidence

**: Statistically significant at 99% level of confidence

Table 6.37 Results of the Analysis of Variance of Test Data: Unaged/Aged Ratio

Source	Sum-of-Squares	DF	Mean-Square	F-Ratio	P
Flexural Strength (Unpressed)					
Curing **	2.225	2	1.112	805.763	0.000
Error	0.012	9	0.001		
Flexural Toughness (Unpressed)					
Curing **	2.343	2	1.172	21.546	0.000
Error	0.489	9	0.054		
Initial Stiffness (Unpressed)					
Curing **	0.648	2	0.324	50.281	0.000
Error	0.058	9	0.006		
Flexural Strength (Pressed)					
Curing **	0.615	2	0.307	127.894	0.000
Error	0.022	9	0.002		
Flexural Toughness (Pressed)					
Curing **	4.652	2	2.326	91.656	0.000
Error	0.228	9	0.025		
Initial Stiffness (Pressed)					
Curing	0.111	2	0.056	3.643	0.069
Error	0.137	9	0.015		

*: Statistically significant at 95% level of confidence

**: Statistically significant at 99% level of confidence

Table 6.38 Statistical Analysis of Test Results: Aged Cases (Unpressed)

	Flexural Strength			Flexural Toughness			Initial Stiffness		
	C1	C2	CO ₂	C1	C2	CO ₂	C1	C2	CO ₂
C1	-			-			-		
C2	**	-		**	-		**	-	
CO ₂	**	**	-	-	-	-	*	-	-

Table 6.39 Statistical Analysis of Test Results: Aged Cases (Pressed)

	Flexural Strength			Flexural Toughness			Initial Stiffness		
	C1	C2	CO ₂	C1	C2	CO ₂	C1	C2	CO ₂
C1	-			-			-		
C2	-	-		-	-		*	-	
CO ₂	**	*	-	*	-	-	-	-	-

Table 6.40 Statistical Analysis of Test Results: Unaged/Aged Ratio (Unpressed)

	Flexural Strength			Flexural Toughness			Initial Stiffness		
	C1	C2	CO ₂	C1	C2	CO ₂	C1	C2	CO ₂
C1	-			-			-		
C2	**	-		**	-		**	-	
CO ₂	**	**	-	**	-	-	-	**	-

Table 6.41 Statistical Analysis of Test Results: Unaged/Aged Ratio (Pressed)

	Flexural Strength			Flexural Toughness			Initial Stiffness		
	C1	C2	CO ₂	C1	C2	CO ₂	C1	C2	CO ₂
C1	-			-			-		
C2	**	-		**	-		-	-	
CO ₂	**	**	-	**	**	-	-	-	-

-: Statistically insignificant difference

*: Statistically significant difference at 95% level of confidence

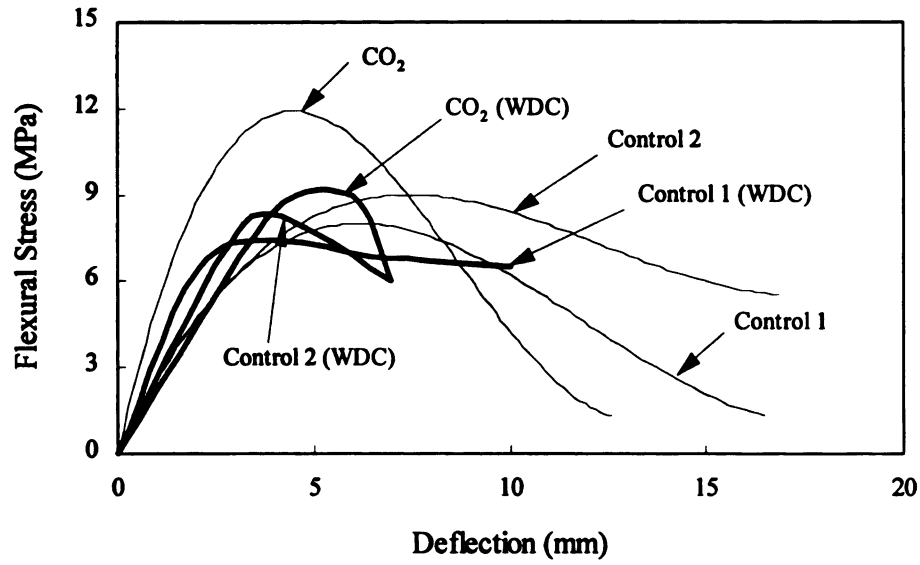
**: Statistically significant difference at 99% level of confidence

C1: Control 1; C2: Control 2

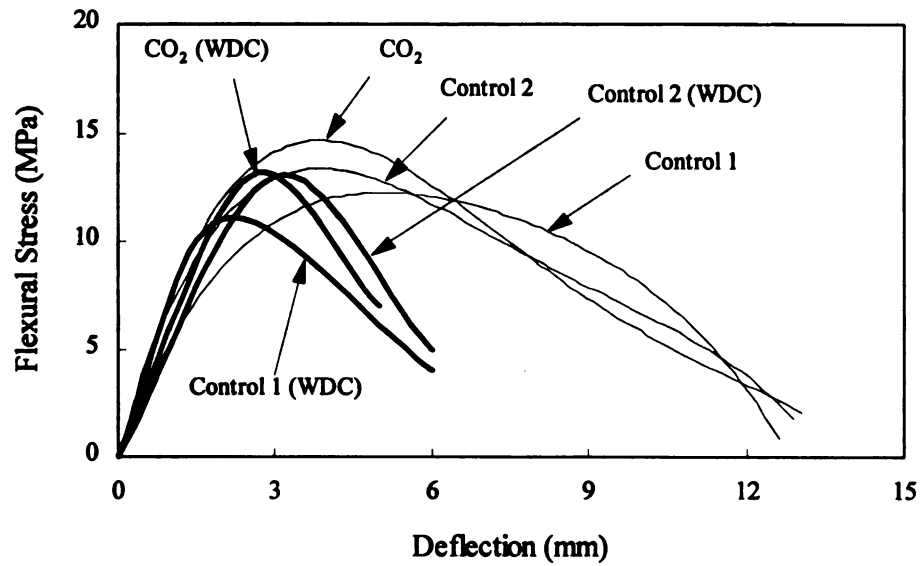
6.3.2.4 Repeated Wetting-Drying-Carbonation Cycles

Figure 6.19 presents the effects of repeated wetting-drying-carbonation cycles on the flexural load-deflection behavior of cellulose fiber reinforced cement composites. The effects of repeated wetting-drying-carbonation cycles on flexural performance are presented in Table 6.42, and in Figures 6.20 and 6.21. There was a tendency in flexural toughness and strength to drop and in flexural stiffness to generally increase after this accelerated aging process. Analysis of variance of the test data suggests that these aging effects were generally of little statistical significance in unpressed boards, but significant in pressed boards. Statistical analysis of repeated wetting-drying-carbonation effects are shown in Tables 6.45 and 6.46. The outcomes of multiple comparisons of the test data are shown on Tables 6.43, 6.44, and 6.47 to 6.50.

Table 6.47 and Figure 6.20 indicate that aged unpressed CO₂-cured boards had higher flexural strength and comparable flexural toughness and stiffness when compared with the aged control unpressed boards, at 95% level of confidence. Table 6.48 and Figure 6.21 indicate that aged pressed CO₂-cured boards offered comparable flexural strength and stiffness values, but lower flexural toughness, when compared with aged control pressed boards, at 95% level of confidence. Figure 6.21, and Table 6.49 and 6.50 show mixed influence of CO₂ curing on the accelerated aging effects on the flexural performance of unpressed and pressed boards.



(a) Unpressed



(b) Pressed

Figure 6.19 Typical Flexural Load-Deflection Behavior After Wetting-Drying-Carbonation Cycles of Cellulose Fiber Reinforced Cement Composites

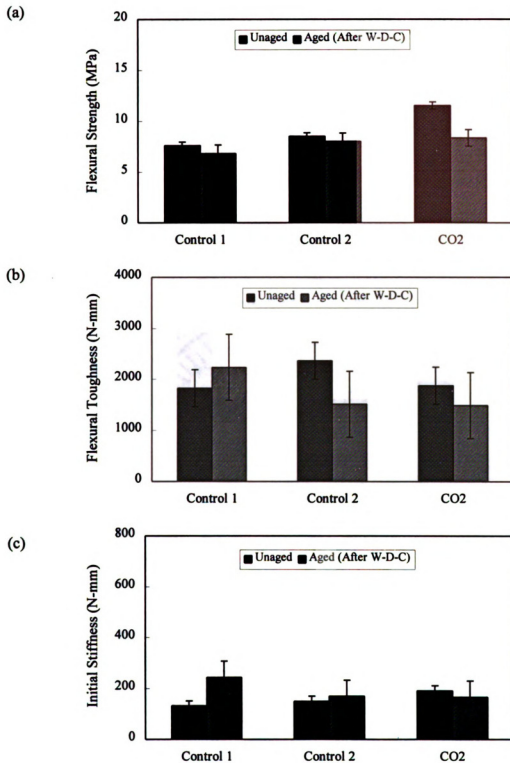


Figure 6.20 Flexural Performance Before and After Wetting-Drying-Carbonation of Unpressed Cellulose Fiber-Reinforced Cement Composites: (a) Flexural Strength; (b) Flexural Toughness; (c) Initial Stiffness

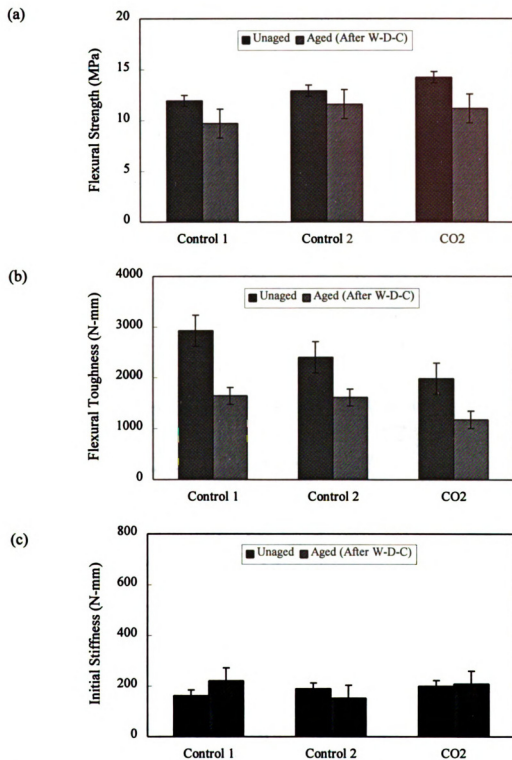


Figure 6.21 Flexural Performance Before and After Wetting-Drying-Carbonation of Pressed Cellulose Fiber-Reinforced Cement Composites: (a) Flexural Strength; (b) Flexural Toughness; (c) Initial Stiffness

Table 6.42 Effects of Repeated Wetting-Drying-Carbonation Cycles on the Flexural Performance of Cellulose Fiber Reinforced Cement Composites

Type of Composite			After Wetting-Drying-Carbonation		
			Strength (MPa) Mean (St. Dev.)	Toughness (N-mm) Mean (St. Dev.)	Stiffness (N/mm) Mean (St. Dev.)
Control	Unpressed	1-1-6	6.97	2631.104	276.675
			6.66	2201.621	152.401
			6.83	2001.312	253.937
			6.92	2102.785	291.525
			6.845 (0.136)	2234.206 (276.948)	243.635 (62.756)
		1-1-8	8.73	1584.392	145.846
			6.90	1524.747	188.069
			8.45	1539.021	159.054
			7.99	1392.004	183.568
			8.018 (0.805)	1510.041 (82.698)	169.134 (20.090)
	Pressed	1-1-4	7.72	1879.831	251.977
			10.11	1621.566	151.604
			10.54	1529.044	238.673
			10.46	1529.894	238.742
			9.708 (1.338)	1640.084 (165.623)	220.249 (46.189)
1-1-8		11.97	1622.375	155.641	
		11.75	1578.873	157.831	
		11.97	1602.834	143.845	
		10.73	1630.638	150.746	
		11.605 (0.592)	1608.680 (23.039)	152.016 (6.200)	
CO ₂	Unpressed	1-1-6	8.04	2433.994	183.301
			8.86	1138.545	150.975
			8.35	1074.753	148.782
			8.23	1292.745	180.746
			8.37 (0.351)	1485.009 (639.241)	165.951 (18.610)
	Pressed	1-1-4	11.33	1266.560	169.306
			10.61	1124.895	242.077
			11.75	1183.638	200.846
			11.09	1109.638	218.740
			11.195 (0.476)	1171.183 (71.139)	207.742 (30.685)
Unaged					
Control	Unpressed	1-1-6	7.66	1767.638	122.327
			7.60	1984.112	141.628
			7.58	1824.312	131.219
			7.68	1722.558	129.214
			7.63 (0.048)	1824.655 (114.166)	131.097 (7.987)
		1-1-8	8.92	2622.431	177.170
			8.39	2100.280	132.792
			8.42	2522.521	149.215
			8.36	2213.216	139.228
			8.523 (0.266)	2364.612 (247.789)	149.601 (19.582)
	Pressed	1-1-4	11.49	2995.953	184.204
			12.39	2877.625	140.094
			11.55	2855.579	150.662
			12.33	2938.243	170.432
			11.94 (0.486)	2928.100 (71.768)	161.348 (19.755)
1-1-8	12.61	2616.021	172.843		
	13.12	2122.374	200.157		
	12.88	2243.215	200.221		
	13.11	2634.562	183.215		
	12.93 (0.24)	2404.043 (260.305)	189.109 (13.477)		
CO ₂	Unpressed	1-1-6	11.72	2281.792	191.313
			11.61	1660.080	194.831
			11.64	1721.514	187.215
			11.14	1834.543	190.216
			11.528 (0.262)	1874.482 (280.989)	190.894 (3.145)
	Pressed	1-1-4	14.24	2275.274	204.420
			14.42	1863.887	192.206
			14.32	1869.213	199.214
			13.99	1922.432	200.513
			14.243 (0.184)	1982.702 (196.831)	199.088 (5.094)

Table 6.43 Results of the Analysis of Variance of Test Data (Unpressed)

		Unaged								
		Flexural Strength			Flexural Toughness			Initial Stiffness		
		C1	C2	CO ₂	C1	C2	CO ₂	C1	C2	CO ₂
Aged	C1	-			-			**		
	C2		-			-			-	
	CO ₂			**			-			-

-: Statistically insignificant difference

*: Statistically significant difference at 95% level of confidence

**: Statistically significant difference at 99% level of confidence

C1: Control 1; C2: Control 2

Table 6.44 Results of the Analysis of Variance of Test Data (Pressed)

		Unaged								
		Flexural Strength			Flexural Toughness			Initial Stiffness		
		C1	C2	CO ₂	C1	C2	CO ₂	C1	C2	CO ₂
Aged	C1	**			**			**		
	C2		-			**			-	
	CO ₂			**			**			-

-: Statistically insignificant difference

*: Statistically significant difference at 95% level of confidence

**: Statistically significant difference at 99% level of confidence

C1: Control 1; C2: Control 2

Table 6.45 Results of the Analysis of Variance of the Test Data: Aged Cases

Source	Sum-of-Squares	DF	Mean-Square	F-Ratio	P
Flexural Strength (Unpressed)					
Curing**	5.100	2	2.550	9.687	0.006
Error	2.369	9	0.263		
Flexural Toughness (Unpressed)					
Curing*	1448447.777	2	724223.888	4.414	0.046
Error	1476503.075	9	164055.897		
Initial Stiffness (Unpressed)					
Curing*	15461.166	2	7730.583	4.947	0.036
Error	14065.189	9	1562.799		
Flexural Strength (Pressed)					
Curing*	7.975	2	3.988	5.052	0.034
Error	7.104	9	0.789		
Flexural Toughness (Pressed)					
Curing**	549677.583	2	274838.791	24.968	0.000
Error	99067.863	9	11007.540		
Initial Stiffness (Pressed)					
Curing*	10556.851	2	5278.425	5.086	0.033
Error	9340.299	9	1037.811		

*: Statistically significant at 95% level of confidence

**: Statistically significant at 99% level of confidence

Table 6.46 Results of the Analysis of Variance of the Test Data: Unaged/Aged Ratio

Source	Sum-of-Squares	DF	Mean-Square	F-Ratio	P
Flexural Strength (Unpressed)					
Curing**	0.228	2	0.114	164.052	0.000
Error	0.006	9	0.001		
Flexural Toughness (Unpressed)					
Curing**	1.139	2	0.570	25.906	0.000
Error	0.198	9	0.022		
Initial Stiffness (Unpressed)					
Curing**	0.755	2	0.377	76.205	0.000
Error	0.045	9	0.005		
Flexural Strength (Pressed)					
Curing**	0.053	2	0.027	23.491	0.000
Error	0.010	9	0.001		
Flexural Toughness (Pressed)					
Curing*	0.168	2	0.084	4.473	0.045
Error	0.169	9	0.019		
Initial Stiffness (Pressed)					
Curing**	0.533	2	0.266	48.786	0.000
Error	0.049	9	0.005		

*: Statistically significant at 95% level of confidence

**: Statistically significant at 99% level of confidence

Table 6.47 Statistical Analysis of Test Results: Aged Cases (Unpressed)

	Flexural Strength			Flexural Toughness			Initial Stiffness		
	C1	C2	CO ₂	C1	C2	CO ₂	C1	C2	CO ₂
C1	-			-			-		
C2	*	-		-	-		-	-	
CO ₂	**	-	-	-	-	-	-	-	-

Table 6.48 Statistical Analysis of Test Results: Aged Cases (Pressed)

	Flexural Strength			Flexural Toughness			Initial Stiffness		
	C1	C2	CO ₂	C1	C2	CO ₂	C1	C2	CO ₂
C1	-			-			-		
C2	*	-		-	-		*	-	
CO ₂	-	-	-	**	**	-	-	-	-

Table 6.49 Statistical Analysis of Test Results: Unaged/Aged Ratio (Unpressed)

	Flexural Strength			Flexural Toughness			Initial Stiffness		
	C1	C2	CO ₂	C1	C2	CO ₂	C1	C2	CO ₂
C1	-			-			-		
C2	*	-		**	-		**	-	
CO ₂	**	**	-	**	*	-	**	**	-

Table 6.50 Statistical Analysis of Test Results: Unaged/Aged Ratio (Pressed)

	Flexural Strength			Flexural Toughness			Initial Stiffness		
	C1	C2	CO ₂	C1	C2	CO ₂	C1	C2	CO ₂
C1	-			-			-		
C2	**	-		*	-		**	-	
CO ₂	-	**	-	-	-	-	**	**	-

-: Statistically insignificant difference

*: Statistically significant difference at 95% level of confidence

**: Statistically significant difference at 99% level of confidence

C1: Control 1; C2: Control 2

6.3.2.2 Moisture Sensitivity

Water has a dramatic effect on the elastic modulus and flexural strength of cellulose fiber irrespective of whether the fibers are bleached or not. The uncollapsed, lignified cellulose fibers retain their strength better than delignified fibers when exposed to moisture. In this section, moisture sensitivity of cellulose fiber reinforced cement composite were investigated.

The flexural load-deflection behavior of carbonated and non-carbonated cellulose fiber reinforced cement composite at different moisture conditions are shown in Figures 6.22 and 6.23. The flexural test results are shown on Figures 6.24 and 6.25, and in Tables 6.51 to 6.53.

The increase in moisture content from air-dried to saturated condition had adverse effects on the flexural strength and stiffness of both conventional and carbonated composites. Ductility and toughness characteristics, however, improved upon saturation. The flexural toughness values did not show this trend because they partly reflect the loss in flexural strength. Oven drying produced adverse effects on flexural performance; this could be partly attributed to the adverse effects of dry heat (48 hours in oven at 102°C) on cellulose fibers. Statistical analysis of variance of test data is presented in Table 6.54. The outcomes of multiple comparison of the results are shown in Table 6.55 to 6.60. These tables generally confirm the statistical significance of moisture effects on the flexural performance of cellulose fiber reinforced cement composites.

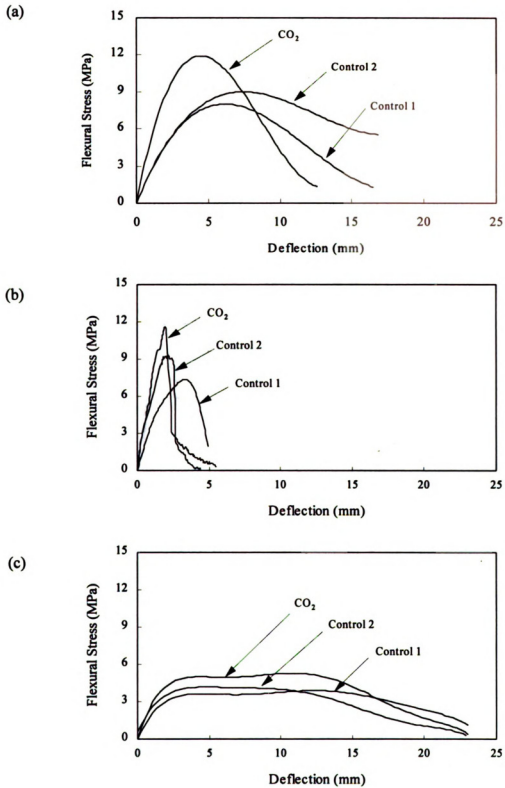


Figure 6.22 Typical Flexural Load-Deflection Behavior in Various Moisture Conditions (Unpressed): (a) Air-Dried; (b) Oven-Dried; (c) Saturated

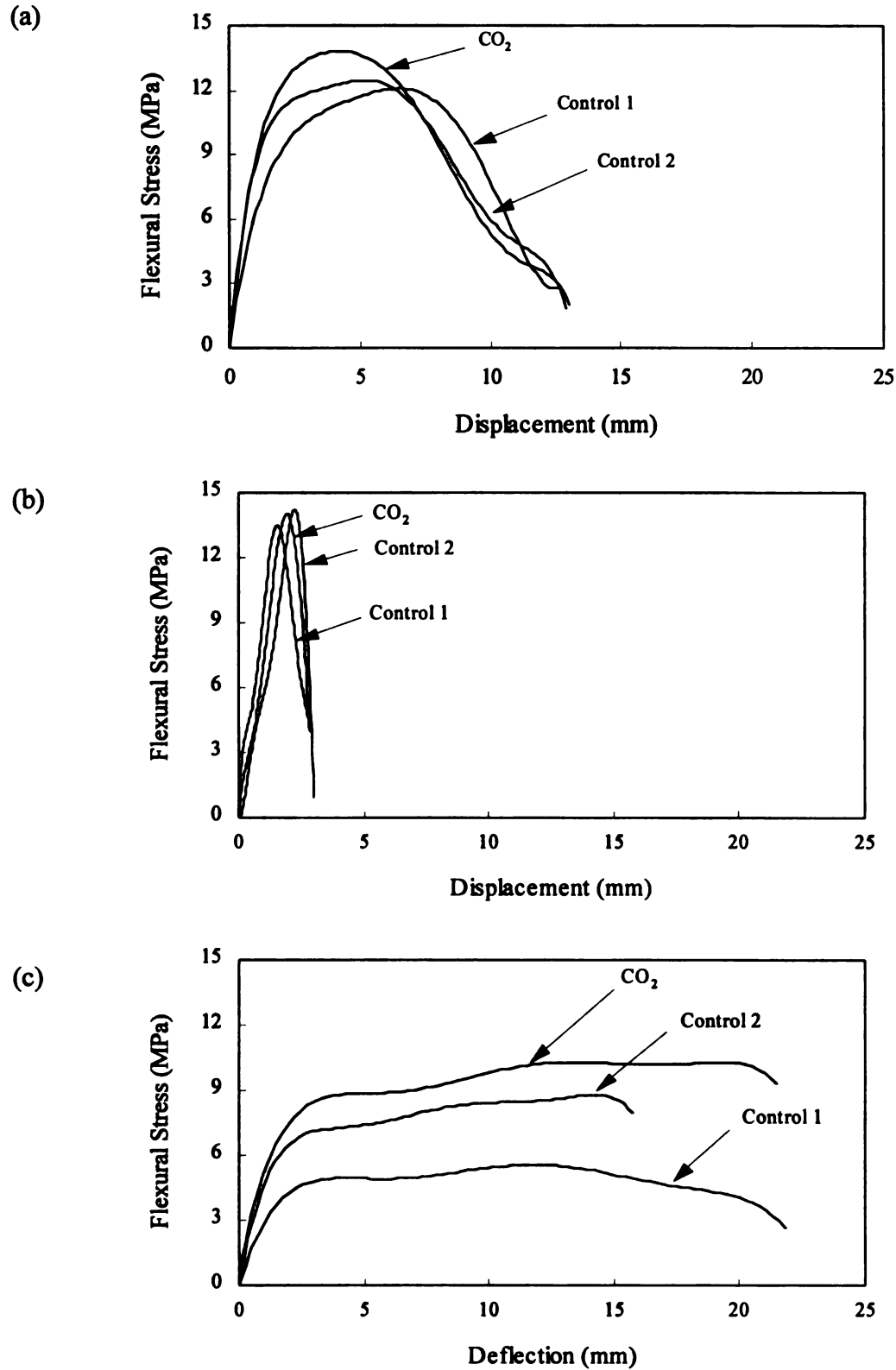
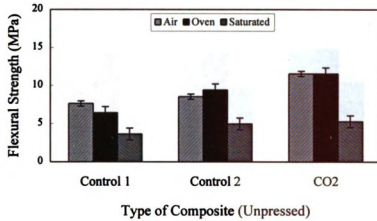
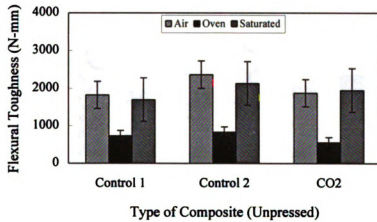


Figure 6.23 Typical Flexural Load-Deflection Behavior in Various Moisture Conditions (Pressed): (a) Air-Dried; (b) Oven-Dried; (c) Saturated

(a)



(b)



(c)

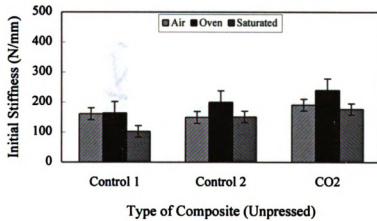
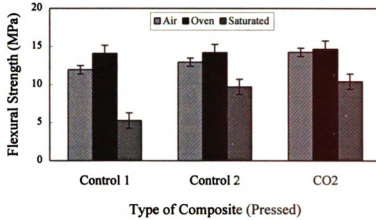
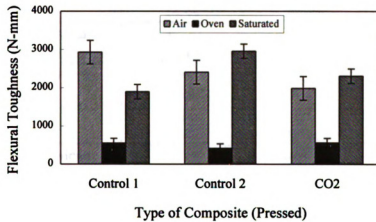


Figure 6.24 Flexural Performance in Various Moisture Conditions (Unpressed): (a) Flexural Strength; (b) Flexural Toughness; (c) Initial Stiffness

(a)



(b)



(c)

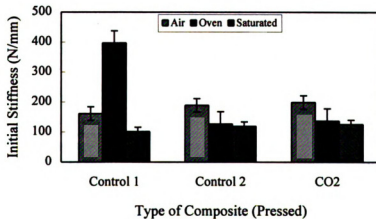


Figure 6.25 Flexural Performance in Various Moisture Conditions (Pressed): (a) Flexural Strength; (b) Flexural Toughness; (c) Initial Stiffness

Table 6.51 Effects of Moisture Condition on the Flexural Strength (MPa)

Type of Composite		Moisture Condition		
		Air-Dried	Oven-Dried	Saturated
Carbonated-Unpressed	1-1-6	11.72	11.67	5.47
		11.61	11.59	5.10
		11.64	11.88	5.55
		11.14	10.98	5.00
	Mean (St. Dev.)	11.528 (0.262)	11.53 (0.387)	5.28 (0.271)
Carbonated-Pressed	1-1-4	14.24	14.36	9.58
		14.42	15.02	10.53
		14.32	15.00	10.89
		13.99	14.28	10.64
	Mean (St. Dev.)	14.243 (0.184)	14.665 (0.400)	10.410 (0.563)
Control-Unpressed	1-1-6	7.66	5.77	3.20
		7.60	7.40	4.44
		7.58	5.99	3.28
		7.68	6.54	3.62
	Mean (St. Dev.)	7.630 (0.048)	6.425 (0.726)	3.635 (0.567)
	1-1-8	8.92	9.34	4.23
		8.39	9.51	5.50
		8.42	9.69	4.86
		8.36	9.11	5.24
	Mean (St. Dev.)	8.523 (0.266)	9.413 (0.247)	4.958 (0.552)
Control-Pressed	1-1-4	11.49	14.45	5.83
		12.39	13.81	4.78
		11.55	13.94	4.93
		12.33	14.16	5.54
	Mean (St. Dev.)	11.940 (0.486)	14.09 (0.280)	5.270 (0.497)
	1-1-8	12.61	12.63	9.07
		13.12	14.73	9.83
		12.88	14.88	10.75
		13.11	14.59	9.13
	Mean (St. Dev.)	12.93 (0.240)	14.208 (1.058)	9.695 (0.783)

Table 6.52 Effects of Moisture Condition on the Flexural Toughness (N-mm)

Type of Composite		Moisture Condition		
		Air-Dried	Oven-Dried	Saturated
Carbonated- Unpressed	1-1-6	2281.792	589.662	2653.090
		1660.080	528.623	1699.143
		1721.514	602.342	1554.334
		1834.543	520.932	1885.599
	Mean (St. Dev.)	1874.482 (280.989)	560.390 (41.565)	1948.042 (489.200)
Carbonated- Pressed	1-1-4	2275.274	644.035	2282.875
		1863.887	504.434	2293.417
		1869.213	500.556	2339.175
		1922.432	605.786	2301.095
	Mean (St. Dev.)	1982.702 (196.831)	563.703 (72.398)	2304.141 (24.521)
Control- Unpressed	1-1-6	1767.638	586.640	1596.002
		1984.112	891.650	2173.015
		1824.312	779.994	1349.216
		1722.558	700.652	1674.638
	Mean (St. Dev.)	1824.655 (114.166)	739.734 (128.666)	1698.218 (345.562)
	1-1-8	2622.431	815.004	1956.227
		2100.280	806.448	2345.003
		2522.521	926.543	2004.321
		2213.216	799.542	2217.438
	Mean (St. Dev.)	2364.612 (247.789)	836.884 (60.106)	2130.747 (182.448)
Control- Pressed	1-1-4	2995.953	433.581	1954.908
		2877.625	610.100	1853.115
		2855.579	634.590	1921.548
		2938.243	549.657	1845.113
	Mean (St. Dev.)	2928.100 (71.768)	556.982 (89.677)	1893.671 (53.322)
	1-1-8	2616.021	360.729	2763.849
		2122.374	476.515	2936.193
		2243.215	380.873	3224.134
		2634.562	450.442	2884.994
	Mean (St. Dev.)	2404.043 (260.305)	417.140 (55.172)	2952.293 (195.104)

Table 6.53 Effects of Moisture Condition on the Initial Stiffness (N/mm)

Type of Composite		Moisture Condition		
		Air-Dried	Oven-Dried	Saturated
Carbonated- Unpressed	1-1-6	191.313	261.451	195.632
		194.831	204.571	151.142
		187.215	209.869	177.432
		190.216	284.675	183.229
	Mean (St. Dev.)	190.894 (3.145)	240.142 (39.239)	176.859 (18.750)
Carbonated- Pressed	1-1-4	204.420	132.881	109.760
		192.206	118.843	102.488
		199.214	128.778	93.488
		200.513	169.052	100.565
	Mean (St. Dev.)	199.099 (5.094)	137.389 (21.916)	101.575 (6.689)
Control- Unpressed	1-1-6	122.327	157.542	105.400
		141.628	177.867	108.416
		131.219	159.532	96.915
		129.214	160.648	100.532
	Mean (St. Dev.)	161.348 (19.755)	163.897 (9.401)	102.816 (5.101)
	1-1-8	177.170	207.654	159.526
		132.792	200.546	142.926
		149.215	188.552	150.338
		139.228	203.746	152.322
Control- Pressed	1-1-4	184.204	385.956	132.885
		140.094	444.614	102.358
		150.662	356.668	122.450
		170.432	400.621	119.251
	Mean (St. Dev.)	161.348 (19.755)	396.965 (36.646)	119.236 (12.670)
	1-1-8	172.843	112.346	119.062
		200.157	136.926	121.549
		200.221	130.664	134.767
		183.215	129.605	128.552
	Mean (St. Dev.)	189.109 (13.477)	127.385 (10.534)	125.983 (7.102)

Table 6.54 Results of Analysis of Variance Regarding Moisture Sensitivity

Source	Sum-of-Squares	DF	Mean-Square	F-Ratio	P
Flexural Strength (Unpressed)					
Curing**	104.125	2	52.063	535.699	0.000
Error	0.875	9	0.097		
Flexural Toughness (Unpressed)					
Curing**	4877103.255	2	2438551.627	22.862	0.000
Error	959995.395	9	106666.155		
Initial Stiffness (Unpressed)					
Curing*	8836.038	2	4418.019	6.972	0.015
Error	5703.377	9	633.709		
Flexural Strength (Pressed)					
Curing**	43.962	2	21.981	126.217	0.000
Error	1.567	9	1.174		
Flexural Toughness (Pressed)					
Curing**	6861338.726	2	3430669.363	230.838	0.000
Error	133756.079	9	14861.787		
Initial Stiffness (Pressed)					
Curing**	19464.311	2	9732.155	52.986	0.000
Error	1653.057	9	183.673		

*: Statistically significant at 95% level of confidence

**: Statistically significant at 99% level of confidence

Table 6.55 Statistical Analysis of the Flexural Strength Test Results for Cellulose Fiber Reinforced Cement Composite under Various Moisture Conditions (Unpressed)

		Control 1			Control 2			CO ₂		
		Air	Oven	Saturated	Air	Oven	Saturated	Air	Oven	Saturated
Control 1	Air	-								
	Oven	**	-							
	Saturated	**	**	-						
Control 2	Air				-					
	Oven				-	-				
	Saturated				**	**	-			
CO ₂	Air							-		
	Oven							-	-	
	Saturated							**	**	-

Table 6.56 Statistical Analysis of the Flexural Toughness Test Results for Cellulose Fiber Reinforced Cement Composite under Various Moisture Conditions (Unpressed)

		Control 1			Control 2			CO ₂		
		Air	Oven	Saturated	Air	Oven	Saturated	Air	Oven	Saturated
Control 1	Air	-								
	Oven	**	-							
	Saturated	-	**	-						
Control 2	Air				-					
	Oven				**	-				
	Saturated				-	**	-			
CO ₂	Air							-		
	Oven							**	-	
	Saturated							-	**	-

-: Statistically insignificant difference

*: Statistically significant difference at 95% level of confidence

**: Statistically significant difference at 99% level of confidence

Table 6.57 Statistical Analysis of the Initial Stiffness Test Results for Cellulose Fiber Reinforced Cement Composite under Various Moisture Conditions (Unpressed)

		Control 1			Control 2			CO ₂		
		Air	Oven	Saturated	Air	Oven	Saturated	Air	Oven	Saturated
Control 1	Air	-								
	Oven	-	-							
	Saturated	-	**	-						
Control 2	Air				-					
	Oven				**	-				
	Saturated				-	**	-			
CO ₂	Air							-		
	Oven							**	-	
	Saturated							-	**	-

Table 6.58 Statistical Analysis of the Flexural Strength Test Results for Cellulose Fiber Reinforced Cement Composite under Various Moisture Conditions (Pressed)

		Control 1			Control 2			CO ₂		
		Air	Oven	Saturated	Air	Oven	Saturated	Air	Oven	Saturated
Control 1	Air	-								
	Oven	**	-							
	Saturated	**	**	-						
Control 2	Air				-					
	Oven				-	-				
	Saturated				**	**	-			
CO ₂	Air							-		
	Oven							-	-	
	Saturated							**	**	-

-: Statistically insignificant difference

*: Statistically significant difference at 95% level of confidence

**: Statistically significant difference at 99% level of confidence

Table 6.59 Statistical Analysis of the Flexural Toughness Test Results for Cellulose Fiber Reinforced Cement Composite under Various Moisture Conditions (Pressed)

		Control 1			Control 2			CO ₂		
		Air	Oven	Saturated	Air	Oven	Saturated	Air	Oven	Saturated
Control 1	Air	-								
	Oven	**	-							
	Saturated	**	**	-						
Control 2	Air				-					
	Oven				**	-				
	Saturated				**	**	-			
CO ₂	Air							-		
	Oven							**	-	
	Saturated							-	**	-

Table 6.60 Statistical Analysis of the Initial Stiffness Test Results for Cellulose Fiber Reinforced Cement Composite under Various Moisture Conditions (Pressed)

		Control 1			Control 2			CO ₂		
		Air	Oven	Saturated	Air	Oven	Saturated	Air	Oven	Saturated
Control 1	Air	-								
	Oven	**	-							
	Saturated	*	**	-						
Control 2	Air				-					
	Oven				**	-				
	Saturated				**	-	-			
CO ₂	Air							-		
	Oven							**	-	
	Saturated							**	-	-

-: Statistically insignificant difference

*: Statistically significant difference at 95% level of confidence

**: Statistically significant difference at 99% level of confidence

6.4 DIMENSIONAL STABILITY OF CELLULOSE FIBER REINFORCED CEMENT UNDER REPEATED WETTING-DRYING-CARBONATION

Dimensional stability of cellulose fiber reinforced cement composites is a key practical issue. This section compares the effects of moisture and aging (after wetting-drying-carbonation) on the dimensions of cellulose fiber reinforced cement composites. The moisture movements were measured as relative humidity increased from 30% to 90%. In the case of aging effects, the dimensions prior to and after aging were both measured in laboratory air at 55% relative humidity. Table 6.61 and Figure 6.26 summarize the test results. Irrespective of the curing process, the aging condition of accelerated wetting-drying-carbonation produced relatively large shrinkage movements in the boards.

Table 6.61 Dimensional Stability Test Results

	Curing Condition	Length (%)		Thickness (%)		Mass (%)	
		Moisture	Aging (W-D-C)	Moisture	Aging (W-D-C)	Moisture	Aging (W-D-C)
Unpressed	Control (1-1-8)	0.058	0.388	0.579	0.66	5.3715	3.857
	CO ₂ (1-1-6)	0.0325	0.298	0.592	0.62	4.9105	2.101
Pressed	Control (1-1-8)	0.062	0.373	0.306	0.398	4.99	1.389
	CO ₂ (1-1-4)	0.035	0.341	0.304	0.387	4.022	1.099

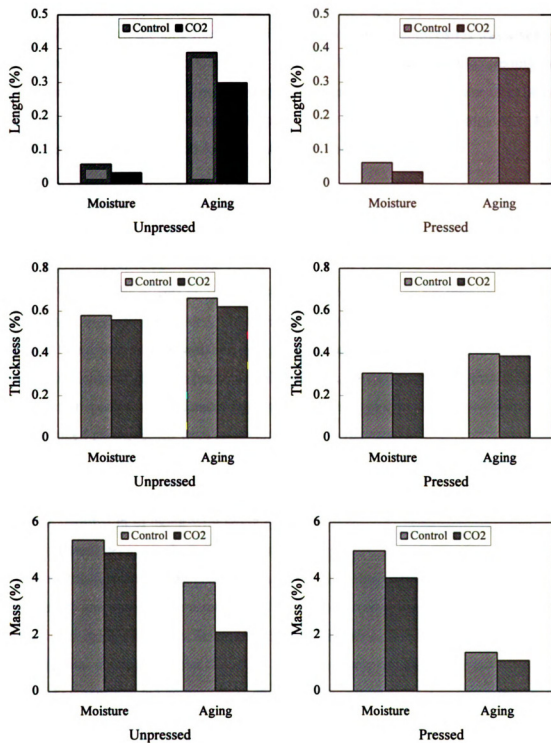


Figure 6.26 Dimensional Stability

6.5 SUMMARY AND DISCUSSION

In this chapter, the long-term durability of wood-cement composites was assessed. The specimens were subjected to repeated cycles of freezing and thawing, wetting and drying, warm water immersion, and wetting-drying-carbonation. In the case of cellulose fiber reinforced cement composites, moisture sensitivity was also investigated. After aging, the specimens were tested for flexural performance.

6.5.1 Cement-Bonded Particleboard

Repeated Wetting-Drying Cycles

In general, repeated wetting-drying cycles led to increased stiffness and reduced toughness values. The effects on flexural strength were mixed. In the case of CO₂-cured boards, wood species (aspen versus southern pine) and wood-cement ratios had statistically significant interactions with the aging effects on the flexural strength of cement-bonded particleboard. From a practical point of view, however, the effects and interactions of wood species, wood-cement ratio and aging in regard to the flexural strength of cement-bonded particleboard were relatively small. In the case of toughness, aging had a definite adverse effect. Wood-cement ratio had a relatively small but statistically significant effect on the stiffness of carbonated boards. Aging led to significant gains in stiffness. The interaction of aging with wood species in relation to toughness, while statistically significant, seems to be rather small from a practical point of view. Statistical analysis of the flexural strength test results suggested that curing conditions (CO₂ vs. conventional) and wood-cement ratio (0.28 vs. 0.35) had statistically significant interactions with the aging effects on flexural strength. The trends in the effect of various factors on flexural strength suggest that, CO₂ curing not only enhanced the initial flexural strength of cement-bonded particleboard, but also improved the resistance to aging effects on the flexural strength. The effects and interaction of wood-cement ratio and aging in regard to flexural strength were relatively small. In the case of flexural toughness, the effects and interactions of curing condition and aging were statistically significant. Flexural toughness was higher with CO₂ curing; aging caused embrittlement in both CO₂ and conventionally cured boards, but flexural toughness after aging remained higher in CO₂

cured boards. The adverse effects of aging on toughness were more pronounced at the higher wood-cement ratio of 0.35. In the case of initial stiffness, aging led to significant gains in stiffness; the interaction of aging with curing condition in relation to stiffness was statistically significant; the CO₂-cured boards showed more gain in stiffness upon aging than conventionally cured boards.

Repeated Freezing-Thawing Cycles

In general, repeated freezing-thawing cycles led to increased stiffness and reduced toughness of cement-bonded particleboard. The effects on flexural strength were mixed but generally negative. Statistical analysis of the flexural strength test results suggested that the effects and interactions of various variables, although statistically significant, are relatively small and of little practical significance. Flexural strength tends to be rather stable under repeated freeze-thaw cycles. Flexural toughness seriously drops with aging under freeze-thaw effects. This adverse effect of repeated freeze-thaw cycles was more pronounced at the higher wood-cement ratio of 0.35. Repeated freeze-thaw cycles produced substantially increased stiffness values. Statistical analysis of the flexural strength test results confirms that flexural strength was rather stable under repeated freeze-thaw cycles. CO₂-curing produced statistically improved flexural strengths before and after the application of freeze-thaw cycles. In the case of toughness, there was a strong interaction of curing and wood-cement ratio with aging. The freeze-thaw effects on toughness were more pronounced at the higher wood-cement ratio and in the case of CO₂-cured boards. The repeated freeze-thaw cycles substantially increased the stiffness of cement-bonded particleboard; the effects and interactions of curing conditions and wood-cement ratio with aging were statistically significant. The increase in the stiffness of cement-bonded particleboard was more pronounced when the boards were subjected to CO₂-curing.

6.5.2 Cellulose Fiber Reinforced Cement Composite

The improvement in flexural strength of boards with CO₂ curing was observed to be statistically significant at 99% level of confidence. Control curing conditions produced flexural toughesses which were higher than those obtained through CO₂ curing.

The improved stiffness with CO₂ curing was statistically significant at 99% level of confidence for unpressed boards; in the case of pressed boards the stiffness obtained with CO₂-curing was statistically comparable to that produced by the longer curing period but, at 95% level of confidence, superior to the stiffness of boards subjected to a similar autoclave curing period without CO₂-curing.

Repeated Wetting-Drying Cycles

Repeated wetting-drying cycles caused an increase in the flexural stiffness and a drop in the flexural toughness of composites, without significantly affecting their flexural strength. In the case of unpressed boards, analysis of variance of flexure test results suggests that repeated wetting-drying cycles had statistically significant effects, at 99% level of confidence, on flexural strength, toughness and stiffness. In the case of pressed boards, the effects of repeated wetting-drying cycles were statistically significant, at 95% level of confidence, only for flexural toughness. CO₂-curing led to higher original strength and stiffness values but did not seem to change the general trends in the effects of wetting-drying cycles.

After aging, the CO₂-cured boards were still superior to conventionally cured ones in all aspects of flexural performance (strength, toughness and stiffness) at 99% level of confidence. CO₂-curing helped control the aging effects on the toughness of unpressed boards. With CO₂-curing, the increase in stiffness with aging was also more pronounced than that for the control curing conditions. Otherwise, similar trends were observed in aging effects on CO₂-cured and conventionally cured composites.

Repeated Freezing-Thawing Cycles

The effects of freeze-thaw cycles on flexural strength were mixed, but flexural stiffness generally increased and toughness decreased after exposure to repeated freeze-thaw cycles. In the case of unpressed boards, analysis of variance of the flexure test data indicates that freeze-thaw cycles generally had statistically significant effects, at 99% level of confidence, on flexural strength, stiffness and toughness. In the case of pressed

boards, effects on flexural strength were not statistically significant, but those on stiffness and toughness were.

The pressed boards, after exposure to repeated freeze-thaw cycles, all performed rather similarly in flexure irrespective of the curing condition. The aged unpressed boards subjected to CO₂ curing possessed strength, toughness and stiffness characteristics which, at 95% level of confidence, were superior to those obtained with control curing condition at similar autoclave curing period and comparable to those obtained with the other control curing condition at elongated autoclave curing period. As far as the aging effects are concerned, the CO₂-curing controlled the adverse aging effects on the flexural toughness of unpressed boards and pronounced the positive effects of aging on initial stiffness. For pressed boards, CO₂ curing did not render improved control over the aging effects on toughness.

Immersion in Warm Water

Warm water immersion had generally adverse effects on flexural strength, toughness and stiffness. Analysis of variance of the test data suggest, that the warm water immersion effects on flexural performance were generally statistically significant for both unpressed and pressed boards.

After aging, the unpressed CO₂-cured boards performed better than boards subjected to the control curing at a similar autoclave period. Elongated autoclave curing (without CO₂ exposure), however, generally produced better aged results. In the case of pressed boards, the aged CO₂ cured boards presented better flexural strength and stiffness and comparable flexural toughness values when compared with the aged boards subjected to control curing conditions. In general, the influence of CO₂ curing on the consequence of warm water immersion were mixed.

Repeated Wetting-Drying-Carbonation Cycles

There was a tendency in flexural toughness and strength to drop and in flexural stiffness to generally increase after this accelerated aging process. Analysis of variance

of the test data suggests that these aging effects were generally of little statistical significance in unpressed boards, but significant in pressed boards.

Aged unpressed CO₂ cured boards had higher flexural strength and comparable flexural toughness and stiffness when compared with the aged control unpressed boards, at 95% level of confidence. The aged pressed CO₂-cured boards offered comparable flexural strength and stiffness values, but lower flexural toughness, when compared with aged control pressed boards, at 95% level of confidence. There was a mixed influence of CO₂ curing on the accelerated aging effects on the flexural performance of unpressed and pressed boards.

Moisture Sensitivity

The increase in moisture content from air-dried to saturated condition had adverse effects on the flexural strength and stiffness of both conventional and carbonated composites. Ductility and toughness characteristics, however, improved upon saturation. The measured flexural toughness values did not show this trend because they partly reflect the loss in flexural strength. Oven drying produced adverse effects on flexural performance; this could be partly attributed to the adverse effects of dry heat (48 hours in oven at 102°C) on cellulose fibers. Analysis of variance and multiple comparison of the results generally confirm the statistical significance of moisture effects on the flexural performance of cellulose fiber reinforced cement composites.

Dimensional Stability

Irrespective of the curing process, the aging condition of accelerated wetting-drying-carbonation produced relatively large shrinkage movements in the boards.

CHAPTER 7

MICROSTRUCTURE OF WOOD-CEMENT COMPOSITES

7.1 INTRODUCTION

The microstructure of pastes made from Portland and other hydraulic cements evolves gradually with time as the hydration proceeds. In the recent years attention has been paid to the evolution of microstructure during the hydration of Portland cement in order to explain the mechanisms of such hydration and the effects it might have on the development of properties such as setting and hardening, permeability and strength.

When wood fibers or particles are added to the paste, it is assumed that the hydration sequences for cement are not altered in any major way but the microstructural development of the composite is affected. In this chapter, the important microstructural features of wood-cement composite, their changes in different environments, and the effects these changes may have on the properties of wood-cement composites are investigated. The environmental scanning electron microscope (ESEM), x-ray diffraction (XRD), thermogravimetric analysis (TGA) and mercury intrusion porosimetry were used to investigate microstructural features. A regular camera with magnification lens was also used to investigate fracture surfaces.

7.2 TEST PROCEDURES

The microstructural test procedures are briefly described in this section.

7.2.1 X-Ray Diffraction (XRD)

X-ray powder diffraction (XRD) is the established and relatively inexpensive method of identifying and quantifying cement mineralogy. Each crystalline compound has its own characteristic “fingerprint” of peak positions and intensities. If a crystalline mineral is exposed to X-rays of a particular wavelength, the layers of atoms diffract the rays and produce a pattern of peaks which is characteristic of the mineral [112]. The horizontal scale of a typical XRD pattern gives the crystal lattice spacing, and the vertical

scale gives the intensity of the diffracted ray. When the specimen being X-rayed contains more than one mineral, the intensity of characteristic peaks from the individual minerals are proportional to their amount.

7.2.2 Environmental Scanning Electron Microscope (ESEM)

ESEM is used to examine the surfaces of specimens. It allows the introduction of a gaseous environment in the specimen chamber [107] which facilitates observations in wet or dry conditions. The ability to observe samples, particularly non-conductors, without the need for conductive coating is the key advantage of ESEM over SEM used. The ESEM was used to examine composite fracture surfaces.

7.2.3 Thermogravimetric Analysis (TGA)

Thermogravimetric is a technique in which the mass of a substance is monitored as a function of temperature over time as the sample is subjected to a controlled temperature history [108]. This relationship was used in this investigation to determine the quantities of calcium hydroxide and calcium carbonate in the aged and unaged composites; these quantities were expected to correlate to the aging effects on wood-cement composites.

Thermogravimetric analysis was used to determine compositional changes (in $\text{Ca}(\text{OH})_2$ and CaCO_3) in the composite under various aging conditions. The TGA curves showed a distinct weight loss in the temperature range typical to $\text{Ca}(\text{OH})_2$ and CaCO_3 , and the contents of these two components could thus be calculated. However, wood decomposes at the same temperature range as $\text{Ca}(\text{OH})_2$, and thus an adjustment had to be made in the calculation of $\text{Ca}(\text{OH})_2$ content. This was done by taking into account the content of the cellulose (wood particle) and its weight loss in this temperature range. A typical weight loss pattern in cement-based composites reflects the initial dehydration which occurs over the 105°C to 440°C (221°F to 824°F) temperature range, followed by dehydroxylation affecting calcium hydroxide in the range 440°C to 580°C (824°F to 1076°F), with calcium carbonate dissociation occurring in the region 580°C to 1000°C (1076°F to 1832°F). The amounts of calcium hydroxide and calcium carbonate can thus

be computed based on weight changes associated with these temperature changes. Free calcium hydroxide can be calculated as follow [110]:

$$\text{Free calcium hydroxide} = 4.11 \times (L_{dx}) + 1.68 \times (L_{dc}) - W \times L_w$$

where, L_{dx} : % weight loss within 440°C to 580°C (824°F to 1076°F)

L_{dc} : % weight loss within 580°C to 1000°C (1076°F to 1832°F)

W : Weight fraction of wood in composite

L_w : % weight loss of wood within 440°C to 580°C (824°F to 1076°F)

The CaCO_3 content can be calculated as follow:

$$\text{CaCO}_3 = \text{weight loss from 580°C to 1000°C (1076°F to 1832°F)}$$

7.2.4 Mercury Intrusion Porosimetry

In this method mercury is forced into the pores of the composite material by means of pressure. When mercury enters the pore, the force acting upon the pore is caused by the pressure applied to the cross section of the pore. This force is counteracted by a force which is caused by the surface tension of the penetrating mercury applied to the circle of the pore. In equilibrium, these forces are equal. The amount of mercury penetrated into pores gives the pore volume directly, as a function of the pressure acting upon the pores. On the other hand, the pressure is inversely proportional to the pore radius. This inverse relationship is expressed by the Washburen equation [111]:

$$D = \frac{4\sigma \cos\theta}{p}$$

which is a capillary law governing liquid penetration into pores, where D is pore diameter, p is pressure, σ is surface tension, and θ is the contact angle. The values used were $\sigma=485 \text{ dynes cm}^{-1}$ and $\theta=130^\circ$.

Mercury porosimetry gives a better appreciation of the larger capillary pore system, which has an important influence on permeability and shrinkage at high humidities [40]. This result can be used to obtain the specific surface of a material.

7.3 TEST RESULTS

7.3.1 Cement-Bonded Particleboard

The mechanical properties of non-aged CO₂-cured composites were superior to those of conventionally cured composites. After repeated wetting-drying, flexural strength increased but after repeated freezing-thawing it decreased. This section reviews the aging effects on the microstructure of cement-bonded particleboard which could describe the corresponding effects on material properties. All composites subjected to control curing conditions which were investigated in this task were made with southern pine wood particles.

7.3.1.1 X-Ray Diffraction

Unaged Cement-Bonded Particleboard

Figure 7. 1 shows the x-ray patterns of unaged composites after 28 days of curing. CO₂-cured composites in the unaged condition had higher CaCO₃ contents and lower Ca(OH)₂ contents than conventionally cured composites. Composite with different wood-cement ratios performed similarly. The conversion of Ca(OH)₂ to CaCO₃ during CO₂-curing illustrates the increase in CaCO₃ content of CO₂ cured composites.

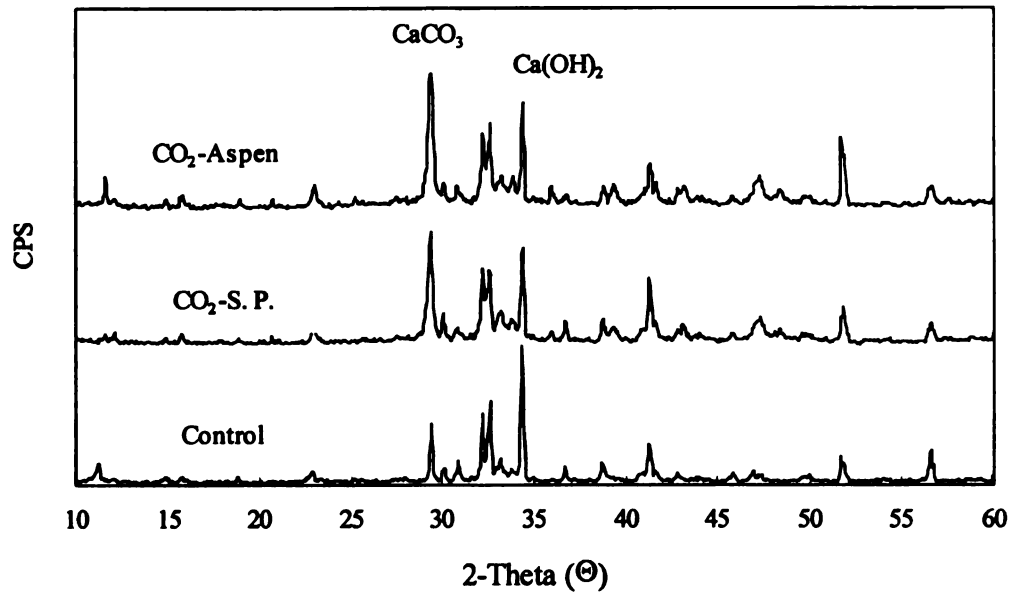
Effects of Repeated Wetting-Drying Cycles

After repeated wetting-drying cycles (Figure 7.2), conventionally cured specimens exhibited an increase in CaCO₃ content and a drop in Ca(OH)₂ content, which could be attributed to carbonation in the atmosphere during the aging process. The x-ray patterns for CO₂ cured composites were rather comparable before and after the application of repeated wetting-drying cycles. There was a general drop in Ca(OH)₂ content all composites upon aging.

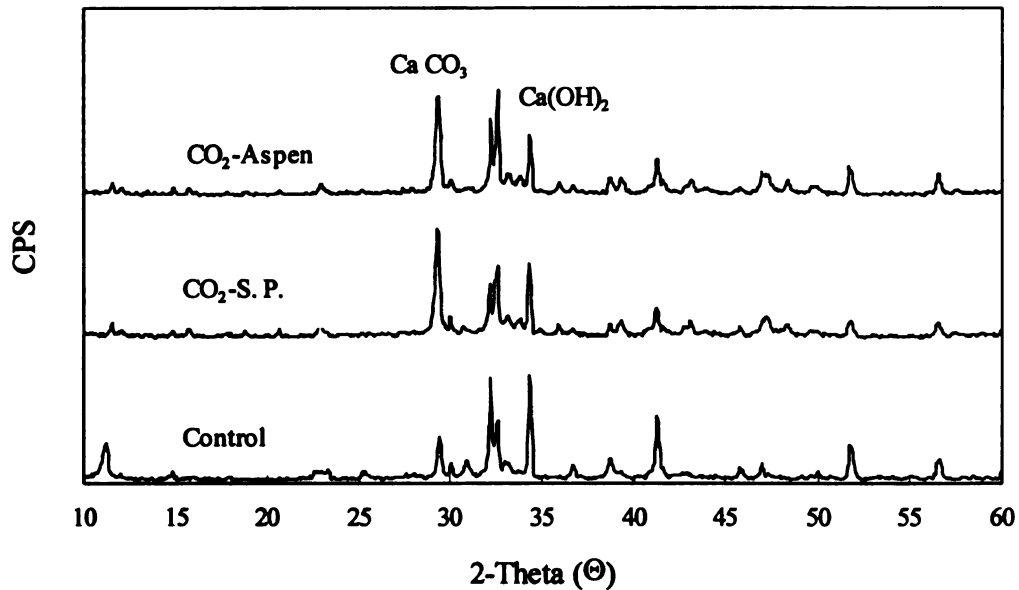
Effects of Repeated Freezing-Thawing Cycles

Figure 7.3 shows the x-ray patterns after repeated freezing-thawing cycles. Comparison of Figures 7.1 and 7.3 indicates that repeated freezing-thawing cycles also pro-

moted the carbonation of conventionally cured specimens. CO_2 -cured specimens did not go through as much mineral changes associated with carbonation. Aging led to reduced $\text{Ca}(\text{OH})_2$ content in all composites.

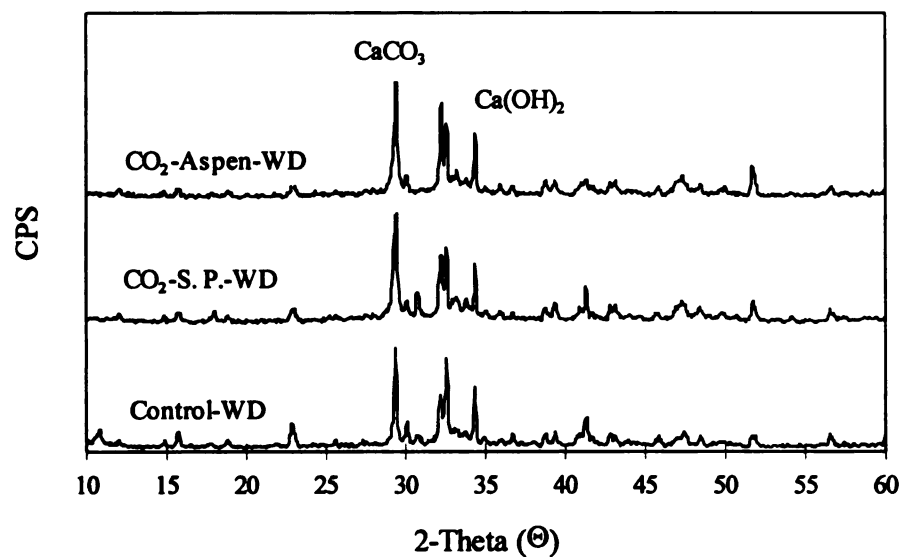


(a) Wood/Cement=0.28

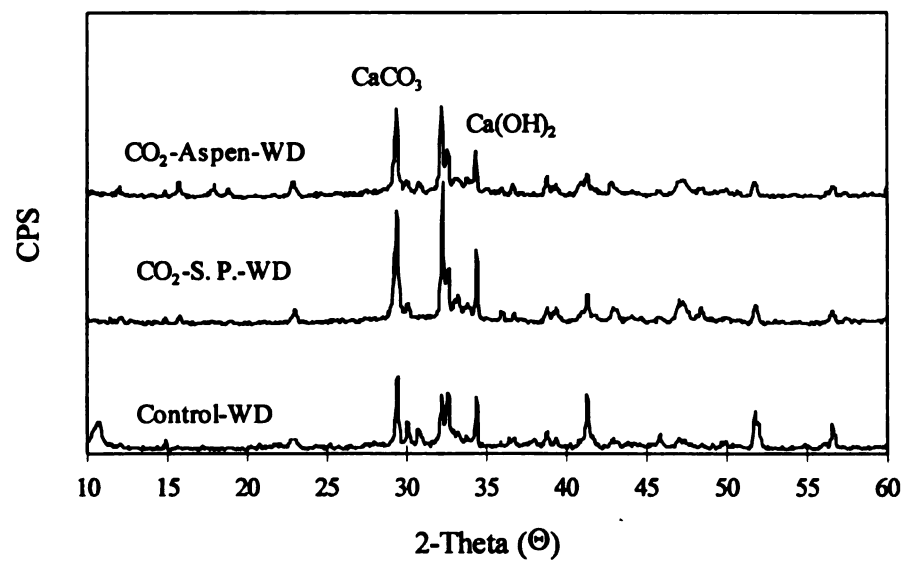


(b) Wood/Cement=0.35

Figure 7.1 X-Ray Patterns for Unaged Specimens of Cement-Bonded Particleboard After 28-Days of Curing

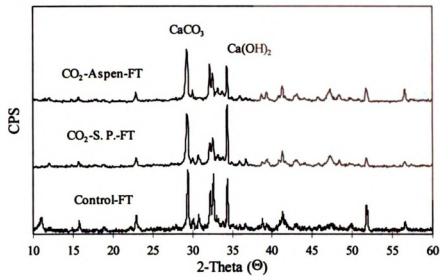


(a) Wood/Cement=0.28

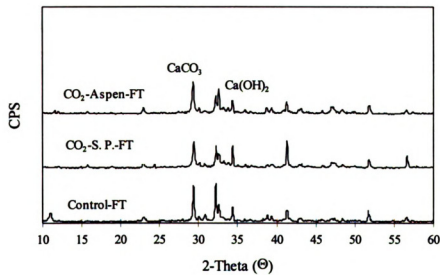


(b) Wood/Cement=0.35

Figure 7.2 X-Ray Patterns After Repeated Wetting-Drying Cycles for Cement-Bonded Particleboard



(a) Wood/Cement=0.28



(b) Wood/Cement=0.35

Figure 7.3 X-Ray Patterns After Repeated Freezing-Thawing Cycles for Cement-Bonded Particleboard

7.3.1.2 Thermogravimetric Analysis (TGA)

The rate of heating was used 20°C (68°F) per minutes and the weight loss with temperature was recorded. Typical trends in weight loss of different wood species are shown in Figure 7.4. From these weight loss curves one may estimate an approximate lignin content of around 25% (lignin decomposes at 450°C, 860°F) in southern pine and aspen (almost identical in the two species). Typical weight loss curves of cement bonded particleboard after 28-days of curing are presented in Figure 7.5; the CaCO_3 and Ca(OH)_2 contents may be calculated from these curves. The weight loss curves of cement-bonded particleboard after repeated wetting-drying and freezing-thawing cycles are shown in Figures 7.6 and 7.7. The amount of free Ca(OH)_2 and CaCO_3 for unaged and various aged particleboards derived from the TGA test results are presented in Table 7.1. The results suggest that control board, when compared with carbonated boards, show more changes in calcium carbonate content upon aging. The carbonated boards, on the other hand, have a high calcium carbonate content prior to aging, which is subject to less change with aging. The additive of lime to the carbonated mixes led to increased Ca(OH)_2 content of unaged carbonated boards. In the control boards, the gradual release of lime associated with the hydration of cement seems to increase Ca(OH)_2 content upon aging.

Table 7.1 Thermogravimetric Compositional Analysis

		Control		Carbonated			
		Wood/Cement Ratio					
		0.28	0.35	0.28		0.35	
		Wood Species		Wood Species			
		S. P*	S. P.*	S. P.*	Aspen	S. P.*	Aspen
Unaged	Ca(OH) ₂	5.104	6.512	12.631	13.128	6.383	7.925
	CaCO ₃	4.372	5.334	7.646	8.560	7.273	9.116
After W-D	Ca(OH) ₂	12.238	7.905	13.571	12.191	7.081	3.265
	CaCO ₃	7.789	6.354	9.050	8.499	8.180	7.771
After F-T	Ca(OH) ₂	10.980	12.033	13.964	9.990	15.104	8.336
	CaCO ₃	7.087	7.617	8.369	7.749	11.290	8.957

*: Southern Pine

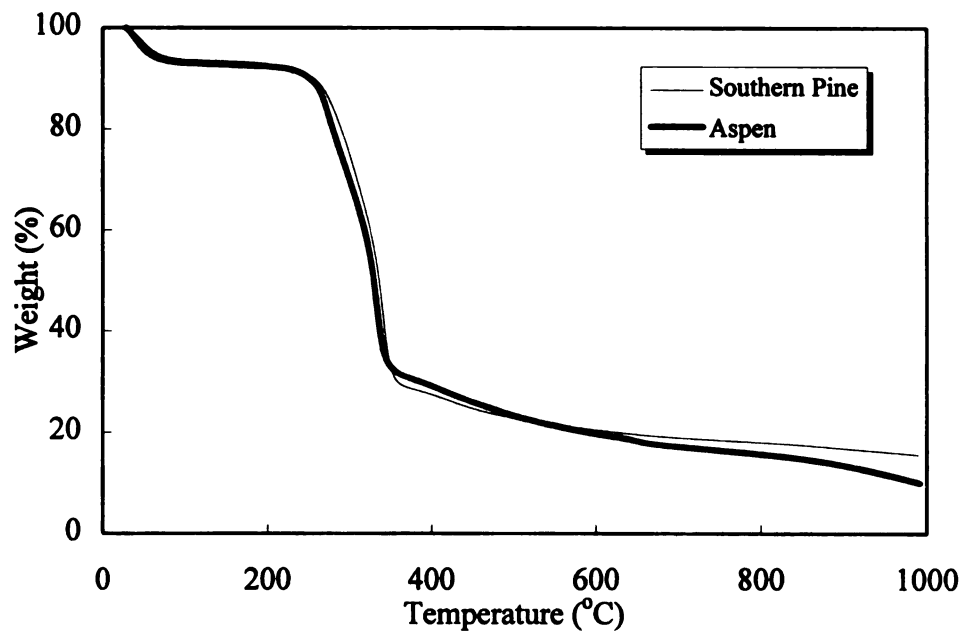
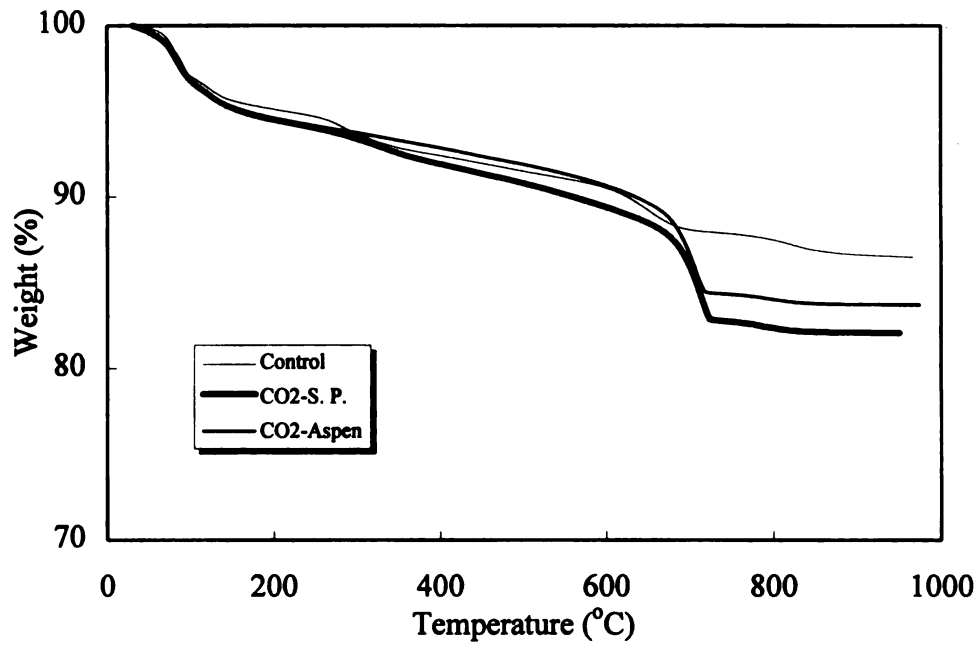
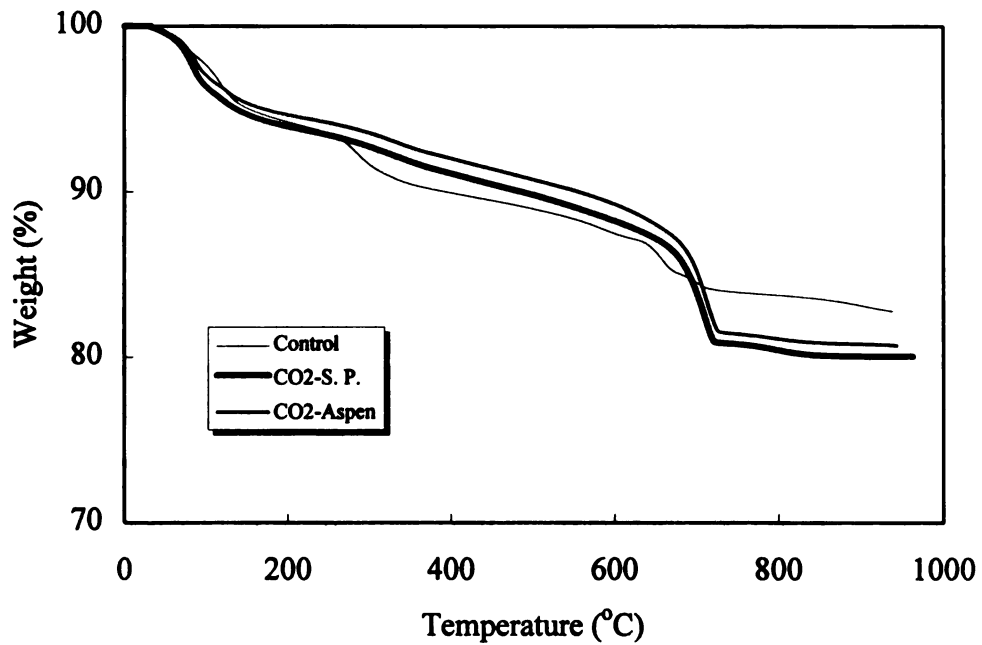


Figure 7.4 Thermogravimetric Analysis of Southern Pine and Aspen

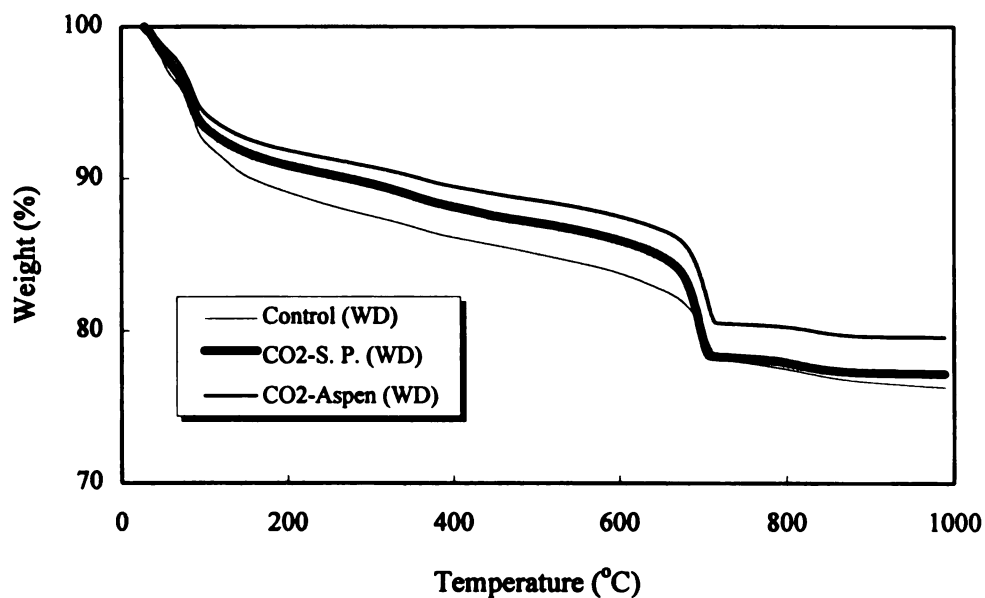


(a) Wood/Cement=0.28

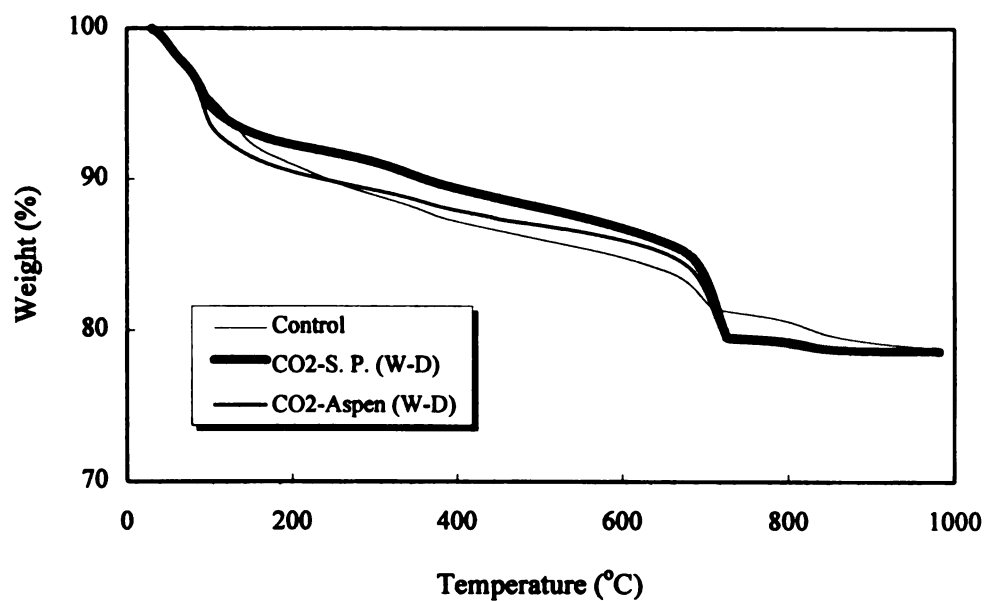


(b) Wood/Cement=0.35

Figure 7.5 Thermogravimetric Analysis of Cement-Bonded Particleboard After 28 Days of Curing

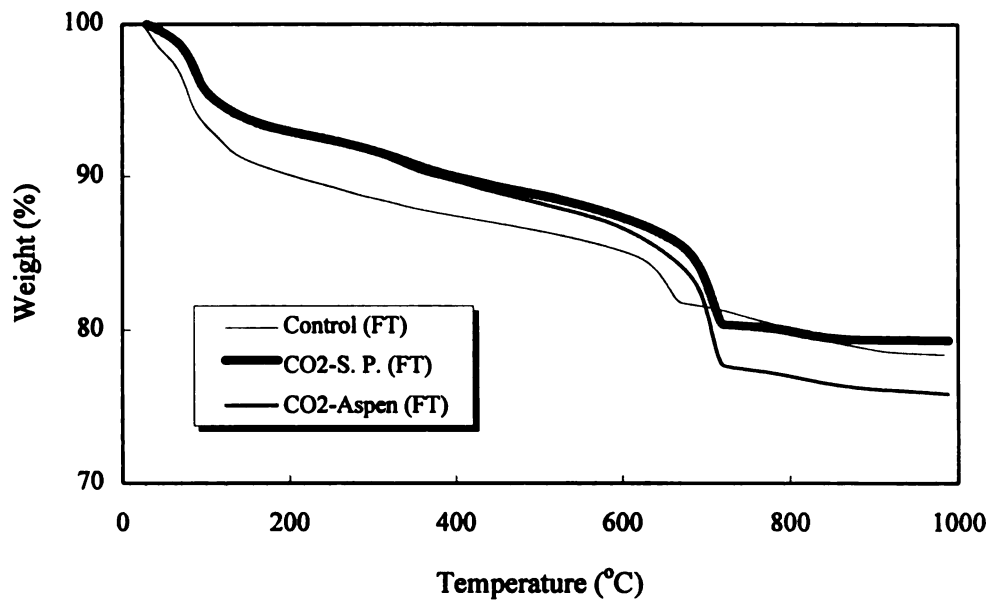


(a) Wood/Cement=0.28

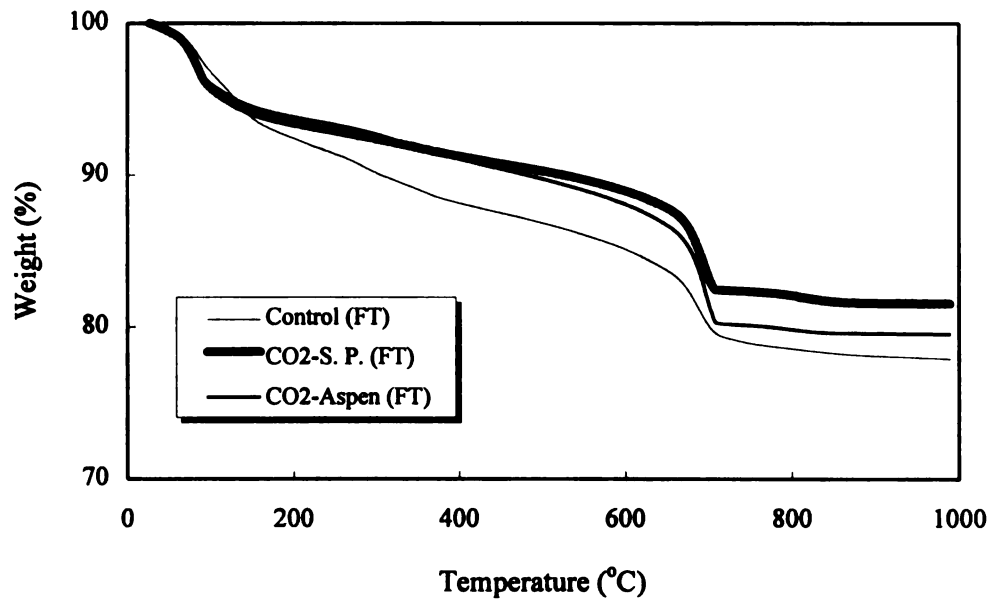


(b) Wood/Cement=0.35

Figure 7.6 Thermogravimetric Analysis of Cement-Bonded Particleboard After Repeated Wetting-Drying Cycles



(a) Wood/Cement=0.28



(b) Wood/Cement=0.35

Figure 7.7 Thermogravimetric Analysis of Cement-Bonded Particleboard After Repeated Freezing-Thawing Cycles

As

ea

ca

al

to

w

b

F

c

c

c

7.3.1.3 Mercury Intrusion Porosimetry

Figure 7.8 shows the pore size distributions of southern pine and aspen species. Aspen seems to have a higher pore volume than southern pine. This is indicative of an easier penetration of gases into aspen, which could illustrate the higher CaCO_3 content of carbonated boards made with aspen. However, one should notice that gas penetration also depends on factors such as the wood specific gravity could thus the pressure needed to produce certain composite specific gravity, and the flat placement of wood particles which subjects the from by to a transverse entry of CO_2 during carbonation. The cement-bonded matrix is another obvious factor controlling gas penetration. Figures 7.9 through Figure 7.11 show the pore size distribution curves (in logarithmic scale) after 28 days of curing, and after different aging processes. Figures 7.9 to 7.11 indicate that the general distribution curves shifted to the left (towards lower-diameter pores) in the case of CO_2 -cured boards; that is, the pore structure became increasing finer when using CO_2 -curing. This is expected be cause CaCO_3 particles produced during carbonation tend to fill some capillary pores. Aging also produces finer pores, which could again be illustrated by carbonation during aging with atmosphere. Table 7.2 summarizes the measurements on total capillary pore volume of cement-bonded particleboard. Unaged carbonated boards possessed a smaller total pore volume, which could result from the filling of pores with CaCO_3 . After aging, however, control (uncarbonated) boards show a large reduction in total pore volume and this aged carbonated and uncarbonated boards have more comparable total capillary porosities.

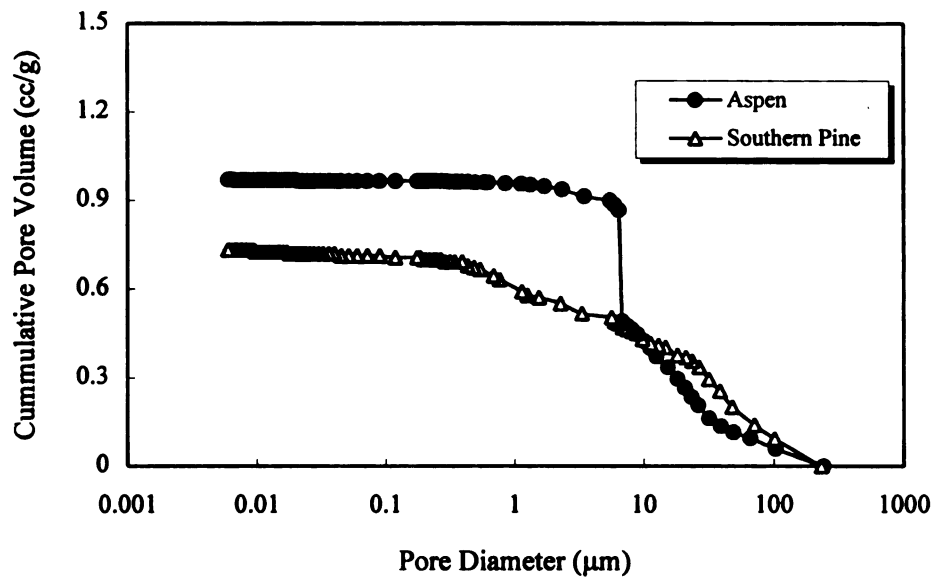
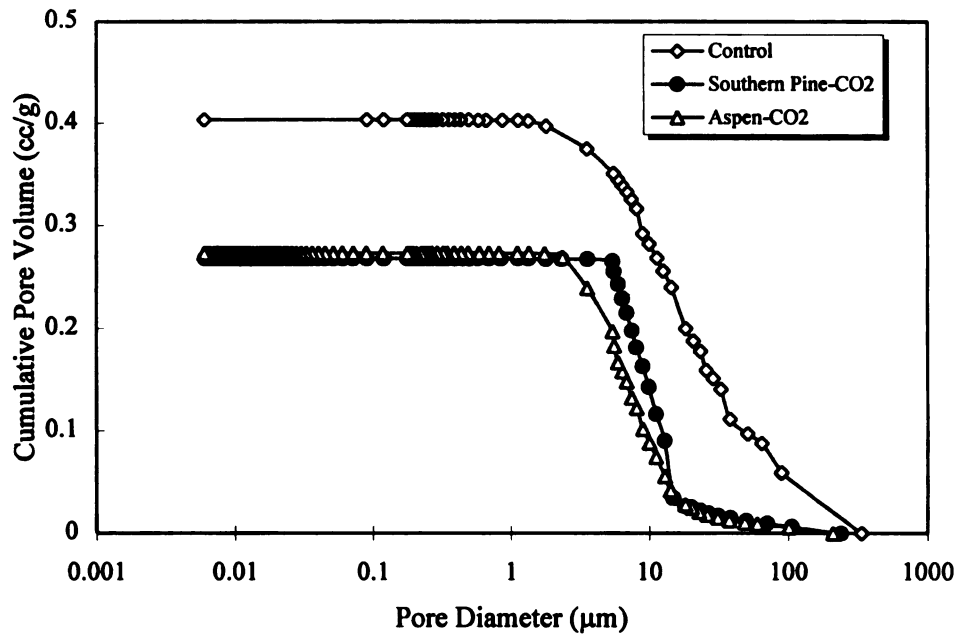


Figure 7.8 Pore Size Distribution of Southern Pine and Aspen Species

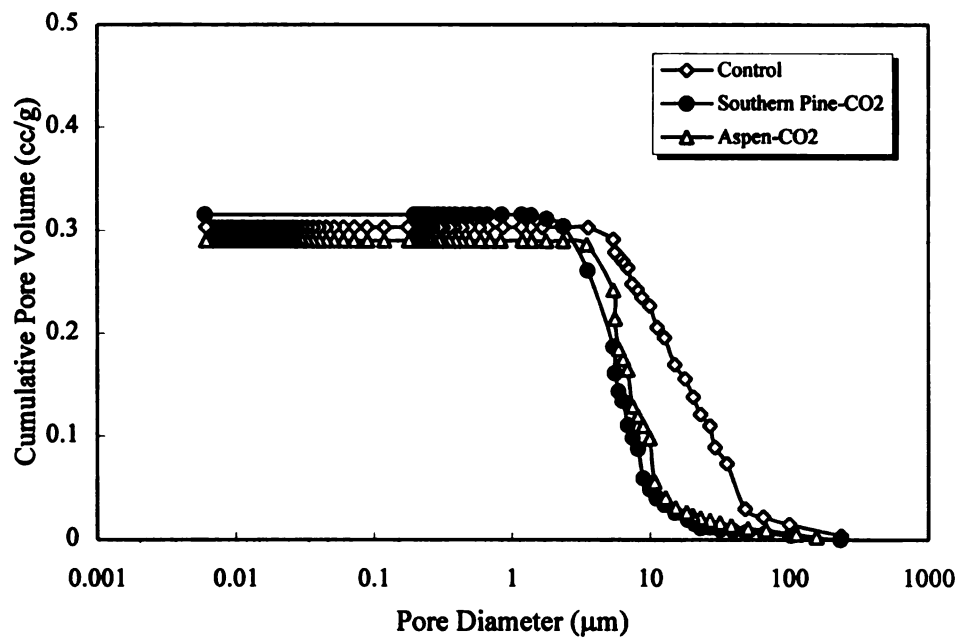
Table 7.2 Comparison of Pore Volumes of Unaged and Aged Cement-Bonded Particleboards

	Wood Species		Control		CO ₂ -Curing			
			Wood/Cement Ratio					
			0.28	0.35	0.28		0.35	
			Wood Species		Wood Species			
	S. P.*	Aspen	S. P.*	S. P. *	S. P.*	Aspen	S. P.*	Aspen
Unaged								
Total Intrusion Volume (cc/g)	0.7327	0.9713	0.4035	0.3034	0.2679	0.2730	0.3153	0.2904
After Repeated Wetting-Drying Cycles								
Total Intrusion Volume (cc/g)			0.2148	0.3871	0.1802	0.2670	0.1703	0.2892
After Repeated Freezing-Thawing Cycles								
Total Intrusion Volume (cc/g)			0.2260	0.1970	0.2405	0.2903	0.2954	0.2712

*: southern pine

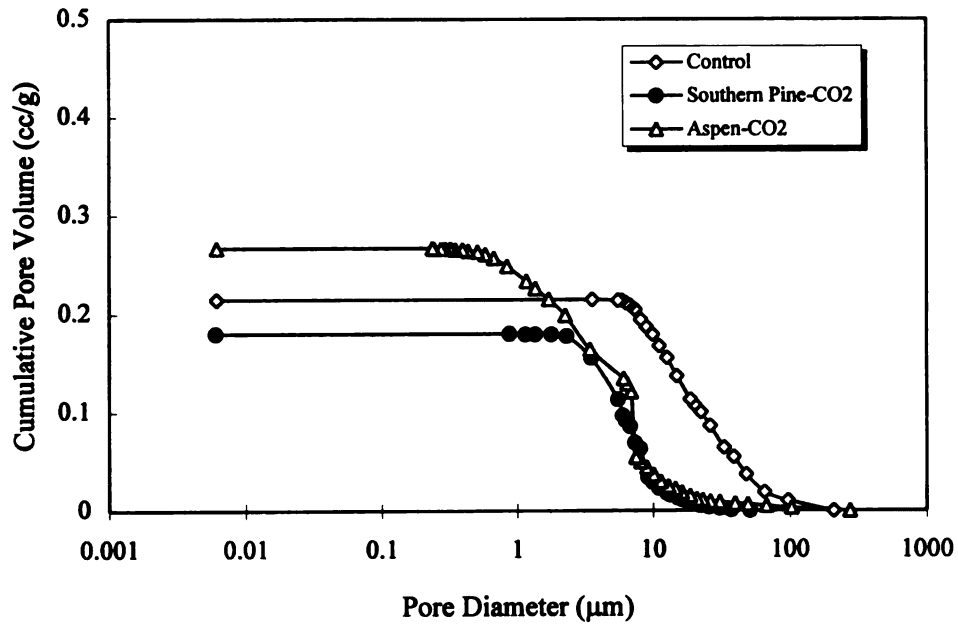


(a) Wood/Cement=0.28

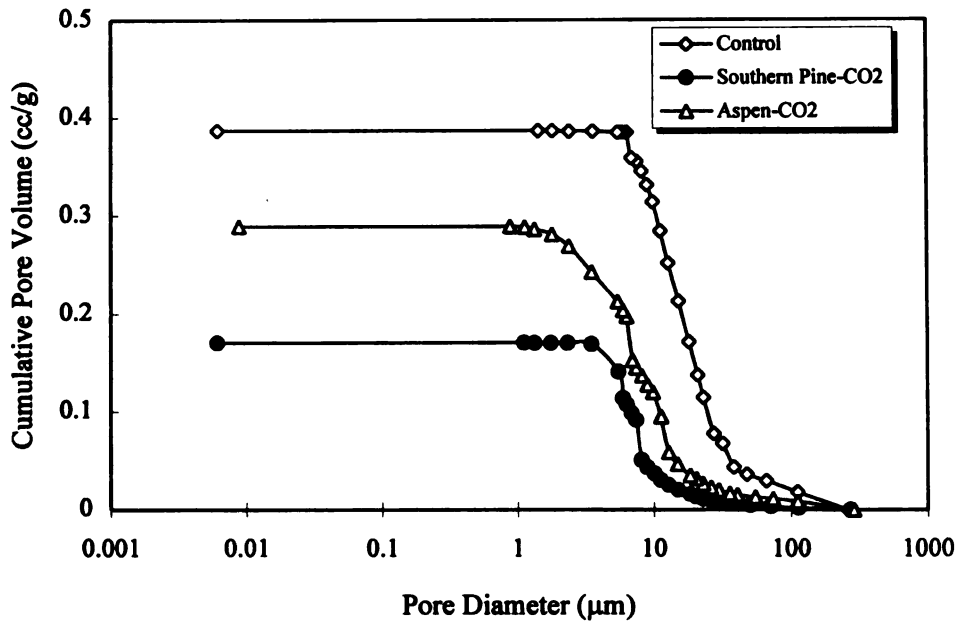


(b) Wood/Cement=0.35

Figure 7.9 Pore Size Distribution of Unaged Cement-Bonded Particleboard After 28 Days of Curing

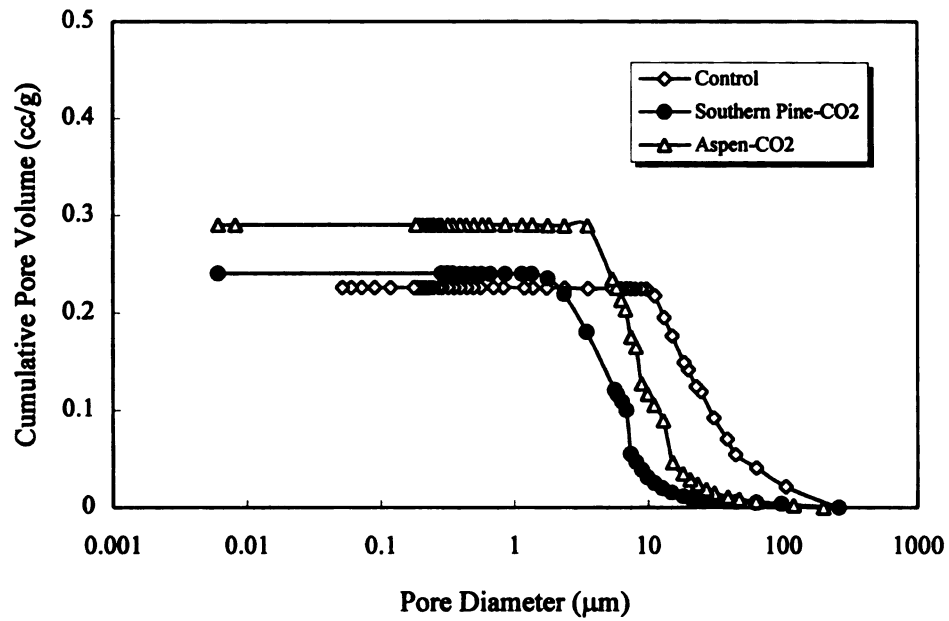


(a) Wood/Cement=0.28

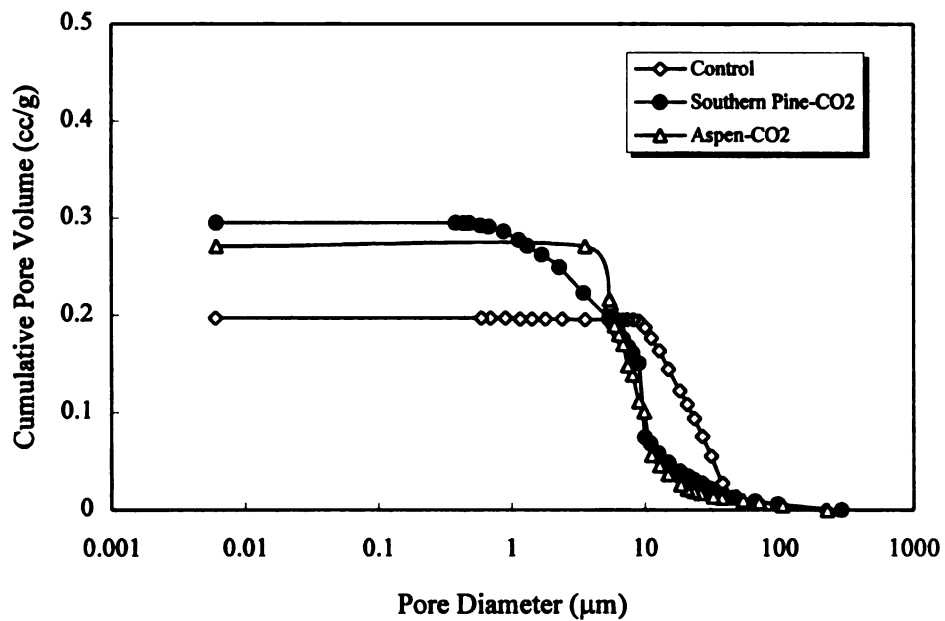


(b) Wood/Cement=0.35

Figure 7.10 Pore Size Distribution of Cement-Bonded Particleboard After Wetting-Drying Cycles



(a) Wood/Cement=0.28



(b) Wood/Cement=0.35

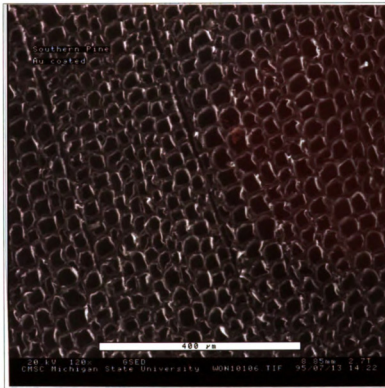
Figure 7.11 Pore Size Distribution of Cement-Bonded Particleboard After Freezing-Thawing Cycles

7.3.1.4 Fracture Surface and Interface

Softwood (southern pine) and hardwood (aspen) have quite different cellular structures when viewed under a microscope. Typically, softwoods have a comparatively simple structure and are more uniform in appearance than hardwoods. They are made up of a few cell types with the long pointed fibrous cells termed tracheids providing both the structural support and the conducting pathways in woods. Hardwood, on the other hand, comprise several different cell types with highly specialized conducting cells of relatively large diameters termed vessels (or pores).

Figures 7.12 shows the cross-section of southern pine and aspen used in this research. Aspen (Figures 7.12b and 7.12d) has large vessels within their cell structure. Southern pine (Figures 7.12a and 7.12c) has a more uniform structure. This may illustrate the ease of penetration of gas into aspen species when compared southern pine species, and also correlates with the density of wood species (aspen is lighter than southern pine). In making boards of same density, however, aspen board needs more volume of particles, which leads too higher pressure in the press for producing a target board density. In spite of this, the more porous nature of aspen may still facilitate the diffusion of CO₂ into the board, may lead to more pronounced petrification of wood particles. Another observation in Figure 7.13 is that the process of size reduction (using a hammer-mill) leaves wood particles with a rough surface. Figures 7.14 through 7.16 show fracture surfaces of unaged and aged cement-bonded particleboard (The pictures were taken using a regular camera with magnification lense). Control unaged boards (without CO₂ curing) tailed mainly pulling out the wood fibers. In CO₂ cured boards, however, a combination of wood fiber fracture and pull-out occurrence. This is indicative of stronger fiber-to-matrix bonding in CO₂ cured boards. Accelerated aging (wetting-drying) cycles led to incurred fiber fracture in both control and CO₂ cured boards: This is indicative of improved bonding after exposure to repeated wetting-drying cycles. Freezing-Thawing cycles seems to also improve bonding but the matrix seems to have received some damage after this accelerated aging process.

(a)



(b)

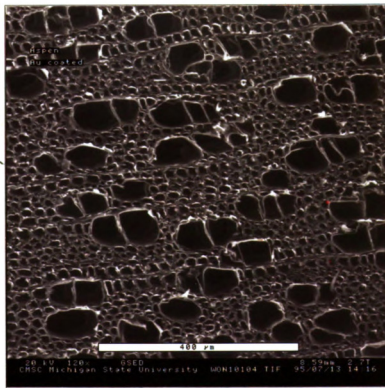


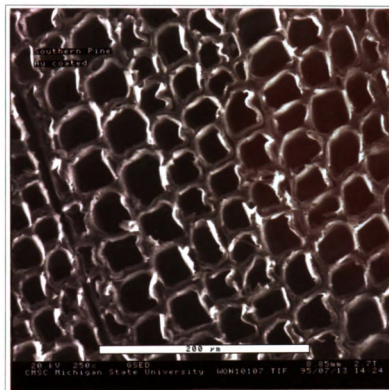
Figure 7.12 Cross-Section of Southern Pine and Aspen: (a) Southern Pine (120x); (b) Aspen (120x); (c) Southern Pine (250x); (d) Aspen (250x)

(c)

(d)

Fig
(12

(c)



(d)

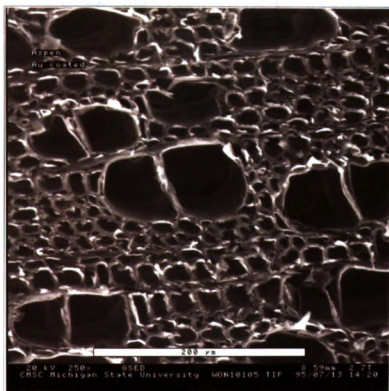
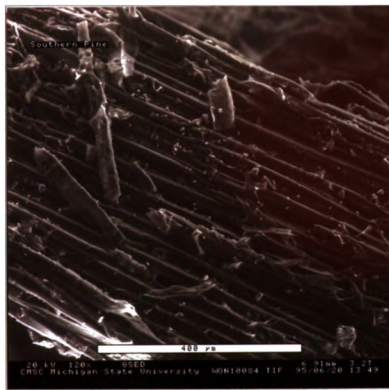


Figure 7.12 (Cont'd) Cross-Section of Southern Pine and Aspen: (a) Southern Pine (120x); (b) Aspen (120x); (c) Southern Pine (250x); (d) Aspen (250x)

(a)



(b)

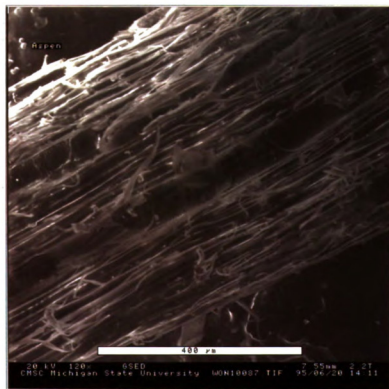


Figure 7.13 Surface of Particles: (a) Southern Pine; (b) Aspen

(a)



(b)



Figure 7.14 Unaged Cement-Bonded Particleboard; (a) Control; (b) CO₂-cured with southern pine used; (c) CO₂-cured with aspen used

(c)



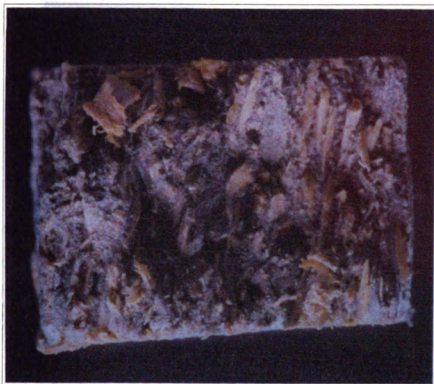
Figure 7.14 (Cont'd) Unaged Cement-Bonded Particleboard; (a) Control; (b) CO_2 -cured with southern pine used; (c) CO_2 -cured with aspen used

(a)



Figure 7.15 After Repeated Wetting-Drying on Cement-Bonded Particleboard; (a) Control; (b) CO_2 -cured with southern pine used; (c) CO_2 -cured with aspen used

(b)



(c)

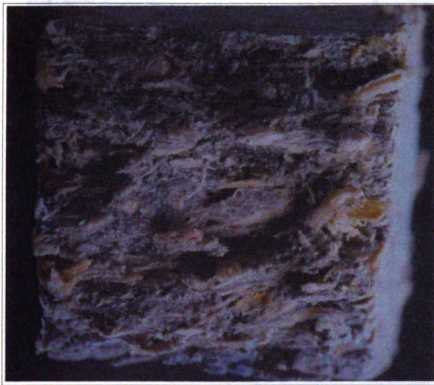


Figure 7.15 (Cont'd) After Repeated Wetting-Drying on Cement-Bonded Particleboard;
(a) Control; (b) CO₂-cured with southern pine used; (c) CO₂-cured with aspen used

(a)



(b)



Figure 7.16 After Repeated Freezing-Thawing on Cement-Bonded Particleboard; (a) Control; (b) CO₂-cured with southern pine used; (c) CO₂-cured with aspen used

(c)



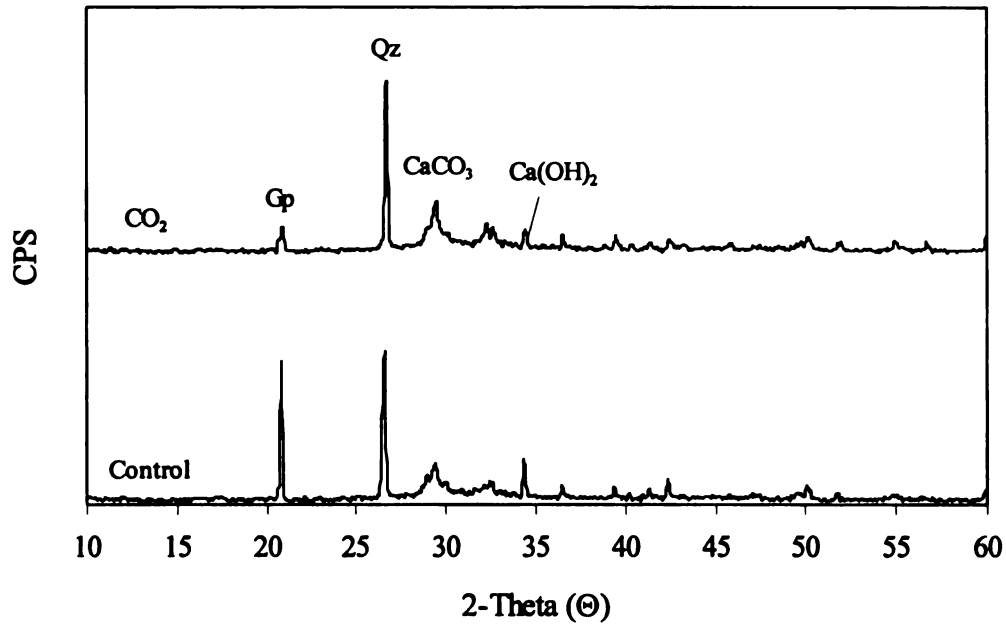
Figure 7.16 (Cont'd) After Repeated Freezing-Thawing on Cement-Bonded Particle-board; (a) Control; (b) CO₂-cured with southern pine used; (c) CO₂-cured with aspen used

7.3.2 Cellulose Fiber Reinforced Cement Composite

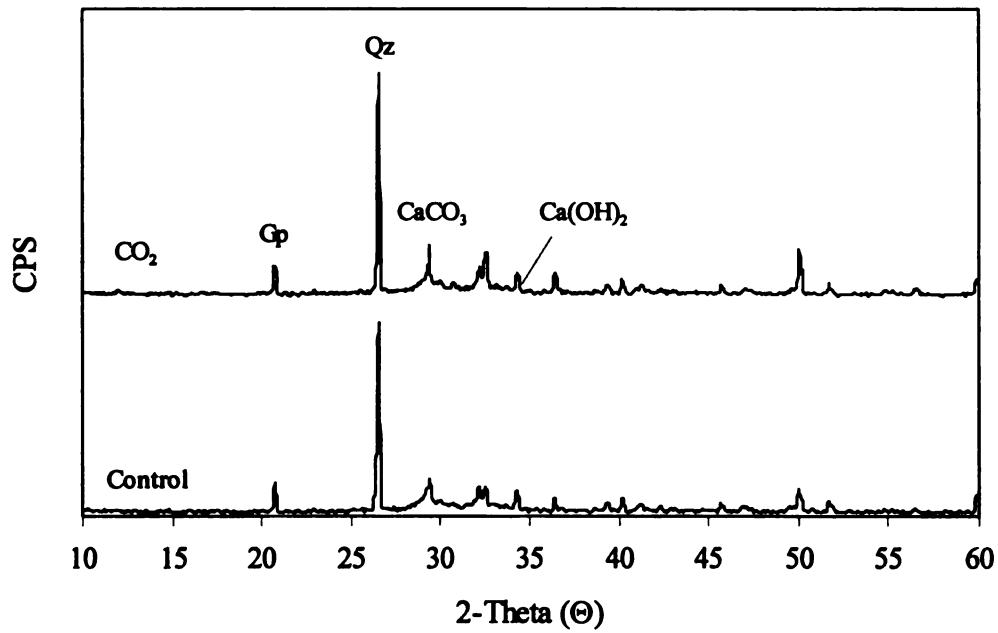
CO₂ curing of cellulose fiber reinforced cement was shown to enhance productivity and engineering properties (including dimensional stability) of the end product. Microstructural studies of this section intend to identify the basic mechanisms which illustrate these effects of the CO₂ curing process. This section compares the CO₂ cured boards versus conventionally cured ones with only longer autoclave curing period (8 hours).

7.3.2.1 X-Ray Diffraction (XRD)

Figure 7.17 through 7.21 show the x-ray patterns of unaged and aged cellulose fiber reinforced cement composites subjected to CO₂ and conventional curing processes. The CO₂ curing process adopted in this study caused little increase in CaCO₃ content of cured boards. Aging process generally increased the CaCO₃ content in both CO₂ and conventionally cured boards. Autoclaved products have do not contain significant amounts of Ca(OH)₂.

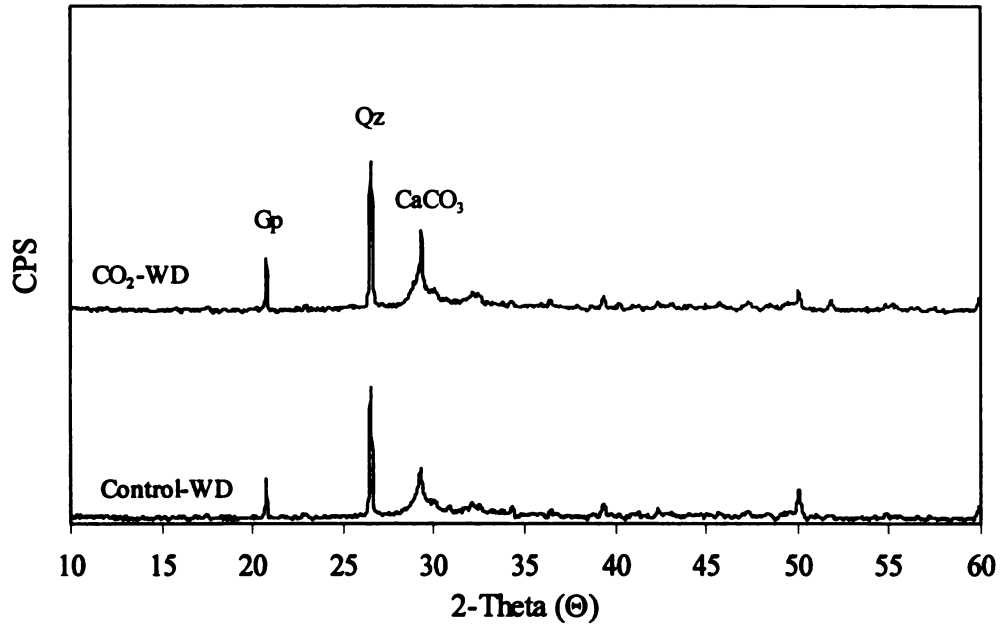


(a) Unpressed

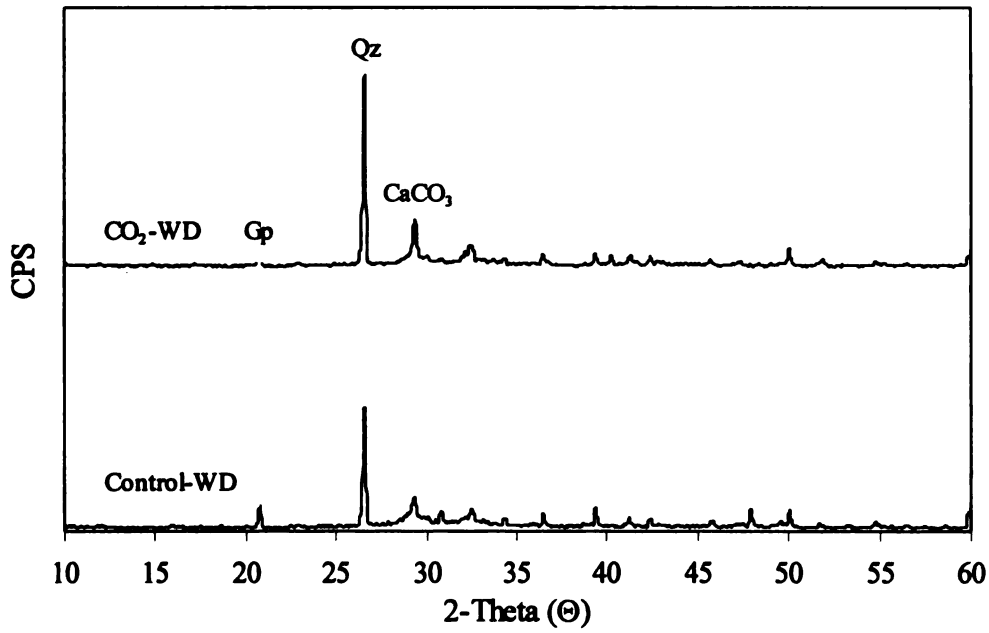


(b) Pressed

Figure 7.17 X-Ray Patterns for Unaged Specimens of Cellulose Fiber Reinforced Cement

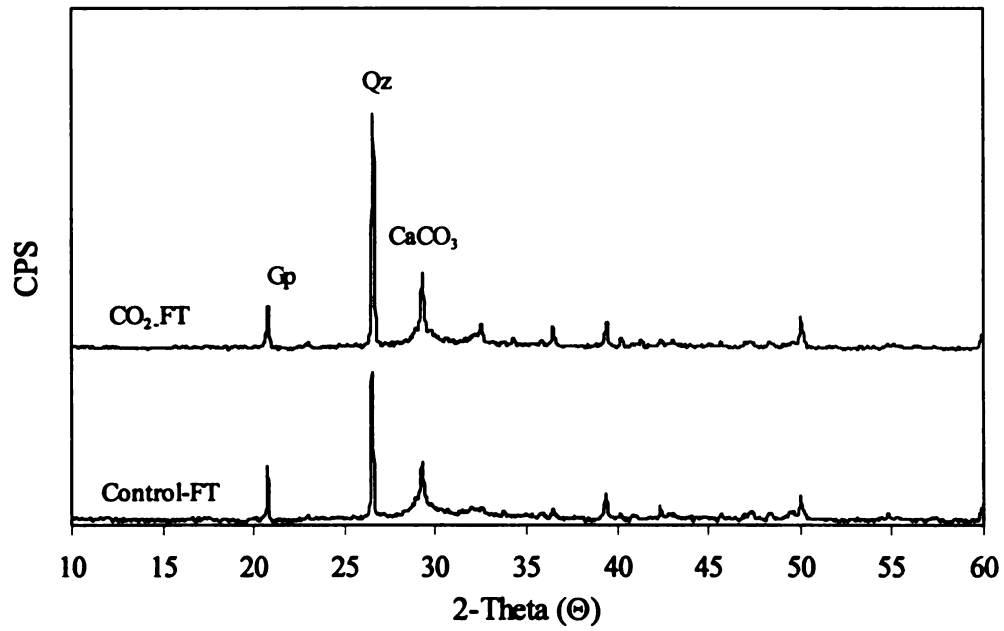


(a) Unpressed

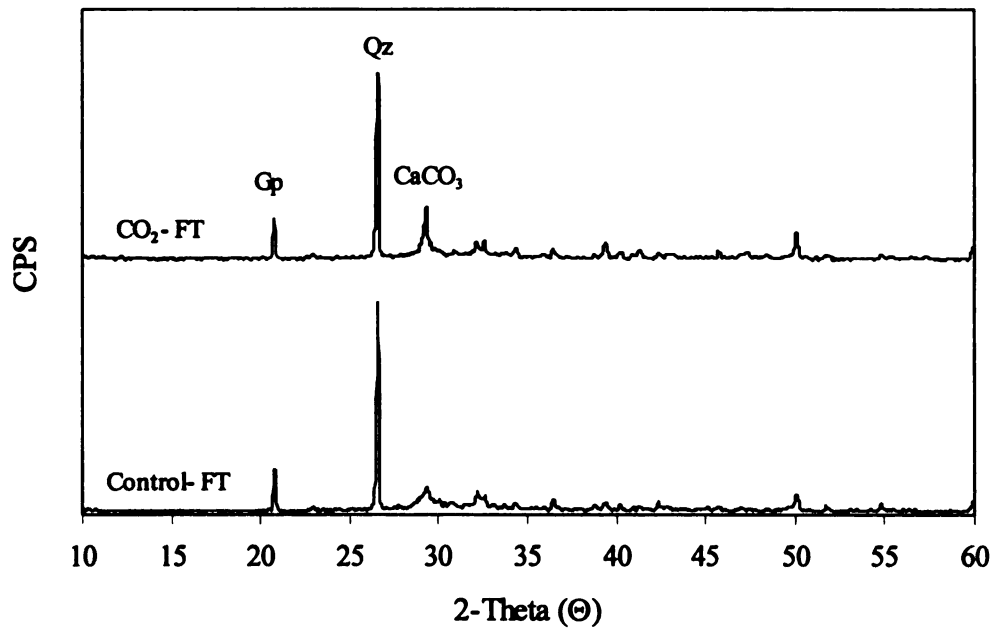


(b) Pressed

Figure 7.18 X-Ray Patterns After Repeated Wetting-Drying Cycles for Cellulose Fiber Reinforced Cement

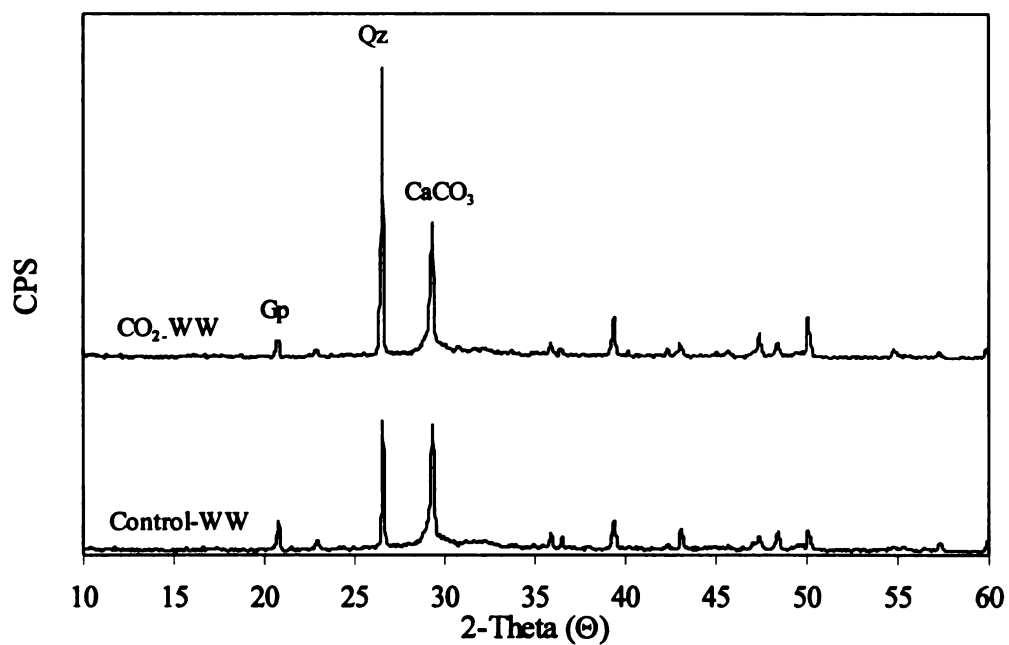


(a) Unpressed

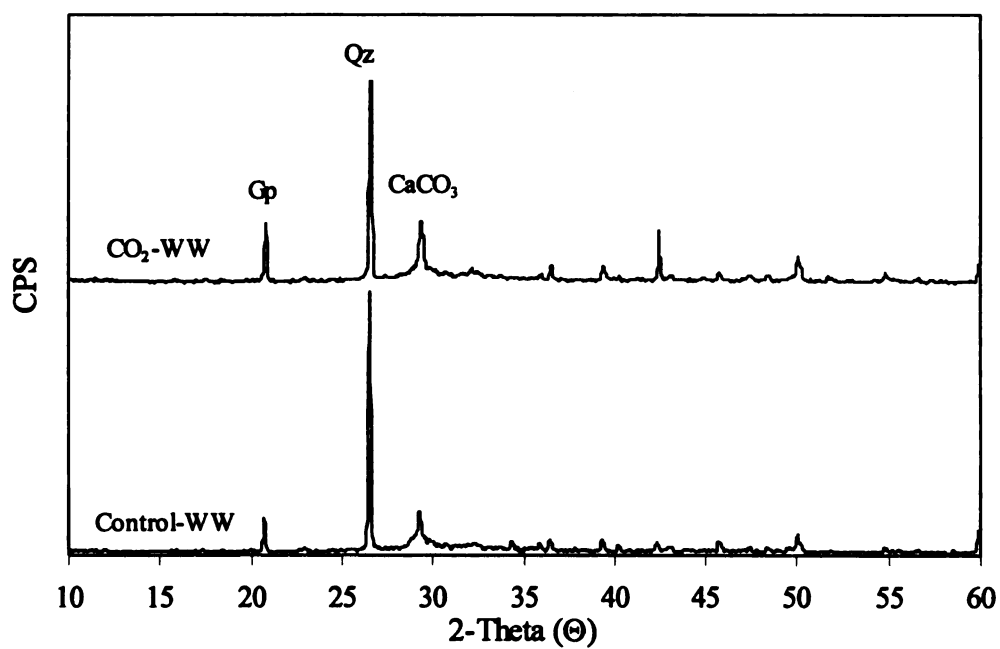


(b) Pressed

Figure 7.19 X-Ray Patterns After Repeated Freezing-Thawing Cycles for Cellulose Fiber Reinforced Cement

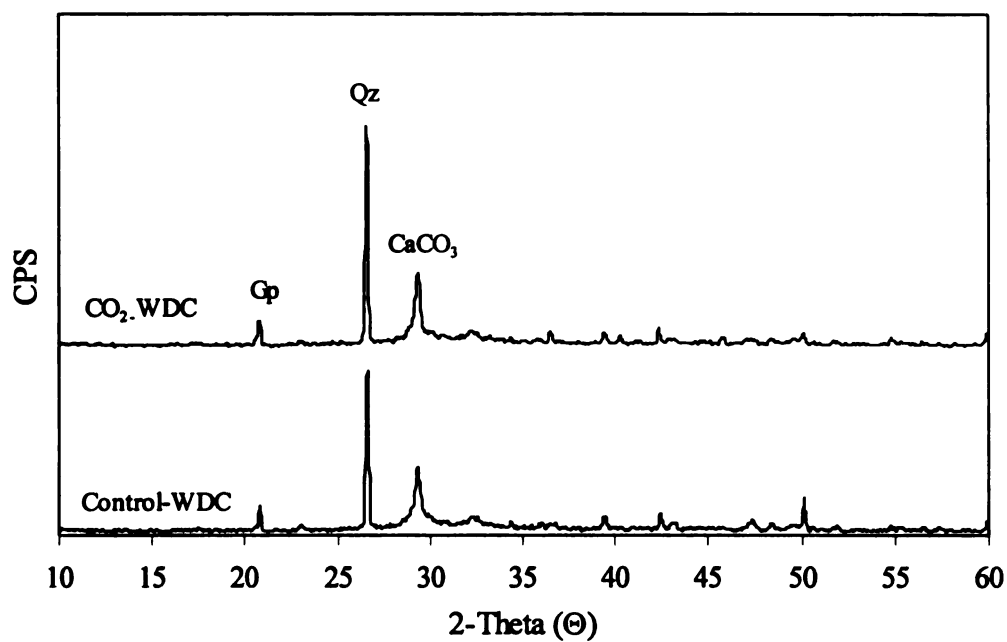


(a) Unpressed

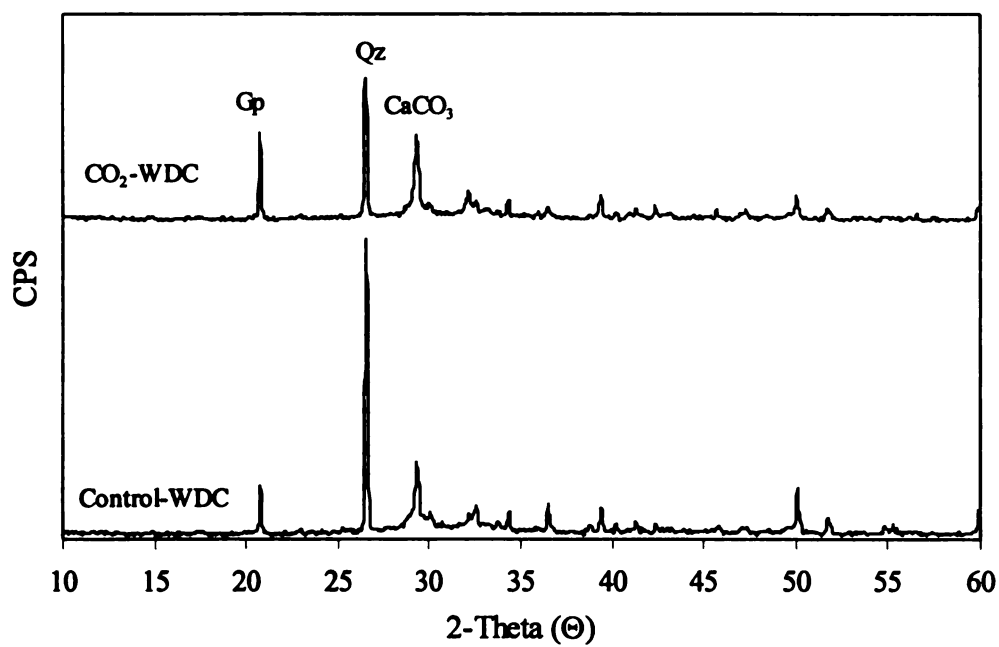


(b) Pressed

Figure 7.20 X-Ray Patterns After Warm Water Immersion for Cellulose Fiber Reinforced Cement



(a) Unpressed



(b) Pressed

Figure 7.21 X-Ray Patterns After Repeated Wetting-Drying-Carbonation Cycles for on Cellulose Fiber Reinforced Cement

7.3.2.2 Thermogravimetric Analysis (TGA)

Table 7.3 shows the amounts of Ca(OH)_2 and CaCO_3 in unaged and aged boards obtained through thermogravimetric analysis. Due to cellulose decompositions at the same temperature range of the Ca(OH)_2 , adjustments had to be made in the calculation of the Ca(OH)_2 content. This was done by taking into account the content cellulose fibers and their weight loss in this temperature range. Figure 7.22 shows Kraft pulp thermogravimetric curves. Figure 7.23 shows typical curves for unaged and aged composites. The following conclusions derived from the TGA analysis. While the results in relation to CaCO_3 content are in general agreement with the findings of x-ray diffraction, the reduced CaCO_3 content after freeze-thaw cycles detected in TGA tests but not in x-ray diffraction. The CaCO_3 content seems to generally correlate with the strength and stiffness of cellulose fiber reinforced cement as far as the effects of CO_2 curing and aging are concerned.

Table 7.3 Thermogravimetric Test Results

		Control		CO_2 -cured	
		UP	P	UP	P
Unaged	Ca(OH)_2	7.09	9.31	10.65	7.19
	CaCO_3	3.72	3.82	6.18	5.07
After Wetting-Drying	Ca(OH)_2	11.07	10.37	8.82	9.11
	CaCO_3	7.04	7.376	8.53	8.84
After Freezing-Thawing	Ca(OH)_2	13.39	10.54	11.04	11.07
	CaCO_3	4.41	4.06	7.32	7.69
After Warm Water	Ca(OH)_2	16.34	13.44	15.08	12.56
	CaCO_3	6.20	4.45	8.24	8.13
After Wetting-Drying-Carbonation	Ca(OH)_2	13.39	11.31	15.75	11.52
	CaCO_3	9.42	8.71	9.53	9.31

UP: Unpressed; P: Pressed

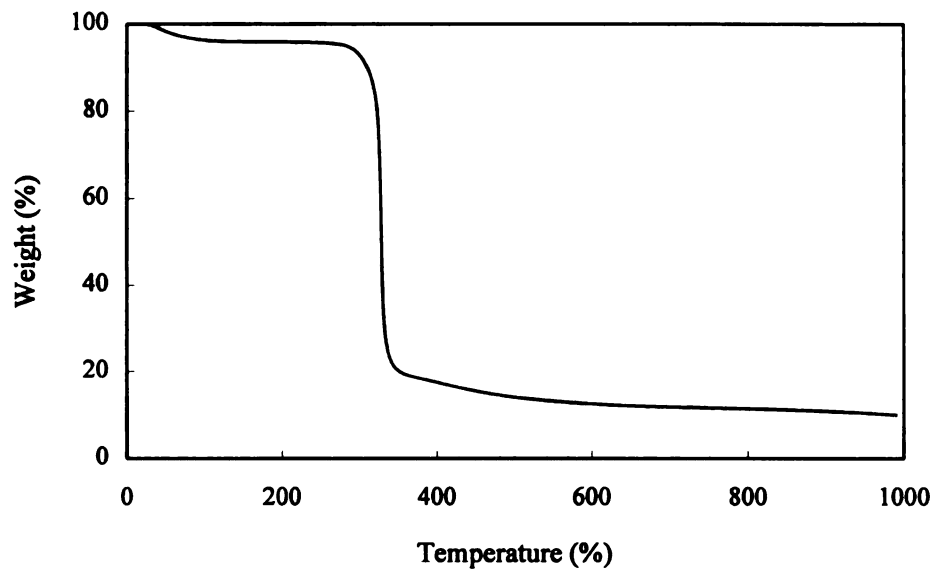


Figure 7.22 Typical Weight Loss Curve for Cellulose (Kraft) Fiber

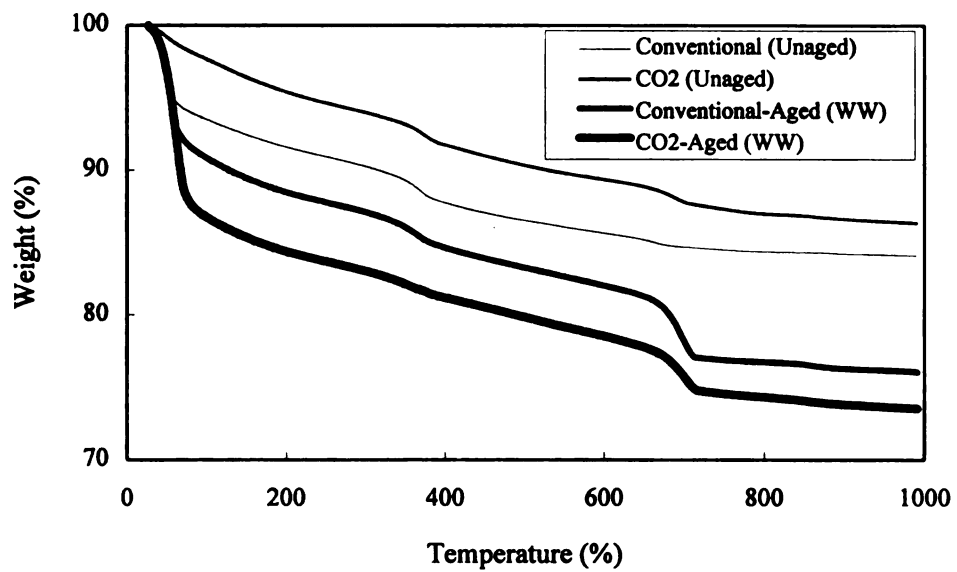


Figure 7.23 Typical Weight Loss Curves for Cellulose Fiber Reinforced Cement

7.3.2.3 Mercury Intrusion Porosimetry

Tables 7.4 and 7.5 present test results for cellulose fiber reinforced cement composites examined by mercury intrusion porosimetry. Figures 7.24 through 7.28 show typical pore size distribution curves for unaged and aged composites. CO₂ curing seems to have reduced the porosity of cement composites. Under aging effects, the porosity of control boards tends to reduce and approach that CO₂ cured boards. In unpressed boards, however, porosity may increase under aging effects in both control and CO₂ cured boards.

Table 7.4 Comparison of Pore Size Distribution of Unaged and Aged Specimens of Cellulose Fiber Reinforced Cement Composite (Unpressed)

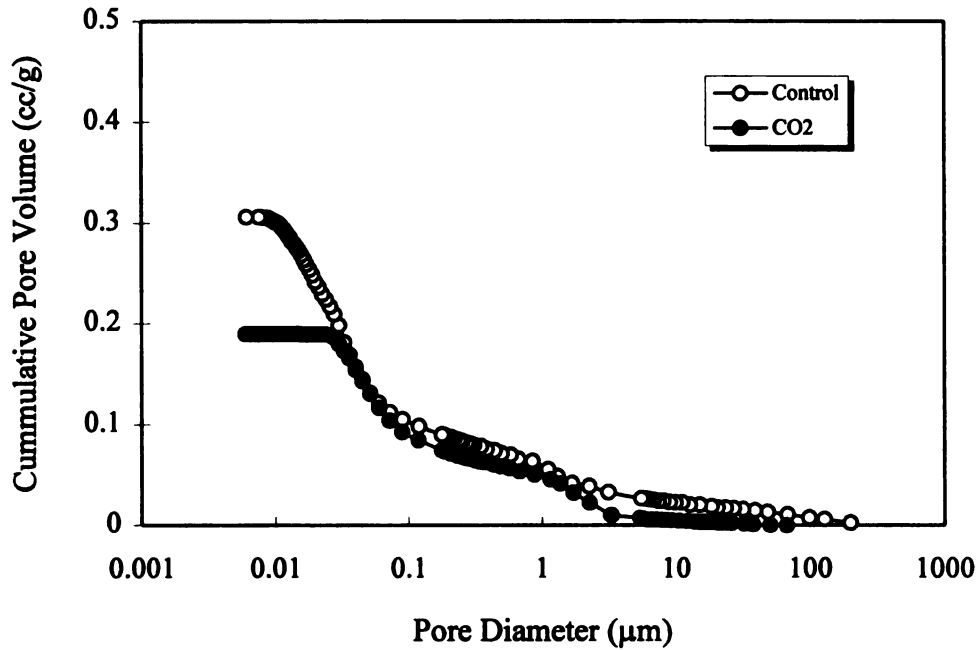
	Unaged		Aged							
	Equilibrium		W-D*		F-T*		W-W*		W-D-C*	
	C**	CO ₂	C**	CO ₂	C**	CO ₂	C**	CO ₂	C**	CO ₂
Total Intrusion Volume (cc/g)	0.3060	0.1896	0.2678	0.2431	0.2564	0.2537	0.3129	0.3371	0.4185	0.3180

Table 7.5 Comparison of Pore Size Distribution of Unaged and Aged Specimens of Cellulose Fiber Reinforced Cement Composite (Pressed)

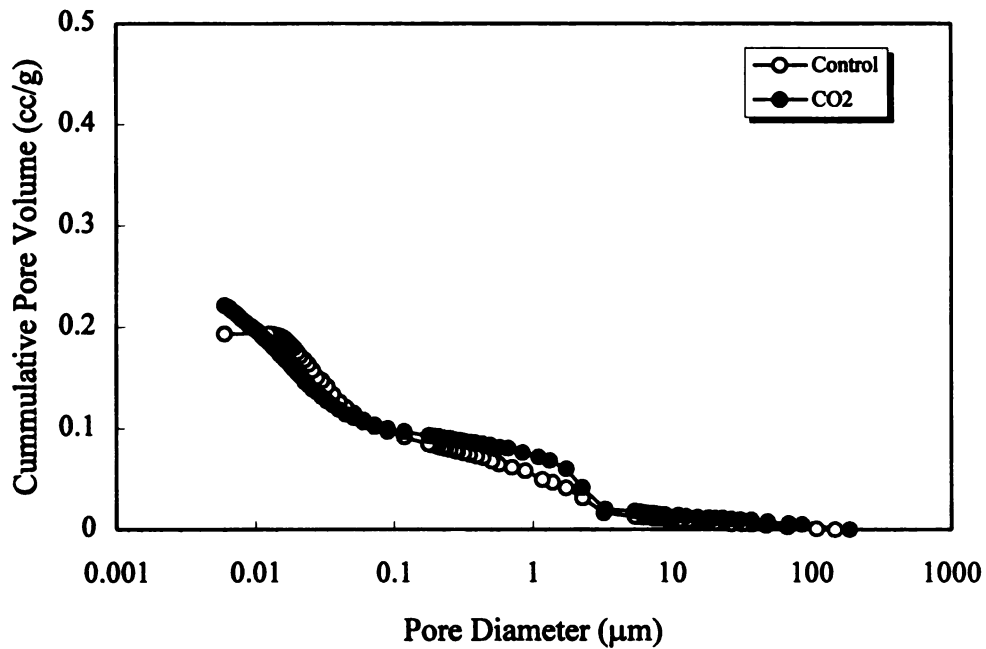
	Unaged		Aged							
	Equilibrium		W-D*		F-T*		W-W*		W-D-C*	
	C**	CO ₂	C**	CO ₂	C**	CO ₂	C**	CO ₂	C**	CO ₂
Total Intrusion Volume (cc/g)	0.2213	0.1734	0.2679	0.1543	0.1560	0.2127	0.1740	0.1729	0.2337	0.2260

*W-D: Wetting-Drying; F-T: Freezing-Thawing; W-W: Warm Water Immersion; W-D-C: Wetting-Drying-Carbonation

**Control

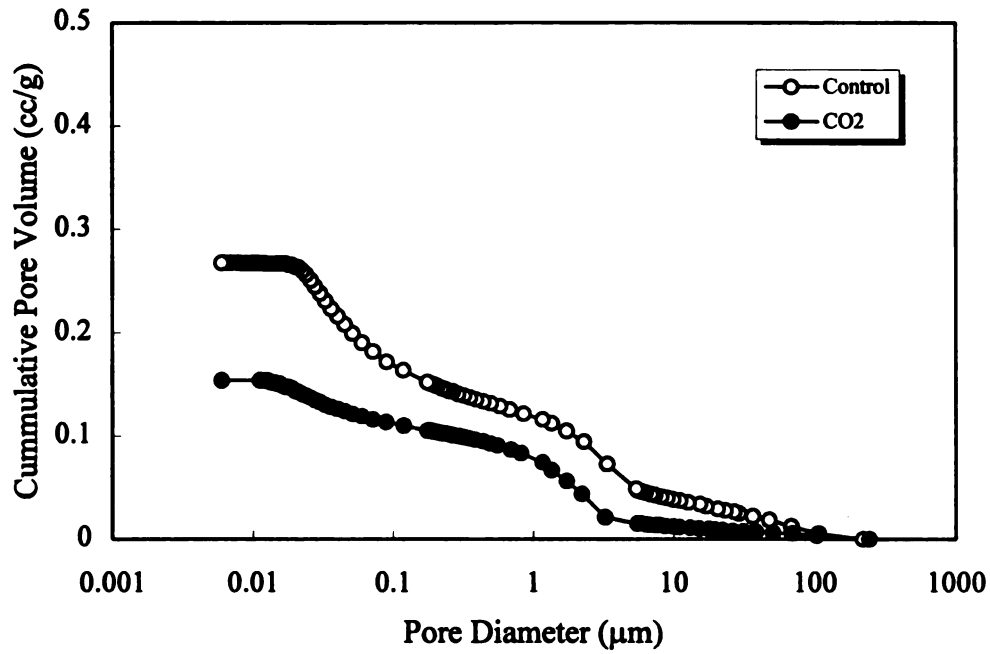


(a) Unpressed

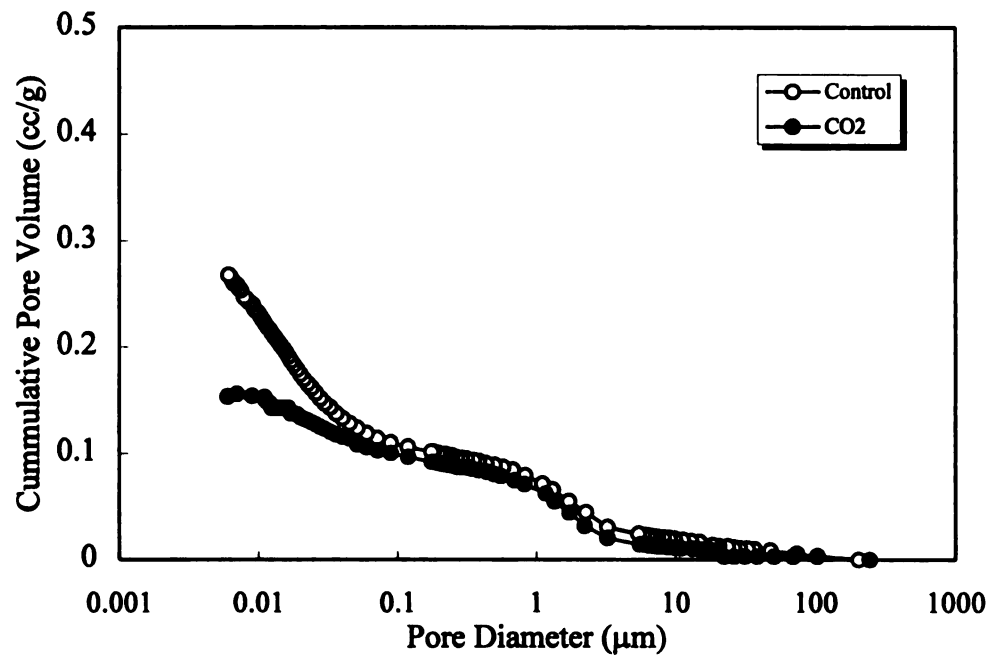


(b) Pressed

Figure 7.24 Pore Size Distribution of Equilibrium Condition on Cellulose Fiber Reinforced Cement Composite

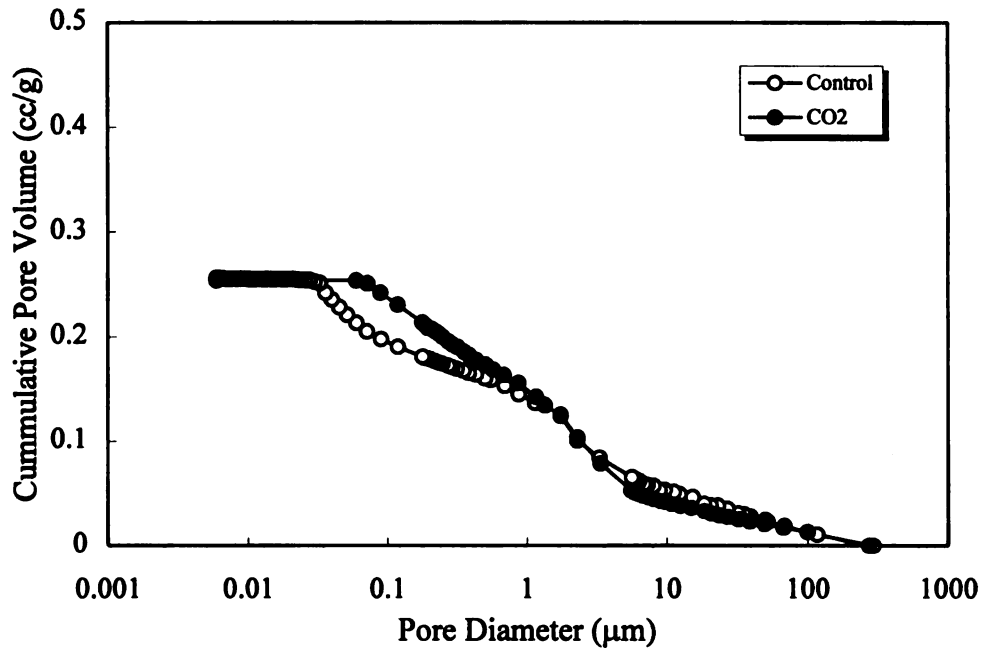


(a) Unpressed

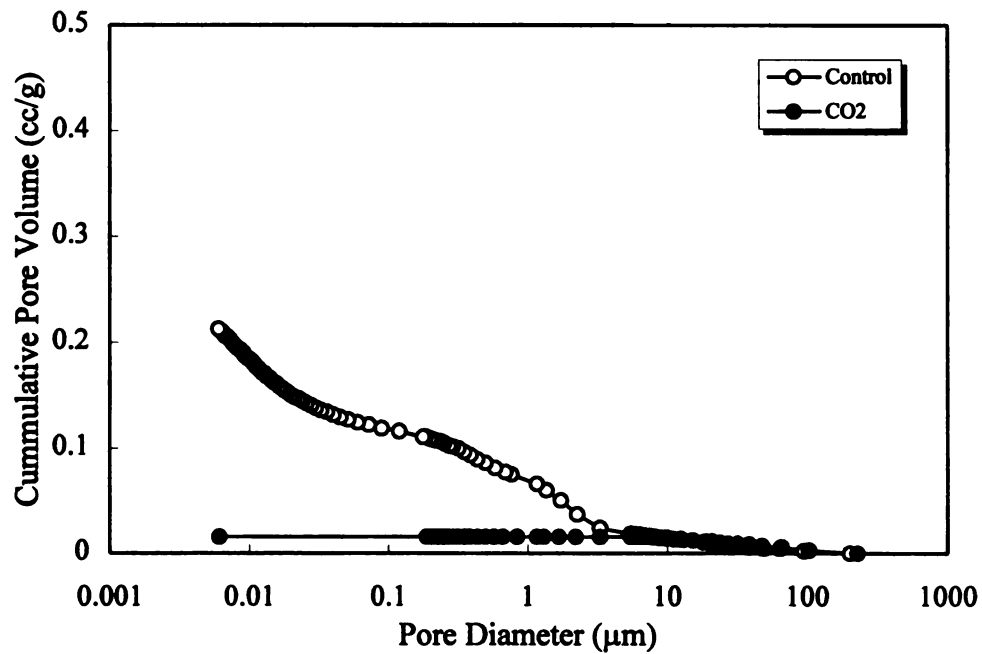


(b) Pressed

Figure 7.25 Pore Size Distribution After Repeated Wetting-Drying on Cellulose Fiber Reinforced Cement Composite

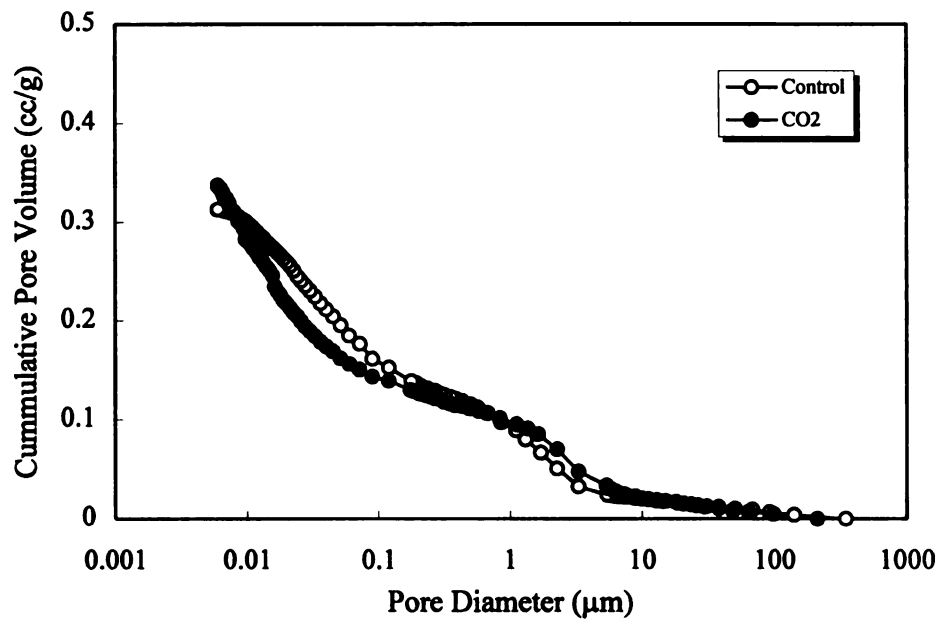


(a) Unpressed

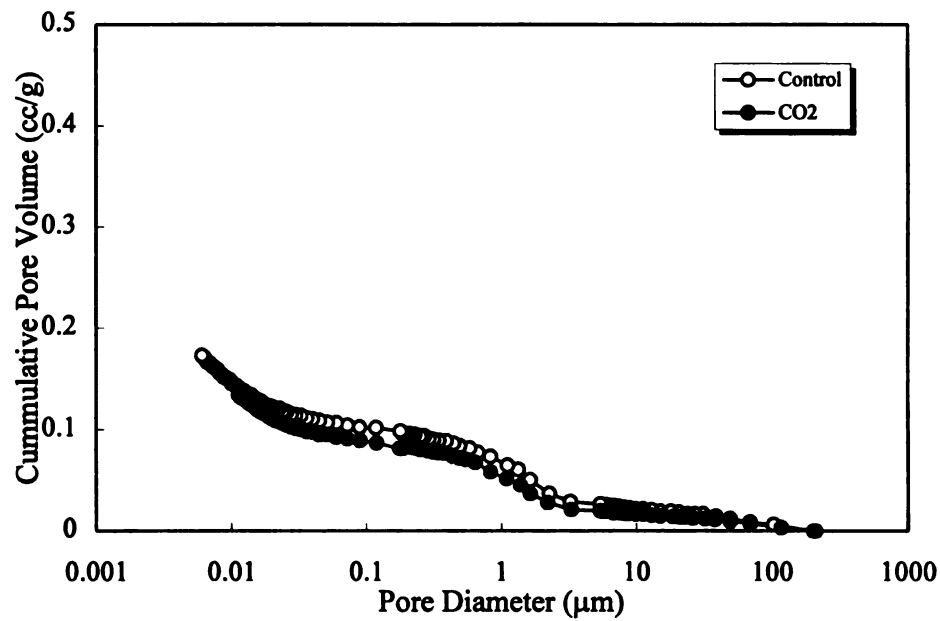


(b) Pressed

Figure 7.26 Pore Size Distribution After Repeated Freezing-Thawing on Cellulose Fiber Reinforced Cement Composite

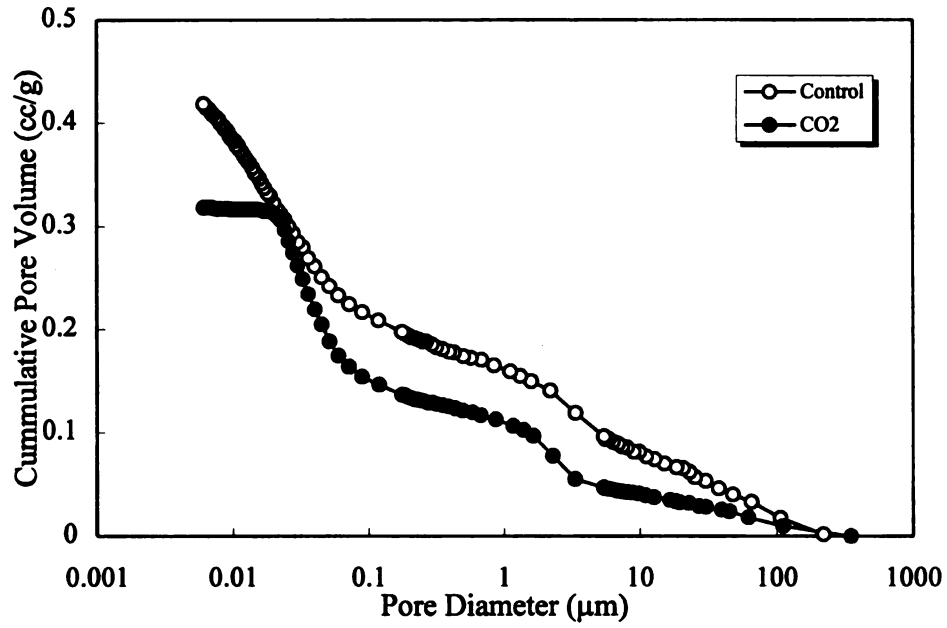


(a) Unpressed

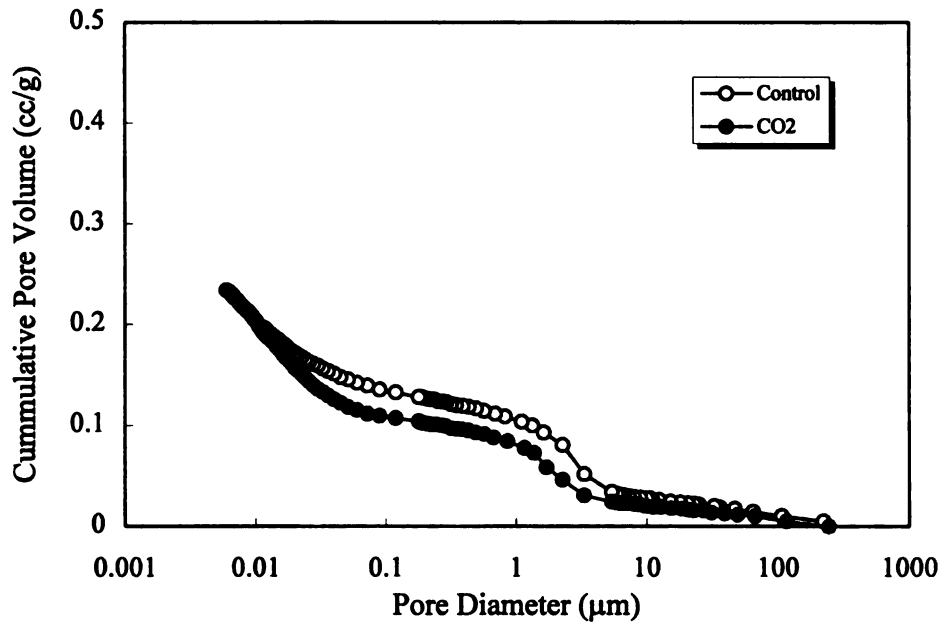


(b) Pressed

Figure 7.27 Pore Size Distribution Immersed Warm Water on Cellulose Fiber Reinforced Cement Composite



(a) Unpressed



(b) Pressed

Figure 7.28 Pore Size Distribution After Repeated Wetting-Drying-Carbonation on Cellulose Fiber Reinforced Cement Composite

7.3.2.4 Fracture Surface and Interface

Figure 7.29 provides some indication for wood petrification in unaged cellulose fiber reinforced cement composites subjected to CO₂ curing. Cellulose fibers pulling out of CO₂ cured boards were partly covered with cement reaction products (see Figure 7.30). Figure 7.31 compares the fracture surfaces of CO₂ and conventionally cured composites. CO₂ curing seems to have reduced microcracking in autoclave. Aging processed, may be except for warm water immersion, seemed to increase the possibility of fiber rupture at the fracture surfaces (see Figure 7.32 through 7.35). This may indicate an increase in bond strength with aging. When compare with saturated boards (Figure 7.36) or air-dried boards (Figure 7.31), oven-dried boards (Figure 7.37) show a greater dominance of fiber rupture at fracture surfaces.

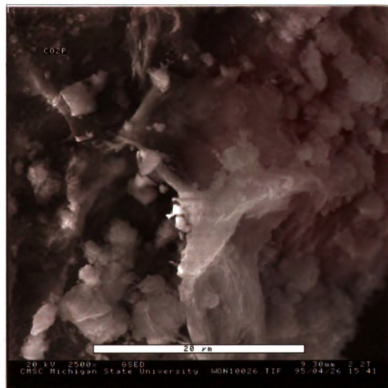


Figure 7.29 Petrified Fibers in CO_2 Cured Cellulose Fiber Reinforced Cement Composites

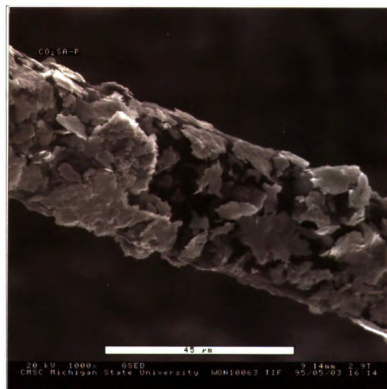
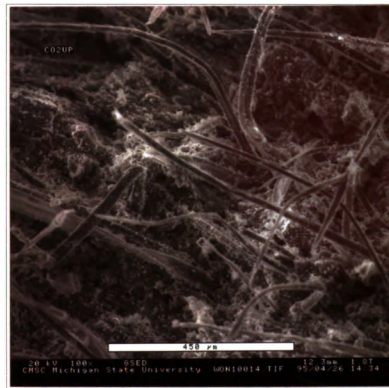


Figure 7.30 Kraft Fiber in CO_2 Cured Cellulose Fiber Reinforced Cement Composites

(a)



(b)

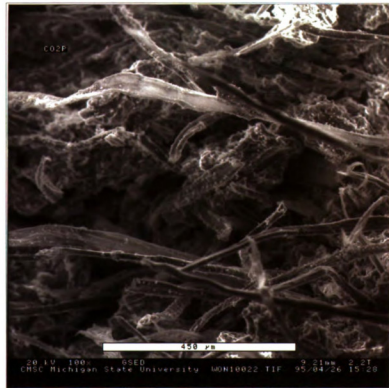
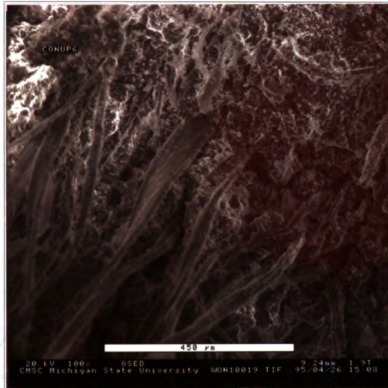


Figure 7.31 Unaged Cellulose Fiber Reinforced Cement Composites: (a) Unpressed and CO₂ Cured; (b) Pressed and CO₂ Cured; (c) Unpressed and Conventionally Cured; (d) Pressed and Conventionally Cured

(c)



(d)

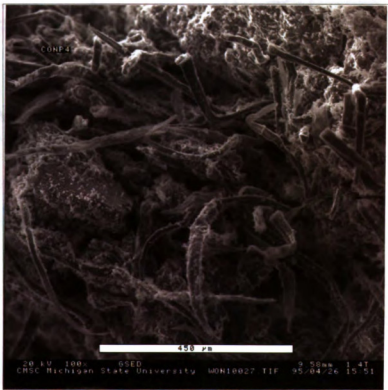
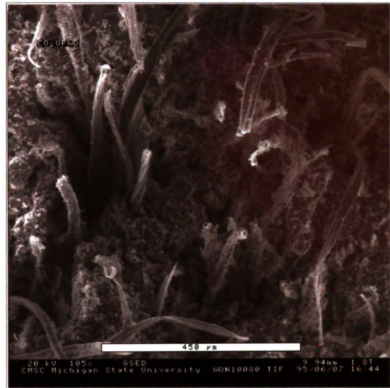
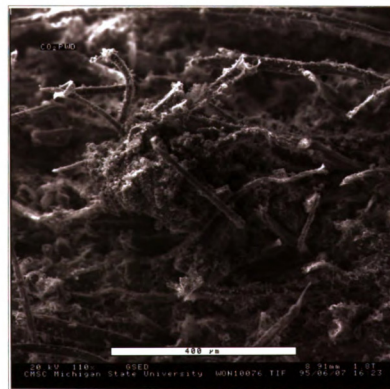


Figure 7.31 (Cont'd) Unaged Cellulose Fiber Reinforced Cement: (a) Unpressed and CO₂ Cured; (b) Pressed and CO₂ Cured; (c) Unpressed and Conventionally Cured; (d) Pressed and Conventionally Cured

(a)



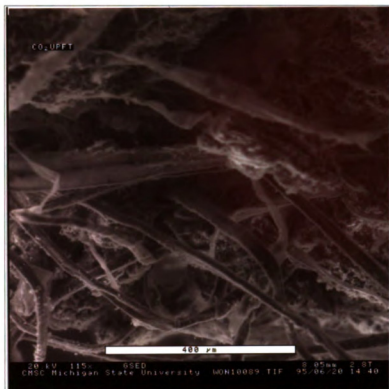
(b)



7.32 After Wetting-Drying Cycles of CO₂ Cured Cellulose Fiber Reinforced Cement:

(a) Unpressed; (b) Pressed

(a)



(b)

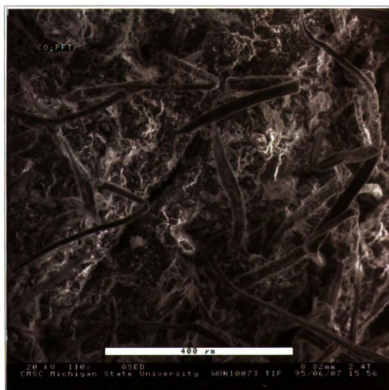
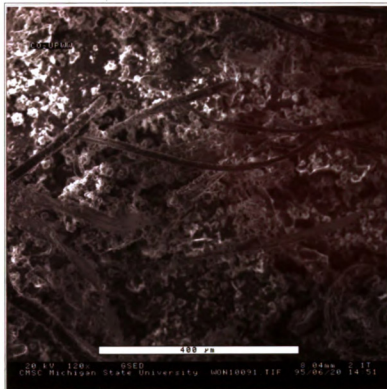


Figure 7.33 After Freezing-Thawing Cycles for CO₂ Cured Cellulose Fiber Reinforced Cement: (a) Unpressed; (b) Pressed

(a)



(b)

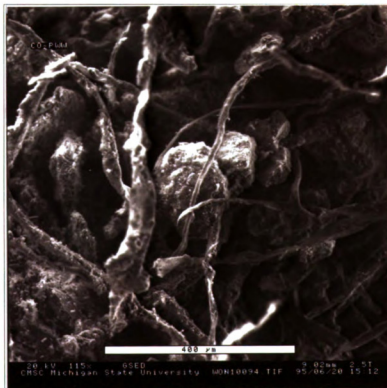
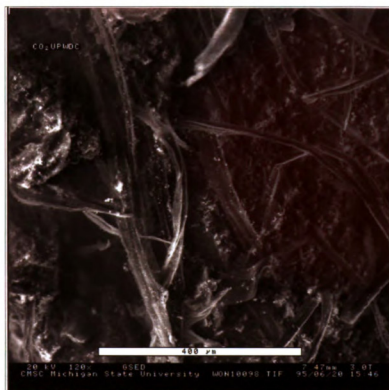


Figure 7.34 After Warm Water Immersion of CO₂ Cured Cellulose Fiber Reinforced Cement: (a) Unpressed; (b) Pressed

(a)



(b)

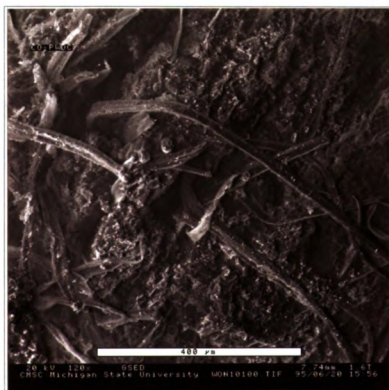
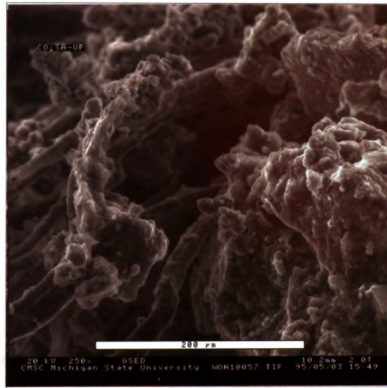


Figure 7.35 After Wetting-Drying-Carbonation Cycles of CO_2 Cured Cellulose Fiber Reinforced Cement: (a) Unpressed; (b) Pressed

(a)



(b)

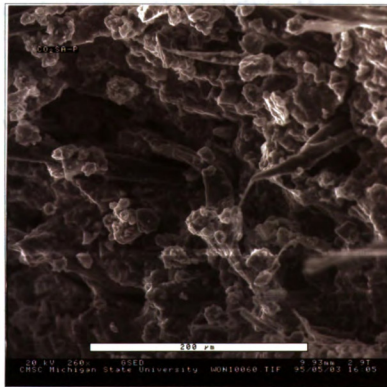
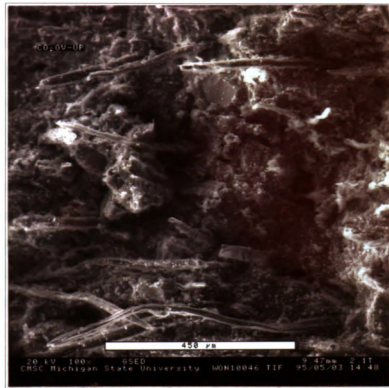


Figure 7.36 Saturated Conditions of CO₂ Cured Cellulose Fiber Reinforced Cement:

(a) Unpressed; (b) Pressed

(a)



(b)

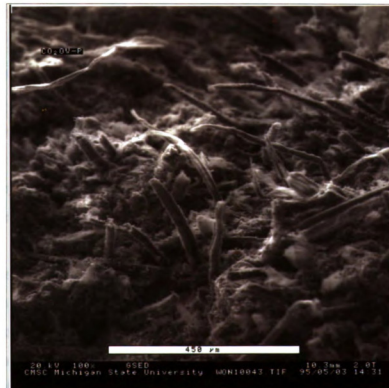


Figure 7.37 Oven-Dried Condition of CO_2 Cured Cellulose Fiber Reinforced Cement:

(a) Unpressed; (b) Pressed

7.4 SUMMARY AND CONCLUSIONS

Microstructural characteristics of unaged and aged wood-cement composites were investigated. The ESEM, TGA, X-ray diffraction and mercury intrusion techniques as well as a regular camera were used in this study.

7.4.1 Cement-Bonded Particleboard

X-Ray Diffraction

- The CO₂-cured composites generally have higher CaCO₃ and lower Ca(OH)₂ contents when compared with the conventionally cured boards. Higher CaCO₃ contents usually correlate with higher flexural strength and stiffness and lower toughness values.
- Aging effects led to increased CaCO₃ and decreased Ca(OH)₂ contents. This is accompanied by increasing CaCO₃ decreasing Ca(OH)₂.

Thermogravimetric Analysis

- Thermogravimetric analysis also showed higher CaCO₃ contents in CO₂-cured composites.
- Aging effects also led to increased CaCO₃ and reduced Ca(OH)₂ contents.

Mercury Intrusion Porosimetry

- CO₂ curing reduced the capillary pore volume on both unaged and aged boards.
- Aging effects generally reduce the pore volume in the case of repeated wetting cycles, but had relatively small effects in the case of freezing-thawing cycles.

Fracture Surfaces and Interface

- Compared with southern pine, aspen had a lower specific gravity and offered a more porous structure for gas penetration.
- In unaged and aged conventionally cured boards, the dominant mode of failure was particle pull-out, and the matrix around the particles was rather weak. In unaged CO₂-cured boards, a combination of particle fracture, peeling and pull-out was ob-

served. After accelerated aging, while the dominant failure modes were the same as unaged boards, the damage to fiber-matrix interfaces was reduced, and the structure was densified under aging effects.

7.4.2 Cellulose Fiber Reinforced Cement Composites

X-Ray Diffraction

- CO₂ curing caused a slight increase in CaCO₃ content. Aging effects generally increased CaCO₃ content in both CO₂ and conventionally cured boards.

Thermogravimetric Analysis (TGA)

- The TGA results generally confirmed the results of x-ray diffraction. The increase in CaCO₃ content under freeze-thaw effect was , however, not confirmed.

Mercury Intrusion Porosimetry

- CO₂ curing reduced the capillary porosity of composites. After aging effects, the porosity of CO₂ and conventionally cured composites seemed to converge.

Fracture Surfaces

- CO₂ curing led to reduced microcracking in the autoclave. Aging seemed to strengthen the interface and provide for more dominance of fiber rupture on fracture surface. Reduced moisture contents of the composite also increased the tendency towards fiber fracture.

CHAPTER 8

SUMMARY AND CONCLUSIONS

An experimental study was conducted to assess the mechanisms of carbonation in accelerated manufacturing of wood-cement composites for achieving balanced improvements in diverse aspects of material properties.

The objectives of this research were reached through the performance of the following tasks:

- Manufacturing and early age characterization of wood-cement composites subjected to carbonation curing
- Investigation of optimum manufacturing conditions, and comprehensive assessment of mechanical and physical properties
- Investigation of the effects of long-term weathering
- Investigation of the microstructural characteristics of wood-cement composites

A comprehensive set of replicated experimental data were generated in this study and analyzed statistically using the analysis of variance, comparisons of means, multiple comparison and response surface analysis techniques in order to derive statistically reliable conclusions.

A summary of the activities in different phases of the project together with the corresponding conclusions are given below.

8.1 MANUFACTURING AND EARLY AGE CHARACTERISTICS UNDER CARBONATION EFFECTS

An experimental study was conducted to assess the effects of the CO₂ curing process variables on wood-cement composites.

8.1.1 Cement -Bonded Wood Particleboard

Hydration Characteristics of Cement in the Presence of Wood

A variety of wood species were selected and characterized based on their interaction with cement. The wood species were: southern pine, red oak, maple, and aspen. The test results indicated that:

- The presence of wood causes delays in the development of the heat of hydration and reduces the peak temperature
- Hardwoods are generally more inhibitory than softwoods

CO₂ Curing Process

Alternative sequences of applying CO₂ and vacuum on faces of the board were investigated and the preferred sequence was selected. The judgment was based on the flexural performance immediately after CO₂ curing.

Effects of CO₂ Concentration

A lower CO₂ concentration (25%) yielded immediate flexural performance characteristics which were generally comparable to those obtained at 100% CO₂ concentration. Initial stiffness was actually higher at the lower CO₂ concentration.

Effects of Mix Composition

A factorial design of experiments was conducted to investigate the effects of wood-cement ratio (0.28 vs. 0.35), CO₂ concentration (25% vs. 100%), and wood species (softwood vs. Hardwood) on the immediate flexural performance. The results suggested that the preferred condition involved the use of a wood-cement ratio of 0.28 and 25% CO₂ concentration.

8.1.2 Cellulose Fiber Reinforced Cement Composites

An experimental study was conducted to assess the effects of CO₂ curing on the flexural performance of autoclaved cellulose fiber reinforced cement composites. The

processing parameters investigated were the oven temperature and autoclaved duration for pressed board; and the oven temperature, oven duration, CO₂ chamber duration, and autoclave duration for unpressed boards. The test results indicated that:

- In pressed boards, all variables (oven temperature and autoclave duration) were statistically significant at the 95% level of confidence. CO₂ curing in some conditions yielded better results than conventional curing process even at half the autoclave duration.
- In the case of unpressed boards, oven duration had statistically significant effects at the 95% level of confidence on flexural strength. In the case of toughness, oven temperature, oven duration, oven duration-CO₂ chamber duration interaction, and CO₂ chamber duration-autoclave duration interaction were statistically significant at the 95% level of confidence. In the case of stiffness, oven duration, oven duration-CO₂ chamber duration interaction, and CO₂ chamber duration-autoclave duration interaction were statistically significant at the 95% level of confidence.
- In both pressed and unpressed cases, an oven temperature of 50°C was chosen as the preferred one. The results yielded preferred processing conditions of pressed board. For unpressed boards, the oven duration, CO₂-curing duration and autoclave duration are to be optimized.

8.2 OPTIMIZATION AND ASSESSMENT OF MECHANICAL AND PHYSICAL PROPERTIES

The results presented in this chapter provided more insight into the optimum processing conditions of wood-cement composites subjected to CO₂-curing. A more comprehensive view was also provided regarding the effects of CO₂-curing on various aspects of composite board performance characteristics.

8.2.1 Cellulose Fiber Reinforced Cement Composite

CO₂-curing helps reduce the manufacturing time and cost of pressed and unpressed cellulose fiber reinforced cement composites, and yields improvements in flex-

ural strength, stiffness, dimensional stability and water absorption of the composite. Flexural toughness tends to be somewhat reduced with CO₂-curing. However, the expected improvements in resistance to aging (carbonation) effects yield improvements even in toughness after aging.

8.2.2 Cement-Bonded Particleboard

CO₂-curing at 25% CO₂ concentration seemed to be more effective at the lower wood-cement ratio of 0.25. At the higher wood-cement ratio of 0.35, however, the combination of CO₂-curing and conventional hydration yielded better 28 day flexural performance. In all cases, the immediate and 28-day flexural performance of CO₂-cured boards were clearly superior to those of conventional boards processed without CO₂-curing. Aspen yielded better results than southern pine when subjected to CO₂ curing. The internal bond strength of CO₂-cured boards, particularly at wood-cement ratio of 0.28 where CO₂-curing was more effective, was substantially greater than the internal bond strength values obtained through conventional processing without CO₂ curing. As far as moisture movements are concerned, CO₂-curing generally enhanced the dimensional stability of the board, or did not markedly influence it.

8.3 DURABILITY CHARACTERISTICS OF CARBONATED WOOD-CEMENT COMPOSITES

In this phase, the long-term durability of wood-cement composites was assessed. The specimens were subjected to repeated cycles of freezing and thawing, wetting and drying, warm water immersion, and wetting-drying-carbonation. In the case of cellulose fiber reinforced cement composites, moisture sensitivity was also investigated. After aging, the specimens were tested for flexural performance.

8.3.1 Cement-Bonded Particleboard

Repeated Wetting-Drying Cycles

In general, repeated wetting-drying cycles led to increased stiffness and reduced toughness values. The effects on flexural strength were mixed. In the case of CO₂-cured

boards, wood species (aspen versus southern pine) and wood-cement ratios had statistically significant interactions with the aging effects on the flexural strength of cement-bonded particleboard. From a practical point of view, however, the effects and interactions of wood species, wood-cement ratio and aging in regard to the flexural strength of cement-bonded particleboard were relatively small. In the case of toughness, aging had a definite adverse effect. Wood-cement ratio had a relatively small but statistically significant effect on the stiffness of carbonated boards. Aging led to significant gains in stiffness. The interaction of aging with wood species in relation to toughness, while statistically significant, seems to be rather small from a practical point of view. Statistical analysis of the flexural strength test results suggested that curing condition (CO_2 vs. conventional) and wood-cement ratio (0.28 vs. 0.35) had statistically significant interactions with the aging effects on flexural strength. The trends in the effect of various factors on flexural strength suggest that CO_2 curing not only enhanced the initial flexural strength of cement-bonded particleboard, but also improved the resistance to aging effects on flexural strength. The effects and interaction of wood-cement ratio and aging in regard to flexural strength were relatively small. In the case of flexural toughness, the effects and interactions of curing condition and aging were statistically significant. Flexural toughness was higher with CO_2 curing; aging caused embrittlement in both CO_2 and conventionally cured boards, but flexural toughness after aging remained higher in CO_2 cured boards. The adverse effects of aging on toughness were more pronounced at the higher wood-cement ratio of 0.35. In the case of initial stiffness, aging led to significant gains in stiffness; the interaction of aging with curing condition in relation to stiffness was statistically significant; the CO_2 -cured boards showed more gain in stiffness upon aging than conventionally cured boards.

Repeated Freezing-Thawing Cycles

In general, repeated freezing-thawing cycles led to increased stiffness and reduced toughness of cement-bonded particleboard. The effects on flexural strength were mixed but generally negative. Statistical analysis of the flexural strength test results suggested that the effects and interactions of various variables, although statistically significant, are

relatively small and of little practical significance. Flexural strength tends to be rather stable under repeated freeze-thaw cycles. Flexural toughness seriously drops with aging under freeze-thaw effects. This adverse effect of repeated freeze-thaw cycles was more pronounced at the higher wood-cement ratio of 0.35. Repeated freeze-thaw cycles produced substantially increased stiffness values. Statistical analysis of the flexural strength test results confirmed that flexural strength was rather stable under repeated freeze-thaw cycles. CO₂-curing produced statistically improved flexural strengths before and after the application of freeze-thaw cycles. In the case of toughness, there was a strong interaction of curing and wood-cement ratio with aging. The freeze-thaw effects on toughness were more pronounced at the higher wood-cement ratio and in the case of CO₂-cured boards. The repeated freeze-thaw cycles substantially increased the stiffness of cement-bonded particleboard; the effects and interactions of curing conditions and wood-cement ratio with aging were statistically significant. The increase in the stiffness of cement-bonded particleboard was more pronounced when the boards were subjected to CO₂-curing.

8.3.2 Cellulose Fiber Reinforced Cement Composites

The improvement in flexural strength of boards with CO₂ curing was observed to be statistically significant at the 99% level of confidence. Control curing conditions produced flexural toughnesses which were higher than those obtained through CO₂ curing. The improved stiffness with CO₂ curing was statistically significant at the 99% level of confidence for unpressed boards; in the case of pressed boards the stiffness obtained with CO₂-curing was statistically comparable to that produced by the longer curing period but, at 95% level of confidence, superior to the stiffness of boards subjected to a similar autoclave curing period without CO₂-curing.

Repeated Wetting-Drying Cycles

Repeated wetting-drying cycles caused an increase in the flexural stiffness and a drop in the flexural toughness of composites, without significantly affecting their flexural strength. In the case of unpressed boards, analysis of variance of flexure test results suggests that repeated wetting-drying cycles had statistically significant effects, at 99% level

of confidence, on flexural strength, toughness and stiffness. In the case of pressed boards, the effects of repeated wetting-drying cycles were statistically significant, at the 95% level of confidence, only for flexural toughness. CO₂-curing led to higher original strength and stiffness values but did not seem to change the general trends in the effects of wetting-drying cycles.

After aging, the CO₂-cured boards were still superior to conventionally cured ones in all aspects of flexural performance (strength, toughness and stiffness) at 99% level of confidence. CO₂-curing helped control the aging effects on the toughness of unpressed boards. With CO₂-curing, the increase in stiffness with aging was also more pronounced than that for the control curing conditions. Otherwise, similar trends were observed in aging effects on CO₂-cured and conventionally cured composites.

Repeated Freezing-Thawing Cycles

The effects of freeze-thaw cycles on flexural strength were mixed, but flexural stiffness generally increased and toughness decreased after exposure to repeated freeze-thaw cycles. In the case of unpressed boards, analysis of variance of the flexure test data indicates that freeze-thaw cycles generally had statistically significant effects, at 99% level of confidence, on flexural strength, stiffness and toughness. In the case of pressed boards, effects on flexural strength were not statistically significant, but those on stiffness and toughness were.

The pressed boards, after exposure to repeated freeze-thaw cycles, all performed rather similarly in flexure irrespective of the curing condition. The aged unpressed boards subjected to CO₂ curing possessed strength, toughness and stiffness characteristics which, at 95% level of confidence, were superior to those obtained with control curing condition at similar autoclave curing period and comparable to those obtained with the other control curing condition at elongated autoclave curing period. As far as the aging effects are concerned, the CO₂-curing controlled the adverse aging-effects on the flexural toughness of unpressed boards and pronounced the positive effects of aging on initial stiffness. For pressed boards, CO₂ curing did not render improved control over the aging effects on toughness.

Immersion in Warm Water

Warm water immersion had generally adverse effects on flexural strength, toughness and stiffness. Analysis of variance of the test data suggest, that the warm water immersion effects on flexural performance were generally statistically significant for both unpressed and pressed boards.

After aging, the unpressed CO₂-cured boards performed better than boards subjected to the control curing at a similar autoclave period. Elongated autoclave curing (without CO₂ exposure), however, generally produced better aged results. In the case of pressed boards, the aged CO₂ cured boards presented better flexural strength and stiffness and comparable flexural toughness values when compared with the aged boards subjected to control curing conditions. In general, the influence of CO₂ curing on the consequences of warm water immersion were mixed.

Repeated Wetting-Drying-Carbonation Cycles

There was a tendency in flexural toughness and strength to drop and in flexural stiffness to generally increase after this accelerated aging process. Analysis of variance of the test data suggests that these aging effects were generally of little statistical significance in unpressed boards, but significant in pressed boards.

Aged unpressed CO₂ cured boards had higher flexural strength and comparable flexural toughness and stiffness when compared with the aged control unpressed boards, at 95% level of confidence. The aged pressed CO₂-cured boards offered comparable flexural strength and stiffness values, but lower flexural toughness, when compared with aged control pressed boards, at 95% level of confidence. There was a mixed influence of CO₂ curing on the accelerated aging effects on the flexural performance of unpressed and pressed boards.

Moisture Sensitivity

The increase in moisture content from air-dried to saturated condition had adverse effects on the flexural strength and stiffness of both conventional and carbonated composites. Ductility and toughness characteristics, however, improved upon saturation.

The measured flexural toughness values did not show this trend because they partly reflect the loss in flexural strength. Oven drying produced adverse effects on flexural performance; this could be partly attributed to the adverse effects of dry heat (48 hours in oven at 102°C) on cellulose fibers. Analysis of variance and multiple comparison of the results generally confirmed the statistical significance of moisture effects on the flexural performance of cellulose fiber reinforced cement composites.

Dimensional Stability

Irrespective of the curing process, the aging condition of accelerated wetting-drying-carbonation produced relatively large shrinkage of boards.

8.4 MICROSTRUCTURE OF WOOD-CEMENT COMPOSITES

Microstructural characteristics of unaged and aged wood-cement composites were investigated. The ESEM, TGA, X-ray diffraction and mercury intrusion techniques as well as a regular camera were used in this study.

8.4.1 Cement-Bonded Particleboard

X-Ray Diffraction

- The CO₂-cured composites generally have higher CaCO₃ and lower Ca(OH)₂ contents when compared with the conventionally cured boards. Higher CaCO₃ contents usually correlate with higher flexural strength and stiffness and lower toughness values.
- Aging effects led to increased CaCO₃ and decreased Ca(OH)₂ contents. This is accompanied by increasing CaCO₃ decreasing Ca(OH)₂.

Thermogravimetric Analysis

- Thermogravimetric analysis also showed higher CaCO₃ contents in CO₂-cured composites.
- Aging effects also led to increased CaCO₃ and reduced Ca(OH)₂ contents.

Mercury Intrusion Porosimetry

- CO₂ curing reduced the capillary pore volume on both unaged and aged boards.
- Aging effects generally reduce the pore volume in the case of repeated wetting cycles, but had relatively small effects in the case of freezing-thawing cycles.

Fracture Surfaces and Interface

- Compared with southern pine, aspen had a lower specific gravity and offered a more porous structure for gas penetration.
- In unaged and aged conventionally cured boards, the dominant mode of failure was particle pull-out, and the matrix around the particles was rather weak. In unaged CO₂-cured boards, a combination of particle fracture, peeling and pull-out was observed. After accelerated aging, while the dominant failure modes were the same as unaged boards, the damage to fiber-matrix interfaces was reduced, and the structure was densified under aging effects.

8.4.2 Cellulose Fiber Reinforced Cement Composites

X-Ray Diffraction

- CO₂ curing caused a slight increase in CaCO₃ content. Aging effects generally increased CaCO₃ content in both CO₂ and conventionally cured boards.

Thermogravimetric Analysis (TGA)

- The TGA results generally confirmed the results of x-ray diffraction. The increase in CaCO₃ content under freeze-thaw effect was, however, not confirmed.

Mercury Intrusion Porosimetry

- CO₂ curing reduced the capillary porosity of composites. After aging effects, the porosity of CO₂ and conventionally cured composites seemed to converge.

Fracture Surfaces

- CO₂ curing led to reduced microcracking in the autoclave. Aging seemed to strengthen the interface and provide for more dominance of fiber rupture on fracture surface. Reduced moisture contents of the composite also increased the tendency towards fiber fracture.

APPENDICES

APPENDIX A

A FRAMEWORK TO MODEL RESTRAINED SHRINKAGE CRACKING OF CELLULOSE FIBER REINFORCED CEMENT COMPOSITES

A.1 INTRODUCTION

Restrained shrinkage cracking is a key issue in practical use of cellulose fiber reinforced cement composites and other building panels.

Many parameters govern the performance of cellulose fiber reinforced cement composite subjected to restrained shrinkage. These parameters include shrinkage, creep, moisture effect on fibers and interfaces, drying state, fiber pull-out and bridging effects, bulk matrix and bond strength development over time, temperature and relative humidity of the environment, etc.

A.2 BACKGROUND

The extent of shrinkage in cement-based materials depends on many factors, including the properties of the material, and the temperature and relative humidity of the environment. Tensile stresses develop if the concrete is constrained from shrinkage, and can lead to cracking. In Figure I.1 schematically shows an installation of cellulose fiber reinforced cement composite. Since the parts are rigidly connected, high tensile stress may build up, and cracking may occur under restrained shrinkage effects.

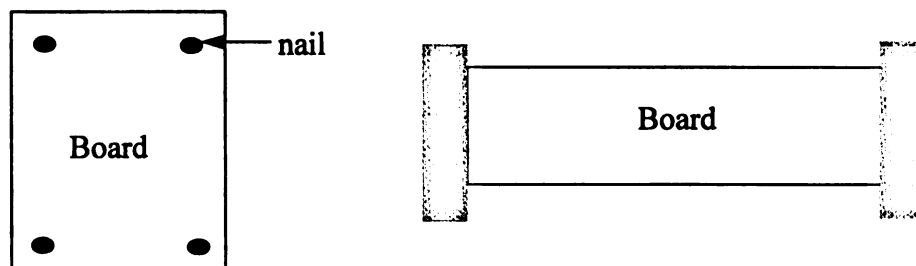


Figure A.1 Typical Construction Pattern of Cellulose Fiber Reinforced Cement Composites

Kraft fibers are very sensitive to changes in moisture content, which affect both the mechanical properties of the fiber and its dimensions. Upon wetting, the fiber loses stiffness and gains ductility. The swelling and shrinkage of the fibers during wetting and drying, with strains greater than those of the matrix, may lead to changes in the contact pressure across the interface, thus causing variations in the actual bond.

The mode of failure involves more fiber pull-out in wet composites. The failure in dry composites is dominated by fiber fracture with only a small extent of pull-out. The change in mechanical properties and fracture mode with variation in moisture content can be explained in terms of changes in fiber properties and the fiber-matrix bond. Fiber failure in wet condition is accompanied by a reduction in cross-sectional area, and twisting and unraveling of the fibers all of which are associated with the ductile behavior of the wet fibers. In the dry composite, there is no significant reduction in the cross sectional area of the broken fiber, and the outer layer of the fibers are stripped away rather than debonded at the interface, indicting a strong bond. The strong bond in the dry state may be the result of hydrogen bridges [98].

A.3 MODEL GENERATION

In this section, a framework for modeling the progressive cracking mechanisms of cellulose fiber reinforced cement composites is presented.

A.3.1 Before Crack Development

If the stress due to imposed shrinkage strain is less than the tensile strength of the element, then the element remains uncracked. There will be relaxation of stress, due to creep, during the time-step. If $\{\dot{\sigma}^R\}$ is the rate of the relaxation of stress, then the constitutive law will have the following form:

$$\{\dot{\sigma}\} = [D]\{\dot{\epsilon}\} + \{\dot{\sigma}^R\} \quad (\text{A.1})$$

or

$$\{\dot{\epsilon}\} = [D^{-1}][\{\dot{\sigma}\} - \{\dot{\sigma}^R\}] \quad (\text{A.2})$$

where D : material stiffness matrix, and the dot represents a differential

A.3.2 After Cracking

When the stress reaches the value of the tensile strength, a cohesive crack is assumed. The crack in the matrix starts developing, but still has the ability to transfer the load, though in a descending manner (the amount of the transferred load decreases as the crack widths). For the case where few elements reach the tensile strength at the same time, as happens, for example, in the case of a linear restrained specimen subjected to drying, a special strain localization mechanisms is introduced in the model. It is assumed that due to some imperfections in the material's structure, only one element incurs cracking at one peak stress. This element is chosen to be in the center between the restraining points. The response of the element between the peak stress and the beginning of a matrix traction-free crack is in this stage, that is, a crack in composite is assumed to resist tensile stresses. However, these cohesive stresses decrease with an increase in crack width. For simplicity, a linear relationship between decreasing stresses and increasing crack width may be assumed. This means that a crack would be traction-free when its width exceeds a certain value ω_{cr} . If the element subjected to restrained shrinkage were unreinforced, then the material outside the fracture zone would incur unloading. For a cellulose fiber reinforced element in the fracture zone, increasing the crack width may provide additional resistance due to fibers bridging at the crack. The resistance provided by fibers consists of two parts: interfacial-transfer in the embedded fibers and the stresses in the exposed fibers.

The representation of cellulose fiber reinforced composite at this stage consists of two subelements; subelement d represents the uncracked part of the element, and subelement cr represents the fracture zone. After cracking, the total strain rate is described between the crack zone $\{\dot{\epsilon}^{cr}\}$ and the uncracked zone $\{\dot{\epsilon}^d\}$, thus:

$$\{\dot{\epsilon}\} = \{\dot{\epsilon}^d\} + \{\dot{\epsilon}^{cr}\} \quad (A.3)$$

The stress rate for the whole element $\{\dot{\sigma}\}$ is equal to the stress rate in subelement, d, and to stress rate in subelement cr.

$$\{\dot{\sigma}\} = \{\dot{\sigma}^d\} = \{\dot{\sigma}^{cr}\}$$

The stress-strain law for the whole element considering subelement d and cr, then;

$$\Delta \varepsilon^{sh} = \left[\frac{1}{E} + \frac{1}{L} \left(f(\omega) - \frac{f_t}{\omega_{cr}} \right)^{-1} \right] \Delta \sigma - \frac{1}{E} \Delta \sigma^R \quad (A.4)$$

or

$$\Delta \sigma = \left[\frac{1}{E} + \frac{1}{L} \left(f(\omega) - \frac{f_t}{\omega_{cr}} \right)^{-1} \right]^{-1} (\Delta \varepsilon^{sh} + \frac{1}{E} \Delta \sigma^R) \quad (A.5)$$

where, E = unloading modulus

L = length of the element

f_t = tensile strength of the matrix material

$\Delta \varepsilon^{sh}$ = imposed shrinkage strain

A.3.3 Crack Developement

In this stage the crack width exceeds its critical value ω_{cr} . There is no more cohesive stress transfer through the matrix. The deformation in the fracture zone results from the deformation in the fibers crossing the crack, and the deformation in the bond between fibers and matrix. The material outside the fracture zone behaves in a way similar to that during cracking.

The whole element is now composed of three subelements connected in series. Subelement d, which represents that part of the material which is outside of the crack zone, and subelement b which represents the interfacial deformation in the crack zone are identical to the corresponding elements after cracking. Subelement f represents the elastic deformation of that part of the fibers which resist crack opening. The total strain rate is distributed in subelement d ($\Delta \varepsilon_i^d$), b ($\Delta \varepsilon_i^b$) and f ($\Delta \varepsilon_i^f$)

$$\Delta \varepsilon_i = \Delta \varepsilon_i^d + \Delta \varepsilon_i^b + \Delta \varepsilon_i^f$$

The stress-strain law is given by

$$\Delta \sigma_i = \left(\frac{1}{D} + \frac{1}{L} \frac{1}{f(\omega_i)} + \frac{\omega_i}{L} \frac{A}{A_f} \frac{1}{E_f} \right)^{-1} (\Delta \varepsilon_i^{sh} + \frac{1}{D} \Delta \sigma_i^R) \quad (A.6)$$

where E_f is the young's modulus of the cellulose fiber, A_f is the effective area of the fibers crossing the crack and A is the cross-section area of the element.

A.4 MODEL COMPONENTS

A.4.1 Shrinkage

Shrinkage can be defined as a time-dependent volume decrease of concrete due to decreasing moisture content during drying. According to Sarja [59], the shrinkage of wood fiber concrete can be described by the following functions of humidity and density:

$$\varepsilon_{sh} = 12 \left(\frac{2800 - \rho}{2400} \right)^2 \left(\frac{200 - RH}{200} \right) \times 10^{-3} \quad (A.7)$$

where, ε_{sh} is the shrinkage strain $\times 10^{-3}$

ρ is the density of concrete dried at RH 40%

RH is the relative humidity (%)

A.4.2 Creep

Creep can generally be defined as a time-dependent deformation of a material subjected to sustained stress. If, as it for example happens in the case of restrained shrinkage, the deformation of a specimen is kept constant, then creep reduces the stress. When a structure or a specimen is subjected to restrained shrinkage, tensile stresses are produced, which can be partly relieved by creep deformations.

It has been experimentally observed that the sum of deformations caused by pure shrinkage (non-loaded drying specimen) and pure creep (loaded but non-drying specimen under constant environmental conditions) is always lower than the deformation caused by simultaneous application of load and drying. This phenomenon was first observed in concrete specimens by Pickett [114]. The same effect, but in tension, was observed by Domone [115]. These observations led to the conclusion that the drying process significantly influences the creep of a loaded specimen. This means that creep and shrinkage interact in determining the creep of a loaded specimen. Creep of a specimen in hygral

equilibrium with the ambient medium (no drying, no swelling) is called basic creep. Creep of a loaded and simultaneously drying specimen is called total creep. The difference between total creep and basic creep is called drying creep

$$\epsilon_{cc}^d = \epsilon_{cc}' - \epsilon_{cc}^b$$

where

ϵ_{cc}' = total creep strain

ϵ_{cc}^b = basic creep strain

ϵ_{cc}^d = drying creep strain

The phenomenon of creep is also observed in tension. Tensile creep occurs at a relative high stress level (close to the tensile strength of concrete) where the behavior is no longer linear. According to some tests, creep in tension is supposed to be equal to creep in compression under stresses of equal magnitude. Other results show that creep in tension is initially higher, but the rate of creep decreases after some time, and finally the long-term creep in tension is lower than in compression. It is also important to relate creep in tension to creep in compression as a function of the stress/strength ratio. Generally, microcracking in tension is more significant and contributes more to creep than in compression. The creep function used here was as follows:

$$\Phi = \frac{1}{E} [1 + \phi] \quad (\text{A.8})$$

where,

E= elastic modulus

ϕ = creep coefficient

The creep coefficient of wood fiber composite increases with decreasing density. The basic creep coefficient can be followed as follow [56]:

$$\phi = 3 \cdot \frac{2400}{\rho}$$

where , ρ is the density dried at 40% RH (kg/cm^3)

A.4.3 Effect of Cyclic Loading

After each new crack formation in a drying specimen under restrained conditions, the material outside the fracture zone is unloaded to some extent. Then, when the tensile stress in the fracture zone is transferred from the matrix to the fibers, the tensile stress increases again until it reaches the value of the tensile strength. A new crack is then formed and the material outside the new fracture zone is again partly unloaded. That means that the material is subjected to a cyclic load. Figure I.2 shows the cyclic tensile stress-strain behavior of concrete. The peak value of the stress decreases with each cycle. Test results are expressed as stress versus displacement relationships. The displacement is the total deformation of the measured zone which usually consists of high deformation in the area closest to the notch where the level of microdamage is high and much lower deformations in the further neighborhood of the notch. The shape of the descending part of $\sigma - \varepsilon$ curve can be analogous to that of the monotonic $\sigma - \omega$ curves. Past investigations[116] indicate that there is no significant difference in post-peak behavior between concrete, mortar and paste. Based on the obtained experimental results, the $\sigma - \omega$ relationship was adopted was as follow:

$$\sigma = f_t \exp(-kw^\lambda) \quad (\text{A.9})$$

where w is the crack width, and k and λ are material constants, assumed, according to reference 116, to be: $k = 0.071$, $\lambda = 1.01$. The following assumption was also made the microdamage density increases by 10% in one cycle and thus the strength of the material decreases by 10%.

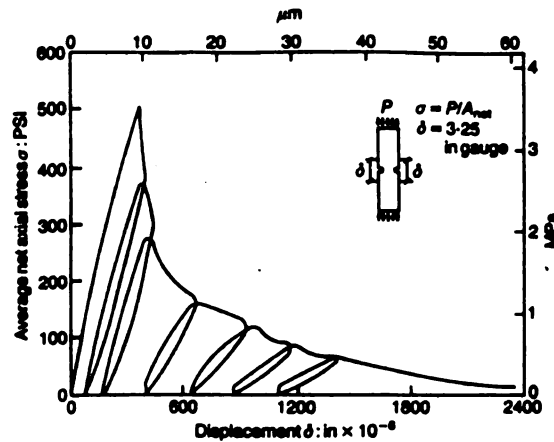


Figure A.2 Response of Concrete Subjected to Uniaxial Cyclic Loading [116]

A.4.4 Bond Behavior

Modeling of the bond between fibers passing across a crack and matrix is essential for the modeling of restrained shrinkage behaviors when we need to establish a constitutive law for the material consisting of a matrix and randomly distributed fibers. According to Jahlenius [117], the relationship between fiber pull-out force P and crack width w in a one fiber model was:

$$P = \pi d \frac{l}{2} \left[\frac{w}{w_s} - \left(\frac{w}{w_s} \right)^2 + \frac{\alpha}{2} \left(\frac{w}{w_s} \right)^2 + K' \frac{w}{w_s} \right] \quad (\text{A.10})$$

assuming that $w > w_s = 1$, where d is the diameter of the fiber, l is the length of the fiber. τ_v is the interfacial shear strength, τ_g is the frictional shear strength, K' is the anchorage force of the end of the fiber, and

$$\alpha = \frac{\tau_g}{\tau_v}$$

w_s is the crack width when all the fibers start sliding.

$$w_s = \frac{\tau_v \ell^2}{d \cdot E_f} \quad \text{if } \alpha + K' \leq 1$$

$$w_s = \frac{\tau_v \ell^2}{d \cdot E_f} (\alpha + K') \quad \text{if } \alpha + K' > 1$$

With the assumption of three-dimension distribution of fibers, the number of fibers per unit area of cross-section through composite is then [118]

$$N = \frac{2V_f}{\pi d^2}$$

A.5 Overall Approach to Modeling

Figure A.3 presents the overall approach for the modeling of the restrained shrinkage behavior of cellulose fiber reinforced cement.

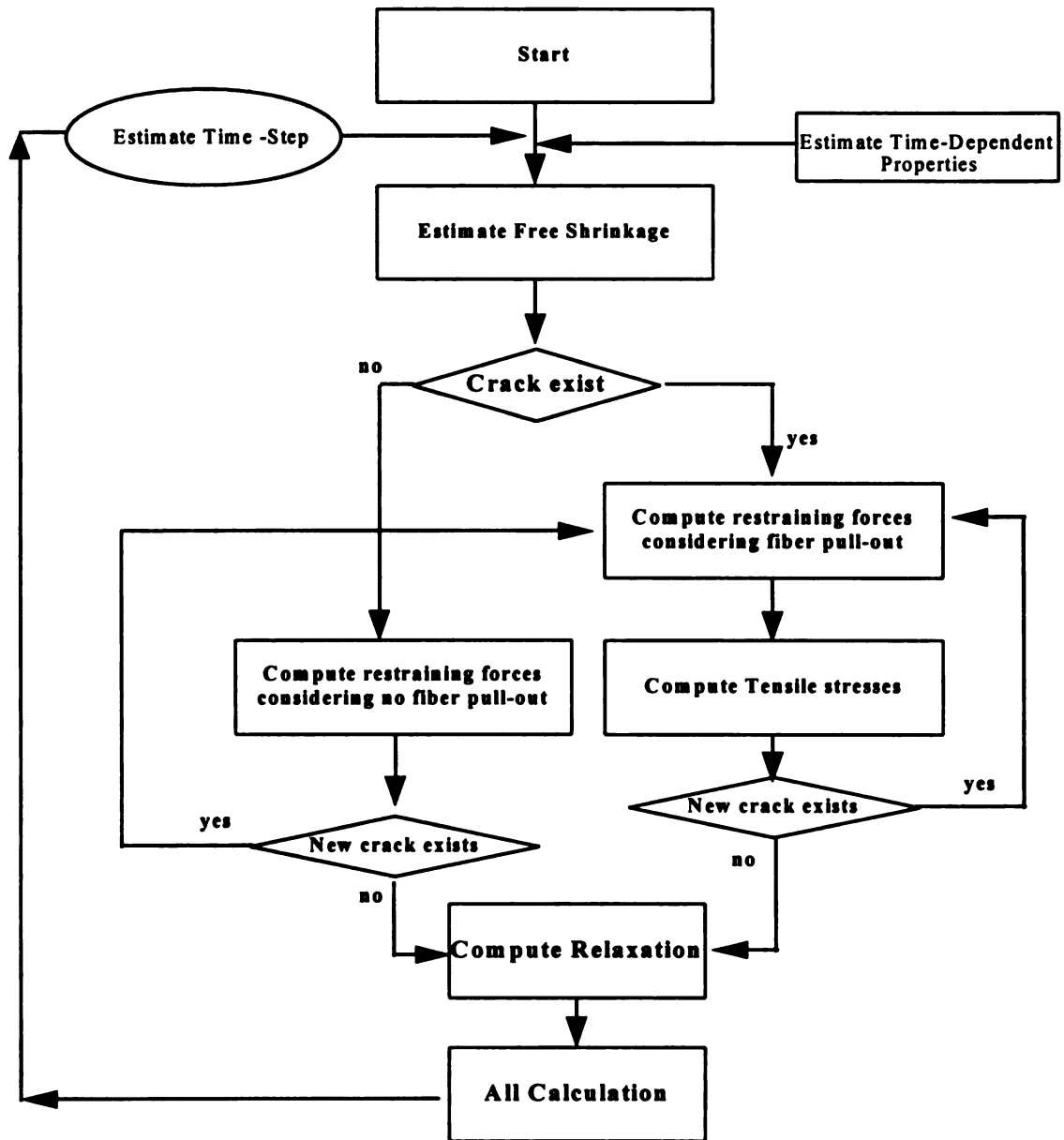


Figure A.3 Flow Chart for Restrained Shrinkage Modeling

A.5.1 Properties of Cellulose Fiber Reinforced Cement Composites

The following data on basic properties of cellulose fiber reinforced cement composite can be used for modeling properties.

- Matrix

$$E_m = 12 \text{ GPa}$$

$$f_t = 2.8 \text{ MPa}$$

$$\varepsilon_{\max} = 0.0001 \text{ [m/m]}$$

$$\beta_{pk} = 0.1$$

$$\omega_{cr} = 40$$

- Fiber (Cellulose)

	Dry	Wet
$E_f(\text{GPa})$	40	4
$f_f(\text{MPa})$	700	700
$V_f(\%)$	8	8
$\ell \text{ (mm)}$	4	4
$d \text{ (mm)}$	0.04	0.04

- Bond

$$\tau_v \text{ (MPa)} = 2, \tau_g \text{ (MPa)} = 0.5$$

A.6 SUMMARY

A framework is presented for modeling the restrained shrinkage behavior of cellulose fiber reinforced cement composites.

APPENDIX B

STANDARD SPECIFICATIONS

The following standard specifications were used in this study:

1. ISO 8335 Cement-Bonded Particleboards- Boards of Portland or Equivalent Cement Reinforced with Fibrous Wood Particles (International Organization for Standardization)
2. BS 5669 Particleboard (British Standard Institution)
3. BS 4624 Methods of Test for Asbestos-Cement Building Products (British Standard Institution)
4. ASTM C1185 Standard Test Methods for Sampling and Testing Non-Asbestos Fiber-Cement Flat Sheet, Roofing, and Siding Shingles, and Clap boards (American Society of Testing and Materials)
5. ASTM D1037 Standard Test Methods of Evaluating the Properties of Wood-Base Fiber and Particle Panel Materials (American Society of Testing and Materials)

LIST OF REFERENCES

BIBLIOGRAPHY

1. Dinwoodie, J.M., "Wood-Cement Particleboards - A Technical Assessment," Building Research Establishment Information Paper, United Kingdom, April 1983.
2. Holderness, S., "Marketing and Application Opportunities for Cement-Bonded Particleboards: Lesson from Great Britain and North Americas," Inorganic Bonded Wood and Fiber Composite Materials, Edited by A.A. Moslemi, Forest Products Research Society, 1992, pp.136-142.
3. White, M.S., "Marketing Wood-Cement Roofing Products in the United States," Inorganic Bonded Wood and Fiber Composite Materials, Edited by A.A. Moslemi, Forest Products Research Society, 1992, pp.127-128.
4. Simatupang, M.H., "Properties and Durability of Rapidly Curing Cement-Bonded Particleboards, Manufactured by Addition of Carbonation," proceeding 2nd International Symposium on Vegetable Plants and Their Fibers as Building Materials, 17-20 September 1990, Salvador, Bahia, Brazil, 1990, pp.239-247.
5. Moslemi, A.A., Garcia, J. F, and Hofstrand, A.D., "Effect of Various Treatments and Additives on Wood-Portland Cement-Water Systems," Wood and Fiber Science, Vol. 15, No. 2, pp.164-176.
6. Bierlich, K.G., "Manufacture of Portland Cement Products," US Patent No. 3468993, September 1969
7. Hsu, W.E., "Blast Furnace Slag Flakeboard," Inorganic Bonded Wood and Fiber Composite Materials, Edited by A. A. Moslemi, Forest Products Research Society, 1993, pp. 48-50.
8. Coutts, R.S.P., "Sticks and Stones," Forest Products Newsletter, CSIRO Division of Chemical and Wood Technology (Australia), Vol. 2, No.1, January, 1986, pp. 1-4.
9. Anon, "New-A Wood-Fiber Cement Building Board," CSIRO Industrial Research News 146, Australia, May,1981, pp. 1-4.
10. Eterline, "High Performance Fiber Reinforced Cement Panels," Eternet Inc., Blandon, Pennsylvania.

11. Hardiflex, "Fiber Reinforced Cement Sheets," James Hardie Building Products, James Hardie, Inc. Mission Viejo, California.
12. Fordos, Z., "Natural or Modified Cellulose Fibres as Reinforcement in Cement Composites," *Natural Fiber Reinforced Cement and Concrete*, Edited by R.N. Swamy, Blackie and Son Ltd, 1988, pp. 173-207.
13. John, G. Haygreen and Jim L. Bowyer, "An Introduction Forest Products and Wood Science," Second Edition, Iowa State University, Ames, Iowa, 1989, pp. 500.
14. H. A. Core, W. A. Cote, and A. C. Day, "Wood-Structure and Identification," Syracuse University Press, Syracuse, New York, 1976, pp. 168.
15. Coutts, R.S.P., "Wood Fiber Reinforced Cement Composites," *Natural Fiber Reinforced Cement and Concrete*, Edited by R.N. Swamy, Blackie and Sons Ltd., 1988, pp. 1-62.
16. Roman Malinowski, "Method of Casting Concrete," US Patent No. 4362679, December 7, 1982.
17. Simatupang, M.H. and Habighorst, C., "The Carbon Dioxide Process to Enhance Cement Hydration in Manufacturing of Cement-Bonded Composites-Comparison with Common Production Method," *Inorganic Bonded Wood and Fiber Composite Materials*, Edited by A. A. Forest Products Research Society, 1993, pp. 114-120.
18. Weatherwax, R.C. and Tarkov, H., "Effects of Wood on the Setting of Portland Cement," *Forest Product Journal*, 14(12), 1964, pp. 567-570.
19. Sanderman, W.R., Kohler, R., "Kurze Eignung Sprufung Von Holzern Fur Zement Gebundene Werkstoffe (Short Aptitude Test of Cement Bound Wood Materials)," *Holzforschung*, 1964, 18(12). pp. 53-59.
20. McIntosh, D.C., "Tensile and Bending Strengths of Loblolly Pine Kraft Fibers Cooked to Different Yield," *Tappi* 46, 1963, pp. 273-277.
21. Beck, S.R., "An Overview of Wood Gasification", In: *Technology and Economics of Wood Residue Gasification*, Edited by Rogers, K.E., Proceedings, 10th Texas Industrial Wood Seminar; March 13, 1979, Lufkin, TX: Texas Forest Service, Texas Forest Products Laboratory, pp. 20-37.
22. Shafizadeh, F. and Chin, P.S., "Thermal deterioration of wood," In Edited by Goldstein, I.S., *Wood Technology: Chemical Aspects*, Washington, D.C.; American Chemical Society; 1977, pp. 57-81.
23. Campert, H., "Faserplatten, Leipzig," VEB Fachbuchverlag, 1967, pp. 453.

24. Moslemi, A.A., "Inorganically Bonded Wood Composites," *Chemtech*, August, 1988, pp. 504-510.
25. Elmendorf, A., "Method of Making a Non-Porous Board Composed of Strands of Wood and Portland Cement," US Patent No. 3271492, 1966.
26. Miller, D.P., 1987, "Wood-Cement Composites: Interactions of Wood Components with Portland Cement," Doctoral Dissertation, University of Idaho. 1987.
27. Hachimi, M.H., "Important Consideration in Wood-Cement Compatibility," Doctoral Dissertation, University of Idaho, 1988.
28. Biblis, E.J. and Lo, C.F., "Sugars and other Wood Extractives; Effects on the Setting of Sodium Pine-Cement Mixtures," *Forest Products Journal*, 18(8), 1968, pp. 28-34.
29. Simatupang, M.H. and Geimer, R.C., "Inorganic Binder for Wood Composites: Feasibility and Limitations," *Wood Adhesives 1990*, Edited by A.H. Conners et al., Forest Products Research Society, 1991, pp. 167-176.
30. Okamura, T., H. Irifune, H. Yoshida, "Aluminum Hydroxide-Based Building Materials and Method for Manufacturing Same," Kogyo, K.K., Great Britain Pattern 2083088., 1982
31. Sekisui chemical Co., "Wood Chip Cement Products," Japanese Patent 56/140059, CA 96(10) 73740., 1981.
32. Galer, R.E. and P.C. Web, "Non-Expansive, Rapid Setting Cement," US Patent 4488909., 1984
33. Berger, R.C., Young, J.F., and Leung, U., "Accelerate of Hydration of Calcium Silicate by Carbon Dioxide Treatment," *Nature Physical Science*, Vol. 240, No. 91, 1972, pp. 16-18.
34. Coutts, R.S.P. and Campbell, M.D., "Coupling Agents in Wood Fiber Reinforced Cement Composites," *Composites*, Vol. 10, 1977, pp. 228-232.
35. Campbell, M.D. and Coutts, R.S.P., "Wood Fiber-Reinforced Cement Composites," *Journal of Material Science*, Vol. 15, 1980, pp. 1962-1970.
36. Cook, D.J., "Concrete and Cement Composites Reinforced with Natural Fibres," *Concrete International 1980: Proceeding Symposium on Fibrous Concrete in London*, Construction Press, New York, NY, 1980, pp. 99-114.

37. Krenchel, H. and Jansen, H.W., "Organic Reinforcing Fibres for Cement and Concrete," Concrete International 1980: Proceeding Symposium on Fibrous Concrete in London, Construction Press, New York. 1980.
38. Harper, S., "Developing Asbestos-Free Calcium Silicate Building Boards," Composites, 13(2), 1980, pp. 123-128.
39. Wells, R.A., "Future Development in Fiber Reinforced Cement, Mortar, and Concrete," Composites, 13(2), 1982, pp. 169-172.
40. Mindess, S. and Young, J.F., "Concrete," Printice-Hall, Inc., Englewood Cliffs, Inc., NJ., 1981, pp. 671.
41. Hachimi, M'Hamed and Campbell, Alton, G., "Wood-Cement Chemical Relationships," Fiber and Particle Boards Bonded with Inorganic Binders, Forest Products Research Society, 1989, pp. 43-47.
42. Kuroki, Y., Nagatomi, W., and Yamada, J., "Manufacture of Light-Weight Cement-Bonded Particleboard in Japan," Inorganic Bonded Wood and Fiber Composite Materials, Edited by A. A. Moslemi, Forest Products Research Society, 1993, pp. 136-142.
43. Lahtinen, Pentti K., "Experiences with Cement-Bonded Particleboard Manufacturing when Using a Short-Cycle Press Line," Inorganic Bonded Wood and Fiber Composite Materials, Edited by A. A. Moslemi, 1991 pp. 32-34.
44. Geimer, Robert L., Suoza, Mario R., Moslemi, A.A., and Simatupang, M. H., "Carbon Dioxide Application for Rapid Production of Cement Particleboard," Inorganic-Bonded Wood and Fiber Composite Materials, Edited by A.A. Moslemi, Forest Products Research Society, 1993, pp. 31-41.
45. Sanderman, W., "Chemische Holzverwertung," Muenchen, BLV Verlagsgesellschaft.
46. Moorehead, N.R. and Davis, M., "Method of Producing a Building Elements," Britain Patent No. 20270, 85 B, 1979.
47. Masatake, U. and Kawaguchi, T., "Manufacture of Wood-Based Boards by Carbonation," Japanese Patent No. 63155 174 A2, Ca/09(6): 42675. 1986.
48. Simatupang, M.H., Lange, H., Kasim, A., and Sedding, N., "Influence of Wood Species on the Setting of Cement and Gypsum," Inorganic Bonded Wood and Fiber Composite Materials, Edited by A. A. Moslemi, Forest Products Research Society, 1992, pp. 33-42.

49. Cox, H.L., "The Elasticity and Strength of Paper and other Fibrous Materials," *British Journal of Applied Physics*, 3, 1952, pp. 72-79.
50. Andonian, R., Mai, Y.W., and Cotterell, B., "Strength and Fracture Properties of Cellulose Fiber Reinforced Cement Composites," *The International Journal of Cement Composites*. Vol. 1, No. 3, 1979, pp. 151-158.
51. Baluch, H., Ziraba, Y.N., and Azod, A.K., "Fracture Characteristics of Sisal Fibre Reinforced Concrete," *The International Journal of Cement Composites and Lightweight Concrete*, Vol. 9, No. 3, 1987, pp. 157-168.
52. Mindess, S., and Bentur, A., "Technical Notes: the Fracture of Wood Fibre Reinforced Cement", *The International Journal of Cement Composites and Lightweight Concrete*, Vol. 14, No. 4, 1982, pp. 245-249.
53. Morrissey, F.E., Coutts, R.S., and Grossman, P.U.A., "Bond between Cellulose Fibers and Cement", *The International Journal of Cement Composite and Lightweight Concrete*, Vol. 7, 1985, pp. 73-80.
54. Dinwoodie, J.M. and Paxton, B.H., " A Technical Assessment of Cement-Bonded Particleboard," *Fiber and Particleboards Bonded with Inorganic Binders*, Edited by A. A. Moslemi, Forest Product Research Society, 1988, pp. 115-124.
55. Sorfa, P., "Properties of Wood-Cement Composites," *Journal of Applied Polymer Science: Applied Polymer Symposium* 40, 1984, pp. 209-216.
56. Lee, Andy W.C., "Physical and Mechanical Properties of Cement Bonded Southern Pine Excelsior Board," *Forest Product Journal*, 34(4), 1984, pp. 30-34.
57. Lee, Andy W.C., "Effect of Cement/Wood Ratio on Bending Properties of Cement-Bonded Southern Pine Excelsior Board," *Wood and Fiber Science*, 17(3), 1985, pp. 361-364.
58. Lee, Andy W.C. and Hong, Z., "Compressive Strength of Cylindrical Samples as an Indicator of Wood-Cement Compatibility," *Forest Product Journal*, Vol. 36, No. 11/12, 1986.
59. Sarja, A., "Wood Fibre Reinforced Concrete," *Natural Fiber Reinforced Cement and Concrete*, Edited by R. N. Swamy, Blackie and Sons Publication, 1988, pp. 63-91.
60. Das Gupta, N. C., Paramasivam, P., and Lee, S.L., "Mechanical Properties of Coir Reinforced Cement Paste Composites," *International Journal of Housing Science and its Applications*, 2, 1978, pp. 391-406.

61. Swift, D.G. and Smith, R.L., "The Flexural Strength of Cement-Based Composites using Low Modulus (Sisal) Fibers," *Composites*, 10, 1979, pp. -145-148.
62. Mai, Y. W. and Hakeem, M. I., "Slow Crack Growth in Bleached Cellulose Fibre Cements," *Journal of Materials Science Letters*, 3, 1984, pp. 127-130.
63. Hughes, D.C. and Hannant, D.J., "Reinforcement of Griffith Flaws in Cellulose Reinforced Cement Composites," *Journal of Materials Science Letters*, 4, 1985, pp. 101-102.
64. Coutts, R. S. P., "Wood Fibers in Inorganic Matrices," *Chemistry in Australia*, Vol. 50, No. 5, May, 1983, pp. 143-148.
65. Blankenhorn, P.R., Labosky, P., Dicola, M., and Stover, L.R., "The use of Eastern Hardwoods in the United States for the Production of Cement-Bonded Particle-board," *Inorganic Bonded Wood and Fiber Composite Materials*, Edited by A. A. Moslemi, Forest Product Research Society, 1991, pp. 28-31.
66. Coutts, R. S. P. "Air-Cured Wood Pulp Fiber-Cement Matrices," *Composites*, Vol. 18, No. 4, 1987, pp. 325-328.
67. Coutts, R. S. P. and Warden, P.G., "Air Cured Wood Pulp Fibre Cement Composites," *Journal of Material Science*, 4, 1985, pp. 117-119.
68. Coutts, R. S. P., "Autoclaved Beaten Wood Fibre-Reinforced Cement Composites," *Composites*, 15, 1984, pp. 139-144.
69. Coutts, R. S. P., "Flax Fibers as a Reinforcement in Cement Mortars," *International Journal of Cement Composite and Lightweight Concrete*, 5, 1983, pp. 257-262.
70. Coutts, R. S. P., "Eucalyptus Wood Fibre-Reinforced Cement," *Journal of Material Science and Letters*, 6, 1987, pp. 955-957.
71. Bugrinal, M.G., G.A. Buzhevich, V.R. Garashin, A. Z. Koketkina, and A. S. Sheherbakov, "Effect of Carbohydrates on Hydration and Hardening Processes of Cement," *Sb. Rub. Mosk Lesotkh Inst. No. 30*, 1968, As Cited in Chem Abstr. 71: 128218k.
72. Sanderman, W., "Research Results of a Wood-Cement System," Translation from *Chemie und Chemische Technol. Mineralgebundener Holzwerkstoff*, Internationale Arbeitstagung, 1969, pp. 5-21, As cited in Forest Abstract 31:5559.
73. Bentur, A., "Durability of Carbonated Glass Fibre Reinforced Cement Composites," *Durability of Building Material*, 1, 1983, pp. 313-326.

74. Moslemi, A.A., and Lim, Y.T., "Compatibility of Southern Hardwoods with Portland Cement," *Forest Products Journal*, 34(7/8), 1984, pp. 22-26.
75. Geimer, Robert L., "Steam Injection Pressing," *Proceeding of the 16th Washington State University International Symposium on Particleboard*, 1982, pp. 115-134.
76. Geimer, Robert L., "Method of Pressing Reconstituted Lignocellulosic Materials," *US Patent No. 4393019*, July 12, 1983.
77. International Standard, ISO 8335: Cement-Bonded Particleboards-Boards of Portland or Equivalent Cement Reinforced with Fibrous Wood Particles, International Organization for Standardization.
78. Food and Agriculture Organization of the United Nations (FAO), 1985, *World Forest Resources*, 1980.
79. Haygreen, John G. and Bowyer, Jim L., "Forest Products and Wood Science-An Introduction," Second edition, Iowa State University Press, 1989, pp. 500.
80. H.A. Core, W.A. Cote, and A.C. Day, "Wood: Structure and Identification," *Syracuse University Press*, 1976, pp. 168.
81. Fischer, K., "Modern Flaking and Particle Reduction," *Proceeding of Washington State University Particleboard Symposium*, 6, 1972, pp. 195-213.
82. Suchsland, Otto and Woodson, George E., "Fiberboard Manufacturing Practices in the United States," *Forest Products Research Society*, 1991, pp. 263.
83. Paper Grade wood pulp HP-11, Proctor and Gamble Cellulose, Memphis, Tennessee
84. NALCLEAR 9708 PULV Flocculent, Nalco Chemical Company, Naperville, Illinois.
85. Lange, H., Simatupang, M.H., and Neubauer, A., "Influence of Latent Hydraulic Binders on the Properties of Wood-Cement Composite," Edited by A.A. Moslemi, 1989, pp. 48-52.
86. Basheer, P.A.M., Montgomery, F.R., and Long, A.E., "Factorial Experimental Design for Concrete Durability Research," *Proceeding Institute Civil Engineers-Structures and Buildings*, 104, Nov. 1994, pp. 449-462.
87. Sharman, W.R. and Vautier, B.P., "Accelerated Durability Testing of Autoclaved Wood-Fiber Reinforced Cement Sheet Composites," *Durability of Building Materials*, 3, 1986, pp. 255-275.

88. Bentur, A. and Akers, S.A.S., "The Microstructure and Aging of Cellulose Fiber Reinforced Cement Composites Cured in a Normal Environment," *International Journal of Cement Composite and Lightweight Concrete*, 11(2), 1989, pp. 99-109.
89. Akers, S.A.S. and Studinka, J.B., "Ageing Behavior of Cellulose Fibre Cement Composites in Natural Weathering and Accelerated Tests," *International Journal of Cement Composites and Lightweight Concrete*, 11(2), 1989, pp. 93-97.
90. Klemm, W.A. and Berger, R.L., "Accelerated Curing of Cementitious Systems by Carbon Dioxide, Part I. Portland Cement," *Cement and Concrete Research*, 2(5), 1972, pp. 567-576.
91. Dinwoodie J.M. and Paxton, B.H., "The Long-Term Performance of Cement-Bonded Wood Particleboard," *Inorganic Bonded Wood and Fiber Composite Materials*, Edited by A.A. Moslemi, Forest Product Research Society, 1991, pp. 45-54.
92. Simatupang, M.H., Seddig, N., Habighorst, C., and Geimer, R.L., "Technologies for Rapid Production of Mineral-Bonded Wood Composite Boards," *Inorganic Bonded Wood and Fiber Composite Materials*, Edited by A.A. Moslemi, Forest Product Research Society, 1991, pp. 18-27.
93. Brown, Paul Wencil and Clifton, James R., "Mechanisms of Deterioration in Cement-Based Materials and in Lime Mortar," *Durability of Building Materials*, Elsevier Science Publishers, May 1988, pp. 409-420.
94. BS 5669, "British Standard: Particleboard," British Standard Institution, 1989.
95. ASTM: D1037-89, "Standard Test Methods of Evaluating the Properties of Wood-base Fiber and Particle Panel Materials," American Society of Testing and Materials.
96. ASTM: C1185-92, "Standard Test Methods for Sampling and Testing Non-Asbestos Fiber-Cement Flat Sheet, Roofing, and Siding Shingles, and Clapboards".
97. BS 4624, "Methods of Test for Asbestos-Cement Building Products," British Standard Institution, 1981.
98. Bentur, A. and Mindess, S., "Fibre Reinforced Cementitious Composites," Elsevier Applied Science, pp 449.
99. Goodbrake, C.J., Young, J.F., and Berger, R.L., "Reaction of Hydraulic Calcium Silicated with Carbon Dioxide and Water," *Journal of the American Ceramic Society*, Vol. 62, No. 9-10, Sept.-Oct. 1979, pp. 488-491.

100. Staley, R.W., "Method of Curing Cement-Type Cold Molding Composites," US Patent No. 2496895, February 7, 1950.
101. Young, J.F., Berger, R.L., and Breese, J., "Accelerated Curing of Compacted Calcium Silicate Mortars on Exposure to CO₂," *Journal of the American Ceramic Society*, September, 1974, pp. 394-397.
102. Neville, A.M., "Properties of Concrete," Third Edition, Longman Scientific & Technical, 1981, pp. 779.
103. Gram, H.E., "Durability Studies of Natural Organic Fibres in Concrete, Mortar or Cement," 3rd International Symposium on Developments in Fibre Reinforced Cement and Concrete, RILEM Symposium Fiber Reinforced Concrete, July 1986.
104. Gram, H.E., "Durability of Natural Fibres in Concrete," CBI Fo 1.83, CBI S-100 44, Swedish Cement and Concrete Research, Stockholm, Sweden, 1983, pp. 255.
105. Laws, V., "On the Mixture Rule for Strength of Fiber Reinforced Cements," *Journal of Material Science Letters*, 2, 1983, pp. 527-531.
106. Drack, E.R., "An Introduction to Process Visualization Capabilities and Considerations in the Environmental Scanning Electron Microscope (ESEM)," *Microscopy Research and Technique*, 25, 1993, pp. 487-492.
107. Danilatos, G.D., "Introduction to the ESEM Instruments," *Microscopy Research and technique*, 25, 1993, pp. 354-361.
108. Earnest, C.M., "The Modern Thermogravimetric Approach to the Compositional Analysis of Materials," *Compositional Analysis by Thermogravimetric*, ASTM STP 997, Edited by Earnest, C.M., American Society of Testing and Materials, 1988, pp. 1-18.
109. Becker, R. And Laks, J., "Cracking Resistance of Asbestos-Cement Panels Subjected to Drying," *Durability of Building Materials*, No. 3, 1985, pp. 35-49.
110. Bhatti, Javed I, I. Reid, K.J., Dellimore, D., Gamlen, G.A.C., Mangabhai, R.J., Rogers, D.F., and Shah, Tahir H., "The Derivation of Kinetic Parameters in Analysis of Portland Cement for Portlandite and Carbonate by Thermogravimetric," *ASTM STT 997*, 1988, pp. 204-215.
111. Pirie, B.J., Glasser, F.P., Schmitt-Henco, C., and Akers, S.A.S., "Durability Studies and Characterization of the Matrix and Fiber-Cement Interface of Asbestos-Free Fibre Cement Products," *Cement & Concrete Composites*, 12, 1990, pp. 233-244.

112. Mehta, P.K. and Monteiro, P.J.M., "Concrete-Structure, Properties, and Materials," 2nd Edition, Printice-Hall, Inc., 1993, pp. 548.
113. Balaguru, P.N. and Shah, S.P., "Fiber Reinforced Cement Composites," McGraw-Hill, Inc., 1992, pp. 530.
114. Pickett, G., "The Effects of Change in Moisture Content on the Creep of Concrete under a Sustained Load," ACI Journal, Vol. 38, No. 4, 1942, pp. 333-355.
115. Domone, P.L., "Uniaxial Tensile Creep and Failure of Concrete," Magazine of Concrete Research, Vol. 26, No. 88, Sept. 1974, pp. 144-152.
116. Gopalnratnam, V.S. and Shah, S.P., "Softening Response of Plain Concrete in Direct Tension," ACI Journal, Vol. 82, No. 3, May-June 1985, pp. 310-323.
117. Jahlenius, A., "Fiber Concrete as Structural Materials," Publication 1/83, Department of Structural Engineering, Royal Institute of Technology, Stockholm, Sweden, 1983.
118. Hannant, D.J., "Fibre Cements and Fibre Concretes," John Wiley & Sons, 1978, pp. 219.

MICHIGAN STATE UNIV. LIBRARIES



31293014000586